Selective C−F and Ni−C Bond Activation of Fluoronickelacycles as a Function of Ancillary Ligands

Kaitlyn Anne Giffin

Thesis submitted to the

Faculty of Graduate and Postdoctoral Studies

in partial fulfillment of the requirements for the degree of

Doctor of Philosophy, Chemistry

Center for Catalysis Research and Innovation

Department of Chemistry and Biomolecular Sciences, University of Ottawa

Abstract

The development of new unconventional routes to small functionalized fluorocarbons (FCs) continues to be an attractive target due to the high utility of FCs in a broad range of applications, including their use as refrigerants, solvents, and surfactants. With the phasing out of hydrofluoroalkanes as refrigerants, there is a growing interest in the synthesis of new hydrofluoroolefins (HFOs), which are known to have significantly reduced global warming potential relative to hydrofluoroalkanes. Currently, energy-intensive conditions and toxic starting materials are typically necessary for their syntheses, making these processes environmentally problematic. The approach we have proposed for alternative 'greener' methods for functionalized FC production targets a transition metal-catalyzed synthesis involving the formation of metallacyclic intermediates through the oxidative cycloaddition of simple fluorinated alkenes, *e.g.*, tetrafluoroethylene (TFE) and trifluoroethylene (TrFE), at low-valent nickel centres.

There is precedent for the generation of short fluoroalkyl chain (C_4-C_6) compounds through homogeneous catalysis. For example, Baker *et al.* showed that you could catalytically hydrodimerize two molecules of tetrafluoroethylene (TFE) or one molecule of TFE with one molecule of ethylene using low valent Ni catalysts and π-acidic monodentate ancillary ligands, affording octafluorobutane and 1,1,2,2-tetrafluorobutane respectively.

The objective of this Thesis is to further the *state-of-the-art* in fluoroorganometallic chemistry by gaining a deeper understanding of transition metal fluoroalkyl complexes as a function of metal−fluoroalkyl and carbon−fluorine bond reactivity. The over-arching goal is to harness said reactivity for the synthesis of new value-added fluorocarbons.

Due to the robust nature of carbon−fluorine and metal−fluoroalkyl bonds in transition metal fluoroalkyl complexes, intensive conditions are often necessary to achieve any reactivity. Recently, bifunctional ligands have proven to be useful at effecting challenging transformations through unconventional ligand-assisted substrate activation pathways. Chapters 2 and 3 herein explore the

use of a bidentate phosphinothiol ligand in the context of perfluoronickelacyclopentane reactivity. Synthetic approaches for the formation of phosphinothioether- and phosphinothiolate-supported perfluorometallacycles are outlined along with ensuing reactivity studies, including examples of $C_\alpha-F$, $C_\beta-F$, and $Ni-C_\alpha$ bond activation. Furthermore, a metal-mediated synthesis of functionalized FC, (*E*)-1,2,3,3,4,4-hexafluoro-1-butene, is provided. Chapter 4 sheds light on the comparatively underdeveloped chemistry of fluorinated nickelacycles generated from TrFE. A systematic study of monodentate phophine and phosphite ligand effects on metallacyclopentane regio-/stereochemistry is presented. The behaviour of the generated hydrofluoronickelacyclopentanes in the presence of acidic additives allows for a direct analogy to be made regarding the effects of the extent of metallacycle fluorination on C−F and Ni−C activation. In search of new approaches to novel functionalized FC synthesis, Chapter 5 will re-visit the use of bifunctional ligands, investigating the formation and reactivity of new perfluoronickelacycles featuring **[P,NH]** and **[P,N$^-$]** bidentate ligands. Finally, Chapter 6 summarizes the findings of this Thesis and discusses some of the future opportunities that will build on this work.

The increased understanding of the stoichiometric systems presented herein will be directly important to the development of nickel-catalyzed routes to HFOs. As the demand for new “greener” refrigerants and propellants increases, the synthesis of small-molecule functionalized FCs using transition metal catalysis and waste fluorinated feedstocks can offer a mild, atom economical approach to new, unique candidates that will be appealing to industrial partners.

Acknowledgements

First and foremost I would like to thank my supervisor, Prof. Tom Baker. You started off as my hippie Organometallics professor who encouraged me to pursue my graduate studies. Right from the get-go, your passion and curiosity of all things chemistry has rubbed off on me and I can't thank you enough for that. I am so grateful for the valuable lessons I have learned working for you, including the importance of independent/creative thinking, the importance of working hard, and of course the importance of having a ton of fun while you're at it. I will miss most our NMR sessions where we solved puzzles together, and I had the opportunity to observe your brain power in action!

Although there are too many to name, I would like to thank all the Baker group members who have come and gone over the years. You made the lab a truly enjoyable place to be. To Graham, Matt, Mehdi, Nick and Alex Sicard who have been there for the long haul with me, thank you for your teamwork and all of the good times we've had together in and out of the lab. Our many bowling, pool, and La Maison excursions kept me going throughout the years. A special thanks to Sarah Piotrkowski and Lorraine Pua who were awesome undergraduate students to mentor and work with. I would like to especially thank Mr. Uttam Das. As a labmate, you were always there to help and provide advice when I needed it, and our lengthy chemistry discussions were always very helpful. I'm so grateful to have you as a friend and will miss sitting next to you in the lab. To Christian, I am so happy we've had the chance to work together the past five years. Your advice, support and friendship mean the world to me, so thank you.

Last but not least I would like to thank all my family and friends for their endless amount of support and understanding throughout all my years of schooling. I would not be where I am today without the constant support I have received from my Mom, Dad, Sister, Grandma and Granny. I am so thankful that they have always encouraged me to take on challenges and to pursue what makes me happy.

Table of Contents

Abbreviations

Ar	Aryl
atm	Atmosphere
BTB	1,3-bis(trifluoromethyl)benzene
C_6H_6	Benzene
CFC	Chlorofluorocarbon
CH_3CN	Acetonitrile
CNAr	2,6-dimethylphenyl isocyanide
cod	1,5-cyclooctadiene
cot	1,3,5-cyclooctatriene
COSY	Correlation spectroscopy
ca.	*circa*, approximately
cf.	compare
DCE	1,2-dichloroethane
DCM	Dichloromethane
DEE	Diethyl ether
DFT	Density functional theory
DPEPhos	(oxydi-2,1-phenylene)bis(diphenylphosphine)
DMF	Dimethylformamide
ESI-MS	Electrospray ionization mass spectrometry
Equiv	Equivalents
Et	Ethyl
FC	Fluorocarbon
h	Hour(s)
HF	Hydrofluoric acid
HFB	Hexafluorobenzene
HFO	Hydrofluoroolefin
HMQC	Heteronuclear multiple quantum coherence
HRMS	High resolution mass spectrometry
Hz	Hertz
i.e.	It is
i-Pr	Isopropyl
IPr	(1,3-bis(2,6-diisopropylphenyl)imidazole-2-ylidene)
L	Ligand
LA	Lewis acid
Me	Methyl
ND	Not detected
NEt_3	Trimethylamine
NHC	N-heterocyclic carbene
NMR	Nuclear magnetic resonance
OTf	Trifluoromethanesulfonate
PFOA	Perfluorooctanoic acid

Ph	Phenyl
PTFE	Polytetrafluoroethylene
Pyr	Pyridine
R^F	Fluoroalkyl group
RB	Round-botom
RT	Room temperature
TFE	Tetrafluoroethylene
TrFE	Trifluoroethylene
THF	Tetrahydrofuran
Tol	Toluene
UV-vis	Ultraviolet-visible sprectrometry

List of Schemes

List of Charts

List of Figures

List of Tables

List of Compounds

Metal Complexes:

Label	Complex	Label	Complex
Ni-1	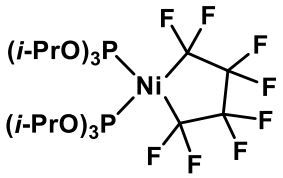	Ni-2	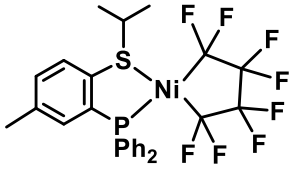
Ni-3	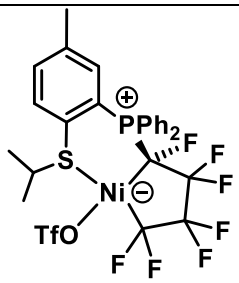	Ni-3 • CH_3CN	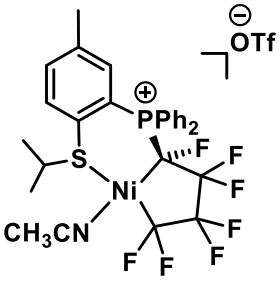
Ni-4	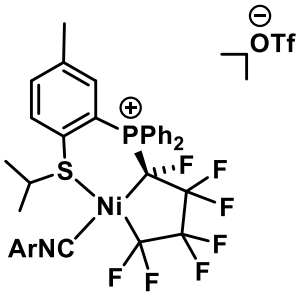	Ni-5	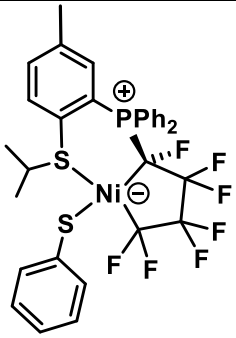
Ni-6	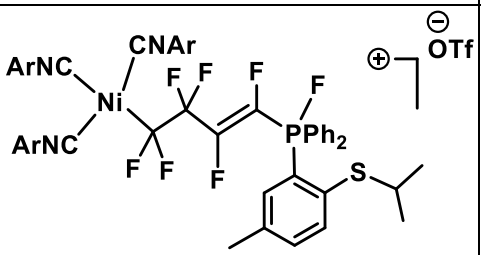	Ni-7	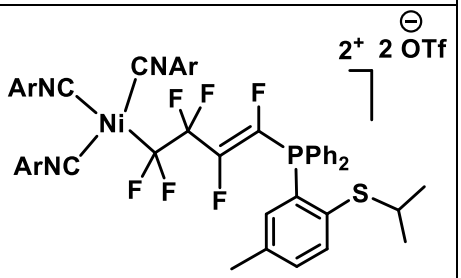
Ni-8	$Ni[P(O\text{-}o\text{-}tol)_3]_4$	Ni-9a	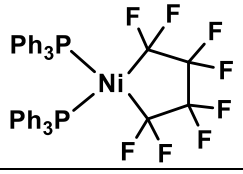
Ni-9b	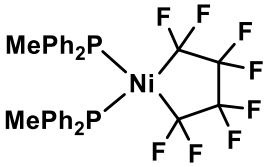	Ni-9c	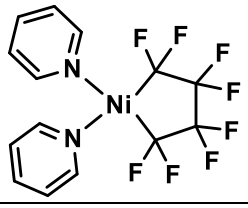

Label	Complex	Label	Complex
Ni-10a	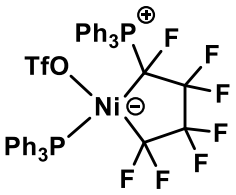	Ni-10b	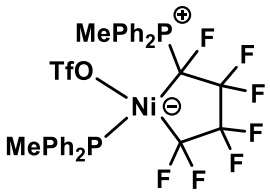
Ni-10c	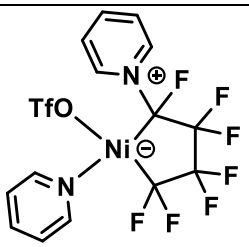	Ni-11a	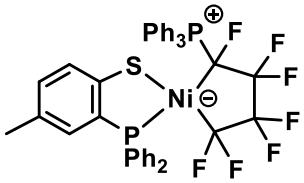
Ni-11b	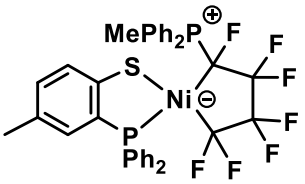	Ni-12	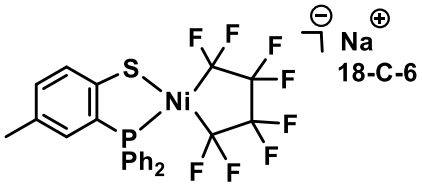
Ni-13	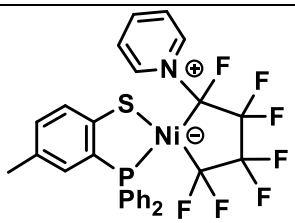	Ni-14	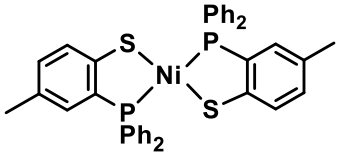
Ni-15a	$Ni(cod)_2 + 2PPh_3$	Ni-15b	$Ni[P(O\text{-}o\text{-}tol)_3]_4$
Ni-15c	$Ni(cod)_2 + 2PPh_2Me$	Ni-15d	$Ni(cod)_2 + 2PPhMe_2$
Ni-15e	$Ni(cod)_2 + 2PMe_3$	Ni-16a	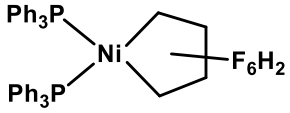
Ni-16b	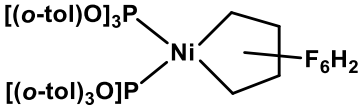	Ni-16c	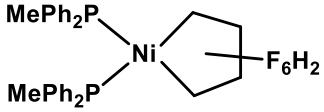
Ni-16d	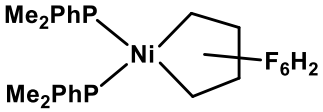	Ni-16e	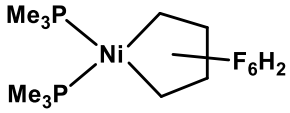
Ni-17	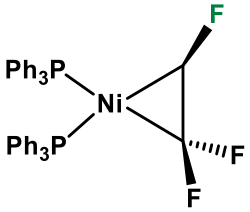	Ni-18’	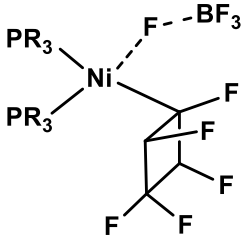

Ni-19'	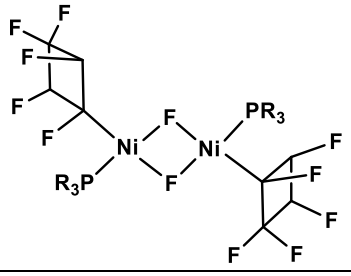	**Ni-20**	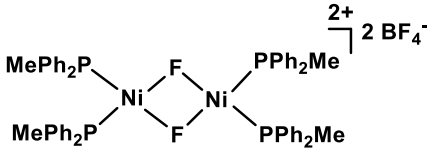
Ni-21	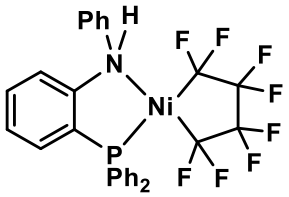	**Ni-22•Na**	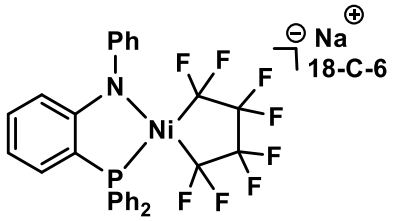
Ni-23	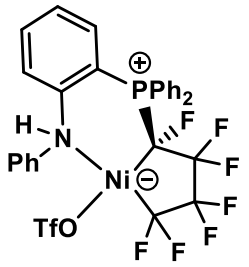	**Ni-24**	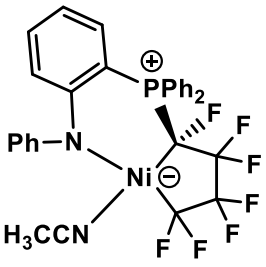

Organic Compounds:

Label	Compound	Label	Compound
O1	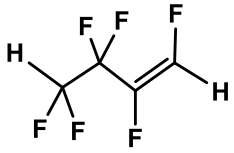	**O2**	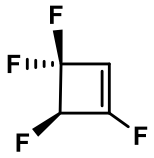
O3	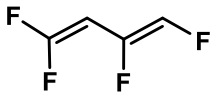	**O4a-f**	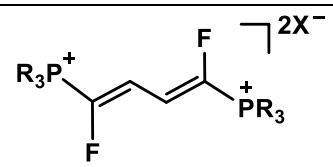
O5a-f	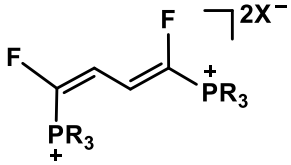	**O6**	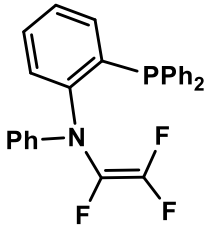
[P,SH]	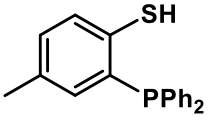	**[P,NH]**	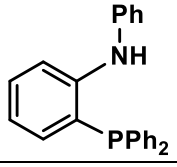

List of Contributions

Publications resulting from the chapters of this Thesis (F = Full article)*:*

F4. Giffin, K. A.; Pua, L. A.; Korobkov, I.; Baker, R.T. Formation and C−F bond functionalization of [P,N]-coordinated perfluoronickelacyclopentanes, **2017**, *manuscript in preparation*.

F3. Giffin, K. A.; Pua, L. A.; Piotrkowski, S.; Gabidulin, B. M.; Korobkov, I.; Hughes, R. P.; Baker, R. T. Generation of Hydrofluoronickelacycles from Trifluoroethylene and Ni(0): Ligand Effects on Regio-/Stereoselectivity and Reactivity, *J. Am. Chem. Soc.* **2017**, *139*, 4075-4086.

F2. Giffin, K. A.; Korobkov, I.; Baker, R. T. Brønsted acid-promoted C−F bond activation in [P,S]-ligated neutral and anionic perfluoronickelacyclopentanes, *Dalton Trans.* **2015**, *44*, 19587-19596 (***Fluorine***-themed issue).

F1. Giffin, K. A.; Harrison, D. J.; Korobkov, I.; Baker, R. T. Activation of C-F and Ni-C Bonds of [P,S]-Ligated Nickel Perfluorometallacycles, *Organometallics* **2013**, *32*, 7424-7430.

Presentations:

10. Giffin, K. A.; Baker, R. T. (2016) A Study of Ligand Effects on the Regio-/Stereo-Selectivity and Reactivity of Fluorinated Metallacycles. Canadian Symposium on Catalysis. (poster presentation)

9. Giffin, K. A.; Pua, L.; Piotrkowski, S.; Korobkov, I.; Baker, R. T. (2015) Selective C-F and Ni-C Bond Activation of Fluoronickelacycles. Organometallic Gordon Research Conference. (poster presentation)

8. Giffin, K. A.; Pua, L.; Piotrkowski, S.; Korobkov, I.; Baker, R. T. (2015) Selective C-F and Ni-C Bond Activation of Fluoronickelacycles. Organometallic Gordon Research Seminar. (poster presentation)

7. Giffin, K. A.; Korobkov, I.; Baker, R. T. (2015) Selective C-F Bond Functionalization of Perfluoronickelacyclopentanes. 98th Canadian Chemistry Conference (CSC). (poster presentation, poster prize inorganic section)

6. Giffin, K. A.; Korobkov, I.; Baker, R. T. (2014) Accessing Greener Routes to Functionalized Fluorocarbons using Nickel Metallacycles. International Symposium on Homogeneous Catalysis (ISHC). (poster presentation)

5. Giffin, K. A.; Korobkov, I.; Baker, R. T. (2014) Accessing Greener Routes to Functionalized Fluorocarbons using Nickel Metallacycles. ACS Summer School on Green Chemistry and Sustainable Energy. (poster presentation)

4. Giffin, K. A.; Harrison, D. J.; Korobkov, I.; Baker, R. T. (2013) Nickel Perfluorometallacycles as Intermediates to Small-Molecule Fluorocarbon Derivatives. Ottawa-Carlton Chemistry Institute (OCCI) Day. (poster presentation, 1ST place poster prize in organometallic/inorganic section)

3. Giffin, K. A.; Harrison, D. J.; Korobkov, I.; Baker, R. T. (2013) Nickel Perfluorometallacycles as Intermediates to Small-Molecule Fluorocarbon Derivatives. 96TH Canadian Chemistry Conference (CSC). (poster presentation, poster prize inorganic section)

2. Giffin, K. A.; Harrison, D. J.; Korobkov, I.; Baker, R. T. (2012) Towards Functionalized Fluorocarbons from Nickel Perfluorometallacycles. Inorganic Discussion Weekend (IDW). (poster presentation)

1. Giffin, K. A.; Harrison, D. J.; Baker, R. T. (2012) Nickel Perfluorometallacycles: Intermediates for Sustainable Routes to Functionalized Fluorocarbons? 95th Canadian Chemistry Conference (CSC). (oral presentation).

Chapter 1. Introduction

1.1. Organofluorine Compounds

The importance of organofluorine compounds is highlighted by their wide range of uses, including as refrigerants, surfactants, solvents, pharmaceuticals, agrochemicals, and polymers.[1] The global fluorochemicals market was valued at $18.90 billion in 2015 and is expected to reach a value of $36.40 billion by 2025.[2] As marketed fluorochemical products are ever-evolving, this type of growth provides opportunity for innovations in both synthesis and product development. Many of the unique properties that make fluorocarbons (FCs) so valuable in a multitude of industrial applications and that furthermore make their syntheses more challenging are imparted by the strength of the C−F bonds in comparison to the C−H bonds of their hydrocarbon analogues. In Nature, fluorine is estimated to be the thirteenth most abundant element and is mostly sourced from fluorite (CaF_2) mining.[1] Interestingly, C−F bonds are very rarely found in Nature, and consequently all C−F bonds of organofluorine compounds are synthetically introduced. Of particular interest for this *Thesis* are small highly fluorinated organics that are important as refrigerants, blowing agents, surfactants and as treatments for various materials to impart water/oil-repellent properties. Quantitatively, refrigerants account for the majority of fluorocarbon production, with their market continuously growing with that of the automotive industry. In contrast, fluorosurfactants account for a minor amount of fluorocarbons by mass, but are still significant economically with an over $1 billion market annually based on their high cost.[3]

1.2 Fluorinated Refrigerants

1.2.1 Properties

Industry based on organofluorine compounds only came to be in 1930 with the discovery of the attractive refrigeration properties of chlorofluorocarbons (CFCs) by Frigidaire, first synthesized earlier by Swarts.[4] This led to the development of a cheaper, lighter and safer refrigerator, thus

instigating widespread use of refrigerators in households. The high electronegativity of the fluorine atom accounts for its low polarizability, which in turn leads to low surface energies and weak cohesive forces between fluorocarbon molecules.[5] This property is evident in the high volatilities of fluorocarbons, which have similar boiling points to their hydrocarbon analogues, even though their molecular weights are significantly higher. The low boiling points of fluorocarbons lend to their efficiency as refrigerants in addition to their high heats of vaporization and critical temperature, and their density in liquid/gaseous form.[6] The two qualities which really set FCs apart from other refrigerants such as ammonia, diethyl ether, sulfur dioxide, and propane are their low flammability and low toxicity. The major drawbacks of fluorinated refrigerants compared to the other options are their environmental impacts. Although chlorofluorocarbons and hydrochlorofluorocarbons make excellent refrigerants, their significant contribution to ozone depletion led to their complete phase out initiated by the Montreal Protocol in 1987 and the Vienna Conference in 1995.[7] Following this phase out, hydrofluorocarbons (HFCs) were developed as the next generation of refrigerants, wherein the absence of chlorine atoms completely eliminates their ozone depletion potential. These compounds, however, still have high global warming potentials (GWP; how much heat a gas traps in the

Figure 1.1 History of fluorocarbon refrigerants.

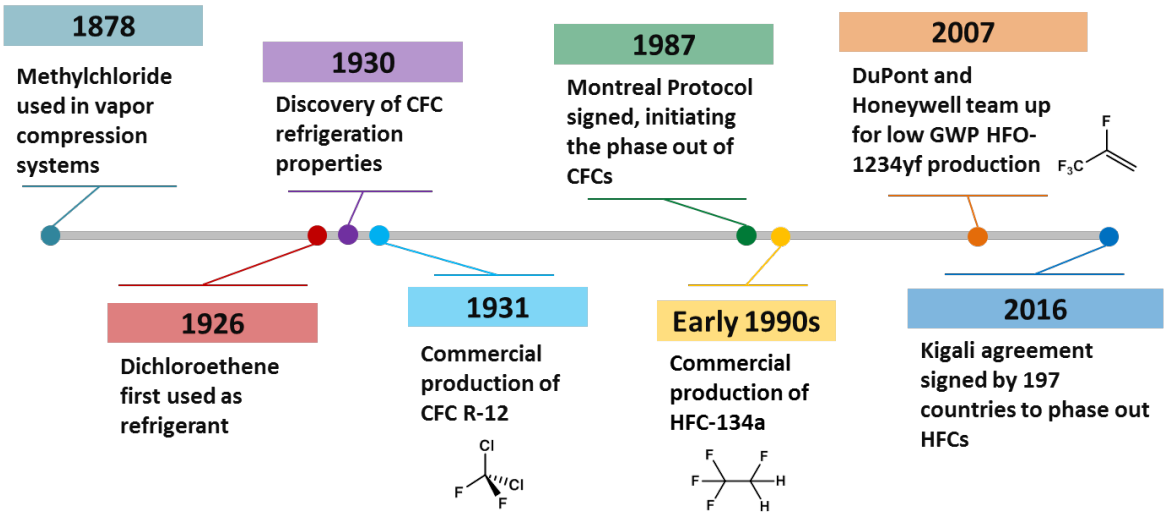

atmosphere). Currently, the most commonly used fluorinated refrigerant is HFC-134a (see Chart 1.1), which has a GWP of 1430 relative to CO_2 = 1. These high GWPs have translated to the phasing out of saturated HFCs which was very recently accelerated on a global scale by the Kigali agreement.[8] Some of the more attractive refrigerants emerging from the phasing out of HFCs include hydrofluoroolefins (HFOs) which are known to retain the attractive refrigeration properties of HFCs while possessing significantly reduced GWPs (*e.g.*, HFO-1234yf has a GWP of 4).[9] Two major players in the commercialization of the fourth generation HFO refrigerants are HFO-1234yf and HFO-1234ze, both based on a C_3 backbone. There are only a few lesser known HFOs to date based on C_4 backbones, including HFO-1336mzz(e) and HFO-1345fz.

Chart 1.1 Important HFC and HFO refrigerants.

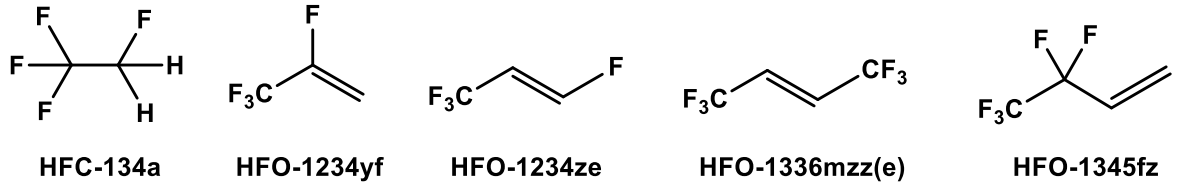

1.2.2 Synthesis

Historically, CFCs were synthesized on industrial scales using the original Swarts Process, in which chlorocarbons react with anhydrous hydrogen fluoride in the presence of a Lewis acid (typically SbF_5 or SbF_3Cl_2), exchanging the chlorine for a fluorine at carbon to form the stronger Sb−Cl bond (*vs.* Sb−F, Scheme 1.1a).[4b] A similar process was adapted for the synthesis of HFCs starting from hydrochlorocarbons and utilizing Cr(III)-based catalysts (Scheme 1.1b).[10] To obtain a higher extent of fluorination as is often needed for the generation of targeted refrigerants, more extreme conditions are necessary. Current methods for the production of emerging HFO refrigerants on an industrial scale draw some similarities to the methods previously/currently used for CFC and HFC production, and will be discussed further below.

Scheme 1.1 a) Formation of C−F bonds using the Swarts process; b) Synthesis of HFC 134a.

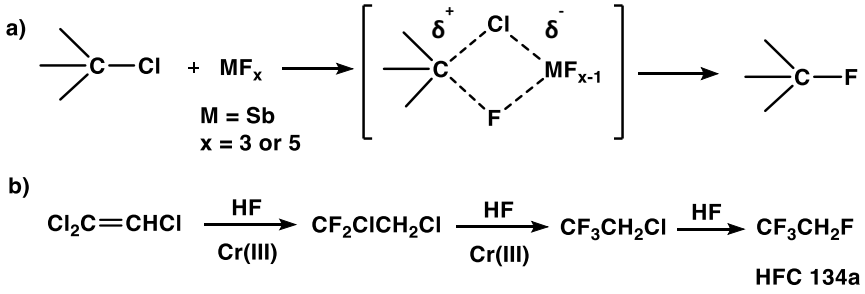

1.2.3. 2,3,3,3-Tetrafluoropropene (HFO-1234yf)

HFO-1234yf (GWP of 4) is one of the most promising HFC replacements. Its performance characteristics match those of HFC-134a (GWP of 1430), making it the ideal candidate to directly replace HFC-134a for automobile air conditioning.[11] Indeed, the EPA approved the use of HFO-1234yf for automobile use back in 2011, and it has already been implemented by a handful of car companies in select models, with this number expected to grow exponentially in the near future, given the new regulations to limit saturated HFCs. In 2007, Du Pont and Honeywell announced a joint manufacturing venture for the production of HFO-1234yf.[12] In 2008, Du Pont patented a method for HFO-1234yf synthesis involving initial hydrogenation (using H_2 gas) of $CF_3CF{=}CHF$ at 85 ^oC over Pd/C catalyst.[13] The effluent from this reactor proceeds to a second catalyst bed of gamma-alumina for dehydrofluorination. When the temperature of the reactor reaches 400 $^\circ C$, targeted HFO-1234yf and HF are obtained in high conversions (Scheme 1.2a). One of the major drawbacks of this method is that the starting olefin, $CF_3CF{=}CHF$, requires several synthesis steps, increasing the costs of the overall reaction. A patent published by Van der Puy from Honeywell Inc. in 2011 outlines the synthesis of 2,3,3,3-tetrafluoropropene involving a two-reactor process (Scheme 1.2b).[14] Chlorotrifluoroethylene (CTFE) and a methyl halide are fed into a reactor (R1) at 700 $^\circ C$ to form an

Scheme 1.2 Methods for the synthesis of HFO-1234yf.

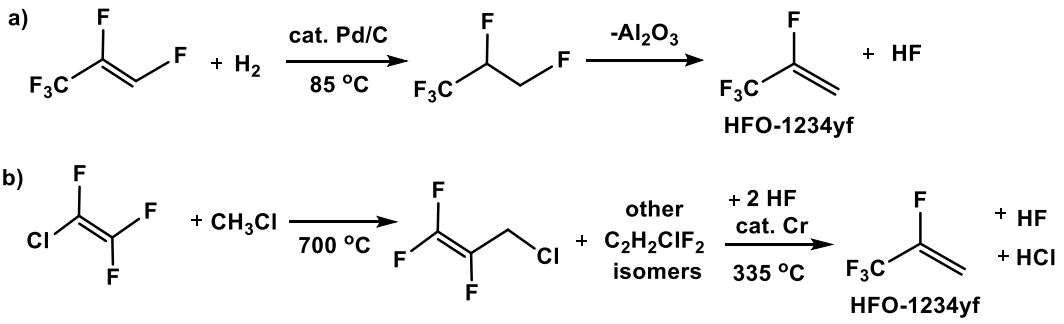

intermediate product stream consisting of $C_3H_2ClF_3$ isomers and minor amounts of other HFCs. This stream is fed into a second reactor (R2, containing a catalytic amount of fluorinated chromium oxide) with a superstoichiometric amount of HF (2 moles *vs.* CTFE for optimal yield) kept at 335 °C. The product stream after R2 consists mainly of the desired product, $CF_3CF=CH_2$ (HFO-1234yf), alongside by-products (HCl and HF), unreacted intermediates (mainly $CF_3CH_2CF_2H$; HFC-245fa), and other minor impurities. HCl and HF can be removed by scrubbing and the significant difference in boiling points between HFO-1234yf and HFC-245fa allow for purification of the product by cryogenic distillation. Some of the major drawbacks of this refrigerant include its current price and its flammability (*vs.* the currently employed HFC-134a), but recent regulations on HFC-134a should provide incentives for the discovery of more economical synthetic routes.

1.2.4 1,3,3,3-Tetrafluoropropene (HFO-1234ze)

Before HFO-1234ze was attractive as a fourth generation refrigerant, it was useful along with other fluorinated propenes as a monomer in the synthesis of homo- and co-polymers.[15] It was traditionally synthesized by catalytic dehydrofluorination of HFC-245fa in the presence of a phase transfer catalyst, or by catalytic dehalogenation of CF_3CH_2CHFCl (HCFC-244fa). However the many steps required to get to both 245fa and 244fa alone make this process undesirable based on cost and availability of starting materials. After renewed interest in HFO-1234ze as a low GWP refrigerant and blowing agent, Honeywell recently patented routes based on more readily available starting materials for its synthesis. In 2008, Van Der Puy and co-workers described a process for the synthesis

of HFO-1234ze using a sequential method, where CF_3X and H_2C=CFH in the presence of a Pd catalyst are heated to 200°C for 48 h, resulting in a mixture of products (Scheme 1.3a).[16] The targeted intermediate CF_3CH_2CFHX is separated from the other by-products by distillation, followed by its addition to an aqueous solution of KOH. After 24 h at 40 °C, GC reveals that the reaction product consists of 75 mol% of the desired 1,3,3,3-tetrafluoropropene.

A more recent Honeywell patent from 2013 disclosed the invention of a four-step process starting with fluorine-free 1,2-dichloroethylene and CCl_4 (Scheme 1.3b).[17] Initially, the starting materials are converted to the addition product, $CCl_3CHClCHCl_2$, in the presence of a molecular Ru or Rh catalyst [*e.g.*, $RuCl_2(PPh_3)_3$] with an isolated yield ranging between 40-50%. The intermediate is then added dropwise to a zinc dust/methanol mixture to afford 60-70% of the dechlorinated product CCl_2=CHCHCl_2. Thirdly, a fluorination reaction is performed using $SbCl_5$ (or SbF_5) on activated carbon as a catalyst and an excess of anhydrous HF to yield CF_3CH_2CHClF as the major product. Lastly, dehydrochlorination of CF_3CH_2CHClF over activated carbon gives targeted HFO-1234ze in a 40-60% yield, purified by distillation.

Scheme 1.3 Patented methods for the synthesis of HFO-1234ze.

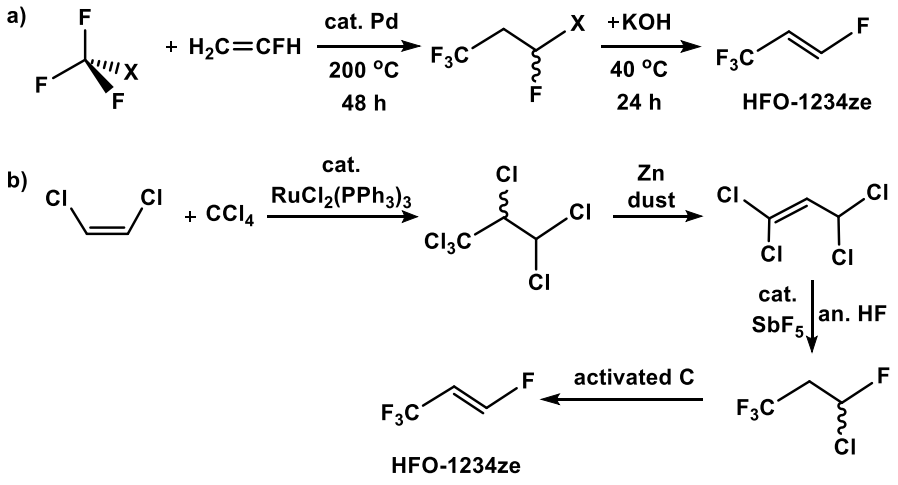

1.2.5 1,1,1,4,4,4-Hexafluoro-2-butene (HFO-1336mzz)

An HFO that meets the low GWP requirements, but has received less attention to date is C4-based HFO-1336mzz which has desirable properties as a blowing agent for insulating foams. A 2013 Du

Pont patent describes the utility of azeotrope-like mixtures of the *E/Z* isomers of HFO-1336mzz in applications as a blowing agent, refrigerant, a fire extinguisher, an aerosol product, and as a solvent.[18] *Z*-HFO-1336mzz can be synthesized by selective hydrogenation (using H_2) of hexafluoro-2-butyne in the presence of a Lindlar catalyst.[19] Alternatively, the *E* isomer can be obtained by treating 1,2-dichloro-1,1,4,4,4-pentafluorobutane with dried KF in distilled tetramethylene sulfone.[20]

1.3 Fluorosurfactants

1.3.1 Properties

Highly fluorinated compounds are known to be the most effective surfactants for many different applications. This is mainly attributable to their low surface energies, water repellency and chemical inertness. They consist of hydrophilic "heads" and fluorophilic "tails" that also make them the most effective surfactants for the solubilisation of fluorinated monomers in emulsion polymerization.[1] Perfluorinated products are indispensable in applications where chemical and thermal robustness play a key role. Their stability stems from the great strength of C−F bonds and C−C bonds of perfluorinated groups, which also accounts for their indefinite persistence in the environment. For example, long-chain fluorocarbons, in particular perfluorooctanoic acid (PFOA) and perfluorooctanesulfonic acid (PFOS, Chart 1.2), are known to bioaccumulate and can be found at low levels everywhere, from municipal wastewater to the blood and organs of most mammals, including polar bears and humans.[21] Upon discovery of this bioaccumulation in the 1990s by 3M, the company voluntarily terminated production of C8-based PFOS-related products (important components in their Scotchgard brand of stain-protection products) and replaced them with shorter-chain pefluorobutane analogues that degrade to perfluorobutane sulfonate (PFBS).[22] This was a surprising discovery as it

was previously believed that longer perfluoroalkyl chains (> C6) were vital to maintain the desirable chemical and thermal properties of these fluoroalkyl materials. Not only were C4-based fluorinated products just as effective as their C8 analogues, they were also found to be much less bioaccumulative, and consequently presumed to be less toxic. For instance, PFBS has a half-life of one month in a person whereas PFOS has a half-life of 4.5 years.[22] Given the evidence for the carcinogenicity and the disruption of sexual development in lab animals with exposure to PFOA, a PFOA Stewardship Program was set in place by the EPA and the 8 major companies that manufacture PFOA agreed to completely eliminate production by 2015.[23] Many of the replacements for PFOA are also based on shorter-chain perfluoroalkyl derivatives, with Du Pont's short-chain perfluoroether-based surfactant as the major player for polymer production. While the new shorter-chain products are an improvement on the phased out longer-chain analogues, more innovation towards fluorinated alternatives that are even less persistent, more environmentally benign, and that furthermore retain properties uniquely associated to fluorocarbons is desired.

Chart 1.2 Long- and short-chain fluorosurfactants.

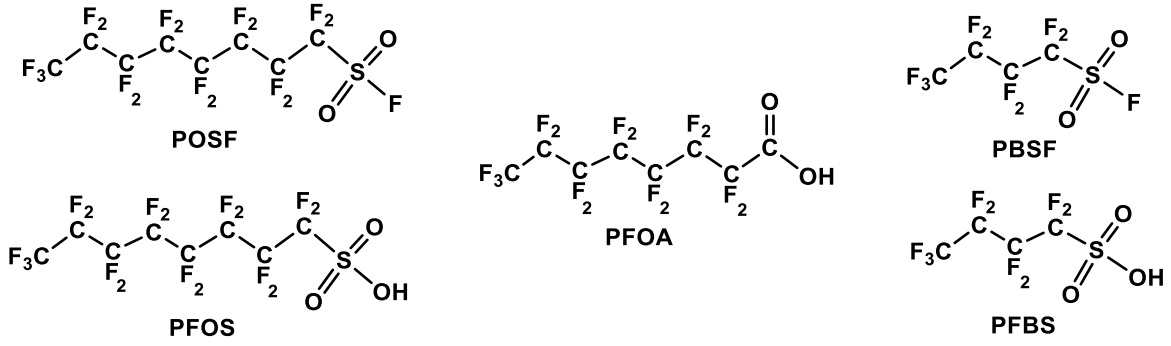

1.3.2 Synthesis

Traditionally, the method of choice for the synthesis of fluorosurfactant precursors employs electrochemical fluorination (ECF), a process developed by Simons in 1950 that is still commonly used on large scales today.[24] The process is especially valuable when a high extent of fluorination is desired, and entails the application of a direct electric current to a solution of organic compound

dissolved in anhydrous HF. Some of the major drawbacks typical of electrochemical fluorination include low yield, long reaction times, and low selectivity towards the desired product(s). 3M's industrial scale synthesis of both PFOA and perfluorooctanesulfonyl fluoride (abbreviated POSF, a precursor for PFOS and PFOS-based compounds) involved ECF of octanoyl chloride and octanesulfonyl fluoride respectively.[25] Although the mechanism of fluorination using ECF is not completely understood, it is proposed to either proceed by formation of high-valent nickel fluorides at the surface of the anode, or by formation of radical cation intermediates (Scheme 1.4). Alternatively, Du Pont employed a telomerisation method for the synthesis of PFOA, involving the addition of tetrafluoroethylene (TFE) to a perfluoroiodine compound in the presence of a catalyst (mixture of iodine pentafluoride and antimony pentafluoride), followed by oxidation with SO_3.[26] With the phasing out of the C8-based products, many of the technologies previously employed for their syntheses were adapted for the synthesis of shorter-chain derivatives. Notable examples from recent patents published by 3M and Du Pont will be highlighted below.

Scheme 1.4 Proposed mechanism for C−F bond formation in ECF.

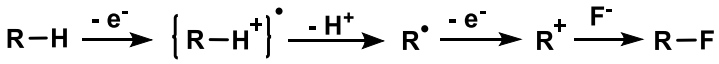

1.3.3 Scotchgard

Scotchgard was famously discovered by Patsy Sherman and Samuel Smith at 3M back in 1952 when an accidental chemical spill on Smith's white shoe proved to effect stain resistance. Scotchgard is now used as a treatment on a wide array of products to impart stain and water resistance, including clothing fabrics, furniture, and carpets. Originally, Scotchgard was patented as a block co-polymer which incorporates a segment that is highly fluorinated and a segment with a high number of polar groups, making materials treated with Scotchgard autoadaptable (*i.e.*, change from net oleophobic and hydrophobic in air to net oleophobic and hydrophilic in water).[27] In 2002, a newer version was patented by 3M, wherein it was first shown that shorter chain fluoroalkyl groups can be effective at

imparting the same desirable qualities.[28] The new Scotchgard treatment is a chemical composition typically considered to be an oligomer which results from the condensation of a) fluorinated polyol, b) polyisocyanate, and c) a monofunctional fluorine-containing terminal group (Chart 1.3). One of the preferred embodiments uses the diol, $C_4F_9SO_2N(C_2H_4OH)_2$ as the fluorinated polyol, which is synthesized by first treating perfluorobutanesulfonyl fluoride (PBSF; obtained from ECF of *n*-butanesulfonyl chloride) with an equimolar amount of NH_3, followed by successive treatments with ethylene chlorohydrin and sodium hydroxide. The monofunctional fluorine-containing terminal group is ideally a C4-based compound that is at least 50 % fluorine by weight, and contains a functional group that must be reactive with either the terminal isocyanate group (from the polyisocyanate) or hydroxyl group (from the polyol). Such functional groups include secondary amino, carboxyl, hydroxyl, isocyanato, epoxy, or oxazolinyl groups. One of the more preferred fluorinated monofunctional compounds is the alcohol, $C_4F_9SO_2N(CH_3)CH_2CH_2OH$, prepared by the reaction of PBSF with methylamine and ethylenechlorohydrin. The three main components of Scotchgard listed above are condensed to afford the fluorochemical oligomer in the presence of a catalytic amount of dibutyltin dilaurate.

Chart 1.3 Formula for the fluorochemical urethane composition of Scotchgard.

$$R^FQ(\text{-CONH-}R^1\text{-NHCO-}OR^2O\text{-})_n(\text{CONH-}R^1\text{-NHCO})\text{-}QR^F$$

where R^F = perfluoroalkyl group
Q = isocyanate linking group
R^1 = straight chain alkylene (1-14 carbons)
R^2 = fluorinated polyol
n = number from 1-10

1.4 Fluoroorganometallic Chemistry

Focus has recently shifted to the development of more sustainable, "greener" routes for the synthesis of small highly fluorinated compounds. In this context, transition metal-mediated transformations of fluorinated building blocks are attractive alternatives to the current methods

highlighted above. Homogeneous catalysts for fluorination and trifluoromethylation have been well-established in the past decade. Some heterogeneous methods for the synthesis of highly fluorinated compounds have emerged as well. This *Thesis* will focus on the selective functionalization of fluorinated compounds at transition metal centres with the goal of developing more sustainable and energy efficient routes towards new value-added fluorochemicals.

1.4.1 Historical Context

One of the first examples of a transition metal fluoroalkyl complex, $Mn(CF_3)(CO)_5$, was almost simultaneously reported by three independent groups in 1960: Gordon Stone and co-workers, the Ethyl Corporation, and W.R. McClellan of Du Pont.[29] The perfluoroalkylmanganese complex was synthesized by the thermal decarbonylation of the acetyl precursor, $CF_3COMn(CO)_5$. Around this same time, it was also discovered that transition metal fluoroalkyl complexes could be accessed by exploiting the pseudohalide characteristics of perfluoroalkyl groups. For example, perfluoroalkyliodides oxidatively add to low valent iron and cobalt centres to afford new metal fluoroalkyl bonds.[30] The 1960s witnessed an explosion in the field of fluoroorganometallic chemistry in large part due to the prolific work of Stone. The first metallacyclopentanes were synthesized by addition of tetrafluoroethylene (TFE) to low valent $Fe(CO)_5$ and $Co(CO)_2(\eta^5\text{-}C_5H_5)$ respectively (Chart 1.4).[30a,31] Evidence for TFE insertion into M−H bonds was also demonstrated by formation of $Mn(CF_2CF_2H)(CO)_5$ from the reaction between TFE and $MnH(CO)_5$.[32] Shortly after the synthesis of the iron and cobalt metallacyclopentanes, Stone expanded this reactivity to low valent Ni and TFE. By widening the scope of the ancillary ligands employed, he was able to conclude that the ligand(s) steric bulk dictated the size of metallacycle formed, with the bulkiest ancillary ligand(s) favouring formation of metallacyclopropane products (Scheme 1.5).[33] The study of mono- and bidentate phosphine ancillary ligands was more recently elaborated by Ogoshi *et. al.* in 2013,

Chart 1.4 First reported perfluorometallacycles.

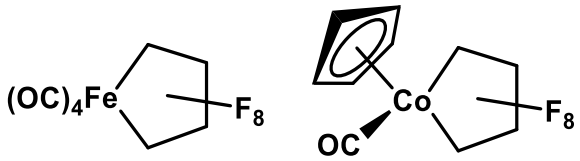

Scheme 1.5 Ligand effects on perfluoronickelacycle formation.

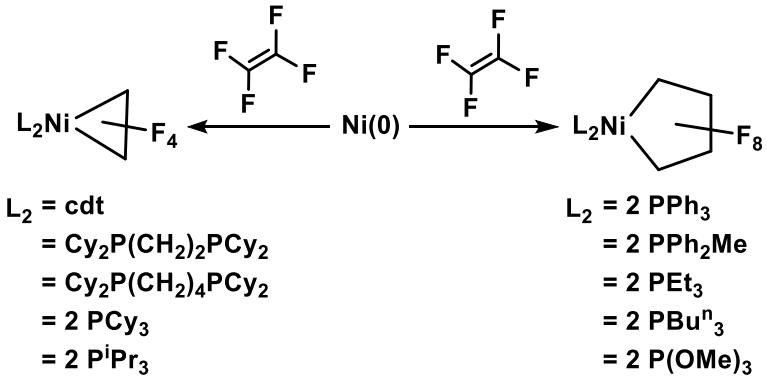

increasing the number of examples of both metallacyclopropane and -pentane complexes.[34] The propensity for Ni(0) to favour the formation of metallacyclopentane products with TFE contrasts the reactivity Stone reported with Pt(0). Platinum and palladium complexes such as $Pt(PR_3)_4$ (where R = alkyl or aryl) and $Pd(C_2H_4)(PPh_3)_2$ exclusively form stable metallacyclopropane products[34,35] with TFE and interestingly, in the presence of excess TFE, $Pt(cod)_2$ gives a diplatinum TFE-bridged product (Chart 1.5, right).[36] This type of reactivity has more recently been extended to Ir complexes by Cowie and co-workers, and will be discussed further in *Chapter 4*.[37] Early studies by Stone were also performed with other fluorinated feedstocks, including hexafluoropropene (HFP) and trifluoroethylene (TrFE). Hexafluoropropene exclusively forms 3-membered metallacycles with both Pt and Ni (Chart 1.5, left).[38] Presumably due to the larger steric bulk of the olefin, no examples of 5-membered rings with HFP have been reported to date. TrFE reacts with $Ni(PPh_2Me)_4$ and $(PPh_3)_2Ni(C_2H_4)$ to give nickelacyclopentanes[33,39], which will be elaborated on later in *Chapter 4*.

Chart 1.5 Reactivity of Pt(0) with TFE and HFP.

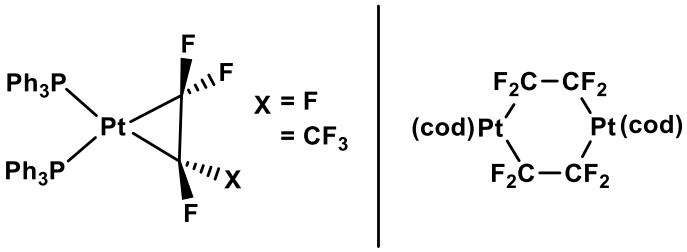

In parallel to this work, Stone also investigated other fluorinated feedstocks such as $(CF_3)_2$=O, $(CF_3)_2$=NH, CF_2=CFX (where X = Br, Cl) that are beyond the scope of this *Thesis*.[40] In his perspective on fluorine as a ligand substituent in organometallic chemistry[41], Hughes pointed out that the initial excitement in the field of fluoroorganometallic chemistry seemed to fade over the years, which he states is "perhaps due to the observations that complexes of fluorinated ligands were almost invariably more stable and much less chemically reactive than their hydrocarbon counterparts."

1.4.2 Comparison of M−Alkyl and M−Perfluoroalkyl Bonds

The strength of mid to late transition metal perfluoroalkyl bonds compared to their hydrocarbon analogues has been highlighted over the years through their difference in reactivity. While metal alkyl bonds are best known in classic organometallic reactions such as migratory insertions and reductive eliminations, metal perfluoroalkyl complexes are famous for their lack of reactivity via these same pathways.[40] For example, $Mn(CH_3)(CO)_5$ is known to undergo facile migratory insertion in the presence of CO (Scheme 1.6a) while $Mn(CF_3)(CO)_5$ is surprisingly resistant to insertion even under high pressures of CO (Scheme 1.6b).[42]

Scheme 1.6 Comparative reactivity of Mn−CH_3 and M−CF_3 bonds.

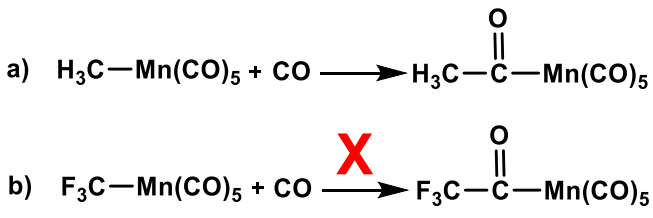

There has been some controversy over the years as to the theory behind the shortening of M−perfluoroalkyl bonds relative to M−alkyl[43], but two recent independent studies by Hughes[44] and Macgregor[45] combined both DFT and experimental studies to conclude that there are a number of factors which contribute to the overall strength of M−CF_3 *vs.* M−CH_3 in mid to late transition metals: a) M−C bonds are predominantly covalent, therefore bond ionicity does not play a major role (no correlation between M or C charges and M−C bond length variations); b) a higher σ interaction in M−CF_3 due to an increase in C 2s character (consistent with Bent's rule)[46] contributes to bond shortening; and c) a minor contribution from metal π-back-bonding into the C−F σ* orbital exists. Notably, Hughes' computational study also compared trends for M−$CF_2CF_2CF_2CF_3$ complexes and found them to be identical to the M−CF_3 analogue.

As mentioned earlier, the strength of C−F bonds (attributed mainly to the large electronegativity difference between fluorine and carbon), creates challenges for the derivatization of fluorocarbons. This is however noticeably changed upon coordination to a transition metal, wherein C−F bonds α to the metal centre are known to be significantly elongated. The NBO analysis by Macgregor on a series of M−CF_3 complexes suggests that two factors contribute to C_α−F weakening: a) the delocalization of the C lone pair in CF_3^- into the C−F σ* orbitals; and b) the minor metal π back-donation contribution into C−F σ* orbitals.[44] The effect of this bond weakening in terms of reactivity will be discussed below.

1.5 Transition Metal-Mediated C−F Bond Activation of Fluorinated Ligands

1.5.1 Selected Examples of M−Fluoroalkyl Reactivity

Reger and Dukes were the first to examine the effect of C_α−F elongation on reactivity, rationalizing that such bonds would be more susceptible to electrophilic attack.[47] Indeed, they successfully synthesized a metal difluorocarbene complex by treatment of Mo−CF_3 with Lewis acidic SbF_5. By using the same strategy on a higher fluoroalkyl complex, they were able to demonstrate that the C_α−F bonds are selectively activated by the transition metal. Treatment of

Mo−$CF_2CF_2CF_3$ with Lewis acid afforded exclusive formation of the monofluorocarbene product **I1** (Scheme 1.7). The fluorocarbene products were unstable and therefore only characterized *in situ* by

Scheme 1.7 Selective activation of C_α−F with a Lewis acid.

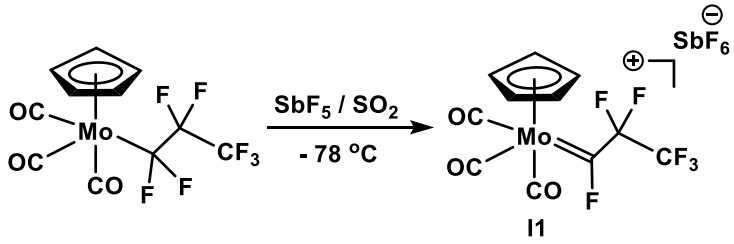

NMR. Shortly after this initial report, a series of new mono- and difluorocarbene complexes were published, mainly from the groups of Roper, Shriver, and Hughes.[48] These subsequent studies demonstrated that the fluoride abstraction generally works well with other acids (both Lewis and protic acids), and also with other M−perfluoroalkyl derivatives, including examples with Mn, Fe, Ru, Os, and Ir. Another early report that clearly highlights the activation of the C_α−F bonds is the electrophilic halogen exchange reaction published by Richmond and Shriver.[49] In the presence of BX_3 (where X = Cl, Br), regiospecific halogen exchange occurs at the α carbon of $CpMo(CO)_3(CF_2CF_3)$ and $CpMo(CO)_3(CF_2CF_2CF_3)$, affording $CpMo(CO)_3(CX_2CF_3)$ and $CpMo(CO)_3(CX_2CF_2CF_3)$ respectively.

1.5.2 Perfluorometallacyclopropane Complexes

Early studies by Stone and Kemmitt investigated the reactivity of Pt HFP[50] and TFE[51] adducts towards Lewis acids (Scheme 1.8). In the case of $(PPh_3)_2Pt(C_2F_4)$, only the weakly Lewis acidic LiI is needed to achieve C−F activation and rearrangement to the vinyl product, presumably due to the favourable formation of LiF. More recently, Ogoshi *et. al.* performed a more in-depth investigation of various Ni and Pd TFE adducts, concluding that a number of Lewis acids and metal halogens are capable of affording the C−F bond-activated vinyl products.[34] These stoichiometric reactions were further exploited to achieve catalytic C−C bond forming reactions in the presence of LiI and aryl zinc compounds formed *in situ* from $ZnCl_2$ and a Grignard reagent.[52]

Scheme 1.8 C−F activation of a) Pt HFP and b) Pt TFE complexes.

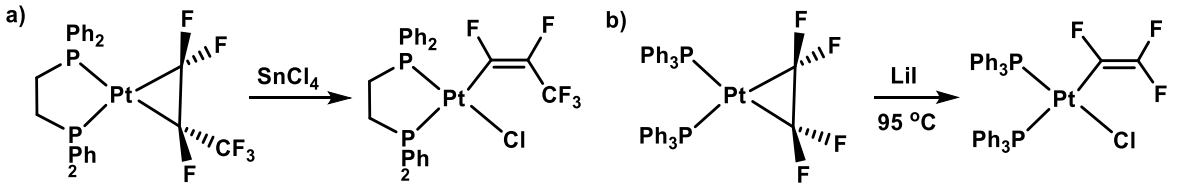

Another more recent report from Xiaoyan Li and colleagues which was published in parallel with the work of this *Thesis*, outlined the synthesis and reactivity of a new Ni HFP adduct.[53] Upon addition of $ZnCl_2$, five coordinate $(PMe_3)_3Ni(C_3F_6)$ undergoes selective C−F activation at the 2-position, giving vinyl product **I2** (Scheme 1.9). Further studies investigating the reactivity of complex **I2** with Grignard reagents resulted in multiple C−F activations, affording *trans*-$[NiBr\{CF_3CH{=}C(CH_2CH_2C_6H_5)\}(PMe_3)_2]$.

Scheme 1.9 C−F bond activations in Ni HFP adduct.

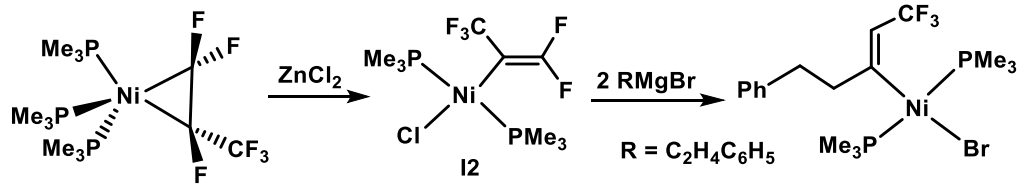

Li's HFP study was followed up shortly thereafter by a report of a Pd HFP analogue from Ogoshi *et al.*, wherein the selectivity of C−F activation (C_α−F *vs.* C_β−F) could be tuned based on the Lewis acid co-additive employed.[54] While a stoichiometric amount of $BF_3{\cdot}OEt_2$ afforded the expected vinylic product upon addition to $(PCy_3)_2Pd(C_3F_6)$ (**I3**), treatment of **I3** with one equivalent of a bulkier Lewis acid, $B(C_6F_5)_3$, gave cationic perfluoroallylpalladium complex **I4**, resulting from the unexpected activation of a CF_3 C_β−F bond (Scheme 1.10). An in depth NMR study demonstrated the fluxionality of the perfluoroallyl ligand and also confirmed its η^2-coordination mode.

Scheme 1.10 Tuning C−F bond activation in I3 by varying the Lewis acid.

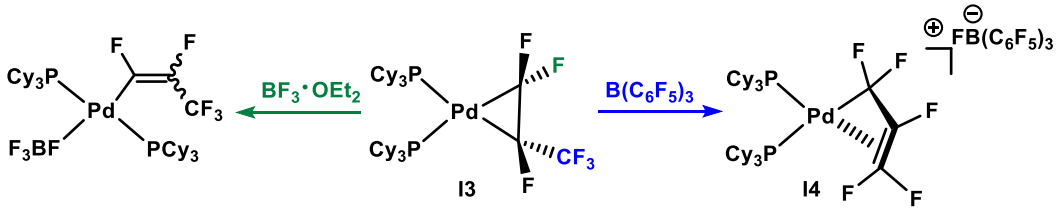

1.5.3 Perfluorometallacyclobutane Complexes

Our group recently published the synthesis of new cobalt fluorocarbenes[55], $CpCo(PR_3)(=CF_2)$ where PR_3 = PPh_3, PPh_2Me and $P(OMe)_3$. The PPh_2Me analogue demonstrates its decidedly *nucleophilic* character by affording perfluorocobaltacyclobutane complex **I5** upon treatment with TFE.[56] Harnessing the reactivity of such fluorocarbenes and fluorometallacyclobutanes is highly desirable in pursuit of more selective homogeneous catalyzed routes (relative to current radical and heterogeneous catalyzed methods)[57], for the polymerization of fluorinated alkenes. In the presence of either stoichiometric Me_3SiOTf or a catalytic amount (3-6 mol%) of $HNTf_2$, fluoride abstraction from **I5** yields the *trans*-vinyl **I6** and the isomerization/ring contraction metallacyclopropane **I7** (where the abstracted fluoride returns to the rearranged product), respectively (Scheme 1.11). Both acid reactions were proposed to proceed through a formal C_β−F activation, which was supported by generation of the β-phosphine functionalized metallacycle **I8** upon addition of $[HPPh_2Me][NTf_2]$ to perfluorometallacyclobutane (Scheme 1.12). These results have been reproduced in our lab with nickel analogues $P_2Ni(-CF_2CF_2-CF_2-)$ where P_2 = 2 $P(OMe)_3$ or bis(diphenylphosphino)ethane (DPPE).[58] New developments including examples of fluoroalkene metathesis have been achieved and are currently being expanded upon by PhD candidate, Mr. Alex Daniels.[59]

Scheme 1.11 Formation and acid reactivity of perfluorocobaltacyclobutane complex I5.

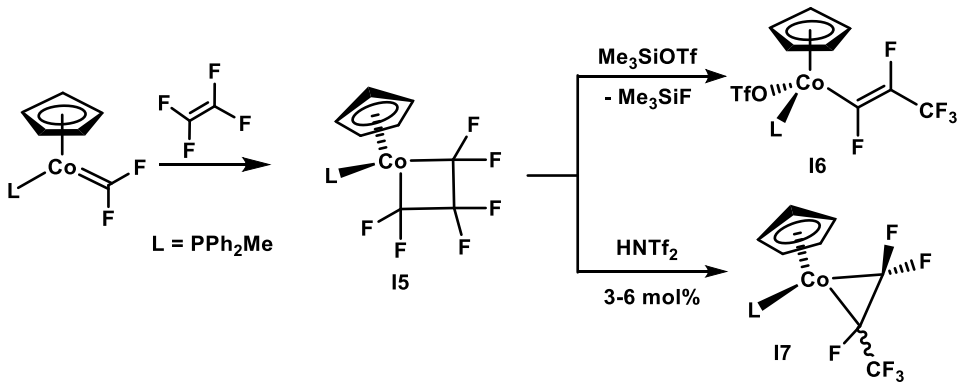

Scheme 1.12 Synthesis of C_β phosphine-functionalized metallacyle.

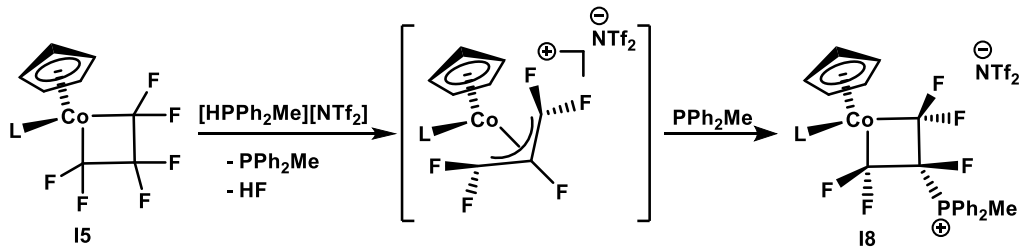

In 2015, Vicic and colleagues reported the synthesis of perfluoroplatinacyclobutanes from perfluoroalkyl iodide complex **I9**. Heating **I9** at 90 °C for 36 h in CH_2Cl_2, or for 16 h in pyridine led to the synthesis of metallacyclobutanes **I10** and **I11**, respectively (Scheme 1.13).[60] Interestingly, the cyclooctadiene analogue **I10** undergoes double C_α−F activation when subjected to column chromatography, giving a fluorocarboxylate metallacycle. This is proposed to result from the reaction between the perfluorometallacyclobutane and water/air.

Scheme 1.13 Formation and reactivity of perfluoroplatinacyclobutanes.

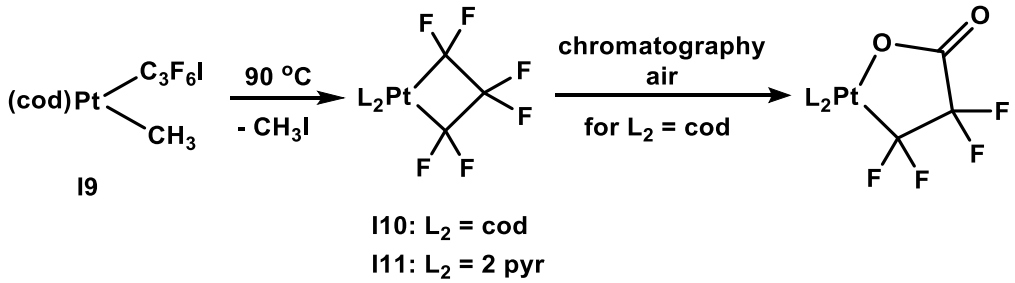

1.5.4 Perfluorometallacyclopentane Complexes

The stability of perfluorometallacyclopentanes was highlighted with the very first example, $(CO)_4Fe(C_4F_8)$, introduced by Stone in 1961.[30a] The metallacycle was found to be indefinitely stable at room temperature, and in the presence of Br_2 or excess phosphine. Heating at 160°C for 12 days resulted in the formation of perfluorocyclobutene, resulting from the activation of two C−F bonds which were proposed to form iron fluorides as by-product(s). Surprisingly, the reactivity of perfluorometallacyclopentanes remained largely unexplored until Burch *et al.* investigated their reactivity towards Lewis acids in 1988.[61] He found that bis(phosphine) metallacycle $(PEt_3)_2Ni(C_4F_8)$ undergoes a C_α−F activation in the presence of BF_3 followed by phosphine ligand migration to C_α, affording the unusual phosphine-functionalized metallacycle **I12** (Scheme 1.14). Furthermore, addition of a second equivalent of BF_3 results in a subsequent C−F activation at the other C_α position, affording the dicationic product of which was isolated by addition of a bis(phosphine) ligand.

Scheme 1.14 C_α−F abstraction in a bis(phosphine) perfluoronickelacycle.

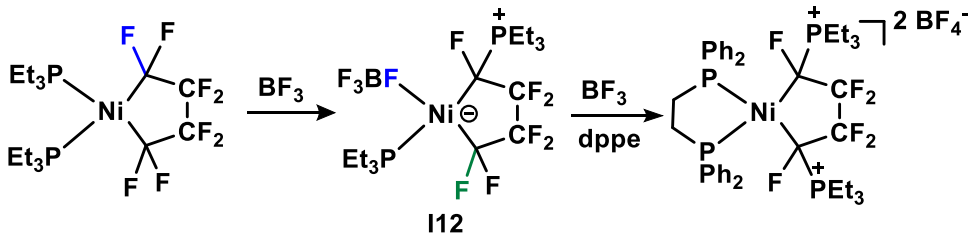

More recently and in parallel with the work of this *Thesis*, Mr. Nicholas Andrella of our group has established alternative reactivity with NHC-coordinated perfluoronickelacycles.[62] Low-coordinate (SIPr)Ni(C_4F_8) [SIPr = 1,3-bis(2,6-diisopropylphenyl)imidazolin-2-ylidene] reacts with one equivalent of Me_3SiOTf to give C_α−F abstraction product **I13**, where the $C_\alpha F_2$ unit migrates to furnish a cyclobutyl ring with the NHC−Ni bond remaining intact (Scheme 1.15). Heating **I13** leads to C_β−F elimination and formation of organic product, perfluorocylobutene; the presumed (SIPr)NiF(OTf) co-product was not fully characterized.

Scheme 1.15 Reactivity of a low-coordinate NHC perfluoronickelacycle.

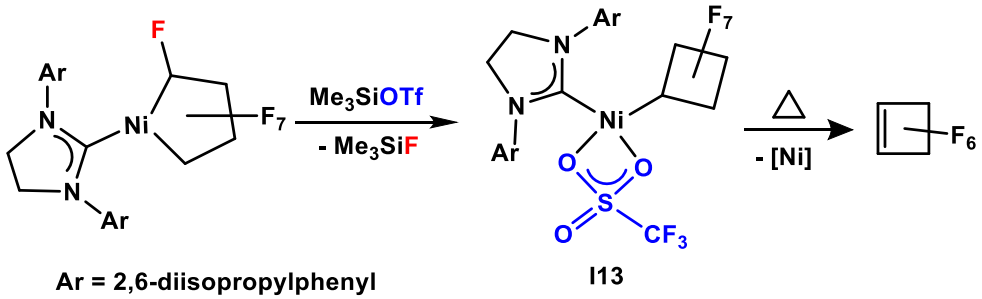

1.6 Formation and Activation of Ni−C_α Bonds in Fluorometallacyclopentanes

As mentioned above, perfluorometallacyclopentanes are classically synthesized by oxidative cyclization of TFE at a low valent metal centre. More recently, Vicic et al. has introduced an alternative method for accessing perfluoronickelacyclopentanes.[63] This method begins with the preparation of a bifunctionalized fluoroalkylzinc reagent from diethyl zinc and 1,4-diiodooctafluorobutane. Upon addition of the dinuclear zinc reagent to [(DME)$NiBr_2$] in the presence of L [where L = CH_3CN or 2,6-dimethylphenyl isocyanide (CNAr)], two new perfluoronickelacyclopentanes are obtained (Scheme 1.16).

Scheme 1.16 Synthesis of perfluoronickelacycles using a transmetallation reaction.

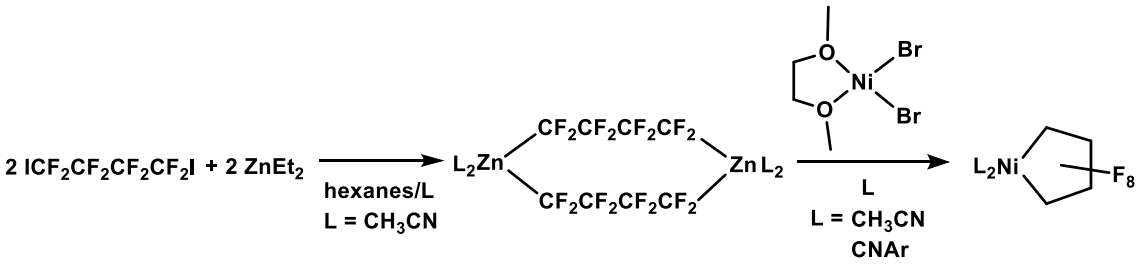

Most examples of Ni−C_α activation in fluorometallacyclopentanes involve mixed metallacycles, derived from the oxidative cyclization of one molecule of TFE with another non-fluorinated alkene or alkyne, in which the non-fluorinated Ni−C_α bond is more prone to insertion reactions. For example, Bennett and colleagues outlined the synthesis of a mixed metallacycle by exposing benzyne nickel(0) complex $(dcpe)_2Ni(\eta^2\text{-}C_6H_4)$ to TFE.[64] Under an atmosphere of CO at 50°C, selective insertion into the nickel aryl bond to give acyl-bound complex **I14** occurs (Scheme 1.17). Increasing the pressure of CO led to the reductive elimination of organic product, **I15**, with concomitant formation of byproduct $(dcpe)_2Ni(CO)_2$.

Scheme 1.17 Reactivity of mixed TFE nickelacyclopentanes.

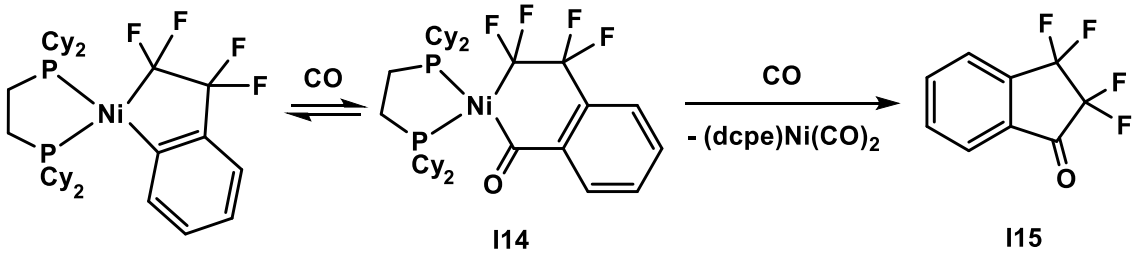

Baker and Ogoshi have also developed catalytic processes that rely on key nickelacyclopentane intermediates derived from one molecule of TFE and one of ethylene, which will be detailed further in *Chapter 4*.[65]

While working at Du Pont, Baker *et al.* developed a catalytic method for the hydrodimerization of TFE, with perfluoronickelacyclopentane and NiL_4 intermediates (Scheme 1.18).[63a] The reaction required elevated temperatures and pressures for the hydrogenolysis of the robust Ni−R^F bonds.

Scheme 1.18 Synthesis of octafluorobutane by hydrodimerization of TFE using low valent Ni.

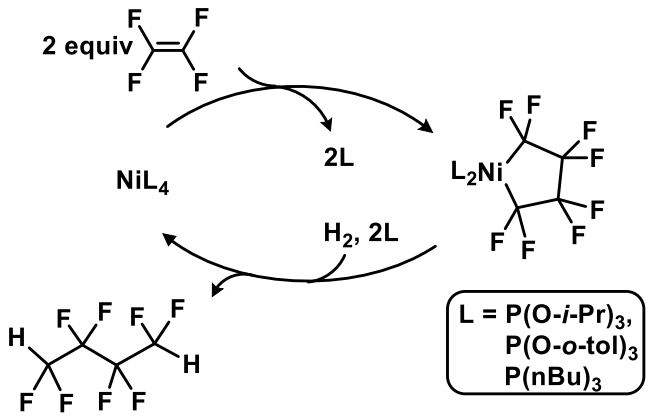

1.7 ^{19}F NMR as a Characterization Tool in Fluoroorganometallic Chemistry

^{19}F NMR spectroscopy has proven to be an invaluable tool in the characterization of fluoroorganometallic complexes. The ^{19}F nucleus is 100% naturally abundant and has a nuclear spin quantum number of ½, allowing for acquisition of useful information about coupling to proximate fluorine, hydrogen, carbon and phosphorus atoms.[66] Another resemblance of ^{19}F to ^{1}H NMR is that the intensity of an individual signal provides an accurate number of fluorines responsible for that given signal. Other advantages of the ^{19}F nucleus are its high magnetogyric ratio (ca. 0.94 times that of ^{1}H) and its expansive chemical shift range. With the complexes synthesized in our group alone, the fluorine chemical shifts span around 1 000 ppm (+ 150 to – 780 ppm)! This huge range is also very informative in terms of determining the chemical environment of the observed fluorine. For example, fluorines in the C_α position of a transition metal fluoroalkyl are known to be shifted significantly downfield relative to a normal aliphatic fluorocarbon.[67] Furthermore, the presence of ^{31}P nuclei can be highly beneficial for characterization purposes. The ^{31}P nucleus is also 100% naturally abundant, has a nuclear spin quantum number of ½, and couples strongly and distinctly to adjacent fluorines.

1.8 Bifunctional Ligands: Uses and Advantages

Classical homogeneous catalysis typically employs ancillary ligands such as phosphines/phosphites that act as two electron donors to stabilize the transition metal centre and remain unchanged throughout the course of the reaction. With a greater understanding of metalloenzymes and how they function in nature to perform essential catalytic reactions, it has become clear that these systems rely heavily on cooperative effects between the metal and its ligand environment. In many cases, the ligand environment is considered to be involved directly in bond activation processes. For example, the enzyme [FeFe]-hydrogenase catalyzes either H_2 production or uptake at its active site (Scheme 1.19).[68] A combination of experimental and theoretical studies has shown that a pendant amine group in this enzyme is key for heterolytic H_2 cleavage.[69]

Scheme 1.19 H_2 activation at [FeFe]-hydrogenase.

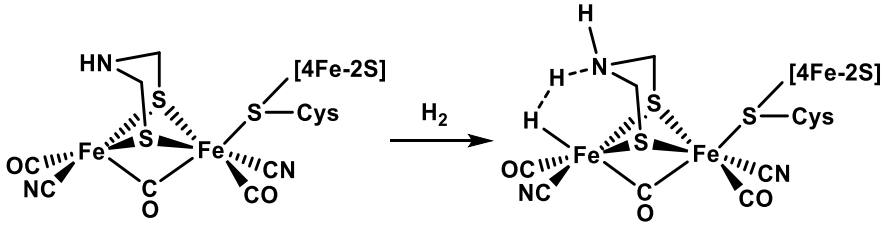

This type of bifunctional reactivity is also highlighted by H_2 oxidation to H^+ in the heterobimetallic [NiFe]-hydrogenase enzyme, where it is proposed that the Ni-coordinated thiolate group participates directly in H_2 splitting (Scheme 1.20).[70]

Scheme 1.20 H_2 activation at [NiFe]-hydrogenase.

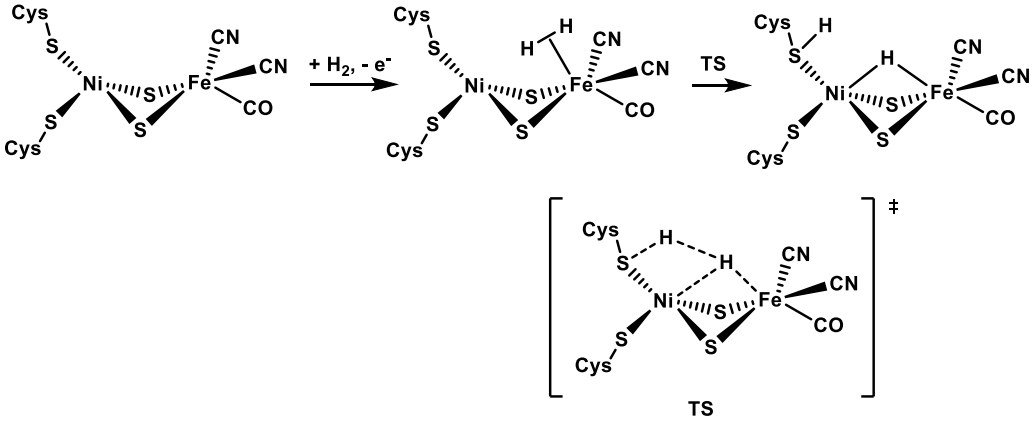

1.8.1 Metal−NH/N Bond

The most studied bifunctional systems in homogeneous catalysis to date are based on metal-coordinated amine and amido ligands.[67c] The first example of heterolytic H_2 cleavage by a metal amido group was established with Fryzuk's disilylamido complexes.[71] The remarkable activity of Noyori's catalyst (based on a Ru ethylenediamine platform) in the asymmetric hydrogenation of ketones to alcohols demonstrates the significance of the "NH effect", which attributes the high catalyst performance to metal-ligand cooperativity.[72] Importantly, this "NH effect" was supported by a loss of catalyst performance when tetramethylethylenediamine was employed as the ligand.[69a]

Although it has been traditionally accepted that the amine ligand participates directly in the ketone hydrogenation (**TS_1**; involving simultaneous transfer of a hydride from Ru and a proton from NH_2 and **TS_2**; heterolytic H_2 cleavage, Scheme 1.21)[73], this mechanism and the exact role of the NH group in metal-ligand cooperativity has recently been debated by Gordon and colleagues.[74] A plethora of transition metal complexes designed to incorporate this "NH effect" have opened the door for the application of homogeneous catalysis to a wider range of more challenging chemical transformations, operating with higher activities and comparatively milder conditions than previous systems. Similar motifs based on **[P,N]** ligand scaffolds have been designed and reported independently by Fagnou[75], Schneider[76], and Baker[77] for the dehydrogenation of ammoniaborane, a targeted substrate for chemical hydrogen storage.

Scheme 1.21 Catalytic cycle for the hydrogenation of ketones under basic conditions.

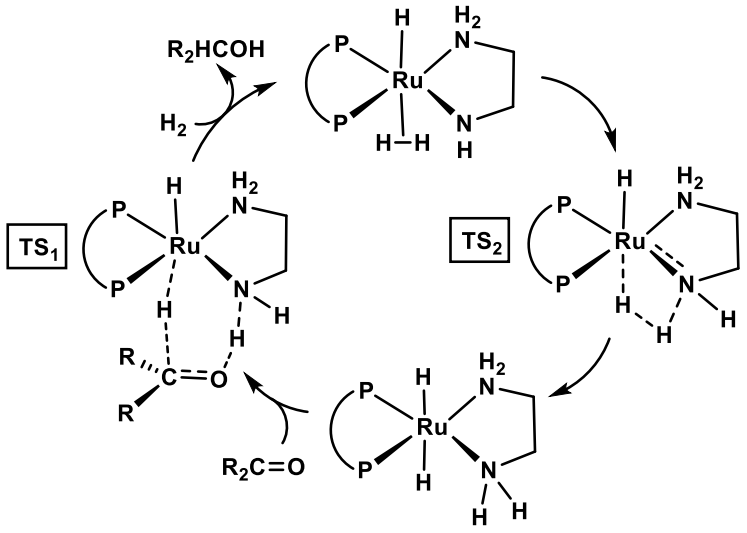

1.8.2 Metal−S Bond

There have been a handful of reports highlighting the metal-ligand cooperativity of thiolato-coordinated metal complexes. One example communicated by Stradiotto *et al.* detailed the reversible activation of Si−H bonds by a **[P,S]**-coordinated cationic Ir complex (Scheme 1.22).[78] This system was shown to achieve stoichiometric ketone hydrosilylation but was not effective as a hydrosilylation catalyst.

Scheme 1.22 Si−H activation by a thiolate-coordinated Ir complex.

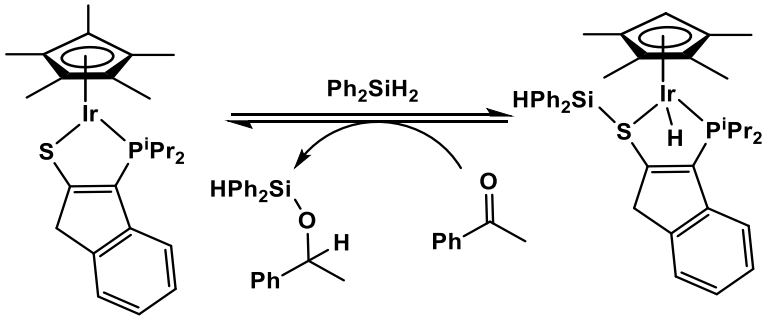

In 2011, Oestreich and co-workers reported a Ru thiolate complex that catalyzes both the electrophilic borylation and the C−H silylation of indoles.[79] Furthermore, they provided evidence

Scheme 1.23 B−H activation by a Ru thiolate complex.

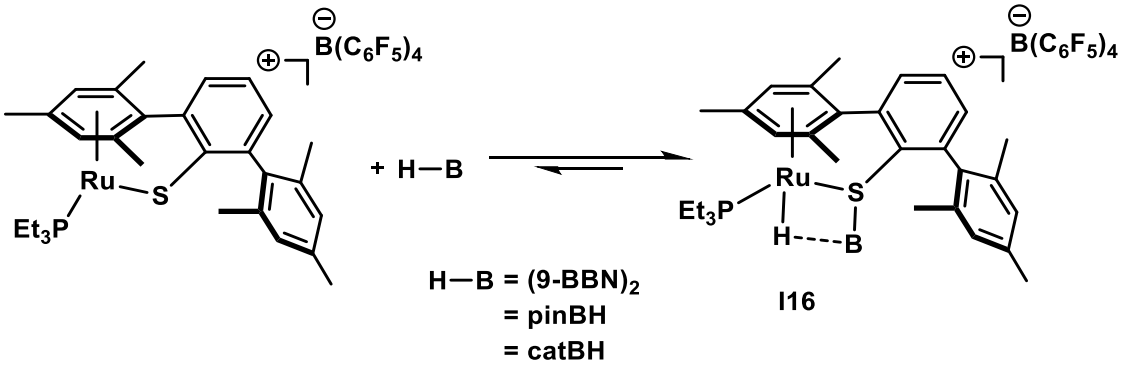

for the metal-ligand cooperative activation of the B−H bond by characterizing complex **I16** by NMR and X-ray crystallography (Scheme 1.23). They have also demonstrated that the same ruthenium complex effectively catalyzes hydrodefluorination of $C(sp^3)$−F bonds, a reaction of particular interest in the context of this *Thesis* (Scheme 1.24).[80] Interestingly, they propose that catalytically generated silicon cations are responsible for the C−F abstraction reaction.

Scheme 1.24 Ru−S catalyzed hydrodefluorination with silanes.

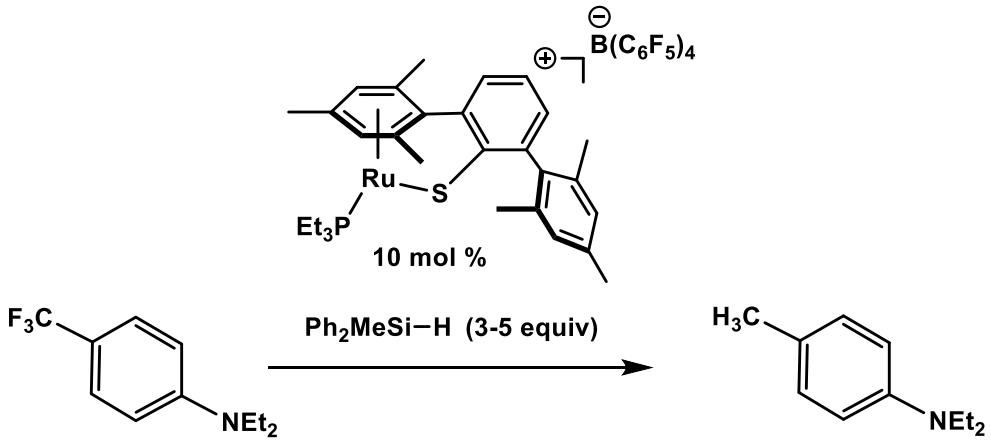

Although we have outlined examples above of metal thiolate complexes capable of activating H_2 and H−X bonds, the magnitude of metal-ligand cooperation at play in catalytic reactions still needs to be elucidated through more thorough mechanistic studies.

1.9 Scope of Thesis Work

The work highlighted in this *Thesis* aims to develop methods for the selective functionalization of FCs at a transition metal centre to obtain novel small-molecule functionalized FCs that are of potential interest for application as refrigerants and fluorosurfactants, among others. The following Chapters will examine the effect that bifunctional ligands have on the reactivity of perfluoronickelacyclopentanes, synthesized by the oxidative cyclization of TFE at Ni(0) centres. The TFE used in these studies is generated by pyrolysis of waste polytetrafluoroethylene (PTFE). Specifically, Chapter 2 will detail the synthesis of a phosphinothioether-coordinated perfluorometallacycle and its ensuing reactivity towards Lewis acids, with examples of $C_\alpha-F$, $C_\beta-F$ and $Ni-C_\alpha$ bond activation. Chapter 3 will highlight the synthesis of phosphinothiolate-coordinated fluoronickelacycles, including the first example of an anionic Ni^{II} metallacycle. Chapter 4 will take a different approach to the synthesis of small-molecule functionalized FCs, examining the effects of replacing TFE with TrFE in metallacycle formation and their subsequent reactivity. Lastly, Chapter 5 will compare and contrast the formation and reactivity of new perfluoronicelacycles featuring **[P,NH]** and **[P,N$^-$]** bidentate ligands {where **[P,NH]** is 2-(diphenylphosphino)phenyl-*N*-phenylaniline} with previously studied systems.

1.10 References

[1] a) Chambers, R.D. *Fluorine in Organic Chemistry, 2nd Ed.*, Blackwell: Oxford, **2004**. b) Kirsch, P. *Modern Fluoroorganic Chemistry: Synthesis, Reactivity, Applications, 1st ed.*, Wiley-VCH: Weinheim, Germany, **2004**.

[2] Wood, L. Global Fluorochemicals Market to Reach $36.4 Billion by 2025 – Driven by Increasing Market for Refrigerants. https://globenewswire.com/news-release/2017/02/06/914184/0/en/Global-Fluorochemicals-Market-to-Reach-36-4-Billion-by-2025-Driven-by-Increasing-Market-for-Refrigerants.html (accessed Apr 4, 2017).

[3] Renner, R. *Environ. Sci. Technol.* **2006**, *40*, 12.

[4] a) Midgley, T.; Henne, A. L. *Ind. Eng. Chem.* **1930**, *22*, 542. b) Wang, Z. Swarts Reaction. In *Comprehensive Organic Name Reactions and Reagents*. **2010**, 2744-2747.

[5] Lemal, D. M. *J. Org. Chem.* **2004**, *69*, 1.

[6] Haaf, S.; Henrici, H. Refrigeration Technology. In *Ullmann's Encyclopedia of Industrial Chemistry* **2003**, 411-448.

[7] Norman, C; DeCanio, S.; Fan, L. *Glob. Environ. Chang.* **2008**, *18*, 330.

[8] Vidal, J. Kigali deal on HFCs is big step in fighting climate change. https://www.theguardian.com/environment/2016/oct/15/kigali-deal-hfcs-climate-change (accessed Apr 4, 2017).

[9] Yang, L.; da Rocha, S. R. P. *J. Phys. Chem. B* **2014***, 118*, 10675.

[10] Rao, V. N. M. In *Organofluorine Chemistry. Principles and Commercial Applications, ed.* Banks, R. E.; Smart, B. E.; Tatlow, J. C. New York, **1994**, 145.

[11] Reisch, M. *Chem. Eng. News* **2010**, *88*, 23.

[12] Krauss, N.; Straitman, R. Honeywell and DuPont Announce Joint Venture to Manufacture New Automotive Refrigerant. http://www51.honeywell.com/honeywell/news-events/press-releases-details/10_0520_Honeywell_Du Pont.html (accessed Apr 4, 2017).

[13] Rao, V. N. M.; Sievert, A. C.; Nappa, M. J. WO 2008/030440 A2, **2008**, E. I. Du Pont de Nemours & Co., USA.

[14] Van Der Puy, M. US 8071826 B2, **2011**, Honeywell International Inc.

[15] a) Potts, J. E.; Ashcraft Jr, A. C.; Wise, E. W. US3472826 A, **1969**, Union Carbide Corp. b) Van Der Puy, M. US 5986151 A, 1999, Alliedsignal Inc.

[16] Mukhopadhyay, S.; Nair, H. K.; Tung, H. S.; Van Der Puy, M. US 7345209 B2, **2008**, Honeywell International Inc.

[17] Nair, H. K.; Singh, R. R.; Wajek, D.; Poss, A. J. WO 2013/122790 A1, **2013**, Honeywell International Inc.

[18] Robin, M. L.; Creazzo, J. A.; Loh, G. WO 2013/123184 A1, **2013**, E. I. Du Pont De Nemours and Company.

[19] Swearingen, E. N. US 8618339 B2, **2008**, E. I. Du Pont De Nemours and Company.

[20] Lui, N.; Marhold, A.; Bielefeldt, D. US 5463150 A, **1995**, Bayer Aktiengesellschaft.

[21] Boulanger, B.; Vargo, J. D.; Schnoor, J. L.; Hornbuckle, K. C. *Environ. Sci. Technol.* **2005**, *39*, 5524.

[22] a) Ritter, S. K. *Chem. Eng. News*, **2015**, *93(28)*, 27. b) Renner, R. *Environ. Sci. Technol.* **2006**, *40*, 12.

[23] PFOA Stewardship Program Baseline Year Summary Report. https://www.epa.gov/assessing-and-managing-chemicals-under-tsca/pfoa-stewardship-program-baseline-year-summary-report (accessed Apr 4, 2017).

[24] E.A. Kauck and J.H. Simons, G.B. Pat. 666 733 (1952); Chem. Abstr., 1952, 46, 6015c.

[25] a) Brice, T. J.; Trott, P. W. US 2732398, **1956**, Minnesota Mining and Manufacturing Company. b) Ahlbrecht, A. H.; Brown, H. A. US 2803656, **1957**, Minnesota Mining and Manufacturing Company.

[26] a) Parsons, R. E. US 3132185, **1964**, E. I. Du Pont De Nemours and Company. b) Blanchard, W. A.; Rhode, J. C. US 3226449, **1965**, E. I. Du Pont De Nemours and Company. c) Parsons, R. E. US 3234294, **1966**, E. I. Du Pont De Nemours and Company. d) Hamada, M.; Ohmura, J.; Muranaka, F. US 4425199, **1984**, Asahi Kasei Kogyo Kabushi Kaisha.

[27] Sherman, P. O.; Smith, S.US 3574791, **1971**, Minnesota Mining and Manufacturing Company.

[28] Qiu, Z-M.; Clark, J. C.; Fan, W. W.; Jariwala, C. P.; Flynn, R. M. WO 02/072657 A1, **2002**, 3M Innovative Properties Company.

[29] a) Coffield, T. H.; Kozikowski, J.; Closson, R. D. Abstr. I.C.C.C Conference, vol. Special Publication No. 13, The Chemical Society, London, 1959, 126. b) Kaesz, H. D.; King, R. B.; Stone, F. G. A. Z. *Naturforsch* 1960, 15b, 763. c) McClellan, W. R. *J. Am. Chem. Soc.* **1961**, *83*, 1598.

[30] a) Manuel, T.; Stafford, S. L.; Stone, F. G. A. *J. Am. Chem. Soc.* **1961**, *83*, 249. b) King, R. B.; Treichel, P. M.; Stone, F. G. A. *J. Am. Chem. Soc.* **1961**, *83*, 3593. c) King, R. B.; Stafford, S. L.; Treichel, P. M.; Stone, F. G. A. *J. Am. Chem. Soc.* **1961**, *83*, 3604.

[31] Coyle, T. D.; King, R. B.; Pitcher, E.; Stafford, S. L. Treichel, P. M.; Stone, F. G. A. *J. Inorg. Nucl. Chem.* **1961**, *20*, 172.

[32] a) King, R. B.; Treichel, P. M.; Stone, F. G. A. *Proc. Chem. Soc.* **1961**, 69. b) Treichel, P. M.; Pitcher, E.; Stone, F. G. A. *Inorg. Chem.* **1962**, *1*, 511.

[33] a) Browning, J.; Cundy, C. S.; Green, M.; Stone, F. G. A. *J. Chem. Soc. (A)*, **1969,** 20. b) Cundy, C. S.; Green, M.; Stone, F. G. A. *J. Chem. Soc. (A)*, **1970,** 1647.

[34] Ohashi, M.; Shibata, M.; Saijo, H.; Kambara, T.; Ogoshi, S. *Organometallics* **2013**, *32*, 3631.

[35] a) Green, M.; Osborn, R. B. L.; Rest, A. J.; Stone, F. G. A. *J. Chem. Soc. Chem. Commun.* **1966**, 502. b) Green, M.; Osborn, R. B. L.; Rest, A. J.; Stone, F. G. A. *J. Chem. Soc. A* **1968**, 2525.

[36] Green, M.; Laguna, A.; Spencer, J. L.; Stone, F. G. A. *J. Chem. Soc., Dalton Trans.* **1977**, 1010.

[37] a) Ristic-Petrovic, D.; Anderson, D. J.; Torkelson, J. R.; McDonald, R.; Cowie, M. *Organometallics* **2003**, *22*, 4647. b) Anderson, D. J.; McDonald, R.; Cowie, M. *Angew. Chem. Int. Ed.* **2007**, *46*, 3741. c) Slaney, M. E.; Anderson, D. J.; Ferguson, M. J.; McDonald, R.; Cowie, M. *J. Am. Chem. Soc.* **2010**, *132*, 16544. d) Slaney, M. E.; Ferguson, M. J.; McDonald, R.; Cowie, M. *Organometallics* **2012**, *31*, 1384.

[38] a) Green, M.; Osborn, R. B. L.; Rest, A. J.; Stone, F. G. A. *J. Chem. Soc. Chem. Commun.* **1966**, 502. b) Green, M.; Osborn, R. B. L.; Rest, A. J.; Stone, F. G. A. *J. Chem. Soc. A* **1968**, 2525.

[39] Maples, P. K.; Green, M.; Stone, F. G. A. *J. C. S. Dalton*, **1973**, 388.

[40] Stone, F. G. A. *J. Fluorine Chem.* **1999**, *100*, 227.

[41] Hughes, R. P. *J. Fluorine Chem.* **2010**, *131*, 1059.

[42] a) Calderazzo, V. F. Angew. Chem. 1977, 89, 305. b) Hughes, R. P. *Adv. Organomet. Chem.* **1990**, *31*, 183.

[43] a) King, R. B.; Bisnette, M. B.; *J. Organomet. Chem.* **1964**, *2*, 15. b) Wilford, J. B.; Stone, F. G. A. *Inorg. Chem.* **1965**, *4*, 389. c) Clark, H. C.; Tsai, J.-H. *J. Organomet. Chem.* **1967**, *2*, 515. d) Cotton, F. A.; Wing. R. M. *J. Organomet. Chem.* **1967**, *9*, 511. e) Graham, W. A. G. *Inorg. Chem.* **1968**, *7*, 315. f) Hall, M. B.; Fenske, R. F. *Inorg. Chem.* **1972**, *11*, 768.

[44] Taw, F. L.; Clark, A. E.; Mueller, A. H.; Janicke, M. T.; Cantat, T.; Scott, B. L.; Hay, P. J.; Hughes, R. P; Kiplinger, J. L. *Organometallics* **2012**, *31*, 1484.

[45] Algarra, A. G.; Grushin, V. V.; Macgregor, S. A. *Organometallics* **2012**, *31*, 1467.

[46] a) Bent, H. A.; *Chem. Rev.* **1961**, *61*, 275. b) Kaupp, M. *Chem. Eur. J.* **1999**, *5*, 3631.

[47] Reger, D. L.; Dukes, M. D. *J. Organomet. Chem.* **1978**, *153*, 67.

[48] Brothers, P. J.; Roper, W. R. *Chem. Rev.* **1988**, *88*, 1293 and references therein.

[49] a) Richmond, T. G.; Shriver, D. F. *Organometallics* **1983**, *2*, 1061. b) Richmond, T. G.; Shriver, D. F. *Organometallics* **1984**, *3*, 305.

[50] Maples, P. K.; Green, M.; Stone, F. G. A. *J. Chem. Soc., Dalton Trans.* **1973**, 2069.

[51] Hacker, M. J.; Littlecott, G. W.; Kemmitt, R. D. W. *J. Organomet. Chem.* **1973**, *47*, 189.

[52] a) Ohashi, M; Kambara, T.; Hatanake, T.; Saijo, H.; Doi, R.; Ogoshi, S. *J. Am. Chem. Soc.* **2011**, *133*, 3256. b) Ohashi, M.; Saijo, H.; Shibata, M.; Ogoshi, S. *Eur. J. Org. Chem.* **2013**, 443.

[53] Xu, W.; Sun, H.; Xiong, Z.; Li, X. *Organometallics* **2013**, *32*, 7122.

[54] Ohashi, M.; Shibata, M.; Ogoshi, S. *Angew. Chem. Int. Ed.* **2014**, *53*, 1.

[55] Harrison, D. J.; Gorelsky, S. I.; Lee, G. M.; Korobkov, I.; Baker, R. T. *Organometallics* **2012**, *32*, 12.

[56] Harrison, D. J.; Lee, G. M.; Leclerc, M. C.; Korobkov, I.; Baker, R. T. *J. Am. Chem. Soc.* **2013**, *135*, 18296.

[57] Kim, C. U.; Lee, J. M.; Ihm, S. K.; *J. Fluorine Chem.* **1999**, *96*, 11.

[58] Harrison, D. J.; Daniels, A. L.; Korobkov, I.; Baker, R. T. *Organometallics* **2015**, *34*, 5683.

[59] Unpublished work.

[60] Xu, L.; Solowey, D. P.; Vicic, D. A. *Organometallics* **2015**, *34*, 3474.

[61] Burch, R. R.; Calabrese, J. C.; Ittel, S. D. *Organometallics* **1988**, *7*, 1642.

[62] Andrella, N. O.; Sicard, A. J.; Gorelsky, S. I.; Korobkov, I.; Baker, R. T. *Chem. Sci.* **2015**, *6*, 6392.

[63] Kaplan, P. T.; Xu, L.; Chen, B.; McGarry, K. R.; Yu, S.; Wang, H.; Vicic, D. A. *Organometallics* **2013**, *32*, 7552.

[64] Bennett, M. A.; Glewis, M.; Hockless, D. C. R.; Wenger, E. *J. Chem. Soc., Dalton Trans.* **1997**, 3105.

[65] a) Baker, R. T.; Beatty, R. P.; Farnham, W. B.; Wallace, R. L. Jr. EP 0783472 A1, **1997**, E. I. Du Pont de Nemours & Co., USA. b) Ogoshi, S.; Kikushima, K.; Taniguchi, T.; Kawashima, T.; Ohashi, M. *Organometallics*, **2015**, *34*, 1604. c) Ogoshi, S.; Kikushima, K.; Shirataki, H.; Ohashi, M. *J. Am. Chem. Soc.*, **2015**, *137*, 6496.

[66] Dolbier, W. R. Jr. In *Guide to Fluorine NMR for Organic Chemists, 2nd Ed.*, John Wiley and Sons Inc. **2016**, 1-8.

[67] Kiplinger, J. L.; Richmond, T. G.; Osterberg, C. E. *Chem. Rev.* **1994**, *94*, 373.

[68] a) Kubas, G. J. *Chem. Rev.* **2007**, *107*, 4152. b) Vignais, P. M.; Billoud, B. *Chem. Rev.* **2007**, *107*, 4206. c) Fontecill-Camps, J. C.; Volbeda, A.; Cavazza, C.; Nicolet, Y. *Chem. Rev.* **2007**, *107*, 4273. d) Gordon, J. C.; Kubas, G. J. *Organometallics* **2010**, *29*, 4682. e) Nicolet, Y.; Piras, C.; Legrand, P.; Hatchikian, C. E.; Fontecilla-Camps, J. C. *Structure* **1999**, *7*, 13.

[69] a) Nicolet, Y.; de Lacey, A. L.; Vernède, X.; Fernandez, V. M.; Hatchikian, E. C.; Fontecilla-Camps, J. C. *J. Am. Chem. Soc.* **2001**, *123*, 1596. b) Fan, H.-J.; Hall, M. B. *J. Am. Chem. Soc.* **2001**, *123*, 3828. c) Barton, B. E.; Olsen, M. T.; Rauchfuss, T. B. *J. Am. Chem. Soc.* **2008**, *130*, 16834. d) Silakov, A.; Wenk, B.; Reijerse, E.; Lubitz, W. *Phys. Chem. Chem. Phys.* **2009**, *11*, 6592.

[70] a) Ogata, H.; Mizoguchi, Y.; Mizuno, N.; Miki, K.; Adachi, S.-i.; Yasuko, N.; Yagi, T.; Yamauchi, O.; Hirota, S.; Higuchi, Y. *J. Am. Chem. Soc.* **2002**, *124*, 11628. b) Lubitz, W.; Ogata, H.; Rüdiger, O.; Reijerse, E. *Chem. Rev.* **2014**, *114*, 4081. c) Khusbutdinova, J. R.; Milstein, D. *Angew. Chem. Int. Ed.* **2015**, *54*, 12236.

[71] a) Fryzuk, M. D.; McNeil, P. A. *Organometallics* **1983**, *2*, 355. b) Fryzuk, M. D.; McNil, P. A. *Organometallics* **1983**, *2*, 682. c) Fryzuk, M. D.; McNeil, P. A.; Rettig, S. J. *Organometallics* **1985**, *4*, 1145. d) Fryzuk, M. D.; McNeil, P. A.; Rettig, S. J. *Organometallics* **1986**, *5*, 2469. e) Fryzuk, M. D.; McNeil, P. A.; Rettig, S. J. *J. Am. Chem. Soc.* **1987**, *109*, 2803.

[72] a) Noyori, R.; Ohkuma, T. *Angew. Chem. Int. Ed.* **2001**, *40*, 40. b) Hems, W. P.; Groarke, M.; Zanotti-Gerosa, A.; Grasa, G. A. *Acc. Chem. Res.* **2007**, *40*, 1340.

[73] a) Abdur_Rashid, K.; Clapham, S. E.; Hadzovic, A.; Harvey, J. N.; Logh, A. J.; Morris, R. H. *J. Am. Chem. Soc.* **2002**, *124*, 15104. b) Sandoval, C. A.; Okhuma, K.; Muñiz, K.; Noyori, R. *J. Am. Chem. Soc.* **2003**, *125*, 13490. c) Clapha, S. E.; Hadzovic, A.; Morris, R. H. *Coord. Chem. Rev.* **2004**, *248*, 2201. d) Muñiz, K. *Angew. Chem. Int. Ed.* **2005**, *44*, 6622. e) Ikariya, T.; Blacker, A. J. *Acc. Chem. Res.* **2007**, *40*, 1300. f) Ito, M.; Ikariya, T. *Chem. Commun.* **2007**, 5134.

[74] a) Dub, P. A.; Henson, N. J.; Martin, R. L.; Gordon, J. C. *J. Am. Chem. Soc.* **2014**, *136*, 3505. b) Dub, P. A.; Gordon, J. C. *Dalton Trans.* **2016**, *45*, 6756.

[75] Blaquiere, N.; Diallo-Garcia, S.; Gorelsky, S. I.; Black, D. A.; Fagnou, K. *J. Am. Chem. Soc.* **2008**, *130*, 14034.

[76] a) Käß, M.; Friedrich, A.; Drees, M.; Schneider, S. *Angew. Chem. Int. Ed.* **2009**, *48*, 905. b) Askevold, B.; Roesky, H. W.; Schneider, S. *ChemCatChem* **2012**, *4*, 307.

[77] Mal, S. S.; Stephens, F. H.; Baker, R. T. *Chem. Commun.* **2011**, *47*, 2922.

[78] Hesp, K. D.; McDonald, R.; Ferguson, M. J.; Stradiotto, M. *J. Am. Chem. Soc.* **2008**, *130*, 16394.

[79] a) Klare, H. F. T.; Oestreich, M.; Ito, J.-i.; Nishiyama, H.; Ohki, Y.; Tatsumi, K. *J. Am. Chem. Soc.* **2011**, *133*, 3312. b) Stahl, T.; Müther, K.; Ohki, Y.; Tatsumi, K.; Oestreich, M. *J. Am. Chem. Soc.* **2013**, *135*, 10978.

[80] Stahl, T.; Klare, H. F. T.; Oestreich, M. *J. Am. Chem. Soc.* **2013**, *135*, 1248.

Chapter 2. Activation of C−F and Ni−C Bonds of [P,S^{iPr}]-Ligated Fluoronickelacycles

2.1 Published Contributions

Activation of C−F and Ni−C Bonds of [P,S]-Ligated Nickel Perfluorometallacycles.
K. A. Giffin, D. J. Harrison, I. Korobkov, R. T. Baker *Organometallics* **2013**, *32*, 7424.

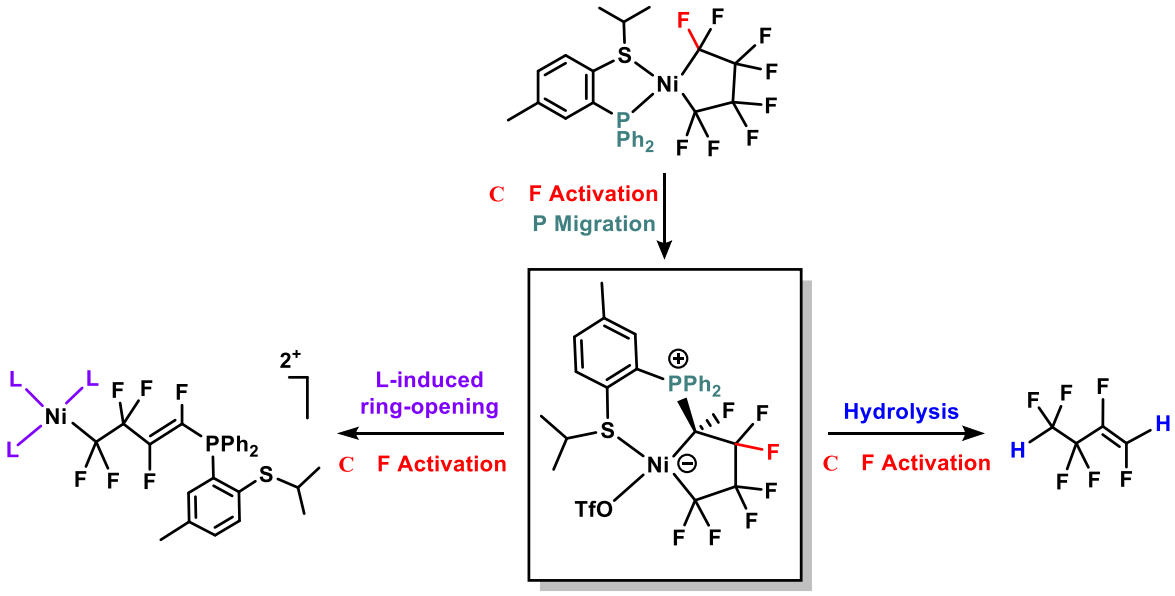

Author Contributions

Giffin, Harrison, and Baker wrote the manuscript. Giffin performed all experiments presented. Korobkov was responsible for X-ray diffraction studies.

Abstract

The first example of a **[P,S^{iPr}]**-ligated metal perfluorocyclopentane is reported. The new metallacycle undergoes C_α−F activation in the presence of a Lewis acid, followed by chemoselective ligand migration, affording a fused metallabicyclic product. Reactivity of this product includes an unprecedented nucleophile-induced ring-opening reaction, involving loss of a β-fluoride.

Additionally, hydrolysis of the metallabicyclic product affords a single isomer of hexafluoro-1-butene.

2.2 Introduction

The importance of fluorocarbons and their derivatives can be seen through their wide range of uses: small-molecule fluorocarbon derivatives are employed, for example, as refrigerants, solvents, surfactants, and pharmaceutical compounds.[1] Despite the attractive features of fluorocarbons and their derivatives (*e.g.,* thermal and chemical/biochemical stability), their syntheses are typically energetically intensive and environmentally problematic.[2] High temperatures or large electrochemical potentials are needed, along with toxic reagents. For example, the Swarts process for synthesizing highly fluorinated organic compounds requires antimony-based catalysts with chlorocarbon and hydrofluoric acid feedstocks (Scheme 1.1).[3] These harsh conditions are also incompatible with most functional groups. Our goal is to develop more sustainable routes to *functionalized* small-molecule fluorocarbons *via* base-metal catalysis, using fluoroalkenes obtained from waste fluoropolymers (*e.g.,* PTFE) as feedstocks.[4] We are currently studying the stoichiometric reactions of new nickel polyfluorocyclopentane complexes, with emphasis on challenging C−F and M−R^F (R^F = fluoroalkyl) activation processes, to assess their viability for future catalytic applications.

In the 1960s, Stone and co-workers synthesized the first nickel perfluorometallacycles by reacting TFE with tetrakis(phosphine) or -(phosphite) nickel(0) complexes (Scheme 1.5). Various metal systems were studied, including nickel, platinum, cobalt and iron. It was concluded that the choice of metal and ancillary ligands dictated whether three- or five-membered metallacycles were formed.[5] Since these complexes surfaced nearly five decades ago, very few studies have focused on their reactivity and most reports have been limited to substitution of the ancillary ligands.[6] Reactions of the typically inert perfluorometallacyclic fragment are even rarer.[7] In 1988, Burch and co-workers demonstrated the activation of a C_α−F bond in $(PEt_3)_2Ni(CF_2)_4$ using BF_3; upon fluoride abstraction,

one of the phosphine ligands migrated to the α-carbon, giving the phosphonium ylide $Ni(PEt_3)(BF_4)[CF(PEt_3)(CF_2)_3]$, and a transient fluorocarbene was proposed as an intermediate (Scheme 1.14).[8] Baker *et al.* later developed a *catalytic* method for the hydrodimerization of TFE, with perfluoronickelacyclopentane and NiL_4 intermediates (Scheme 1.18).[9] The reaction required elevated temperatures/pressures and hydrogenolysis of the typically robust Ni−R^F bonds was only observed when π-acidic phosphite ligands were employed.[9,10] Catalysis with transition metal perfluoroalkyl intermediates is inherently challenging due to the general stability of M−R^F bonds,[11,18a] but a number of new metal-based methods for introducing R^F (predominantly CF_3) groups to organic molecules have appeared recently.[12]

2.3 Results and Discussion

One approach to metal-catalyzed fluorocarbon synthesis involves metallacycle modification through C−F bond functionalization prior to hydrogenolysis. As a result, we have initiated extensive studies of fluoride abstraction as a function of metal and ancillary ligands. Herein we report the first nickel perfluorometallacycle complex with a bidentate **[P,S^{iPr}]** ligand. Most[6b] of the previously reported complexes with the perfluoronickelacyclopentane substructure have two identical monodentate auxillary ligands or a symmetrical bidentate ligand (e.g., 2,2'-bipyridine or 1,2-bis(diphenylphosphino)-ethane; ideal C_{2v} symmetry for the complexes). The reactivity of the **[P,S^{iPr}]**-ligated metallacycle has been examined and below we describe several reactions, including the activation of $C_α$−F and M−C bonds, as well as an unusual ring-opening reaction that appears to proceed through β-fluoride elimination.

The bis(phosphite) nickel perfluorometallacycle **Ni-1** was synthesized according to reported methods.[3,9] Treatment of **Ni-1** with the thiol form of the ligand, 1,2,4-(HS),(Ph_2P),Me(C_6H_3) [variation of the known ligand, 1,2-(HS),(Ph_2P)(C_6H_4)][13] led to unexpected migration of an isopropyl group of the phosphite ligand to the sulfur atom of the bidentate ligand, cleanly yielding complex **Ni-2** (86% isolated yield). The di-isopropyl phosphonate side-product was observed by $^{31}P\{^1H\}$ NMR

at 1.1 ppm with an equimolar amount of free phosphite appearing at 135.8 ppm. The mechanism for the formation of **Ni-2** is speculative at this point, but likely involves a transient nickel-coordinated thiol, which is deprotonated by the phosphite; the resulting phosphorus acid then transfers an alkyl group to the nickel-bound thiolate (Scheme 2.1).[14] This proposed mechanism is similar to the organic Michaelis-Arbuzov reaction which involves formation of a phosphonate from a trialkylphosphite and an alkyl halide; the potently electrophilic P-alkylated phosphite transfers another alkyl group to the halide.[15]

Scheme 2.1 Proposed mechanism for the formation of [P,S^{iPr}]-ligated metallacycle.

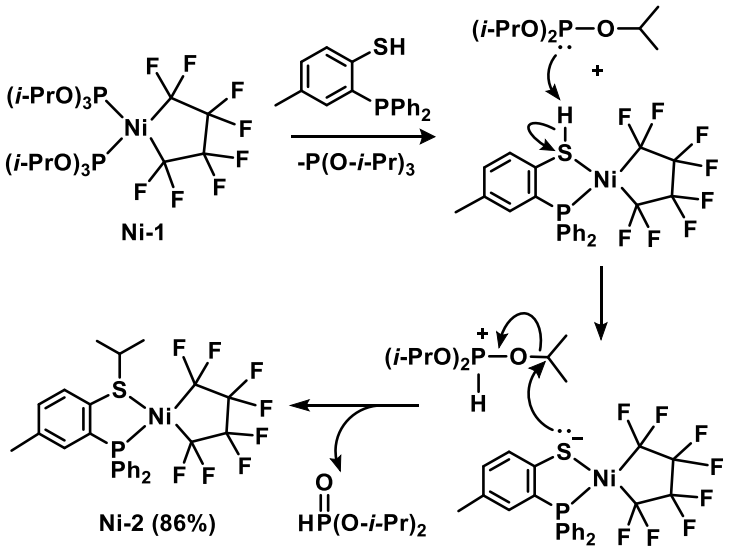

The ^{19}F NMR data for **Ni-2** are consistent with the loss of symmetry (apparent C_s), relative to **Ni-1** (C_{2v}) and show four unique fluorine environments. Considering that the nickel-coordinated sulfur atom is chiral, and pyramidal inversion is unlikely (based on previous reports of sulfonium salts and metal-coordinated thioethers),[16] we propose that the thioether group rapidly coordinates/decoordinates from the metal, resulting in the apparent equivalence of the two faces of the perfluorometallacycle. The ^{31}P{^{1}H} signal for **Ni-2** (44.0 ppm) is an apparent quintet due to coupling with the fluorines on the C_α atoms. Complex **Ni-2** was characterized by single-crystal X-ray diffraction (Figure 2.1).[17] Crystals were grown by slow evaporation of a diethyl ether solution. Bond angles are consistent with a distorted-square-planar Ni(II) centre. As expected,[11] the C_α–F

bonds are significantly elongated in comparison to C_β−F bonds (*e.g.*, 1.3897(17) Å and 1.3507(18) Å respectively). The Ni(1)-C(26) bond in **Ni-2** is appreciably longer than the Ni(1)-C(23) bond *trans* to the sulfur donor (1.9470(13) Å and 1.9204(14) Å respectively), reflecting the larger *trans* influence of the phosphine in comparison to the thioether.

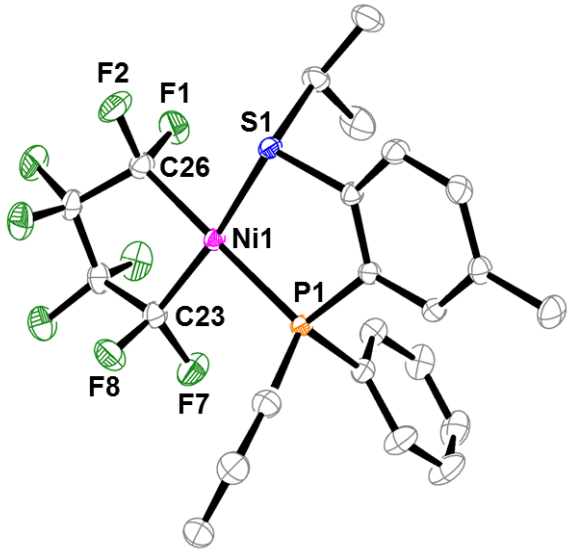

Figure 2.1 ORTEP representation of the molecular structure of complex **Ni-2**. Thermal ellipsoids set at 40% probability and hydrogen atoms are omitted. Selected bond lengths [Å] and angles [°]. Ni1-C23 1.9204(14), Ni1-C26 1.9470(13), Ni1-S1 2.2147(3), Ni1-P1 2.2194(3), C26-F1 1.3852(17), C26-F2 1.3897(17), C23-F7 1.3743, C23-F8 1.3823(18), C23-Ni1-C26 85.82(6), C26-Ni1-S1 91.12(4), C23-Ni1-P1 93.57(4), S1-Ni1-P1 89.860(13).

When the **[P,S^{iPr}]** perfluorometallacycle **Ni-2** was treated with Lewis acid Me_3SiOTf (Tf = SO_3CF_3), a fluoride was abstracted from the metallacycle, presumably from one of the metal-activated C_α positions,[18] yielding the fused metallabicyclic complex **Ni-3** in 95% isolated yield (48 h, 60°C in toluene) (Scheme 2.2, top). At this stage, it is not clear which of the α-fluoride atoms is activated: the C_α−F bond lengths in the solid state structure of **Ni-2** are very similar for the carbon atoms *trans* to P and S and thus offer no insight into the likely site of fluoride abstraction. When BF_3-etherate was employed as the Lewis acid, the BF_4-ligated analogue of **Ni-3** was not formed and only minor, unidentified products were observed (C_6D_6, 60°C, <10% conversion of starting material after 48 h). Complex **Ni-3** is air-stable and did not decompose upon heating (80°C) in CD_3CN for 24 h.

The reactivity described above is reminiscent of Burch's observation of monodentate phosphine (PEt_3) migration upon fluoride abstraction (see above).[8] Interestingly, Burch noted that fluoride abstraction/phosphine migration was *not* observed when excess BF_3 was combined with perfluoronickelacyclopentane bearing a bidentate **[P,P]** ligand {Ni[κ^2-(*i*-Pr)$_2$PCH$_2$CH$_2$P(*i*-Pr)$_2$)](CF$_2$)$_4$}, even upon heating.[8] The failure of the **[P,P]** complex to undergo fluoride abstraction derives presumably from the increased Lewis basicity and/or size of the phosphine groups, relative to the P and S donors in **Ni-2**. However, BF_3 also failed to abstract fluoride from complex **Ni-2** (see above) and it is possible the **[P,P]** metallacycle could be activated using Me_3SiOTf. Burch proposed the fluoride-activation reaction proceeds through a short-lived nickel fluorocarbene.[8] In keeping with this proposal, we speculate that the reaction proceeds through one of two possible intermediates: a fluorocarbene (Scheme 2.2, bottom left), or a carbocation intermediate[19] (Scheme 2.2, bottom right). The highly electrophilic[18a,20] intermediate is attacked, chemoselectively, by the more nucleophilic phosphine group of the **[P,S^{iPr}]** ligand to give **Ni-3**.

The ^{19}F NMR spectrum of **Ni-3** shows eight unique fluorine environments (including the CF_3 from the triflate group), consistent with loss of apparent mirror-plane symmetry (C_s to C_1) and the formation of a new chiral carbon centre upon phosphine migration. Again, the sulfur atom is chiral, but the ^{1}H NMR data show only two methyl environments for the S-bound isopropyl group, indicating either the formation of only one diastereomer or rapid racemization at sulfur (see above).[16] Geminal F-F ($^2J_{FF}$) coupling constants range between 250 and 275 Hz and the fluorine geminal to P is shifted significantly upfield to -198.4 ppm ($^2J_{FP}$ = 69 Hz). All seven of the metallacyclic fluorine environments were assigned by ^{19}F NOESY NMR experiments (see Appendix for 2D spectrum).

Single crystals of **Ni-3** were obtained by slowly cooling a benzene solution. Distorted-square-planar geometry is again observed at the Ni centre. For the Ni−C−P fragment, the Ni−C bond is approximately the same length or shorter than the three Ni−CF$_2$R^F bonds in structures **Ni-2** and **Ni-3** (Figure 2.2). Presumably, the weak *trans* influence of the OTf ligand contributes to the short metal−carbon bond, although the effects of replacing a fluoride with a phosphine substituent are

unclear at present.

Scheme 2.2 C_α−F activation of Ni-2 with Lewis acid.

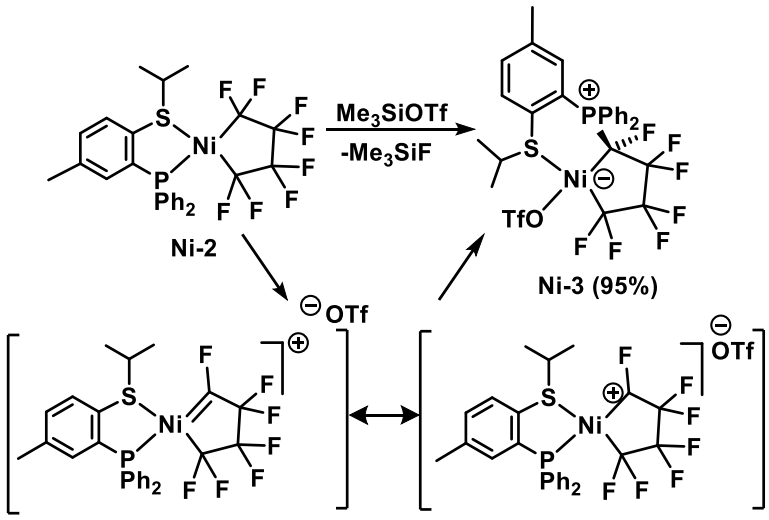

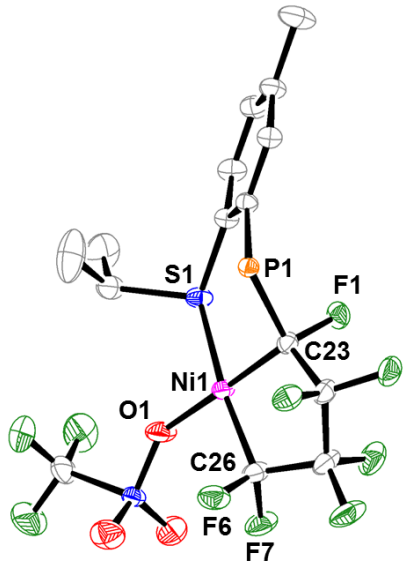

Figure 2.2 ORTEP representation of the molecular structure of complex **Ni-3**. Thermal ellipsoids set at 40% probability and hydrogen atoms are omitted. Two phenyl groups are omitted from P1 for clarity. One of two orientations of the disordered OTf group is depicted. Selected bond lengths [Å] and angles [°]. Ni1-C23 1.9160(15), Ni1-C26 1.9149(15), Ni1-S1 1.2777(4), P1-C23 1.8494(14), O1-Ni1-S1 84.49(14), C23-Ni1-S1 93.58(4), O1-Ni1-C26 95.07(15), C23-Ni1-C26 86.73(6).

We began to explore the reactivity of complex **Ni-3**, initially focusing on ligand substitution reactions with a variety of nucleophiles. Dissolving **Ni-3** in acetonitrile leads to displacement of the triflate ion with acetonitrile to yield **Ni-3·CH$_3$CN** (Scheme 2.3, left). Substitution of the triflate group

was also observed when **Ni-3** was treated with 1 equiv of 2,6-dimethylphenyl isocyanide (CNAr) or sodium thiophenolate, to afford **Ni-4** and **Ni-5**, respectively (Scheme 2.3). Thus, the triflate ion of **Ni-3** can be displaced from nickel by a variety of nucleophiles, while the thioether group remains coordinated in the products.

Scheme 2.3 Ligand substitution reactions of Ni-3.

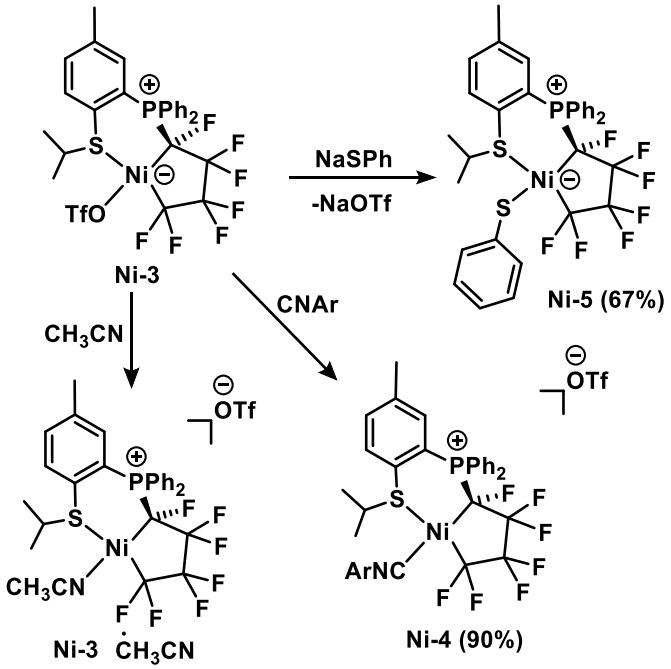

When **Ni-3** is treated with > 1 equiv of CNAr, a surprising ligand–induced ring-opening reaction occurs, in which Ni−S, Ni−C, and C_β−F bonds are cleaved and P−F/C−C bonds are formed. Treatment of **Ni-3** with 3 equiv of CNAr yields complex **Ni-6** (room temperature, 1 h, C_6D_6) (Scheme 2.4, top right), which was observed using multinuclear NMR.[21,22] Evidence for the P−F group is provided by ^{19}F and ^{31}P NMR: the large coupling constant of 660 Hz is strongly indicative of one-bond P-F coupling and the downfield ^{19}F shift of +16.5 ppm also supports a fluorine−phosphorus bond. The $^{31}P\{^1H\}$ NMR resonance for **Ni-6** is found significantly upfield at -73.8 ppm, suggestive of a five-coordinate phosphorus atom.[23] For the alkenyl fluorine atoms, $^3J_{FF}$ = 135 Hz, pointing to exclusive formation of the F,F-*trans* (*E*) double bond isomer. Attempts to isolate **Ni-6** led to decomposition; we obtained the more stable compound **Ni-7** (91% isolated yield) by fluoride

abstraction from the phosphorus centre of **Ni-6**, using Me_3SiOTf (Scheme 2.4). Complex **Ni-7** was characterized by ^{1}H, ^{19}F and $^{31}P\{^{1}H\}$ NMR, UV-vis, and ESI-MS.

Upon hydrolysis, **Ni-3** releases exclusively the F,F-*trans* (*E*) double bond isomer fluoroalkene **O1**, shown in Scheme 2.4 (bottom) and uncharacterized co-products.[24] This is the first example of a transition metal-mediated process for the selective formation of (*E)*-1,2,3,3,4,4-hexafluoro-1-butene.[25] An experiment with D_2O confirms that the hydrogens of the product originate from water. We suspect the obtained NMR yield of the hydrofluoroalkene (27% based on 3 trials) is artificially low due to liquid-gas phase partitioning and/or supersaturation of the benzene solvent. The crude ^{19}F NMR spectrum for the hydrolysis reaction showed only minor impurities and (*E*)-1,2,3,3,4,4-hexafluoro-1-butene as the only major product.

Scheme 2.4 Ligand-induced ring-opening reaction of Ni-3.

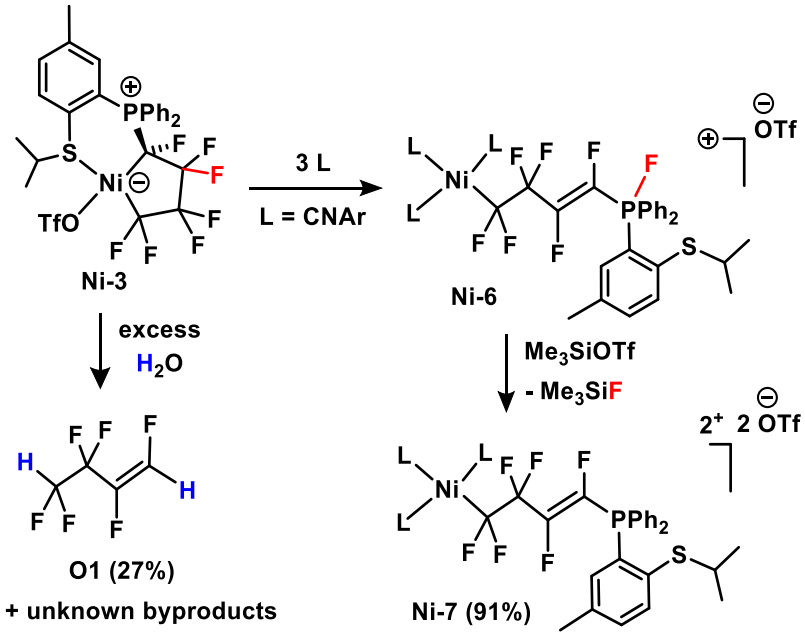

Treating complex **Ni-7** with water *does not* generate (*E*)-1,2,3,3,4,4-hexafluoro-1-butene. ^{19}F and $^{31}P\{^{1}H\}$ NMR data indicate that an intact P−C(F) bond is present among the unknown hydrolysis products, on the basis of geminal coupling between the phosphorus and one fluorine atom.

2.4 Conclusions

In summary, the synthesis of a new nickel perfluorometallacycle (**Ni-2**), with a hemilabile phosphine/thioether ligand, has been described. Fluoride abstraction from this complex yielded a phosphine migration product (**Ni-3**), featuring weakly bound thioether and triflate groups on the nickel atom. Ligand substitution studies revealed that the triflate ligand may be displaced from the metal, producing neutral or cationic complexes by employing different nucleophiles. The reaction of **Ni-3** with CNAr (≥ 3 equiv) produced an unexpected ring-opened product *via* Ni−C and C−F activation pathways. Finally, hydrolysis of **Ni-3** afforded a single isomer of hexafluoro-1-butene (**O1**), thus demonstrating the potential of metallacycle modification for selective production of unsaturated hydrofluorocarbons. The stoichiometric systems reported here will be studied more extensively with the goal of designing *catalytic* systems for the synthesis of functionalized fluorocarbons.

2.5 Experimental Section

2.5.1 General

Experiments were conducted under nitrogen, using Schlenk techniques or an MBraun glove box. All solvents were deoxygenated by purging with nitrogen. Toluene, hexanes, diethyl ether and tetrahydrofuran (THF) were dried on columns of activated alumina using a J. C. Meyer solvent purification system. Benzene-d_6 (C_6D_6) was dried by stirring over activated alumina (ca. 10 wt.%) overnight, followed by filtration. Acetonitrile (CH_3CN), acetonitrile-d_3 (CD_3CN), and dichloromethane (DCM) were dried by refluxing over calcium hydride under nitrogen. After distillation, they were dried further by stirring over activated alumina (ca. 5 wt.%) overnight, followed by filtration. All solvents were stored over activated (heated at ca. 250^{o}C for >10 h under vacuum) 4 Å molecular sieves. Glassware was oven-dried at 150^{o}C for >2 h. The following chemicals were obtained commercially, as indicated: trimethylsilyl trifluoromethanesulfonate (Me_3SiOTf, Aldrich, 99%), bis(1,5-cyclooctadiene)nickel ($Ni(cod)_2$, Strem, 98+%), tri-*iso*-propyl phosphite

($P(O\text{-}i\text{-}Pr)_3$, Aldrich, 95%), 4-methylbenzenethiol (1,4-$(HS)Me(C_6H_4)$, Aldrich, 98%), diphenylchlorophosphine (PPh_2Cl, Strem, min. 95%), 2,6-dimethylphenyl isocyanide (CNAr; Aldrich, 96%), sodium thiophenolate (NaSPh, Aldrich, ≥96.5%). Tetrafluoroethylene was purchased from ABCR (99%) or made by pyrolysis of polytetrafluoroethylene (Scientific Polymer Products, powdered) under vacuum, using a slightly modified literature procedure [10-20 mTorr, 650°C, 30 g scale, product stabilized with R(+)-limonene (Aldrich, 97%), giving TFE of *ca.* 97% purity].[26] Compound $[P(O\text{-}i\text{-}Pr)]_2Ni(C_4F_8)$ was made by oxidative addition of tetrafluoroethylene to $Ni[P(O\text{-}i\text{-}Pr)_3]_4$ using a slightly modified literature procedure.[3,9] $Ni[P(O\text{-}i\text{-}Pr)_3]_4$ complex was prepared from $Ni(cod)_2$ following reported methods.[3] ^1H, ^{19}F, $^{31}P\{^1H\}$ and $^{13}C\{^1H\}$ NMR spectra were recorded on a 300 MHz Bruker Avance instrument at room-temperature (21-23°C). ^1H NMR spectra were referenced to the residual proton peaks associated with the deuterated solvents (C_6D_6: 7.16 ppm; CD_3CN: 1.94 ppm). ^{19}F NMR spectra were referenced to internal 1,3-bis(trifluoromethyl)benzene (BTB) (Aldrich, 99%, deoxygenated by purging with nitrogen, stored over activated 4 Å molecular sieves), set to –63.5 ppm. $^{31}P\{^1H\}$ NMR data were referenced to external H_3PO_4 (85 % aqueous solution), set to 0.0 ppm. Electrospray ionization mass spectral data were collected using an Applied Biosystem API2000 triple quadrupole mass spectrometer. UV-vis spectra were recorded on a Cary 100 instrument, using sealable quartz cuvettes (1.0 cm pathlength). Elemental analyses were performed by Canadian Microanalytical Service Ltd. (Delta, British Columbia, Canada).

2.5.2 X-ray Crystallography

For **Ni-2** and **Ni-3**: samples were mounted on thin glass fibers using paraffin oil and were cooled to 200 K prior to data collection. Data were collected on a Bruker AXS KAPPA single crystal diffractometer equipped with a sealed Mo tube source (wavelength 0.71073 Å) APEX II CCD detector. Raw data collection and processing were performed with APEX II software package from BRUKER AXS.[27] Diffraction data were collected with a sequence of 0.5° ω scans at 0, 90, 180, and 270° in ϕ. Initial unit cell parameters were determined from 60 data frames collected at the different sections of the Ewald sphere. Semi-empirical absorption corrections based on equivalent reflections

were applied. Systematic absences in the diffraction data set and unit-cell parameters were consistent with triclinic systems. Solutions in centrosymmetric space group yielded chemically reasonable and computationally stable results of refinement. The structures were solved by direct methods, completed with difference Fourier synthesis, and refined with full-matrix least-squares procedures based on *F*.[27] In the structure, compound molecules are situated in the general position. All non-hydrogen atoms were refined anisotropically with satisfactory thermal parameters values. Additional crystallographic data and selected data collection parameters are reported below.

2.5.3 Synthesis of [1,2,4-(*i*-Pr-S),(Ph_2P),Me(C_6H_3)]Ni(C_4F_8) (Ni-2)

[(P(O-*i*-Pr)$_3$)$_2$Ni(C_4F_8)] **(Ni-1)** (1.00 g, 1.48 mmol) was placed in a 100 mL round-bottom flask and dissolved in ca. 10 mL of toluene. [1,2,4-(HS),(Ph_2P),Me(C_6H_3)] (480 mg, 1.56 mmol) was added to the stirred **[**(P(O*i*-Pr)$_3$)$_2$Ni(C_4F_8)]/toluene mixture, and stirring was continued at room temperature for ca.12 h. The cloudy yellow-orange reaction mixture was concentrated in vacuo until ca. 2 mL of yellow paste remained. Around 20 mL of hexanes was then added to the round-bottom flask, precipitating a light yellow powder. The flask was placed in a -35°C freezer for 24 h. The product was filtered cold (30 mL medium pore fritted funnel), washed with pre-cooled hexanes (2 x 3 mL), and dried in vacuo, affording a light yellow powder. Yield: 776 mg, 1.27 mmol, 86% based on **Ni-1**. UV-vis (0.7 mM in diethyl ether): $\lambda_{max}(\varepsilon)$ = 332(2082). ^{1}H NMR (300 MHz, C_6D_6) δ 0.96 (d, J ≈ 7 Hz, 6H, 2 *i*-Pr Me), 1.64 (s, 3H, Me), 3.58 (sept, 1H, *i*-Pr H), 6.60 (d m, 1H, Ar-H), 6.98 (ov m, 8H, Ar-H), 7.60 (ov m, 4H, Ar-H). ^{19}F NMR (282 MHz, C_6D_6) δ -96.3 (d m, 2Fα, $^3J_{FP}$ = 32 Hz), -104.7 (d m, 2Fα, $^3J_{FP}$ = 27 Hz), -137.8 (m, 2Fβ), -138.6 (m, 2Fβ). ^{31}P{^{1}H} NMR (121 MHz, C_6D_6) δ 44.0 (tr tr, $^3J_{PF}$ = 27, 32 Hz). Anal. Calc. for $C_{26}H_{23}F_8NiPS$: C, 51.26, H, 3.81. Found: C, 51.48, H, 3.65. See Figures A1-A2 for ^{19}F and ^{31}P{^{1}H} NMR spectra.

2.5.4 Synthesis of [1,2,4-(*i*-Pr-S),(Ph_2P),Me(C_6H_3)]Ni(C_4F_7)(OTf) (Ni-3)

[1,2,4-(*i*-Pr-S),(Ph_2P),Me(C_6H_3)]Ni(C_4F_8) **(Ni-2)** (831 mg, 1.36 mmol) was dissolved in ca. 20 mL of toluene and transferred to a 100 mL Schlenk ampoule. To the **Ni-2**/toluene solution was added Me_3SiOTf (296 μL, 1.64 mmol). The ampoule was sealed and placed in a 60°C oil bath for 48 h. A

dark yellow precipitate was formed over the course of the reaction. The product was filtered through a 30 mL medium pore fritted funnel under nitrogen. The collected dark yellow powder was washed with hexanes (2 x 3 mL), and dried in vacuo. Yield: 958 mg, 1.30 mmol, 95% based on **Ni-2**. ^{1}H NMR (300 MHz, CD_2Cl_2) δ 1.59, 1.74 (d, J = 7 Hz, 3H, *i*-Pr Me), 2.33 (s, 3H, Me), 3.81 (sept, J = 7 Hz, 1H, *i*-Pr H), 7.06 (d, J_{HP} = 14 Hz, 1H, Ar-H), 7.47-8.00 (ov m, 10H, Ar-H), 8.39 (ov d m, 2H, Ar-H). ^{19}F NMR (282 MHz, CD_2Cl_2) δ -78.5 (s, 3F, OTf), -99.2 (d tr, $^{2}J_{FF}$ = 242 Hz, $^{3}J_{FF}$ = 12 Hz, 1Fα), -115.6 (d d, $^{2}J_{FF}$= 242 Hz, $^{3}J_{FF}$ = 17 Hz, 1Fα), -117.8 (d m, $^{2}J_{FF}$ = 272 Hz, 1Fβ), -129.9 (d m, $^{2}J_{FF}$ = 272 Hz, 1Fβ), -132.5 (d d d, $^{2}J_{FF}$ = 245 Hz, ^{3} J_{FF} = 35, 16 Hz, 1Fβ), -137.3 (d m, $^{2}J_{FF}$ = 245 Hz, 1Fβ), -196.2 (d d d, $^{2}J_{FP}$ = 75 Hz, $^{3}J_{FF}$ = 31, 7 Hz, 1Fα). ^{31}P{^{1}H} NMR (121 MHz, CD_2Cl_2) δ 14.8 (d tr, $^{2}J_{PF}$ = 75, $^{3}J_{PF}$ = 14 Hz). Anal. Calc. for $C_{27}H_{23}F_{10}NiO_3PS_2$: C, 43.87, H, 3.14. Found: C, 43.73, H, 2.95. See Figures A3-A4 for ^{19}F and ^{1}H NMR spectra.

2.5.5 {[1,2,4-(*i*-Pr-S),(Ph_2P),Me(C_6H_3)](CD_3CN)Ni(C_4F_7)}$^{+}$(OTf)$^{-}$ (Ni-3·CD_3CN)

[1,2,4-(*i*-Pr-S),(Ph_2P),Me(C_6H_3)]Ni-(C_4F_7)(OTf) **(Ni-3)** (10 mg, 0.0135 mmol) was dissolved in deuterated acetonitrile. UV-vis (0.7 mM in acetonitrile): $\lambda_{max}(\varepsilon)$ = 396(907). ^{1}H NMR (300 MHz, CD_3CN) δ 1.18 (d d, J ≈ 7, 1 Hz, 3H, *i*-Pr Me), 1.38 (d, J ≈ 7 Hz, 3H, *i*-Pr Me), 2.34 (s, 3H, Me), 3.43 (sept, 1H, *i*-Pr H), 7.29 (d d m, 1H, Ar-H), 7.5-8.1 (ov m, 10H, Ar-H), 8.35 (ov d m, 2H, Ar-H). ^{19}F NMR (282 MHz, CD_3CN) δ -79.4 (s, 3F, OTf), -96.8 (d tr m, $^{2}J_{FF}$ = 250 Hz, $^{3}J_{FF}$ = 12 Hz, 1Fα), -109.2 (d d, $^{2}J_{FF}$ = 250 Hz, $^{3}J_{FF}$ = 16 Hz, 1Fα), -118.5 (d m, $^{2}J_{FF}$ = 273 Hz, 1Fβ), -130.0 (d tr m, $^{2}J_{FF}$ = 273 Hz, $^{3}J_{FF}$ = 15 Hz, 1Fβ), -132.4 (d m, $^{2}J_{FF}$ = 248 Hz, 1Fβ), -135.8 (d m, $^{2}J_{FF}$ = 248 Hz, 1Fβ), -198.4 (d d m, $^{2}J_{FP}$ = 69 Hz, $^{3}J_{FF}$ = 30 Hz, 1Fα). ^{31}P{^{1}H} NMR (121 MHz, CD_3CN) δ 15.8 (d tr, $^{2}J_{PF}$ = 69, $^{3}J_{PF}$ = 13 Hz).

2.5.6 Synthesis of {[1,2,4-(*i*-Pr-S),(Ph_2P),Me(C_6H_3)](CNAr)Ni(C_4F_7)}$^{+}$(OTf)$^{-}$ (Ni-4)

[1,2,4-(*i*-Pr-S),(Ph_2P),Me(C_6H_3)] Ni(C_4F_7)(OTf) **(Ni-3)** (50 mg, 0.068 mmol) was dissolved in ca. 8 mL of DCM and transferred to a 50 mL round-bottom flask. To the **Ni-3**/DCM solution was added one equiv of CNAr (9 mg, 0.068 mmol). No significant colour change was observed. The reaction mixture was stirred at room temperature for 12 h. The product was concentrated, dried in vacuo, and

stored at room temperature under nitrogen. Yield: 53 mg, 0.061 mmol, 90% based on **Ni-3**. UV-vis (0.7 mM in DCM): $\lambda_{max}(\varepsilon)$ = 352(1118). ^{1}H NMR (300 MHz, CD_2Cl_2) δ 1.52, 1.55 (d, J = 7 Hz, 3H, *i*-Pr Me), 2.31 (s, 6H, CNAr Me), 2.39 (s, 3H, Me), 3.75 (sept, 1H, *i*-Pr H), 7.06 (d, $^{2}J_{PH}$ = 14 Hz, 1H, Ar-H), 7.2 (d, 2H), 7.34 (m, 1H, Ar-H), 7.51-8.08 (ov m, 12H, Ar-H). ^{19}F NMR (282 MHz, CD_2Cl_2) δ -79.0 (s, 3F, OTf), -87.5 (br d, $^{2}J_{FF}$ = 257 Hz, 1Fα), -94.2 (d tr, $^{2}J_{FF}$ = 257 Hz, J_{FF} = 10 Hz, 1Fα), -116.9 (d m, $^{2}J_{FF}$ = 275 Hz, 1Fβ), -128.8 (d m, $^{2}J_{FF}$ = 275 Hz, 1Fβ), -132.5 (br AB doublets, $^{2}J_{FF} \approx$ 262 Hz, 2Fβ), -199.0 (d d, $^{3}J_{FF}$ = 31 Hz, $^{2}J_{FP}$ = 67 Hz, 1Fα). ^{31}P{^{1}H} NMR (121 MHz,CD_2Cl_2) δ 17.2 (d d d, $^{2}J_{PF}$ = 67, $^{3}J_{PF}$ = 17, 10 Hz). MS-ESI (positive mode), solvent: CH_3OH]: *m/z* calcd for {[1,2,4-(*i*-Pr-S),(Ph_2P),Me(C_6H_3)](CNAr)Ni(C_4F_7)}$^{+}$ (% intensity): 720.1 (100), 722.1 (51), 721.1 (39), 723.1 (20), found: 720.2 (100), 722.3 (51), 721.3 (39), 723.4 (22).

2.5.7 Synthesis of [1,2,4-(*i*-Pr-S),(Ph_2P),Me(C_6H_3)](SPh)Ni(C_4F_7) (Ni-5)

[1,2,4-(*i*-Pr-S),(Ph_2P),Me(C_6H_3)]Ni(C_4F_7)(OTf) **(Ni-3)** (70 mg, 0.095 mmol) was dissolved in ca. 6 mL of acetonitrile and transferred to a 50 mL round-bottom flask. To the above solution was added sodium thiophenolate (13 mg, 0.099 mmol). An immediate colour change from light orange to bright red was observed. The reaction mixture was stirred at room temperature for 12 h. The solution was concentrated in vacuo, and the product was extracted with DCM, precipitating out the sodium triflate salt. The DCM solution was filtered through a Celite Pasteur pipet and concentrated in vacuo in a round-bottom flask. Hexanes was added (ca. 20 mL), precipitating out a light orange solid. The flask was placed in a -35°C freezer for 12 h. The product was filtered cold (15 mL medium pore fritted funnel) and washed with 3 mL hexanes. The light orange powder was dried in vacuo. Yield: 44 mg, 0.063 mmol, 67% based on **Ni-3**. UV-vis (0.7 mM in acetonitrile): $\lambda_{max}(\varepsilon)$ = 310 (5886) (shoulder on off-scale signals in the UV range), 353 (2551) (shoulder/tail), 515(322). ^{1}H NMR (300 MHz, CD_3CN) δ 1.33, 1.38 (d, J ≈ 7 Hz, 3H, *i*-Pr Me), 2.28 (s, 3H, Me), 4.15 (sept, J ≈ 7 Hz, 1H, *i*-Pr H), 6.82 (ov m, 3H, Ar-H), 6.93 (ov m, 2H, Ar-H), 7.17 (d, $J_{HP} \approx$ 14 Hz, 1H, Ar-H), 7.46-7.69 (ov m, 6H, Ar-H), 7.86 (ov m, 3H, Ar-H), 8.00 (m, 1H, Ar-H), 8.32 (ov d, 2H, Ar-H). ^{19}F NMR (282 MHz, CD_3CN) δ -93.0 (d m, $^{2}J_{FF}$ = 269 Hz, 1Fα), -114.6(d d d, $^{2}J_{FF}$ = 269 Hz, $^{3}J_{FF}$ = 20, 5 Hz, 1Fα), -117.3 (d m, $^{2}J_{FF}$

= 270 Hz, 1Fβ), -130.4 (d m, $^2J_{FF}$ = 270 Hz, 1Fβ), -130.9 (d m, $^2J_{FF}$ = 244 Hz, 1Fβ), -135.9 (d m, $^2J_{FF}$ = 244 Hz, 1Fβ), -198.8 (d d, $^2J_{FP}$ = 73 Hz, $^3J_{FF}$ = 36 Hz, 1Fα). $^{31}P\{^1H\}$ NMR (121 MHz, CD_3CN) δ 13.5 (d tr, $^2J_{PF}$ = 73, $^3J_{PF}$ = 15 Hz). MS[ESI(positive mode), solvent: CH_3CN]: *m/z* calcd for {[1,2,4-(*i*-Pr-S),(Ph_2P),Me(C_6H_3)] Ni(C_4F_7)$^+$} (% intensity): 589.0 (100), 591.0 (43), 590.1 (28), found: 589.8 (100), 591.7 (48), 590.8 (43).

2.5.8 Observation of Ni-6

[1,2,4-(*i*-Pr-S),(Ph_2P),Me(C_6H_3)]Ni(C_4F_7)(OTf)) **(Ni-3)** (20 mg, 0.027 mmol) was dissolved in C_6D_6 (ca. 1 mL) in a medium screw cap vial, and CNAr (12 mg, 0.095 mmol) was added. The colour changed immediately from opaque yellow to clear orange. The reaction mixture was stirred at room temperature for 30 min and then transferred to a J Young NMR tube to obtain NMR spectra of compound **Ni-6**. NMR data in benzene-d_6 (broad peaks in fluorine and proton spectra associated with intermediate(s) en route to **Ni-6** are not reported; integrations for proton peaks are not reported due to overlap between product peaks from **Ni-6** and broad intermediate peaks): ^1H NMR (300 MHz, C_6D_6) δ 0.95 (d, J = 7 Hz, *i*-Pr Me), 2.15 (s, Me), 2.22 (s, CNAr Me), 3.11 (sept, *i*-Pr H), 6.62-6.69 (ov m, Ar-H), 6.77-6.83 (m, Ar-H), 7.66-7.78 (ov m, Ar-H). ^{19}F NMR (282 MHz, C_6D_6) δ 14.5 (br d, J_{FP} = 660 Hz, 1F), -55.9 (br s, 2Fα), -78.3 (s, 3F, OTf), -105.0 (d d, $^4J_{FF}$ = 27, $^3J_{FF}$ = 11 Hz, 2Fβ), -128.2 (br d, $^3J_{FF(trans)}$ = 135 Hz, 1F), -151.2 (br d, $^3J_{FF(trans)}$ = 135 Hz, 1F). $^{31}P\{^1H\}$ NMR (121 MHz, C_6D_6) δ -73.3 (br d, J_{PF} = 660 Hz). See Figures A6-A7 for $^{31}P\{^1H\}$ and ^{19}F NMR spectra.

2.5.9 {[1,2,4-(*i*-Pr-S),(Ph_2P),Me(C_6H_3)][(1,2,6-(CN)($Me)_2$(C_6H_3)]$_3$Ni(C_4F_6)}$^{2+}$[2(OTf)]$^-$ (Ni-7)

[1,2,4-(*i*-Pr-S),(Ph_2P),Me(C_6H_3)]Ni(C_4F_7)(OTf) **(Ni-3)** (70 mg, 0.095 mmol) was dissolved in ca. 10 mL of C_6H_6 in a 50 mL round-bottom flask. A 3.5 equiv portion of CNAr (44 mg, 0.333 mmol) was added, and the reaction mixture was left to stir for 20 min at room temperature. To the **Ni-3**/CNAr benzene solution was added Me_3SiOTf (18.9 μL, 0.104 mmol). The reaction mixture was stirred at room temperature for 14 h. The product was concentrated in vacuo and washed with 2 x 3 mL of benzene, affording a yellow-gold solid. Yield: 109 mg, 0.086 mmol, 91% based on **Ni-3.** UV-vis (0.7 mM in acetonitrile): $\lambda_{max}(\varepsilon)$ = 369 (2233) (shoulder on off-scale signals in UV range), 453 (1018). ^1H

NMR (300 MHz, CD_3CN) δ 0.93 (d, J = 7 Hz, 6H, *i*-Pr Me), 2.32 (s, 3H, Me), 2.41 (ov s, 18H, CNAr Me), 3.17 (sept, 1H, *i*-Pr H), 7.23 (ov m, 6H, Ar-H), 7.36 (ov m, 5H, Ar-H), 7.75 (ov m, 9H, Ar-H), 7.94 (ov m, 2H, Ar-H). ^{19}F NMR (282 MHz, CD_3CN) δ -58.7 (br s, 2Fα), -79.4 (s, 6F, OTf), -107.3 (d d, $^4J_{FF}$ = 23, $^3J_{FF}$ = 11 Hz, 2Fβ), -133.9 (d m, $^3J_{FF(trans)}$ = 144, $^4J_{FF}$ = 11 Hz, 1F), -151.0 (d t t, $^3J_{FF(trans)}$ = 144 Hz, $^2J_{FP}$ = 60 Hz, J_{FF} = 23, $^3J_{FF}$ = 8 Hz, 1F). $^{31}P\{^1H\}$ NMR (121 MHz, CD_3CN) δ 15.6 (d d, $^2J_{PF}$ = 60, $^3J_{PF}$ = 7 Hz). MS[ESI (positive mode), solvent: CH_3CN]: *m/z* calcd for [{[1,2,4-(*i*-Pr-S),(Ph_2P),Me-(C_6H_3)][(1,2,6-(CN)($Me)_2$(C_6H_3)]$_3$Ni(C_4F_6)}$^{2+}$($OTf)^-$ - H + K^+]: 1150.2 , found: 1150.5; {[[1,2,4-(*i*-Pr-S),(Ph_2P),Me-(C_6H_3)][(1,2,6-(CN)($Me)_2$(C_6H_3)]$_3$Ni(C_4F_6)}$^{2+}$ 481.6, found: 481.3.

2.5.10 Hydrolysis of [1,2,4-(*i*-Pr-S),(Ph_2P),Me(C_6H_3)]Ni(C_4F_7)(OTf) (Ni-3)

Ni-3 (60 mg, 0.081 mmol) was transferred to a 50 mL Schlenk ampoule in a minimal amount of deuterated benzene (~ 2 mL). To the **Ni-3**/benzene solution was added 0.2 mL of water. The flask was sealed and left to stir at 75°C for 72 h. The reaction mixture was cooled to room temperature and the flask was connected directly to the Schlenk line. Three freeze-pump-thaw cycles were performed on the flask. The J. Young NMR was then evacuated and cooled to – 196°C. With the ampoule and J. Young tube both under vacuum, ca. 0.5 mL of the reaction mixture was transferred to the J. Young tube under static vacuum, isolating *(E)*-1,2,3,3,4,4-hexafluoro-1-butene from the nickel-containing and other non-volatile co-products. ^{19}F NMR yield (by integration of product CF_2 peaks relative to an internal standard) of 27% based on three trials was calculated. Note: No reaction occurred upon addition of an excess of water to **Ni-2** with heating. NMR data in benzene-d_6: ^1H NMR (300 MHz, C_6D_6) δ 0.44 (s, H_2O), 5.06 (tr tr m, $^2J_{HF}$ = 53, $^3J_{HF}$ = 3 Hz, 1H), 6.19 (d d m, J_{HF} = 71, 4 Hz, 1H). ^{19}F NMR (282 MHz, C_6D_6) δ -122.1 (m, J_{FH} = 3 Hz, 2F), -137.3 (d m, $^2J_{FH}$ = 53 Hz, 2F), -166.8 (d d tr tr, $^3J_{FH(gem)}$ = 71 Hz, $^3J_{FF(trans)}$ = 135 Hz, J_{FF} = 21, 4 Hz, 1F), -178.5 (d m, $^3J_{FH(cis)}$ = 4 Hz, $^3J_{FF(trans)}$ = 135 Hz, 1F). $^{19}F\{^1H\}$ NMR (282 MHz, C_6D_6) δ -122.1 (m, 2F), -137.3 (m, 2F), -166.8 (d tr tr, $^3J_{FF(trans)}$ = 135 Hz, J_{FF} = 21, 4 Hz, 1F), -178.5 (d tr tr, $J_{FF(trans)}$ = 135 Hz, 1F). $^{13}C\{^1H\}$ NMR (75 MHz, C_6D_6) δ 109.2 (tr tr d, J_{CF} = 251 Hz, $^2J_{CF}$ = 38 Hz, $^3J_{CF}$ = 3 Hz, 1C), 142.9 (d d, J_{CF} = 244 Hz, $^2J_{CF(trans)}$ = 33

Hz, 1C), 144.8 (d d tr, J_{CF} = 264 Hz, $^{2}J_{CF(trans)}$ = 59 Hz, $^{3}J_{CF}$ = 3 Hz, 1C). MS[ESI (positive mode), solvent: CH_3CN]: *m/z* calcd for $[M + H^+]$: 165.0, found: 165.4.

2.6 References

[1] Chambers, R.D. *Fluorine in Organic Chemistry, 2nd Ed.*; Blackwell: Oxford, **2004**.

[2] Kitazume, T., *J. Fluorine Chem.* **2000**, *105*, 265.

[3] Chambers, R. D.; Burton, D. J.; Drakesmith, F. G.; Hutchinson, J.; Kitazume, T.; Lu, L.; Percy, J. M.; Sandford, G.; Yamazaki, T. *Organofluorine Chemistry Techniques and Synthons*, Vol. 193; Springer: New York, **1997**.

[4] (a) Siegle, J. C.; Muus, L. T.; Lin, T. P.; Larsen, H. A. *J. Polym. Sci., Part A : Polym. Chem.* **1964**, *2*, 391. (b) Lonfei, J.; Jingling, W.; Shuman, X. *J. Anal. Appl. Pyrol.* **1986**, *10*, 99. (c) Meissner, E.; Wróblewska, A.; Milchert, E. *Polym. Degrad. Stab.* **2004**, *83*, 163. (d) Bhadury, P. S.; Singh, S.; Sharma, M.; Palit, M. *J. Anal. Appl. Pyrol.* **2007**, *78*, 288.

[5] (a) Green, M.; Osborn, R. B. L.; Rest, A. J.; Stone, F. G. A. *J. Chem. Soc. (A)* **1968,** 2525. (b) Ashley-Smith, J.; Green, M.; Stone, F. G. A. *J. Chem. Soc. (A)* **1969,** 3019. (c) Browning, J.; Cundy, C. S.; Green, M.; Stone, F. G. A. *J. Chem. Soc. (A)* **1969,** 20. (d) Cundy, C. S; Green, M.; Stone, F. G. A. *J. Chem. Soc.(A)* **1970,** 1647. (e) Greco, A.; Green, M.; Shakshooki, S. K; Stone, F. G. A. *J. Chem. Soc. (D)* **1970,** 1374. (f) Stone, F. G. A., *J. Fluorine Chem.* **1999**, *100*, 227. (g) Ohashi, M.; Shibata, M.; Saijo, H.; Kambara, T.; Ogoshi, S. *Organometallics* **2013**, *32*, 3631.

[6] (a) Green, M.; Shakshooki, S. K.; Stone, F. G. A. *J. Chem Soc. (A)* **1971**, 2828. (b) Davies, C. H.; Game, C. H.; Green, M.; Stone, F. G. A. *J. Chem. Soc., Dalton Trans.* **1974**, 357.

[7] Stone reported reactivity studies of a related tetra-carbonyl iron perfluorocyclopentane complex. The product decomposed with heating at 70°C for 120 h, affording perfluorocyclobutane as the major organic product. With heating at 160°C for 12 days, perfluorocyclobutene was obtained as the major organic product: Manuel, T. A.; Stafford, S. L.; Stone, F. G. A. *J. Am. Chem. Soc.* **1961**, *83*, 249.

[8] Burch, R. R; Calabrese, J. C.; Ittel, S. D. *Organometallics* **1988**, *7*, 1642.

[9] Baker, R. T., Beatty, R. P., Farnham, W. B.; Wallace, R. L., Jr. *PCT Int. Appl.* **1997**, U.S Patent 5,670,679, E. I. Du Pont de Nemours & Co., USA. Preparation of unsaturated hydrofluoro-carbons (HFCs) is an attractive target as several such molecules have been shown to have drastically reduced global warming potential (*vs.* saturated HFCs): http://www.unep.org/dewa/portals/67/pdf/HFC_report.pdf

[10] Gasafi-Martin, W.; Oberendfellner, G.; Von Werner, K. *Can. J. Chem.* **1996**, *74*, 1922.

[11] Kiplinger, J. L.; Richmond, T. G.; Osterberg, C. E. *Chem. Rev.* **1994**, *94*, 373.

[12] (a) Dubinina, G. G.; Furutachi, H.; Vicic, D. A. *J. Am. Chem. Soc.* **2008**, *130*, 8600. (b) Dubinina, G. G.; Ogikubo, J.; Vicic, D. A. *Organometallics* **2008**, *27*, 6233. (c) Oishi, M.; Kondo, H.; Amii, H. *Chem. Commun.* **2009**, 1909. (d) Ball, N. D.; Kampf, J. W.; Sanford, M. S. *J. Am. Chem. Soc.* **2010**, *132*, 2878. (e) Cho, E. J.; Senecal, T. D.; Kinzel, T.; Zhang, Y.; Watson, D. A.; Buchwald, S. L. *Science* **2010**, *328*, 1679. (f) McReynolds, K. A.; Lewis, R. S.; Ackerman, L. K. G.; Dubinina, G. G.; Brennessel, W. W.; Vicic, D. A. *J. Fluorine Chem.* **2010**, *131*, 1108. (g) Knauber, T.; Arikan, F.; Röschenthaler, G. V.; Gooßen, L. J. *Chem. Eur. J.* **2011**, *17*, 2689. (h) Zhang, C. P.; Wang, Z. L.; Chen, Q. Y.; Zhang, C. T.; Gu, Y. C.; Xiao, J. C. *Angew. Chem. Int. Ed.* **2011**, *50*, 1896. (i) Tomashenko, O. A.; Escudero-Adán, E . C.; Belmonte, M. M.; Grushin, V. V. *Angew. Chem. Int. Ed.* **2011**, *50*, 7655. (j) Morimoto, H.; Tsubogo, T.; Litvinas, N. D.; Hartwig, J. F. *Angew. Chem. Int. Ed.* **2011**, *50*, 3793. (k) Xu, J.; Luo, D. F.; Xiao, B.; Liu, Z. J.; Gong, T. J.; Fu, Y.; Liu, L. *Chem. Commun.* **2011**, *47*, 4300. (l) Dai, J. J.; Fang, C.; Xiao, B.; Yi, J.; Xu, J.; Liu, Z. J.; Lu, X.; Liu, L.; Fu, Y. *J. Am. Chem. Soc.* **2013**, *135*, 8436.

[13] Block, E.; Ofori-Okai, G.; Zubieta, J. *J. Am. Chem. Soc.* **1989**, *111*, 2327.

[14] (a) McFarlane, W.; White, R. F. M. *J. Chem. Soc. D* **1969**, 744. (b) Olah, G. A.; McFarland, C. W. *J. Org. Chem.* **1971**, *36*, 1374. (c) Weiss, R.; Vande Griend, L. J.; Verkade, J. G. *J. Org. Chem.* **1979**, *44*, 1860.

[15] (a) Arbusow, B. A. *Pure Appl. Chem.* **1964**, *9*, 307. (b) Bhattacharya, A. K.; Thyagarajan, G. *Chem. Rev.* **1981**, *81*, 415.

[16] (a) Darwish, D.; Hong Hui, S.; Tomilson, R. *J. Am. Chem. Soc.* **1968**, *90*, 5631. (b) Stirling, C. J. M. *The Chemistry of the Sulphonium Group, Part 1*; John Wiley and Sons: Chicester, U. K., **1981.** (c) Toru, T.; Bolm, C.; Brière, J-F.; Metzner, P. Synthesis and Use of Chiral Sulfur Ylides. In *Organosulfur Chemistry in Assymetric Synthesis*; Wiley-VCH: Verlag, Germany, **2008**; pp 179-208 and references therein. (d) Arévalo, R.; Pérez, J.; Riera, L. *Inorg. Chem.* **2013**, *52*, 6785.

[17] Additional crystallographic details can be found in the Supporting Information. For complex **Ni-2**; R = 0.0297. For complex **Ni-3**; R = 0.0644.

[18] (a) Clark, G. R.; Hoskins, S. V.; Roper, W. R. *J. Organomet. Chem.* **1982**, *234*, C9. (b) Brothers, P. J.; Roper, W. R. *Chem. Rev.* **1988**, *88*, 1293. (c) Garratt, S. A.; Hughes, R. P.; Kovacik, I.; Ward, A. J.; Willemsen, S.; Zhang, D. *J. Am. Chem. Soc.* **2005**, *127*, 15585. (d) Torrens, H.; *Coord. Chem. Rev.* **2005**, *249*, 1957. (e) Hughes, R. P. *J. Fluor. Chem.* **2010**, *131*, 1059. (f) Huang, D.; Koren, P. R.; Folting, K.; Davidson, E. R.; Caulton, K. G. *J. Am. Chem. Soc.* **2000**, *122*, 8916. (g) Taw, F. L.; Clark, A. E.; Mueller, A. H.; Janicke, M. T.; Cantat, T.; Scott, B. L.; Hay, P. F.; Hughes, R. P.; Kiplinger, J. L. *Organometallics* **2012**, *31*, 1484.

[19] (a) Nieto-Oberhuber, C.; López, S.; Jiménez-Núñez, E.; Echavarren, A. M. *Chem. Eur. J.* **2006**, *12*, 5916. (b) Fürstner, A.; Morency, L. *Angew. Chem. Int. Ed.* **2008**, *47*, 5030.

[20] Harrison, D. J.; Gorelsky, S. I.; Lee, G. M.; Korobkov, I.; Baker, R. T. *Organometallics* **2013**, *32*,

[21] Treatment of **Ni-3** with >1 equiv of sodium thiophenolate results in very minor consumption of **Ni-4** to an uncharacterized product.

[22] Dissolving **Ni-3** in pyridine results in the formation of an analogous ring-opening product. Initial variable temperature NMR experiments in THF suggest the presence of more than one metallacyclic intermediate en route to **Ni-6**.

[23] Burton, D. J.; Yang, Z. Y.; Qiu, W. *Chem. Rev.* **1996**, *96*, 1641, and references therein.

[24] No reaction occurred upon addition of an excess of water to **Ni-2** with heating. Burch observed an ancillary ligand substitution reaction upon reacting his phosphine ligand migration product with an excess of water, resulting in the cationic complex $[Ni(PEt_3)(H_2O)(CF(PEt_3)\text{-}(CF_2)_3]^+[BF_4]^-$ (see ref. 8).

[25] Miller, R. N.; Nappa, M. J.; Rao, V. N. M.; Sievert, A. C. *U. S. Pat. Appl. Publ.* **2006**, U.S Patent 2006106263, E. I. Du Pont de Nemours & Co., USA.

[26] Hunadi, R. J.; Baum, K. *Synthesis* **1982**, *39*, 454.

[27] APEX Software Suite v.2010; Bruker AXS: Madison, WI, **2005**.

Chapter 3. Brønsted acid-promoted C−F bond activation in [P,S]-ligated neutral and anionic perfluoronickelacyclopentanes

3.1 Published Contributions

Brønsted acid-promoted C−F bond activation in [P,S]-ligated neutral and anionic perfluoronickelacyclopentanes.

K. A. Giffin, I. Korobkov, R. T. Baker *Dalton Trans.* **2015**, *44*, 19587.

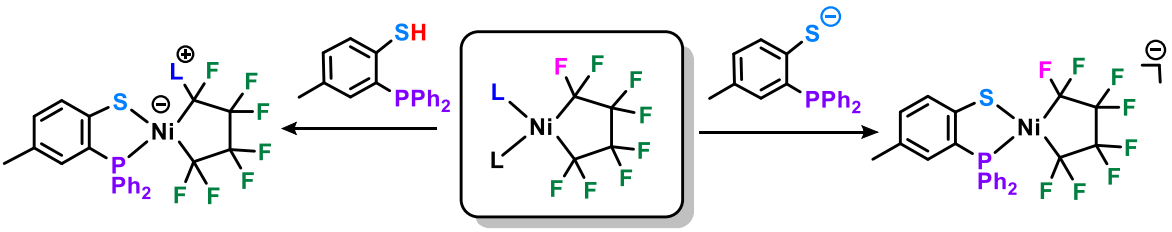

Author Contributions

Giffin and Baker wrote the manuscript. Giffin performed all experiments presented. Korobkov was responsible for X-ray diffraction studies.

Abstract

Treatment of $L_2Ni(C_4F_8)$ (L = PPh_3, PPh_2Me, pyridine) with an external Lewis acid results in the synthesis of new L-functionalized fluoronickelacyclopentanes. $L_2Ni(C_4F_8)$ (L = PPh_3, PPh_2Me) react with the thiol form of the bidentate ligand 1,2,4-(HS)(Ph_2P)Me(C_6H_3) **[P,SH]** through a unique C_α−F bond activation mechanism, affording phosphinothiolate-functionalized nickelacycles. Furthermore, substituting monodentate ligands in $L_2Ni(C_4F_8)$ with the deprotonated form of the bidentate ligand **[P,S$^-$]** leads to the first anionic phophinothiolate-cooordinated perfluoronickelacycle. The anionic metallacyle demonstrates reactivity with phosphonium salts [$PHPh_3$](Br) and [$PHPh_2Me$](Br).

3.2 Introduction

The development of new homogeneous catalytic routes to small functionalized fluorocarbons (FCs) remains an attractive target, given the environmental concerns related to current synthetic routes. Recently, there have been significant advances in homogeneous catalyzed routes for the installment of fluorine ($-F$)[2], trifluoromethyl ($-CF_3$)[3], difluoromethyl ($-CHF_2$)[4], and difluoromethylene ($-CF_2-$)[4] groups to unactivated organic substrates, typically proceeding through M−F or M−R^F (M = transition metal, R^F = fluoroalkyl) intermediates. In contrast, examples of M−R^F complexes containing a perfluoroalkyl fragment with more than one perfluoromethylene unit as intermediates in catalysis are less common, and often require the use of heavier halogenated FCs as precursors for M−R^F synthesis.[4,5] To circumvent this, we investigated the reactivity of perfluorometallacycle complexes synthesized by the oxidative cyclization of tetrafluoroethylene (TFE; obtained from waste PTFE)[6] to low-valent metal centres. Previous studies have concluded that both the metal and ancillary ligands influence whether three- or five-membered metallacycles are formed upon reacting TFE with low-valent metals.[7] To date, there are few reports on Ni−C and C−F bond reactivity studies involving perfluoronickelacyclopentanes. Among these is work patented by Baker *et al.*, wherein catalytic hydrodimerization of TFE resulting in the synthesis of octafluorobutane, a useful solvent in several industrial processes, was achieved.[5c]

Additionally, work published by Burch and co-workers demonstrated the activation of a C_α−F bond of $(PEt_3)_2Ni(C_4F_8)$ in the presence of a stoichiometric amount of the fluorophilic Lewis acid, BF_3.[8] In an effort to develop novel strategies for activation of C−F bonds and functionalization of nickel fluorocyclopentanes, we aim to assess their reactivity as a function of ancillary ligand(s) modification. Our group recently reported a new T-shaped three-coordinate perfluoronickelacyclopentane–NHC complex that undergoes an unusual fluoroalkyl group migration upon C_α−F activation by a Lewis acid. Additionally, the NHC perfluoronickelacycle reacts with

carboxylic acids to afford C_α−F activated/ C_α ester functionalized metallacycles and/or Ni−C bond protonolysis products.[9]

We previously communicated the synthesis of an unsymmetrical **[P,S^{iPr}]**-ligated nickel perfluorocyclopentane (complex **Ni-2**, Scheme 3.1) which displayed examples of C_α−F, C_β−F and Ni−R^F bond activation reactivity.[10] Upon treatment of $[P[O(i\text{-}Pr)]_3]_2Ni(C_4F_8)$ **(Ni-1)** with 1,2,4-(HS)(Ph_2P)Me(C_6H_3) **[P,SH]** an isopropyl transfer from one free phosphite to the sulfur occurred, resulting in the selective formation of the phosphinothioether-coordinated nickel complex **Ni-2**. We speculated that this reaction proceeds through a transient acidic thiol-bound intermediate (***Int 1***) that, upon deprotonation by a free phosphite, results in a short-lived thiolate-coordinated anionic nickel intermediate (***Int 2***). Nucleophilic attack by the nickel-coordinated thiolate on one O−*i*-Pr bond of the phosphorus acid leads to the formation of product **Ni-2**.[11] Treatment of **Ni-2** with the strongly Lewis acidic Me_3SiOTf (OTf = SO_3CF_3) resulted in C_α−F activation followed by chemoselective phosphine migration, affording metallabicyclic product **Ni-3**. Hydrolysis of **Ni-3** with heating led to exclusive formation of the (*E*)-1,2,3,3,4,4-hexafluoro-1-butene as the major product.

Scheme 3.1 Formation and reactivity of [P,S^{iPr}]Ni(C_4F_8).

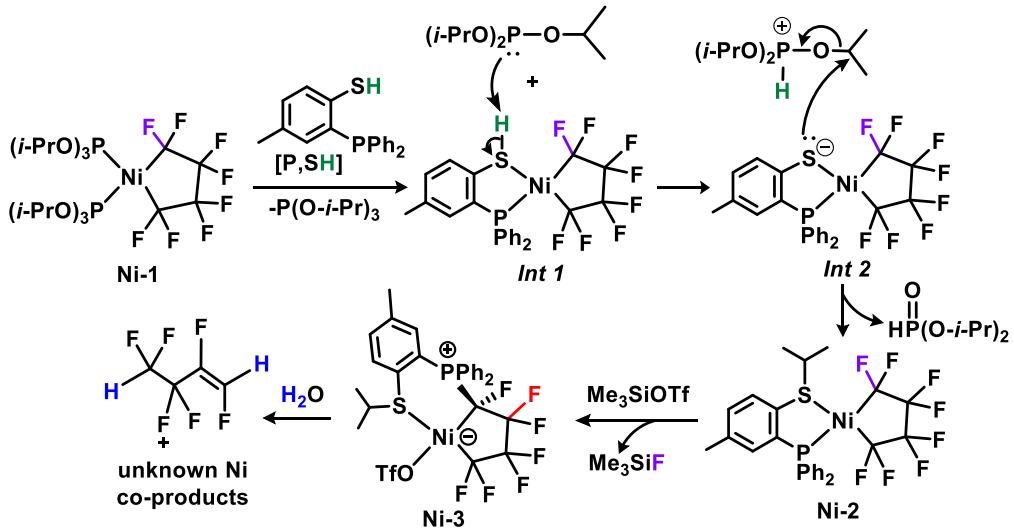

In this work, we turned our focus to other perfluoronickelacyclopentanes bearing two monodentate ancillary ligands, $L_2Ni(C_4F_8)$, where L = PPh_3 **(Ni-9a)**, PPh_2Me **(Ni-9b)**, and pyridine

(Ni-9c). Nickelacycles **Ni-9a** and **Ni-9b** have both been previously characterized by Stone and co-workers. Bis(pyridine)Ni(C_4F_8) **(Ni-9c)** has not been reported, however Stone did characterize the analogous bis(γ-picoline)Ni(C_4F_8).[7d] Complexes **Ni-9a** to **Ni-9c** were of interest for our study as they do not offer potential alkyl transfer to the sulfur atom (see Scheme 3.1, ***Int 2***) as was observed with phosphite ancillary ligands containing O−*i*-Pr bonds susceptible to nucleophilic attack. The phosphinothiol ligand offers versatility as it can be employed in its acidic thiol form **[P,SH]** or in its basic thiolate form **[P,S$^-$]**. A handful of Ni(I) and Ni(II) coordination complexes bearing the 1,2-(S^-)(Ph_2P)(C_6H_4) ligand (slight variation on the ligand used in this study) have been reported to date.[12] Most preceding examples of C_α−F bond activation of nickel perfluorocyclopentanes have required the use of a strong Lewis acid, where the driving force for the reaction is the formation of the stronger B−F or Si−F bond (relative to C−F). Herein, we present the reactivity of the unsymmetrical bidentate ligand **[P,SH]** in substitution reactions with L_2Ni(C_4F_8) **Ni-9a**,**b** and **c**, where a unique ligand-assisted/Brønsted acid-promoted C_α−F activation occurs. Furthermore, the synthesis and characterization of an anionic perfluoronickelacyclopentane will be presented, along with preliminary reactivity studies.

3.3 Results and Discussion

Consistent with previous results from our group and Burch *et al.*[8], C_α−F activation of perfluoronickelacycles **Ni-9** occurs when an equimolar amount of external Lewis acid is added (Scheme 3.2). This result is also congruous with precedent for the weakening of C_α−F *versus* C_β−F bonds in M−R^F (M = Rh, Ir, Pt, Fe, Ni) complexes.[13] The postulated short-lived electrophilic intermediate then undergoes a nucleophilic attack by one L, resulting in the zwitterionic L-functionalized metallacycles **Ni-10a**,**b** and **c**. Dissolving **Ni-10** metallacycles in CD_3CN results in displacement of the $(OTf)^-$ ligand with one molecule of acetonitrile, affording a cationic Ni centre with an outer sphere OTf anion.

Scheme 3.2 Functionalization of perfluoronickelacycles through C_α−F activation.

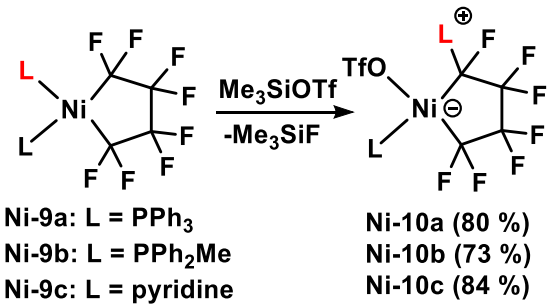

Ni-9a: L = PPh_3
Ni-9b: L = PPh_2Me
Ni-9c: L = pyridine

Ni-10a (80 %)
Ni-10b (73 %)
Ni-10c (84 %)

Notably, C_α−N bond formation to give the pyridine-functionalized nickel fluorometallacycle **Ni-10c** is the first example of N-donor migration to the C_α position. X-ray quality crystals of **Ni-10b** and **Ni-10c** were grown by slow diffusion of hexanes into a dichloroethane solution and slow evaporation from a dichloromethane solution respectively (Figure 3.1). No significant Ni−C_α elongation in comparison to Ni−C_α bonds of **Ni-9c** (See Appendix for ORTEP representation) is observed upon substituting a fluoride with a pyridine group at C_α. In contrast, a quite significant increase in Ni−C_α bond length in **Ni-10b** is observed for the C_α−P functionalized carbon in comparison to perfluorinated C_α *trans* to OTf (1.994(5) Å and 1.864(6) Å respectively).

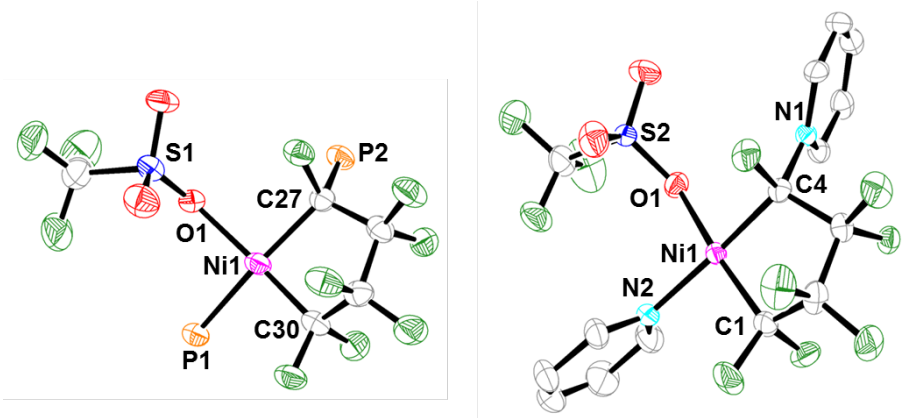

Figure 3.1. ORTEP representation of the molecular structures of complexes **Ni-10b** (left) and **Ni-10c** (right). Thermal ellipsoids are set at the 40% probability level. Hydrogen atoms and phenyl/methyl groups of **P1** and **P2** (left structure) are omitted for clarity. Selected bond lengths (Å) and angles (deg): **Ni-10b:** Ni1−P1 2.2398(16), Ni1−O1 1.988(4), Ni1−C27 1.994(5), Ni1−C30 1.864(6), C27−P2 1.845(5); C30−Ni1−C27 86.4(2), C30−Ni1−P1 93.40(17), C27−Ni1−O1 93.44(19), P1−Ni1−O1 88.76(11). **Ni-10c:** Ni1−N2 1.9213(17), Ni1−O1 1.9733(15), Ni1−C1 1.879(2), Ni1−C4 1.921(2), C4−N1 1.499(3); C1−Ni1−C4 87.09(9), C1−Ni1−N2 91.35(9), C4−Ni1−O1 93.07(8), N2−Ni1−O1 89.87(7).

Upon substitution of $(PR_3)_2Ni(C_4F_8)$ metallacycles **Ni-9a** and **Ni-9b** with the thiol form **[P,SH]** of the bidentate ligand, an unexpected $C_\alpha-F$ bond activation occurs, where a displaced free phosphine is selectively installed in the C_α position of the final product **Ni-11**, proceeding through HF elimination. Monitoring the reaction between **Ni-9a** and **[P,SH]** in C_6D_6 at room temperature using ^{19}F NMR shows immediate consumption of $(PPh_3)_2Ni(C_4F_8)$ and the presence of **Ni-11** as well as an intermediate with four distinct fluorine environments: two $C_\alpha F_2$ peaks at δ_F = -97.4 (d, J_{FP} = 27 Hz) and -102.2 (d, J_{FP} = 24 Hz), and two $C_\beta F_2$ peaks at -137.9 and -138.2 (see Appendix, Figure A8). The $^{31}P\{^1H\}$ NMR spectrum reveals two phosphorus peaks assignable to complex **Ni-11** at δ_P = 54.0 (d, J_{PF} = 57 Hz, Ni−P) and 17.6 (dm, J_{PF} = 65 Hz, $C_\alpha-P$). The phosphorus resonances associated with the intermediate include one apparent quintet at δ_P = 46.4 (1P), and a singlet at -7.8 (2P). After 3 hours, the ^{19}F and $^{31}P\{^1H\}$NMR spectra indicate complete consumption of the intermediate, with only seven unique fluorine peaks associated with **Ni-11** remaining. Carrying out the reaction between **[P,SH]** and **Ni-9a** in THF at -40°C reveals the formation of the same intermediate mentioned above, however no conversion to product **Ni-11** at this temperature is observed. When the reaction between **[P,SH]** and **Ni-9b** is performed in THF at room temperature, product **Ni-11** is formed along with the observation of a distinct HF peak at δ_F = -195.7 ppm (J_{FH} = 453 Hz; see Appendix, Figure A9). The ^{19}F NMR data for the intermediate are consistent with an unsymmetrically substituted perfluorometallacycle.[10]

We reasoned that the intermediate observable by NMR either resembles the thiol-coordinated ***Int 3*** proposed in Scheme 3.3, or a thiolate-coordinated intermediate (***Int 4***, Scheme 3.3). A variable temperature multinuclear NMR experiment between **[P,SH]** and **Ni-9b** in $CDCl_3$ solvent supports a thiolate-coordinated anionic nickel complex as the intermediate (***Int 4***, Scheme 3.3) based on the following observations: a) Initially, the $^{31}P\{^1H\}$ NMR spectrum at room temperature shows one apparent quintet at δ_P = 51 and a broad singlet at δ_P = -16 ($\Delta\nu_{1/2}$ = 200 Hz); b) The broad singlet at -

Scheme 3.3 Formation of functionalized [P,S]-ligated fluoronickelacycles.

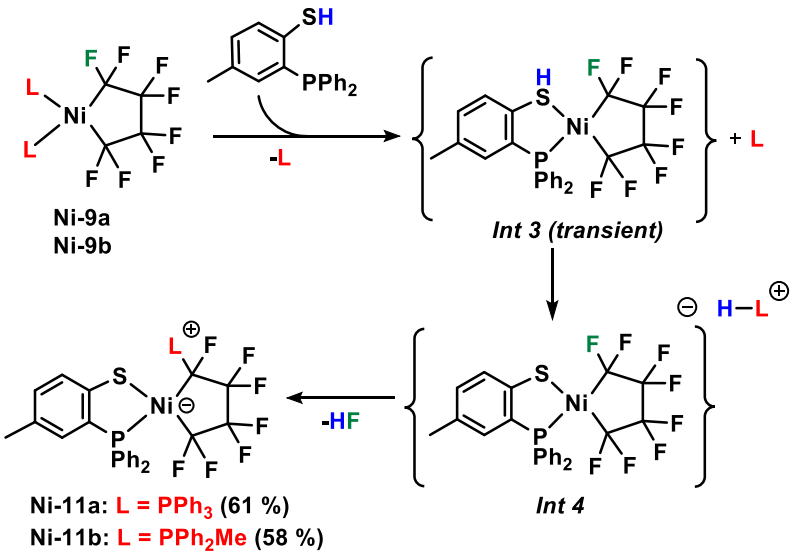

16 ppm splits into two separate singlets at δ_P = -4 and -27 respectively upon cooling to -40°C, revealing a chemical exchange process between two phosphorus atoms;[14] c) Performing a gated decoupled ^{31}P NMR experiment at -40°C shows splitting from a singlet to a doublet peak at -4 ppm with a large $^{1}J_{PH}$ coupling constant of 522 Hz, strongly suggestive of one bond P−H coupling; d) At -40°C, the proton with a consistent $^{1}J_{HP}$ = 522 Hz coupling is assigned at δ_H = 10.0 ppm. The one bond P−H coupling constant in addition to the observation of a significantly downfield chemical shift for the associated proton are in agreement with an outer sphere phosphonium cation as shown in Scheme 3.3, ***Int 4*** (see Appendix, Figures A10-A11).[15] We propose that a transient nickel-coordinated thiol intermediate ***(Int 3)*** should initially form in order to generate a sufficiently acidic proton for deprotonation by free phosphine.[16] These results provide experimental support for the intermediates we originally presented in the proposed mechanism for the synthesis of **Ni-2** (see Scheme 3.1). It is likely that the acidity of the generated secondary phosphonium cation in conjunction with the basicity of the anionic nickel counter ion contribute to the instability of ***Int 4***, leading to C_α−F abstraction and formation of the stable Ni(II) product **Ni-11**. Following HF elimination, a transient electrophilic carbocationic or fluorocarbene intermediate presumably

precedes nucleophilic attack by free phosphine, although this intermediate is not observable by NMR even at low temperatures. Interestingly, exclusive formation of the triphenylphosphine (**Ni-11a**) and methyldiphenylphosphine (**Ni-11b**) functionalized metallacycles is observed with no evidence of **[P,S⁻]** phosphine migration to the C_α as observed previously upon C_α−F activation of **Ni-2** using an external Lewis acid (*vide supra*). Moreover, the reaction is regioselective for a C_α−F bond *trans* to the phosphine group of the **[P,S⁻]** ligand. Complexes **Ni-11a** and **Ni-11b** were fully characterized using multinuclear NMR, UV-vis spectroscopy, X-ray diffraction, and elemental analysis.

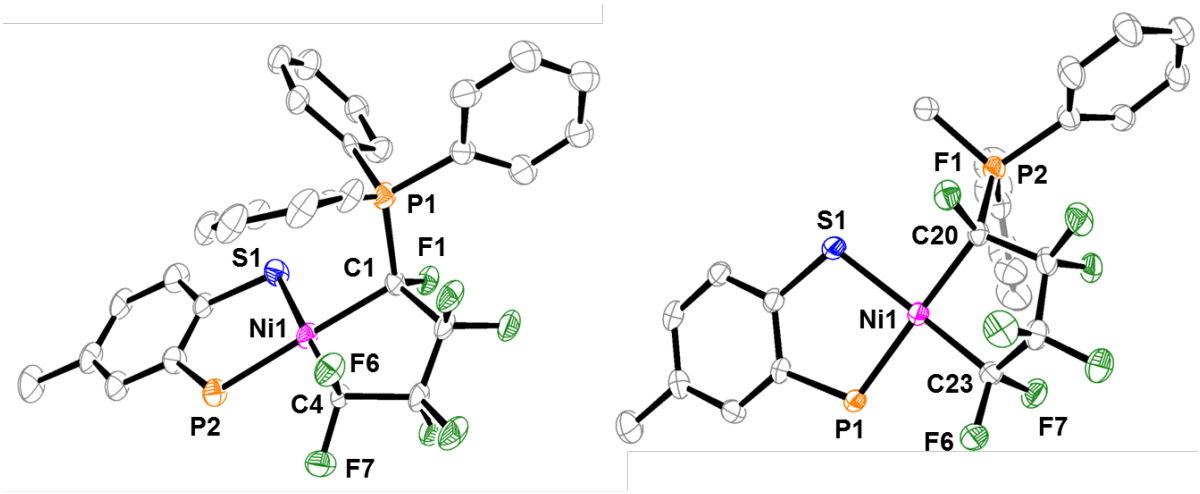

Figure 3.2. ORTEP representation of the molecular structures of complexes **Ni-11a** (left) and **Ni-11b** (right). Thermal ellipsoids are set at the 40% probability level. Hydrogen atoms and phenyl rings of **P2** (left structure) and **P1** (right structure) are omitted for clarity. Selected bond lengths (Å) and angles (deg): **Ni-11a**: Ni1−C1 2.044(11), Ni1−C4 1.947(8), Ni1−P2 2.182(3), Ni1−S1 2.198(2), C1−P1 1.832(9), C1−F1 1.443(10), C4−F6 1.383(9), C4−F7 1.363(10); C4−Ni1−C1 86.7(4), C4−Ni1−P2 93.2(3), P2−Ni1−S1 88.04(11), C1−Ni1−S1 92.0(2). **Ni-11b**: Ni1−C20 2.016(3), Ni1−C23 1.926(3), Ni1−P1 2.1608(9), Ni1−S1 2.1929(10), C20−P2 1.849(4), C20−F1 1.422(3), C23−F6 1.401(4), C23−F7 1.392(4); C23−Ni1−C20 87.72(13), C23−Ni1−P1 90.97(10), P1−Ni1−S1 88.50(3), C20−Ni1−S1 92.72(10).

X-ray quality crystals of **Ni-11a** and **Ni-11b** were grown by slow evaporation of a benzene solution (Figure 3.2, left) and by gradual cooling of a saturated dichloromethane solution (Figure 3.2, right), respectively. Bond angles in the molecular structures of **Ni-11a** and **Ni-11b** confirm a distorted-square-planar geometry about the Ni(II) centres (359.9° and 359.9°, respectively). For the Ni−C−P fragment, both structures reveal a significant elongation of the metal−carbon bond upon replacement of one fluorine with a phosphine substituent. The Ni−C_α bond length associated with

the phosphine-functionalized C_α is significantly longer in comparison to the Ni−C_α bond of the perfluorinated C_α *trans* to sulfur (*e.g.,* 2.044(11) Å and 1.947(8) Å respectively for **Ni-11a**). A similar Ni−C_α bond elongation was noted above for the structure of **Ni-10b**, however was not observed in the previously reported phosphine-functionalized metallacycles presumably due to the minor *trans* influence of the weakly coordinating triflate group in **Ni-3** and the fluoride-bridging tetrafluoroborate group in $(PEt_3)(BF_4)Ni[CF(PEt_3)(CF_2)_3]$ reported by Burch and co-workers.[8,10]

Treatment of $(PR_3)_2Ni(C_4F_8)$ (**Ni-9a, Ni-9b**) with the anionic form **[P,S⁻]** of the bidentate ligand (free ligand deprotonated *in situ* using an equimolar amount of sodium *tert*-butoxide) and one equivalent of 18-Crown-6 (18-C-6)[17] led to quantitative formation of an anionic phosphinothiolate-coordinated nickel perfluorometallacycle **Ni-12**, isolated as a bright yellow powder (Scheme 3.4). To the best of our knowledge, there have been no previously reported stable anionic Ni(II) metallacycles.

Scheme 3.4 Synthesis of phosphinothiolate-coordinated perfluoronickelacycle.

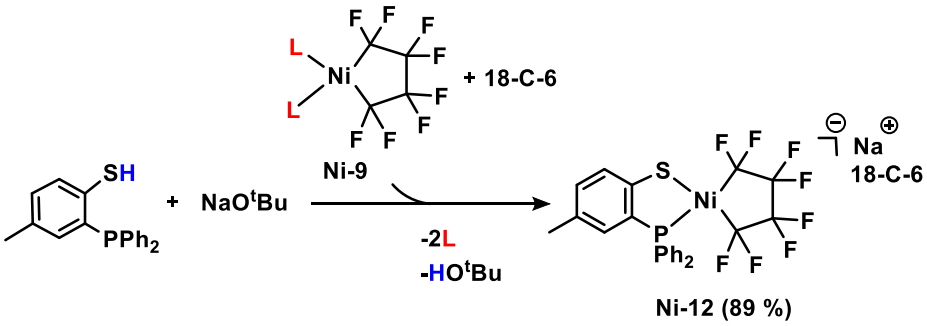

Single crystals of **Ni-12** were grown by gradual cooling of a saturated THF solution (see Figure 3.3). The sum of the angles about the Ni(II) centre in the molecular structure of **Ni-12** demonstrate distorted-square-planar geometry (360.1°). The nickel-thiolate bond length of the anionic complex **Ni-12** (2.1903(15) Å) is similar in comparison to the Ni−S bonds of the neutral complexes **Ni-11a** and **Ni-11b** (2.198(2) Å and 2.1929(10) Å respectively). The Ni−C_α bond length *trans* to phosphine is significantly shorter in relation to the Ni−C_α bonds of the phosphine-functionalized metallacycles **Ni-11a** and **Ni-11b** (*e.g.,* 1.943(5) Å for **Ni-12** and 2.044(11) Å for **Ni-11a**). The sodium cation is

bound by two THF molecules in addition to the six oxygen atoms of 18-Crown-6, making it an octacoordinate metal centre.[18]

Owing to the imparted electron density from the thiolate group and the basic nature of **Ni-12**, we directed our attention to its reactivity with a range of different acids, aiming to develop new strategies for C−F bond functionalization. Of particular interest were Brønsted acids, as these have previously demonstrated reactivity with cobalt perfluorocyclobutane[19], nickel hexafluoropropene complexes[20], and more recently with a three-coordinate perfluoronickelacyclopentane–NHC complex.[9] Indeed, treatment of **Ni-12** with the phosphonium salts $[HPPh_3](Br)$ and $[HPPh_2Me](Br)$ affords zwitterionic products **Ni-11a** and **Ni-11b**, concomitantly eliminating NaBr and HF (Scheme 3.5). At room temperature, full conversion of **Ni-12** to **Ni-11a** and **Ni-11b** is observed within 4 hours (91%) and 16

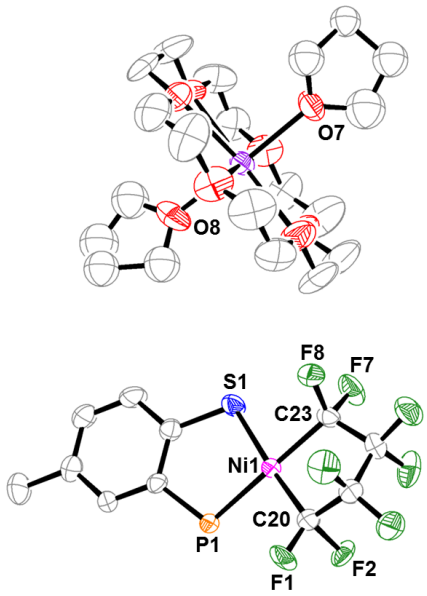

Figure 3.3. ORTEP representation of the molecular structure of [1,2,4-(S),(Ph_2P),Me(C_6H_3)]Ni(C_4F_8)[Na(18-Crown-6)$(THF)_2$] **(Ni-12·2 THF)**. Thermal ellipsoids are set at the 40% probability level. Hydrogen atoms, two phenyl rings of **P1**, and two outer sphere THF molecules are omitted for clarity. One of two orientations of the disordered F atoms of C20 is depicted and one of two orientations for the two disordered Na^+ bound THF molecules. Selected bond lengths (Å) and angles (deg): Ni1−C23 1.943(5), Ni1−C20 1.925(6), Ni1−P1 2.1890(14), Ni1−S1 2.1903(15), C23−F7 1.381(6), C23−F8 1.379(6), C20−F1 1.238(16), C20−F2 1.543(18); C20−Ni1−C23 86.2(2), C20−Ni1−P1 96.75(18), P1−Ni1−S1 87.92(5), C23−Ni1−S1 89.24(16).

hours (78%), respectively (yields were determined using ^{19}F NMR spectroscopy and a quantitative amount of internal standard). Treating **Ni-12** with the more strongly Brønsted acidic trifluoroacetic acid resulted in a complex mixture of products by ^{19}F and $^{31}P\{^{1}H\}$ NMR spectroscopy.

Scheme 3.5 Functionalization of phosphinothiolate-coordinated perfluoronickelacycle.

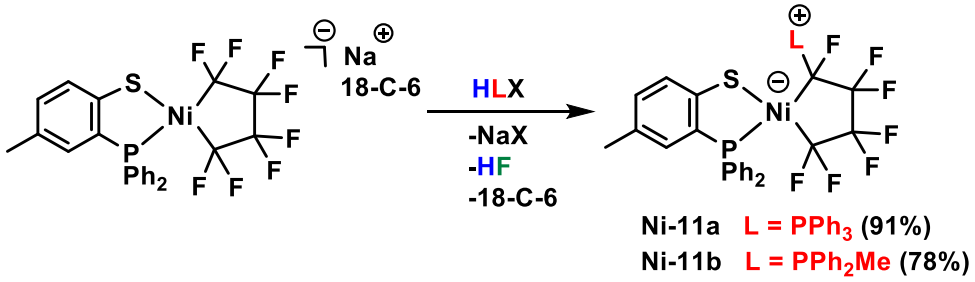

In the presence of an equimolar amount of pyridinium bromide, complex **Ni-12** afforded a mixture of products with only a minor amount of C_{α}−F activated pyridine-functionalized product **Ni-13** observed by multinuclear NMR. Unlike the $(PR_3)_2Ni(C_4F_8)$ perfluorometallacycles, treatment of $(Pyr)_2Ni(C_4F_8)$ **Ni-9c** with 2 equiv. of **[P,SH]** gave a mixture of Ni(II) pyridine-functionalized metallacycle **Ni-13** (48% yield by quantitative ^{19}F NMR), bis(chelate) $[NiS_2P_2]$ product **Ni-14** and other uncharacterized byproducts (Scheme 3.6). Similar $[NiS_2P_2]$ complexes related to **Ni-14** have been reported previously.[12] The *trans* geometry of **Ni-14** was determined by X-ray analysis (see Figure A55) and a characteristic singlet in the $^{31}P\{^{1}H\}$ NMR spectrum at δ_P = 52.9 ppm in C_6D_6.

Scheme 3.6 Reactivity of $(Pyr)_2Ni(C_4F_8)$ with [P,SH] ligand.

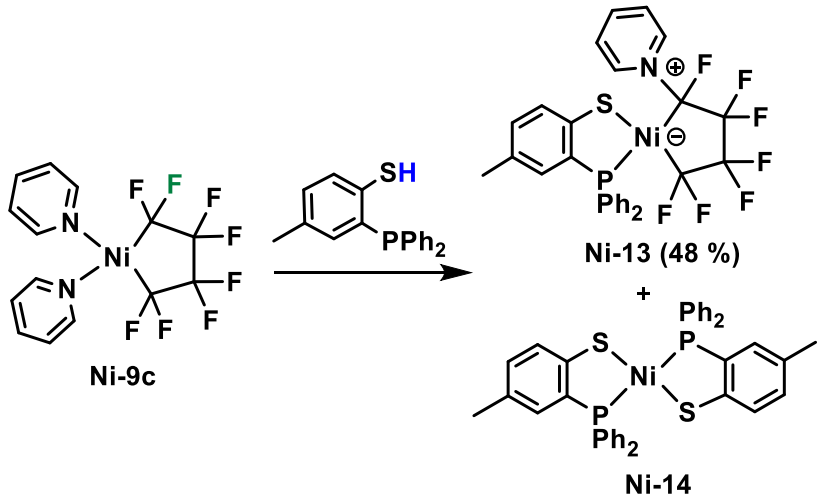

3.4 Conclusions

This work expands our knowledge of C−F bond activation in fluorometallacycles. Lewis acid activation of a C_α−F bond in $L_2Ni(C_4F_8)$ complexes to give zwitterionic functionalized fluoronickelacyclopentanes was extended beyond L = P donors to include the N-donor pyridine. In contrast, treatment of $(PR_3)_2Ni(C_4F_8)$ **Ni-9a** and **Ni-9b** with an equimolar amount of protonated bidentate ligand **[P,SH]** led to a unique ligand-assisted/Brønsted acid-protomoted C_α−F activation, affording phosphine-functionalized nickelacycles bearing the phosphinothiolate ligand **Ni-11a** and **Ni-11b** . A variable temperature NMR study confirmed the presence of an intermediate consisting of an anionic nickel centre with an outer sphere phosphonium counter ion (***Int 4***) in the formation of **Ni-11a** and **Ni-11b**. Finally, substituting the monodentate phosphines in **Ni-9** with the deprotonated chelate **[P,S$^-$]** afforded an anionic phophinothiolate-cooordinated nickelacycle **Ni-12**. Treatment of **Ni-12** with weakly acidic tertiary phosphonium salts reformed **Ni-11** without protonation of the thiolate sulfur. This study has revealed the versatile nature of the **[P,SH]** ligand, and corroborated previous studies that demonstrated the significant influence that ancillary ligand(s) can impart on perfluorometallacycle reactivity. Additional in-depth studies assessing the effects of the basic **[P,S$^-$]**

ligand on the reactivity of perfluoronickelacyclopentanes and their functionalized derivatives is currently underway.

3.5 Experimental Section

3.5.1 General

Experiments were conducted under nitrogen, using Schlenk techniques or an MBraun glove box. All solvents were deoxygenated by purging with nitrogen. Toluene, hexanes, and dichloroethane (DCE) were dried on columns of activated alumina using a J. C. Meyer solvent purification system. Benzene-d_6 (C_6D_6) and chlorobenzene were dried by stirring over activated alumina (ca. 10 wt. %) overnight, followed by filtration. Acetonitrile (CH_3CN), acetonitrile-d_3 (CD_3CN), and dichloromethane (DCM) were dried by refluxing over calcium hydride under nitrogen. After distillation, CH_3CN, CD_3CN and DCM were further dried by stirring over activated alumina (ca. 5 wt. %) overnight, followed by filtration. All solvents were stored over activated (heated at ca. 250^{o}C for >10 h under vacuum) 4 Å molecular sieves. Glassware was oven-dried at 150^{o}C for >2 h. The following chemicals were obtained commercially, as indicated: trimethylsilyl trifluoromethanesulfonate (Me_3SiOTf, Aldrich, 99%), bis(1,5-cyclooctadiene)nickel (0) ($Ni(cod)_2$, Strem, 98+%), 4-methylbenzenethiol (1,4-(HS)Me(C6H4), Aldrich, 98%), and diphenylchlorophosphine (PPh_2Cl, Strem, minimum 95%). Tetrafluoroethylene was made by pyrolysis of polytetrafluoroethylene (Scientific Polymer Products, powdered) under vacuum, using a slightly modified literature procedure (10−20 mTorr, 650 °C, 30 g scale, product stabilized with (R)-(+)-limonene (Aldrich, 97%), giving TFE of ca. 97% purity).[6] Compound $[P(O\text{-}o\text{-}tol)_3)_2]Ni(C_4F_8)$ (**Ni-8**) was made by oxidative addition of tetrafluoroethylene to $Ni[P(O\text{-}o\text{-}tol)_3]_4$ using slightly modified literature procedures.[5c] $(PPh_3)_2Ni(C_4F_8)$ and $(PPh_2Me)_2Ni(C_4F_8)$ complexes were prepared from $Ni(cod)_2$ following reported methods.[7d,7i] ^1H, ^{19}F, $^{31}P\{^1H\}$, $^{13}C\{^1H\}$ NMR spectra were recorded on a 300 MHz Bruker Avance instrument at room-temperature (21-23^{o}C). ^1H NMR spectra were referenced to the residual proton peaks associated with the deuterated solvents (C_6D_6: 7.16 ppm; CD_3CN: 1.94 ppm; $CDCl_3$: 7.26 ppm; CD_2Cl_2: 5.32 ppm). ^{19}F NMR spectra were referenced to

internal 1,3-bis(trifluoromethyl)benzene (BTB) (Aldrich, 99%, deoxygenated by purging with nitrogen, stored over activated 4 Å molecular sieves), set to –63.5 ppm. $^{31}P\{^{1}H\}$ NMR data were referenced to external H_3PO_4 (85 % aqueous solution), set to 0.0 ppm. UV-vis spectra were recorded on a Cary 100 instrument, using sealable quartz cuvettes (1.0 cm pathlength). Electrospray ionization mass spectral data were collected using an Applied Biosystem API2000 triple-quadrupole mass spectrometer. Elemental analyses were performed by Laboratoire d'Analyse Élémentaire de l'Université de Montréal.

3.5.2 X-ray Crystallography

For **Ni-9c**, **Ni-10b**, **Ni-10c**, **Ni-11a**, **Ni-11b**, **Ni-12** and **Ni-14**: samples were mounted on thin glass fibers using paraffin oil and were cooled to 200 K prior to data collection. Data were collected on a Bruker AXS KAPPA single crystal diffractometer equipped with a sealed Mo tube source (wavelength 0.71073 Å) APEX II CCD detector. Raw data collection and processing were performed with APEX II software package from BRUKER AXS.[1] Diffraction data were collected with a sequence of 0.5° ω scans at 0, 90, 180, and 270° in ϕ. Initial unit cell parameters were determined from 60 data frames collected at the different sections of the Ewald sphere. Semi-empirical absorption corrections based on equivalent reflections were applied. Systematic absences in the diffraction data set and unit-cell parameters were consistent with a triclinic system for **Ni-11a**, a tetragonal system for **Ni-9c**, and monoclinic systems for **Ni-10b**, **Ni-10c**, **Ni-11b**, **Ni-12** and **Ni-14**. Solutions in centrosymmetric space group yielded chemically reasonable and computationally stable results of refinement. The structures were solved by direct methods, completed with difference Fourier synthesis, and refined with full-matrix least-squares procedures based on F.[27] In the structure, compound molecules are situated in the general position. All non-hydrogen atoms were refined anisotropically with satisfactory thermal parameters values.

3.5.3 Synthesis of $(Pyr)_2Ni(C_4F_8)$ (Ni-9c)

$[P(O\text{-}o\text{-}tol)_3]_2Ni(C_4F_8)$ **Ni-8** (1.0 g, 0.00104 mol) was placed in a 100 mL round-bottom Schlenk flask, dissolved in a minimal amount of pyridine (ca. 10 mL), and left to stir at room temperature for

16 h. The reaction mixture was concentrated in vacuo until ca. 1 mL of solution was remaining. Hexanes was added (15 mL), precipitating out a light yellow solid. The flask was placed in a -35 °C freezer for 16 h. The product was filtered cold, washed with pre-cooled hexanes (2 x 3 mL), and dried in vacuo, affording a light beige powder. Yield: 338 mg, 0.81 mmol, 78% based on $[P(O\text{-}o\text{-}tol)_3]_2Ni(C_4F_8)$. X-ray quality crystals were grown from a saturated solution of **Ni-9c** in toluene/hexanes/diethyl ether. ^{1}H NMR (300 MHz, C_6D_6) δ 6.27 (br t, 4H, H_{meta}), 6.50 (br t, 2H, H_{para}), 7.16 (solvent), 8.29 (br d, 4H, H_{ortho}). ^{19}F NMR (282 MHz, C_6D_6) δ -63.5 (s, BTB), -111.3 (s, $4F_\alpha$), -139.3 (s, $4F_\beta$). Anal. Calc. for $C_{14}H_{10}F_8NiN_2$: C, 40.33, H, 2.42, N, 6.72. Found: C, 40.59, H, 2.43, N, 6.64.

3.5.4 Synthesis of $(PPh_3)(OTf)Ni[CF(PPh_3)(CF_2)_3]$ (Ni-10a)

$(PPh_3)_2Ni(C_4F_8)$ (100 mg, 0.13 mmol) was dissolved in ca. 10 mL of C_6H_6 in a 50 mL Schlenk ampoule. Me_3SiOTf (25.5 µL, 0.14 mmol) was added via 25 µL syringe and the reaction mixture was heated to 40°C and left to stir for 3 days. The colour changed from clear dark yellow to a cloudy bright orange throughout the reaction. The reaction mixture was filtered, collecting a light orange solid. The product was washed with cold hexanes (3 x 3mL) and the isolated material was dried in vacuo, affording a light orange powder. Yield: 94 mg, 0.10 mmol, 80% based on $(PPh_3)_2Ni(C_4F_8)$. UV-vis (0.3 mM in dichloromethane): $\lambda_{max}(\varepsilon)$ = 451 nm (1095). By NMR in CD_2Cl_2, there is ca. 8 % of a minor shifted functionalized metallacycle, which we propose to be the other regioisomer (C_α–P *trans* to OTf). ^{1}H NMR (300 MHz, CD_2Cl_2) δ 5.32 (solvent), 7.30-7.53 (m, 21H, Ar-H), 7.75 (d m, 3H, Ar-H), 8.02 (d d, $^3J_{HP}$ = 13 Hz, $^3J_{HH}$ = 8 Hz, 6H, Ar-H). ^{19}F NMR (282 MHz, CD_2Cl_2) δ -63.5 (s, BTB), -79.1, (s, 3F, OTf), -94.2 (d, $^2J_{FF}$ = 239 Hz, $1F_\alpha$), -96.2 (d d m, $^2J_{FF}$ = 239 Hz, $^3J_{FP}$ = 65 Hz, $1F_\alpha$), -102.8 (br d, $^2J_{FF}$ = 265 Hz, $1F_\beta$), -124.3 (d, $^2J_{FF}$ = 265 Hz, $1F_\beta$), -128.6 (d m, $^2J_{FF}$ = 243 Hz, $1F_\beta$), -129.8 (d m, $^2J_{FF}$ = 243 Hz, $1F_\beta$), -206.9 (d m, $^2J_{FP}$ = 74 Hz, $1F_\alpha$). $^{31}P\{^1H\}$ (121 MHz, CD_2Cl_2) δ 15.6 (d m, $^3J_{PF}$ = 65 Hz, Ni-P), 19.1 (d d d, $^2J_{PF}$ = 74 Hz, $^3J_{PF}$ = 34 Hz, C_α-P). Repeated elemental analysis resulted in low % Carbon for **Ni-9a**. Anal. Calc. for $C_{41}H_{30}F_{10}NiO_3P_2S$: C, 53.92, H, 3.31, S, 3.51. Found: C, 50.44, H, 3.20, S, 3.84.

3.5.5 Synthesis of $\{(PPh_3)(NCCH_3)Ni[CF(PPh_3)(CF_2)_3]\}^+(OTf)^-$ (Ni-10a·CH_3CN)

$(PPh_3)(OTf)Ni[CF(PPh_3)(CF_2)_3]$ **(Ni-10a)** was dissolved in deuterated acetonitrile. ^1H NMR (300 MHz, CD_3CN) δ 1.94 (solvent), 7.36-7.50 (m, 15 H, Ar-H), 7.70-7.79 (m, 6H, Ar-H), 7.87 (m, 3H, Ar-H), 8.22 (d d, $^3J_{HP}$ = 13 Hz, $^3J_{HH}$ = 8 Hz, 6H, Ar-H). ^{19}F NMR (282 MHz, CD_3CN) δ -63.5 (s, BTB), -79.4 (s, 3F, OTf), -97.9 (br d, $^2J_{FF}$ = 254 Hz, $1F_\alpha$), -107.4 (br d, $^2J_{FF}$ = 254 Hz, $1F_\alpha$), -110.7 (d m, $^2J_{FF}$ = 269 Hz, $1F_\beta$), -126.1 (d t t, $^2J_{FF}$ = 269 Hz, $^3J_{FF}$ = 16 Hz, $^3J_{FF}$ = 2 Hz, $1F_\beta$), -130.8 (d m, $^2J_{FF}$ = 247 Hz, $1F_\beta$), -132.8 (d m, $^2J_{FF}$ = 247 Hz, $1F_\beta$), -203.1 (d d m, $^2J_{FP}$ = 63 Hz, $^3J_{FF}$ = 29 Hz, $1F_\alpha$). $^{31}P\{^1H\}$ (121 MHz, CD_3CN) δ 4.7 (v br s, 1P, Ni-P), 18.5 (d d d, $^2J_{PF}$ = 63 Hz, $^3J_{PF}$ = 24 Hz, $^3J_{PF}$ = 12 Hz, 1P, C_α-P). High-resolution Electrospray Ionisation; mass calculated for $C_{40}H_{30}NiF_7P_2$ (M^+ - CH_3CN) 763.1064, found 763.1003. MS [ESI (positive mode), solvent: CH_3CN] *m/z* calcd for $C_{40}H_{30}F_7NiP_2$ (M^+ - CH_3CN) 763.1, *m/z* found (% intensity) 763.3 (56 %); *m/z* calcd for $C_{26}H_{21}F_7N_2NiP$ (M^+ - PPh_3 + CH_3CN) 583.1, *m/z* found 583.2 (16 %); *m/z* calcd for $C_{24}H_{18}F_7NNiP$ (M^+ - PPh_3) 542.0, *m/z* found 542.2 (51 %); *m/z* calcd for $C_{22}H_{15}F_7NiP$ (M^+ - CH_3CN - PPh_3) 501.0, *m/z* found 501.2 (50 %); *m/z* calcd for $C_{22}H_{15}F_5P$ ($C_4F_5PPh_3$) 405.1, *m/z* found 405.2 (100%).

3.5.6 Synthesis of $(PPh_2Me)(OTf)Ni[CF(PPh_2Me)(CF_2)_3]$ (Ni-10b)

$(PPh_2Me)_2Ni(C_4F_8)$ (100 mg, 0.15 mmol) was dissolved in ca. 10 mL of DCM in a 100 mL Schlenk ampoule. Me_3SiOTf (30.2 µL, 0.17 mmol) was added via 100 µL syringe, heated to 40°C and left to stir for 4 days. The colour changed from clear yellow to a darker clear orange throughout the reaction. The reaction mixture was transferred to a 50 mL RB Schlenk flask, solvent volume was reduced in vacuo to ca. 2 mL and hexanes was added, precipitating out a dark yellow solid. The flask was placed in a -35°C for 16 h. The product was filtered cold and washed with cold hexanes (3 x 3 mL). The isolated material was dried in vacuo, affording a bright yellow powder. Yield: 86 mg, 0.11 mmol, 73% based on $(PPh_2Me)_2Ni(C_4F_8)$. X-ray quality crystals were grown by slow diffusion of hexanes into a supersaturated solution of **Ni-10b** in dichloroethane. UV-vis (0.7 mM in dichloromethane): $\lambda_{max}(\varepsilon)$ = 419 nm (911). ^1H NMR (300 MHz, $CDCl_3$) δ 1.70 (d, $^2J_{HP}$ = 9 Hz, 3H, CH_3), 2.47 (d d, $^2J_{HP}$ = 13 Hz, $^3J_{HH}$ = 3 Hz, 3H, CH_3), 7.26 (solvent), 7.27-7.55 (ov m, 14H, Ar-H), 7.64 (m, 1H, Ar-H),

8.00 (m, 2H, Ar-H), 8.10 (m, 1H, Ar-H), 8.50 (d d, $^{3}J_{HP}$ = 13 Hz, $^{3}J_{HH}$ = 8 Hz, 2H, Ar-H). ^{19}F NMR (282 MHz, $CDCl_3$) δ -63.5 (s, BTB), -77.9 (d, $^{6}J_{FF}$ = 9 Hz, 3F, OTf), -93.5 (d m, $^{2}J_{FF}$ = 258 Hz, 1F$_\alpha$), -100.8 (d d t, $^{2}J_{FF}$ = 258 Hz, $^{3}J_{FF}$ = 15 Hz, $^{3}J_{FP}$ = 67 Hz, 1F$_\alpha$), -114.0 (d m, $^{2}J_{FF}$ = 274 Hz, 1F$_\beta$), -130.0 (d d d, $^{2}J_{FF}$ = 274 Hz, 3J_{FF} = 28 Hz, $^{3}J_{FF}$ = 15 Hz, 1F$_\beta$), -131.9 (app s, 2F$_\beta$), -207.1 (br d d m, $^{2}J_{FP}$ = 74 Hz, $^{3}J_{FF}$ = 31 Hz, 1F$_\alpha$). ^{31}P{^{1}H} (121 MHz, $CDCl_3$) δ 4.8 (d t, $^{3}J_{PF}$ = 67 Hz, 1P, Ni-P), 21.2 (d d, $^{2}J_{PF}$ = 74 Hz, $^{3}J_{PF}$ = 22 Hz, 1P, C$_\alpha$-P).

3.5.7 Synthesis of {(PPh_2Me)($NCCH_3$)Ni[$CF(PPh_2Me)(CF_2)_3$]}$^+$(OTf)$^-$ (Ni-10b·CH_3CN)

(PPh_2Me)(OTf)Ni[$CF(PPh_2Me)(CF_2)_3$] **(Ni-9b)** was dissolved in deuterated acetonitrile. ^{1}H NMR (300 MHz, CD_3CN) δ 1.94 (solvent), 2.03 (br d, $^{2}J_{HP}$ = 7 Hz, 3H, CH_3), 2.72 (d, $^{2}J_{HP}$ = 13 Hz, 3H, CH_3), 7.45-7.89 (m, 15 H, Ar-H), 7.93-8.04 (m, 3H, Ar-H), 8.10 (d d, $^{2}J_{HP}$ = 13 Hz, $^{3}J_{HH}$ = 8 Hz, 2H, Ar-H). ^{19}F NMR (282 MHz, CD_3CN) δ -63.5 (s, BTB), -79.3 (s, 3F, OTf), -96.6 (d m, $^{2}J_{FF}$ = 270 Hz, 1F$_\alpha$), -104.1 (d m, $^{2}J_{FF}$ = 270 Hz, 1F$_\alpha$), -112.2 (d m, $^{2}J_{FF}$ = 272 Hz, 1F$_\beta$), -128.3 (d t, $^{2}J_{FF}$ = 272 Hz, $^{3}J_{FF}$ = 15 Hz, 1F$_\beta$), -131.3 (ov d d, $^{2}J_{FF} \approx$ 267 Hz, 2F$_\beta$), -207.5 (d d, $^{2}J_{FP}$ = 65 Hz, $^{3}J_{FF}$ = 29 Hz, 1F$_\alpha$). ^{31}P{^{1}H} (121 MHz, CD_3CN) δ 12.2 (br s, 1P, Ni-P), 19.6 (d d d, $^{2}J_{PF}$ = 65 Hz, $^{3}J_{PF}$ = 30 Hz, $^{3}J_{PF}$ = 9 Hz, 1P, C$_\alpha$-P). High-resolution Electrospray Ionisation; mass calculated for $C_{32}H_{29}NNiP_2$ (M^+) 680.1017, found 680.0950. MS [ESI (positive mode), solvent: CH_3CN] *m/z* calcd for $C_{32}H_{29}F_7NNiP_2$ (M^+) 680.1, *m/z* found (% intensity) 680.3 (7 %); *m/z* calcd for $C_{30}H_{26}F_7NiP_2$ (M^+ - CH_3CN) 639.1, *m/z* found 639.3 (43 %); *m/z* calcd for $C_{19}H_{16}F_7NNiP$ (M^+ - PPh_2Me) 480.0, *m/z* found 480.2 (24 %); *m/z* calcd for $C_{17}H_{13}F_7NiP$ (M^+ - CH_3CN - PPh_2Me) 439.0, *m/z* found 439.1 (18 %). See Figure A52 for ESI-MS spectrum.

3.5.8 Synthesis of (Pyr)(OTf)Ni[$CF(Pyr)(CF_2)_3$] (Ni-10c)

$(Pyr)_2Ni(C_4F_8)$ (117 mg, 0.28 mmol) was dissolved in ca. 8 mL of DCE in a 50 mL Schlenk ampoule. Me_3SiOTf (66.1 µL, 0.37 mmol) was added via 100 µL syringe. The reaction mixture was heated to 60°C and left to stir for 24 h. The colour changed from clear beige to a cloudy yellow throughout the course of the reaction. The reaction mixture was transferred to a 50 mL RB Schlenk flask, solvent volume was reduced in vacuo to ca. 2 mL and hexanes was added, precipitating out a

bright yellow solid. The flask was placed in a -35°C for 16 h. The product was filtered cold and washed with cold hexanes (3 x 2 mL). The isolated material was dried in vacuo, affording a bright yellow powder. Yield: 130 mg, 0.24 mmol, 84% based on $(Pyr)_2Ni(C_4F_8)$. X-ray quality crystals were grown by slow evaporation of a dichloromethane solution. UV-vis (0.7 mM in dichloromethane): $\lambda_{max}(\varepsilon)$ = 398 nm (627). ^{19}F NMR (282 MHz, CH_2Cl_2/C_6D_6 lock) δ -63.5 (s, BTB), - 79.8 (br s, 3F, OTf), -99.0 (d t, $^2J_{FF}$ = 253 Hz, $^3J_{FF}$ = 11 Hz, $1F_\alpha$), -113.9 (d d d, $^2J_{FF}$ = 253 Hz, $^3J_{FF}$ = 15 Hz, $^3J_{FF}$ = 6 Hz, $1F_\alpha$), -126.1 (d m, $^2J_{FF}$ = 254 Hz, $1F_\beta$), -130.1 (d m, $^2J_{FF}$ = 252 Hz, $1F_\beta$), -141.1 (d m, $^2J_{FF}$ = 252 Hz, $1F_\beta$), -144.4 (d t, $^2J_{FF}$ = 254 Hz, $^3J_{FF}$ = 13 Hz, $1F_\beta$), -153.0 (app t, $^3J_{FF} \approx$ 14 Hz, $1F_\alpha$). Anal. Calc. for $C_{15}H_{10}F_{10}N_2NiO_3S$: C, 32.94, H, 1.84, N, 5.12, S, 5.86. Found: C, 32.69, H, 2.00, N, 5.01, S, 5.72.

3.5.9 Synthesis of $\{(Pyr)(NCCH_3)Ni[CF(Pyr)(CF_2)_3]\}^+(OTf)^-$ (Ni-10c·CH_3CN)

$(Pyr)(OTf)Ni[CF(Pyr)(CF_2)_3]$ **(Ni-10c)** was dissolved in deuterated acetonitrile. ^1H NMR (300 MHz, CD_3CN) δ 1.94 (solvent), 7.49 (br t, $^3J_{HH}$ = 6 Hz, 2H), 7.91 (t, $^3J_{HH}$ = 7 Hz, 1H), 8.13 (t, $^3J_{HH}$ = 7 Hz, 2H), 8.60 (t, $^3J_{HH}$ = 8 Hz, 1H), 8.91 (br d, 2H), 9.59 (d, $^3J_{HH}$ = 6 Hz, 2H). ^{19}F NMR (282 MHz, CD_3CN) δ -63.5 (s, BTB), -79.3 (s, 3F, OTf), -103.5 (br d, $^2J_{FF} \approx$ 263 Hz, $1F_\alpha$), -114.8 (br d, $^2J_{FF} \approx$ 263 Hz, $1F_\alpha$), -126.8 (app d q, $^2J_{FF}$ = 256 Hz, $^3J_{FF}$ = 30 Hz, $^3J_{FF}$ = 15 Hz, $1F_\beta$), -131.6 (d m, $^2J_{FF}$ = 253 Hz, $1F_\beta$), -140.8 (br d, $^2J_{FF}$ = 253 Hz, $1F_\beta$), -142.6 (d m, $^2J_{FP}$ = 256 Hz, $1F_\beta$), -150.7 (v br s, $1F_\alpha$). $^{13}C\{^1H\}$ (75 MHz, CD_3CN) δ 1.3 (solvent), 118.3 (solvent), 126.5 (s, 2C, pyr), 128.8 (d, J_{CF} = 2 Hz, 2C, pyr), 140.2 (s, 1C, pyr), 143.3 (d, J_{CF} = 9 Hz, 2C, pyr), 148.8 (s, 1C, pyr), 150.7 (s, 2C, pyr). High-resolution Electrospray Ionisation; mass calculated for $C_{16}H_{13}NiF_7N_3$ (M^+) 438.0351, found 438.0365. MS [ESI (positive mode), solvent: CH_3CN] *m/z* calcd for $C_{16}H_{13}F_7N_3Ni$ (M^+) 438.0, *m/z* found (% intensity) 438.1 (76%); *m/z* calcd for $C_{13}H_{11}F_7N_3Ni$ (M^+ - Pyr + CH_3CN) 400.0, *m/z* found 400.1 (100%); *m/z* calcd for $C_{11}H_8F_7N_2Ni$ (M^+ - Pyr) 359.0, *m/z* found 359.0 (23%). See Figure A53 for ESI-MS spectrum.

3.5.10 Synthesis of [1,2,4-(S),(Ph_2P),Me(C_6H_3)]Ni[$CF(PPh_3)(CF_2)_3$] (Ni-11a)

NMR scale Ni-11a: $(PPh_3)_2Ni(C_4F_8)$ (**Ni-9a**) (20 mg, 0.03 mmol) was dissolved in a 1:1 mixture of C_6D_6/C_6H_6 (total volume ca. 2 mL). To the solution was added [1,2,4-(HS),(Ph_2P),Me(C_6H_3)]

(dissolved in ca. 2 mL C_6H_6) and the mixture was stirred at RT for 3 h. Integration of product F peaks relative to BTB in the ^{19}F spectrum indicated an 89% yield of **Ni-11a**.

Isolation of Ni-11a: $(PPh_3)_2Ni(C_4F_8)$ (**Ni-9a**) (224 mg, 0.29 mmol) was placed in a 100 mL round-bottom Schlenk flask and dissolved in chlorobenzene (ca. 20 mL). 1,2,4-(HS),(Ph_2P),Me(C_6H_3)] (88 mg, 0.29 mmol) was dissolved in ca. 10 mL of chlorobenzene and added to the $(PPh_3)_2Ni(C_4F_8)$/chlorobenzene solution. A gradual colour change (over 30 min.) from clear yellow to clear bright orange occurred. The reaction mixture was left to stir at RT for 14 h. The clear orange reaction mixture was concentrated in vacuo until 5 mL remained in the flask (cloudy orange). Around 10 mL of hexanes was then added to the round-bottom flask, precipitating a light orange powder. The flask was placed in a -35°C freezer for 16 h. The product was filtered cold, washed with 2 x 2 mL pre-cooled acetonitrile/ 2 x 2 mL pre-cooled hexanes, and dried in vacuo, affording a light orange powder. Yield: 140 mg, 0.17 mmol, 61% based on **(**$PPh_3)_2Ni(C_4F_8)$. X-ray quality crystals were grown by slow evaporation of a saturated solution of **Ni-11a** in benzene. UV-vis (0.7 mM in dichloromethane): $\lambda_{max}(\varepsilon)$ = 377 nm (2814). ^1H NMR (300 MHz, $CDCl_3$) δ 2.04 (s, 3H, CH_3), 6.60 (d, $^3J_{HH}$ = 8 Hz, 1H, Ar-H), 6.74 (m, 2H, Ar-H), 7.26 (solvent), 7.29-7.67 (m, 17H, Ar-H), 7.90 (d d d, $^3J_{HP}$ = 12 Hz, $^3J_{HH}$ = 8 Hz, $^3J_{HH}$ = 2 Hz, 2H, Ar-H), 8.13 (d d, $^3J_{HP}$ = 12 Hz, $^3J_{HH}$ = 8 Hz, 6H, Ar-H). ^{19}F NMR (282 MHz, $CDCl_3$) δ -63.5 (s, BTB), -94.7 (d m, $^2J_{FF}$ = 282 Hz, $1F_\alpha$), -108.3 (d d d d, $^2J_{FF}$ = 282 Hz, $^3J_{FP}$ = 57 Hz, $^3J_{FF}$ = 22 Hz, $1F_\alpha$), -109.3 (d m, $^2J_{FF}$ = 267 Hz, $1F_\beta$), -126.1 (d m, $^2J_{FF}$ = 267 Hz, $1F_\beta$), -129.0 (d m, $^2J_{FF}$ = 245 Hz, $1F_\beta$), -136.3 (d m, $^2J_{FF}$ = 245 Hz, $1F_\beta$), -203.1 (d d d, $^2J_{FP}$ = 65 Hz, $^3J_{FF}$ = 36 Hz, $1F_\alpha$).). $^{31}P\{^1H\}$ (121 MHz, $CDCl_3$) δ 17.3 (d m, $^2J_{PF}$ = 65 Hz, 1P, C_α-P), 54.3 (d m, $^3J_{PF}$ = 57 Hz, 1P, Ni-P). Repeated elemental analysis resulted in low % Carbon for **Ni-11a**. Anal. Calc. for $C_{41}H_{31}F_7NiP_2S$: C, 60.84, H, 3.86, S, 3.96. Found: C, 59.65, H, 3.90, S, 3.94. High-resolution Electrospray Ionisation; mass calculated for $C_{41}H_{32}SNiP_2F_7$ ($M + H^+$) 809.0942, found 809.0920. MS [ESI (positive mode), solvent: CH_3CN] *m/z* calcd for $C_{41}H_{31}SNiP_2F_7K$ ($M + K^+$) 847.1, *m/z* found (% intensity) 847.2 (32%); *m/z* calcd for $C_{41}H_{31}SNiP_2F_6$ $(M - F)^+$ 789.1, *m/z* found 789.3 (34%).

3.5.11 Synthesis of [1,2,4-(S),(Ph_2P),Me(C_6H_3)]Ni[CF(PPh_2Me)(CF_2)$_3$] (Ni-11b)

NMR scale Ni-11b: (PPh_2Me)$_2$Ni(C_4F_8) (**Ni-9b**) (15 mg, 0.023 mmol) was dissolved in a minimum amount (ca. 3 mL) of chlorobenzene. [1,2,4-(HS),(Ph_2P),Me(C_6H_3)] (8 mg, 0.025 mmol) was dissolved in ca. 4 mL of cholorobenzene and transferred to the vial containing the (PPh_2Me)$_2$Ni(C_4F_8)/chlorobenzene solution. After stirring at RT for 15 h the colour had changed from bright clear yellow to clear orange-yellow. Integration of product F peaks relative to BTB in the ^{19}F spectrum indicated 92% yield of **Ni-11b**.

Isolation of Ni-11b: (PPh_2Me)$_2$Ni(C_4F_8) (**Ni-9b**) (250 mg, 0.38 mmol) was placed in a 100 mL round-bottom Schlenk flask and dissolved in chlorobenzene (ca. 20 mL). 1,2,4-(HS),(Ph_2P),Me(C_6H_3)] (123 mg, 0.40 mmol) was dissolved in ca. 15 mL of chlorobenzene and added to the (PPh_2Me)$_2$Ni(C_4F_8)/chlorobenzene solution. A gradual colour change (over 30 min.) from clear yellow to cloudy bright yellow occurred. The reaction mixture was left to stir at RT for 14 h. The clear deep orange reaction mixture was concentrated and dried in vacuo for 2 h, leaving a yellow solid. The product was dissolved/suspended in ca. 5 mL of acetonitrile. The flask was placed in a -35°C freezer for 16 h. The product was filtered cold, washed with 3 x 3 mL pre-cooled hexanes, and dried in vacuo, affording a dark yellow powder. Yield: 165 mg, 0.22 mmol, 58% based on **(**PPh_2Me)$_2$Ni(C_4F_8). X-ray quality crystals were grown by gradual cooling of a supersaturated solution of **Ni-11b** in dichloromethane. UV-vis (0.7 mM in chloromethane): $\lambda_{max}(\varepsilon)$ = 374 nm (1332). ^{1}H NMR (300 MHz, $CDCl_3$) δ 2.07 (s, 3H, CH_3), 2.78 (d d, $^3J_{HP}$ = 14 Hz, $^3J_{HH}$ = 2 Hz, 3H, CH_3), 6.64 (d, $^3J_{HH}$ = 8 Hz, 1H, Ar-H), 6.84 (d m, $^3J_{HH}$ = 8 Hz, 1H, Ar-H), 7.15 (d d, $^3J_{HH}$ = 8 Hz, $^3J_{HH}$ = 3 Hz, 1H, Ar-H), 7.25-7.68 (ov m, 16H, Ar-H/solvent), 7.89 (d d, 2H, Ar-H), 8.18 (d d, $^3J_{HP}$ = 13 Hz, $^3J_{HH}$ = 8 Hz, 2H, Ar-H). ^{19}F NMR (282 MHz, CD_3CN) δ -63.5 (s, BTB), -94.1 (d m, $^2J_{FF}$ = 283 Hz, 1F$_\alpha$), -107.5 (d d d d, $^2J_{FF}$ = 283 Hz, $^3J_{FP}$ = 55 Hz, $^3J_{FF}$ = 21 Hz, 1F$_\alpha$), -111.3 (d m, $^2J_{FF}$ = 272 Hz, 1F$_\beta$), -128.1 (d m, $^2J_{FF}$ = 272 Hz, 1F$_\beta$), -130.0 (d m, $^2J_{FF}$ = 245 Hz, 1F$_\beta$), -135.9 (d m, $^2J_{FF}$ = 245 Hz, 1F$_\beta$), -202.0 (d d d, $^2J_{FP}$ = 75 Hz, $^3J_{FF}$ = 36 Hz, $^3J_{FF}$ = 12 Hz, 1F$_\alpha$). ^{31}P{^{1}H} (121 MHz, CD_3CN) δ 23.0 (d d

d, $^{2}J_{PF}$ = 75 Hz, $^{3}J_{PF}$ = 28 Hz, $^{3}J_{PF}$ = 10 Hz, 1P, C_{α}-P), 53.5 (d m, $^{3}J_{PF}$ = 55 Hz, 1P, Ni-P). Anal. Calc. for $C_{36}H_{29}F_{7}NiP_{2}S$: C, 57.86, H, 3.91, S, 4.29. Found: C, 57.84, H, 3.98, S, 4.00.

3.5.12 Synthesis of [1,2,4-(S^{-}),(Ph_2P),Me(C_6H_3)]Ni(C_4F_8)(Na)(18-Crown-6) (Ni-12)

[1,2,4-(HS),(Ph_2P),Me(C_6H_3)] (130 mg, 0.42 mmol) was placed in a 100 mL round-bottom flask and dissolved in THF (ca. 10 mL). NaO^{t}Bu (40 mg, 0.42 mmol) was added to the [1,2,4(HS),(Ph_2P),Me(C_6H_3)]/THF solution. An immediate colour change from clear to a very pale yellow occurred. After 15 minutes of stirring at room temperature, **(**$PPh_3)_2$Ni(C_4F_8) (330 mg, 0.42 mmol) was added to the mixture. An immediate colour change to clear bright yellow was observed. Immediately after, one equivalent of 18-Crown-6 was added to the flask (111 mg, 0.42 mmol). The reaction mixture was left to stir at RT for 18 h. The yellow-green reaction mixture was concentrated in vacuo until 10 mL solution remained in the flask (precipitate already beginning to form). Around 10 mL of hexanes was then added, precipitating a bright yellow powder. The flask was placed in a -35°C freezer for 4 h. The product was filtered cold, washed with pre-cooled hexanes (3 x 3 mL), and dried in vacuo, affording a bright yellow powder. Yield: 319 mg, 0.37 mmol, 89% based on **(**$PPh_3)_2$Ni(C_4F_8). UV-vis (0.7 mM in dichloromethane): $\lambda_{max}(\varepsilon)$ = 386 nm (1176) (shoulder on off-scale signals in the UV range). ^{1}H NMR (300 MHz, CD_3CN) δ 1.94 (solvent), 2.08 (s, 3H, Me), 3.57 (s, 24H, 18-Crown-6), 6.74 (br d, J_{HP} = 7 Hz, 1H, Ar-H), 6.90 (br d, J_{HH} = 8 Hz, 1H, Ar-H), 7.22 (br dd, J_{HH} = 8 Hz, J_{HP} = 3 Hz, 1H, Ar-H), 7.37-7.52 (m, 6H, Ar-H), 7.64-7.74 (m, 4H, Ar-H). ^{19}F NMR (282 MHz, CD_3CN) δ –63.5 (s, BTB), -100.0 (d, $^{3}J_{FP}$ = 27 Hz, 2F), -107.3 (d, $^{3}J_{FP}$ = 25 Hz, 2F), -138.6 (m, 4F). ^{31}P{^{1}H} (121 MHz, CD_3CN) δ 48.7 (m, J_{PF} = 27 Hz, 25 Hz, 1P). Anal. Calc. for $C_{35}H_{40}F_{8}NaNiO_{6}PS$: C, 49.26, H, 4.72, S, 3.76. Found: C, 49.27, H, 4.78, S, 3.91.

3.5.13 NMR scale reaction of Ni-12 with [$HPPh_3$](Br)

[1,2,4-(S),(Ph_2P),Me(C_6H_3)]Ni(C_4F_8)(Na)(18-Crown-6) (25 mg, 0.029 mmol) **(Ni-12)** was dissolved in ca. 1 mL DCM and transferred to a vial containing [$HPPh_3$](Br) (10 mg, 0.029 mmol) dissolved /suspended in ca. 1 mL DCM. Initial colour of reaction mixture was a clear bright yellow. After stirring at RT for 4 h the colour had changed to clear orange-yellow. Integration of product F

peaks relative to BTB in the ^{19}F spectrum indicated 91% yield of **Ni-11a** (^{19}F NMR indicates ca. 8% of what we propose to be the other regioisomer, with C_α−P *trans* to S).

3.5.14 NMR scale reaction of Ni-12 with [HPPh$_2$Me](Br)

[1,2,4-(S),(Ph_2P),Me(C_6H_3)]Ni(C_4F_8)(Na)(18-Crown-6) (27 mg, 0.032 mmol) **(Ni-12)** was dissolved in ca. 1 mL DCM and transferred to a vial containing [$HPPh_2Me$](Br) (9 mg, 0.032 mmol) dissolved /suspended in ca. 1 mL DCM. Initial colour of reaction mixture was a clear yellow. After stirring at RT for 16 h the colour had changed to clear orange-yellow. Integration of product F peaks relative to BTB in the ^{19}F spectrum indicated 78% yield of **Ni-11b** (^{19}F NMR indicates ca. 15% of what we propose to be the other regioisomer, with C_α−P *trans* to S).

3.5.15 Reaction of Ni-9c with [P,SH]

($Pyr)_2Ni(C_4F_8$) (80 mg, 0.19 mmol) **(Ni-9c)** was dissolved in ca. 6 mL chlorobenzene and transferred to a 50 mL RB Schlenk flask containing [1,2,4-(HS),(Ph_2P),Me(C_6H_3)] (118 mg, 0.38 mmol) dissolved in ca. 6 mL chlorobenzene. An immediate colour change to bright clear yellow was followed by a gradual colour change over 5 minutes to a deep clear red-orange. After stirring at RT for ca. 6 h, integration of product F peaks relative to BTB in the ^{19}F spectrum (average of three separate experiments) indicated a 48% yield of **Ni-13** based on ($Pyr)_2Ni(C_4F_8$) as well as the presence of **Ni-14** by $^{31}P\{^1H\}$ NMR. **Ni-13** was not isolated but was characterized by its ^{19}F and $^{31}P\{^1H\}$ spectra: ^{19}F NMR (282 MHz, C_6H_5Cl with C_6D_6 capillary) δ -63.5 (s, BTB), -94.3 (d m, $^2J_{FF}$ = 288 Hz, $1F_\alpha$), - 107.6 (d d d, $^2J_{FF}$ = 288 Hz, $^3J_{FP}$ = 46 Hz, $^3J_{FF}$ = 19 Hz, $1F_\alpha$), -124.4 (d m, $^2J_{FF}$ = 251 Hz, $^3J_{FF}$ = 18 Hz, $1F_\beta$), -128.5 (d m, $^2J_{FF}$ = 250 Hz, $1F_\beta$), -141.4 (d m, $^2J_{FF}$ = 251 Hz, $1F_\beta$), -143.1 (ov m, $1F_\beta$, $1F_\alpha$). $^{31}P\{^1H\}$ (121 MHz, C_6H_5Cl with C_6D_6 capillary) δ 54.0 (d, $^3J_{PF}$ = 46 Hz, 1P, Ni-P). Cooling an acetonitrile solution resulted in precipitation of X-ray quality crystals of **Ni-14**, isolated as green cubic crystals. $^{31}P\{^1H\}$ (121 MHz, C_6D_6) δ 52.9 (s, 2P).

3.6 References

[1] a) Chambers, R.D. *Fluorine in Organic Chemistry, 2nd Ed.*; Blackwell: Oxford, **2004**. (b) Kirsch, P. *Modern Fluoroorganic Chemistry: Synthesis, Reactivity, Applications, 1st ed.*; Wiley-VCH: Weinheim, Germany, **2004**.

[2] Campbell, M. G.; Hoover, A. J.; Ritter, *Top. Organomet. Chem.*, **2015**, *52*, 1.

[3] (a) Tomashenko, O. A.; Grushin, V. V. *Chem. Rev.*, **2011**, *111*, 4475. (b) Zhu, W.; Wang, J.; Wang, S.; Gu, Z.; Aceña, J. L.; Izawa, K.; Liu, H.; Soloshonok, V. A. *J. Fluor. Chem.* **2014**, *167*, 37 and reference therein.

[4] Chen, B.; Vicic, D. A. *Top. Organomet. Chem.*, **2015**, *52*, 113.

[5] (a) Zhou, Q.; Huang, Y. *J. Fluor. Chem.*, **1988**, *39*, 87. (b) Kamigata, N.; Ohtsuka, T.; Fukushima, T.; Yoshida, M.; Shimizu, T. *J. Chem. Soc. Perkin Trans. 1*, **1994**, 1339. (c) Baker, R. T.; Beatty, R. P.; Farnham, W. B.; Wallace, R. L. Jr. *PCT Int. Appl.* **1997**, U.S Patent 5,670,679, E. I. Du Pont de Nemours & Co., USA. (d) Popov, I.; Lindeman, S.; Daugulis, O. *J. Am. Chem. Soc.*, **2011**, *133*, 9286. (e) Loy, R. N.; Sanford, M. S. *Org. Lett.*, **2011**, *13*, 2548. (f) Litvinas, N. D.; Fier, P. S.; Hartwig, J. F. *Angew. Chem. Int. Ed.*, **2012**, *51*, 536; *Angew. Chem.*, **2012**, *124*, 551. (g) Zatolochnaya, O. V.; Gevorgyan, V. *Org. Lett.*, **2013**, *15*, 2562. (h) Ogoshi, S.; Kikushima, K.; Taniguchi, T.; Kawashima, T.; Ohashi, M. *Organometallics*, **2015**, *34*, 1604. (i) Ogoshi, S.; Kikushima, K.; Shirataki H.; Ohashi, M. *J. Am. Chem. Soc.*, **2015**, *137*, 6496.

[6] (a) Siegle, J. C.; Muus, L. T.; Lin, T. P.; Larsen, H. A. *J. Polym. Sci., Part A : Polym. Chem.* **1964**, *2*, 391. (b) Lonfei, J.; Jingling, W.; Shuman, X. *J. Anal. Appl. Pyrol.* **1986**, *10*, 99. (c) Meissner, E.; Wróblewska, A.; Milchert, E. *Polym. Degrad. Stab.* **2004**, *83*, 163. (d) Bhadury, P. S.; Singh, S.; Sharma, M.; Palit, M. *J. Anal. Appl. Pyrol.* **2007**, *78*, 288.

[7] (a) Green, M.; Osborn, R. B. L.; Rest, A. J.; Stone, F. G. A. *J. Chem. Soc. (A)* **1968,** 2525. (b) Ashley-Smith, J.; Green, M.; Stone, F. G. A. *J. Chem. Soc. (A)* **1969,** 3019. (c) Browning, J.; Cundy, C. S.; Green, M.; Stone, F. G. A. *J. Chem. Soc. (A)* **1969,** 20. (d) Cundy, C. S; Green, M.; Stone, F. G. A. *J. Chem. Soc. (A)* **1970,** 1647. (e) Greco, A.; Green, M.; Shakshooki, S. K; Stone, F.

G. A. *J. Chem. Soc. (D)* **1970,** 1374. (f) Kaschube, W.; Schröder, W.; Pörschke, K. R.; Angermund, K.; Krüger, C. *J. Organomet. Chem.* **1990**, *389*, 399. (g) Schröder, W.; Bonrath, W.; Pörschke, K. R. *J. Organomet. Chem.* **1991**, *408*, C25-C29. (h) Stone, F. G. A., *J. Fluor. Chem.* **1999**, *100*, 227. (i) Ohashi, M.; Shibata, M.; Saijo, H.; Kambara, T.; Ogoshi, S. *Organometallics* **2013**, *32*, 3631.

[8] Burch, R. R; Calabrese, J. C.; Ittel, S. D. *Organometallics* **1988**, *7*, 1642.

[9] N. O Andrella, A. J. Sicard, S. I. Gorelsky, I. Korobkov amd R. T. Baker, *Chem. Sci.*, 2015, DOI: 10.1039/C5SC01886B.

[10] Giffin, K. A.; Harrison, D. J.; Korobkov, I.; Baker, R. T. *Organometallics* **2013**, *32*, 7424.

[11] (a) Arbusow, B. A. *Pure Appl. Chem.* **1964**, *9*, 307. (b) Bhattacharya, A. K.; Thyagarajan, G. *Chem. Rev.* **1981**, *81*, 415.

[12] (a) Block, E.; Ofori-Okai, G. *Inorg. Chim. Acta* **1991**, *188*, 7. (b) Pérez-Lourido, P.; Romero, J.; García-Vázquez, J. A.; Sousa, A.; Zubieta, J.; Maresca, K. *Polyhedron* **1998**, *17*, 4457. (c) Canseco-González, D.; Gómez-Benítez, V.; Hernández-Ortega, S.; Toscano, R. A.; Morales-Morales, D. *J. Organomet. Chem.* **2003**, *679*, 101. d) She, L.; Li, X.; Sun, H.; Ding, J.; Frey, M.; Klein, H. *Organometallics* **2007**, *26*, 566. e) Kraikivskii, P. B.; Frey, M.; Bennour, H. A.; Gembus, A.; Hauptmann, R.; Svoboda, I.; Fuess, H.; Saraev, V. V.; Klein, H. *J. Organomet. Chem.* **2009**, *694*, 1869.

[13] (a) Kiplinger, J. L.; Richmond, T. G.; Osterberg, C. E. *Chem. Rev.* **1994**, *94*, 373 and references therein. (b) Garratt, S. A.; Hughes, R. P.; Kovacik, I.; Ward, A. J.; Willemsen, S.; Zhang, D. *J. Am. Chem. Soc.* **2005**, *127*, 15585. (c) Torrens, H.; *Coord. Chem. Rev.* **2005**, *249*, 1957. (d) Hughes R. P. *Eur. J. Inorg. Chem.* **2009**, *2009*, 4591. (e) Hughes, R. P. *J. Fluor. Chem.* **2010**, *131*, 1059. (f) Ahrens, T.; Kohlmann, J.; Ahrens, M.; Braun, T. *Chem. Rev.* **2015**, *115*, 931 and references therein.

[14] (a) Bain, A.D. *Prog. Nucl. Mag. Res. Sp.* **2003**, *43*, 63. (b) Bain, A. D.; *Ann. Rev. NMR Spect.* **2008**, *63*, 23.

[15] Lambert, J. B.; So, J. *J. Org. Chem.* **1991**, *56*, 5960.

[16] This intermediate is potentially observed by ^{19}F NMR in THF.

[17] (a) Frensdorff, H. K. *J. Am. Chem. Soc.* **1971**, *93*, 600. (b) Christensen, J. J.; Eatough, D. J.; Izatt, R. M. *Chem. Rev.* **1974**, *74*, 351.

[18] Nöth, H.; Warchhold, M. *Eur. J. Inorg. Chem.* **2004**, 1115.

[19] Harrison, D. J.; Lee, G. M.; Leclerc, M. C.; Korobkov, I.; Baker, R. T. *J. Am. Chem. Soc.* **2013**, *135*, 18296.

[20] Xu, W.; Sun, H.; Xiong, Z.; Li, X. *Organometallics* **2013**, *32*, 7122.

[21] APEX Software Suite v.2010; Bruker AXS: Madison, WI, **2005**.

Chapter 4. Hydrofluoronickelacycles: Ligand Effects on Regio-/Stereo-Selectivity and Reactivity

4.1 Published Contributions

Generation of Hydrofluoronickelacycles from Trifluoroethylene and Ni(0): Ligand Effects on Regio-/Stereoselectivity and Reactivity

K. A. Giffin, L. A. Pua, S. Piotrkowski, B. M. Gabidulin, I. Korobkov, R. P. Hughes and R. T. Baker *J. Am. Chem. Soc.* **2017**, *139*, 4075.

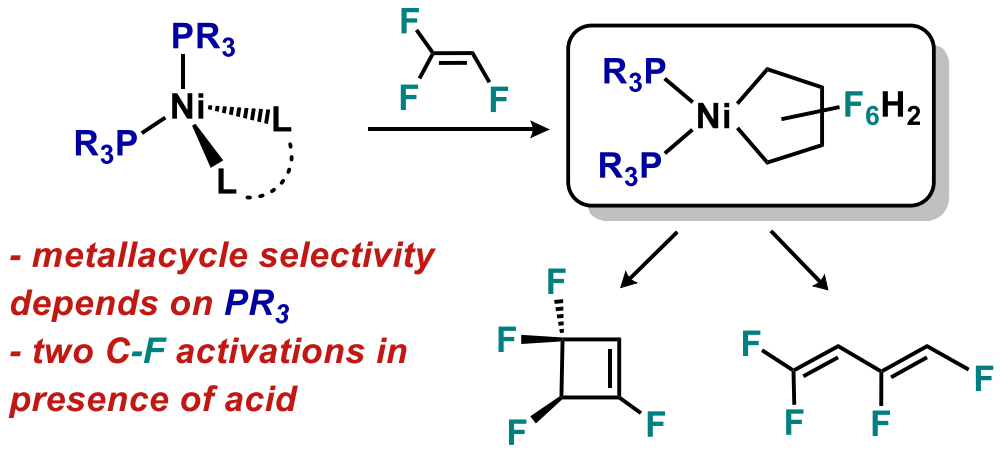

Author Contributions

Giffin and Baker wrote the manuscript. Giffin performed all experiments presented. Pua and Piotrkowski performed preliminary experimental studies under the supervision of Giffin. Korobkov and Gabidulin were responsible for X-ray diffraction studies. Hughes was responsible for DFT studies presented.

Abstract

Treatment of Ni(0) complexes with sub-atmospheric pressures of trifluoroethylene (TrFE) affords hydrofluoronickelacyclopentanes $L_2Ni(C_4F_6H_2)$ (L = PPh_3, $P(O\text{-}o\text{-}tol)_3$, PPh_2Me, $PPhMe_2$, PMe_3). Fluorine NMR analysis demonstrates predominant formation of three (of the possible six) isomers upon oxidative cycloaddition of TrFE: the *cis* and *trans* head-tail isomers and the *trans* head-head isomer, where the CHF group is defined as the TrFE "head". The respective ratios of $L_2Ni(C_4F_6H_2)$

isomers are influenced by the nature of L with smaller phosphines favouring the thermodynamically preferred (from DFT calculations) *trans* head-head isomer (cf. 50% with PMe_3) and the largest affording small amounts of the tail-tail isomers. Lewis and Brønsted acids induce a surprising double C−F bond activation in $L_2Ni(C_4F_6H_2)$ (L = PPh_2Me, $PPhMe_2$), affording small functionalized hydrofluoroalkenes. Interestingly, varying the acid employed dictates the organic product obtained from the head-tail isomers: BF_3•OEt_2 is selective for 1,1,2,3-tetrafluorocyclobutene, whereas Me_3SiOTf and *N,N*-dimethylanilinium bromide yield (*Z,E*)-1,1,3,4-tetrafluorobutadiene as the major fluorinated product. Reaction intermediates were isolated and possible pathways are discussed.

4.2 Introduction

Transition metal-mediated synthesis of fluorinated organic compounds has developed over the past two decades into an invaluable approach for obtaining new value-added fluorocarbons (FCs).[1] FCs find value in a multitude of applications; specifically, small highly fluorinated organics are desirable for use as anesthetics, refrigerants, blowing agents, surfactants and as treatments for various materials to impart water/oil-repellent properties. The strength of C−F compared to C−H bonds (ca. 480 vs. ca. 400 kJ/mol) accounts for the inertness and persistence of FCs in the environment.[2] The latter issue has initiated a major industry shift towards the use of shorter fluoroalkyl chains (i.e. C^F_4), known to be less persistent (and arguably less toxic), to replace their longer chain predecessors (e.g., perfluorooctanoic acid).[3] Another recent change in the fluorochemical industry has been the replacement of hydrofluoroalkanes (known global warming contributors) with new hydrofluoroalkene refrigerants with significantly reduced global warming potential.[4] Environmental concerns with synthetic routes common to FC synthesis stimulate interest in the development of less energy-intensive and more atom economical routes for C^F_4 and HFO production. Moreover, the synthesis of novel small-molecule functionalized FCs that maintain the beneficial properties of FCs and decrease their toxicity/persistence is highly desired.[5]

The oxidative cyclization of unsaturated substrates at M(0) centres to form metallacyclic intermediates is an indispensable technique for atom economical C-C bond forming catalytic processes (cf. selective ethylene oligomerization to 1-hexene or 1-octene).[6] One approach to new highly fluorinated organics is to derivatize fluorometallacycles selectively at a transition metal centre prior to release from the metal.[7] For example, Baker et al. demonstrated nickel phosphite complex-catalyzed hydrodimerization of two molecules of tetrafluoroethylene (TFE) or one molecule of TFE with one of ethylene, affording octafluorobutane or 1,1,2,2-tetrafluorobutane, respectively (Scheme 4.1a).[8] More recently, Ogoshi et al. reported the nickel-catalyzed co-cyclization of TFE and ethylene, yielding 5,5,6,6-tetrafluoro-1-hexene (Scheme 4.1b).[9] Additionally, nickel IPr complexes effected the catalytic co-cyclization of TFE, ethylene and aldehydes was demonstrated, generating new fluorine-containing ketones (IPr = (1,3-bis(2,6-diisopropylphenyl)imidazole-2-ylidene), Scheme 4.1c).[10] These highlighted catalytic processes rely on the oxidative cyclization reaction to afford key nickelacyclopentane intermediates. As a result, we are exploring the reactivity of less studied HFAs with low-valent metal centres. In this initial report, we detail the synthesis and reactivity of new partially fluorinated nickelacycles, generated from trifluoroethylene (TrFE).

Scheme 4.1. Nickel-catalyzed routes to C_4-C_6 functionalized fluorocarbons.

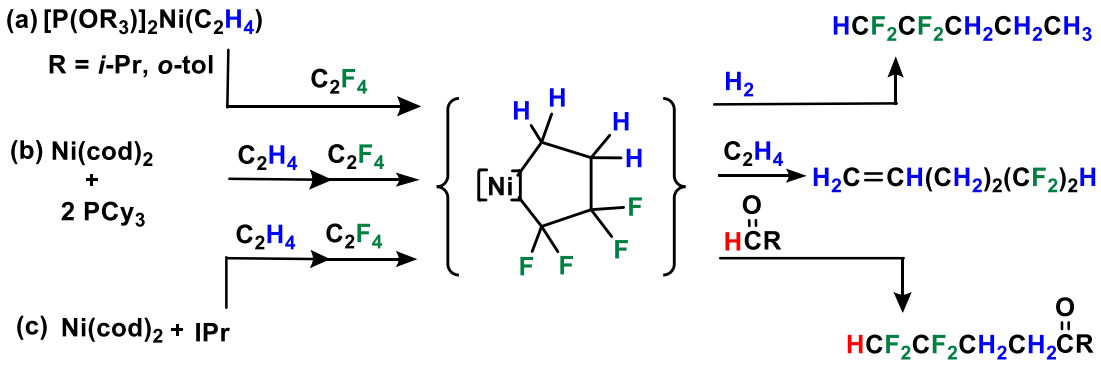

Stone et al. reported previously the oxidative cyclization of TrFE with $Ni(PPh_2Me)_4$ and $(PPh_3)_2Ni(C_2H_4)$ to give $L_2Ni(C_4F_6H_2)$ (Scheme 4.2a, left).[11] The 5-membered nickelacycles were characterized by elemental analysis, melting point, and although NMR spectral data were not provided, they were proposed to be a mixture of isomers based on their complex ^{19}F NMR spectra. Two Ni TrFE complexes with the tridentate ligands $[MeC(CH_2EPh_2)_3]$ (E = P, tpame; As, tdame; Scheme 4.2a, right) have also been prepared.[12] Notably, the P analogue was unstable in the solid state, decomposing readily in solution in the absence of an excess of TrFE. In contrast, the As analogue is stable in the solid state and reacts with excess TrFE to presumably form a mixture of 5-membered nickelacycles, although these were only described as having complex ^{19}F NMR that could not be analyzed due to solubility issues. Finally, Cowie and co-workers have done extensive studies on the reactivity of C_2F_3H-bridged di-iridium complexes, including examples of C−F bond activation using a stoichiometric amount of Lewis acid (Scheme 4.2b).[13]

Scheme 4.2 Reported Ni TrFE complexes and metallacyclopentanes (a) and the Lewis acid reactivity of a TrFE- bridged diiridium complex (b).

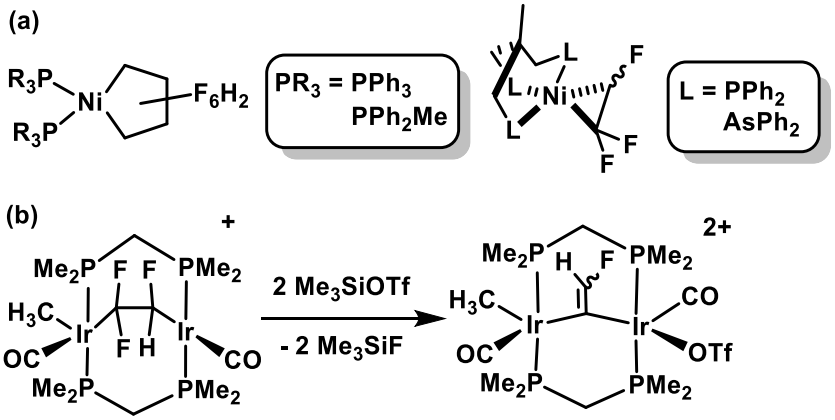

Owing to the reduced symmetry of TrFE vs. TFE, there are six potential nickelacyclopentane isomers that could form upon oxidative cyclization (Chart 4.1). We present herein the effects of ancillary ligand variation on the nature of the nickelacycle formed (3- vs. 5-membered), as well as the regio-/stereoselectivity and reactivity of the ensuing nickelacyclopentanes.

Chart 4.1 Potential nickelacyclopentane regio-/stereoisomers from oxidative cyclization of TrFE.

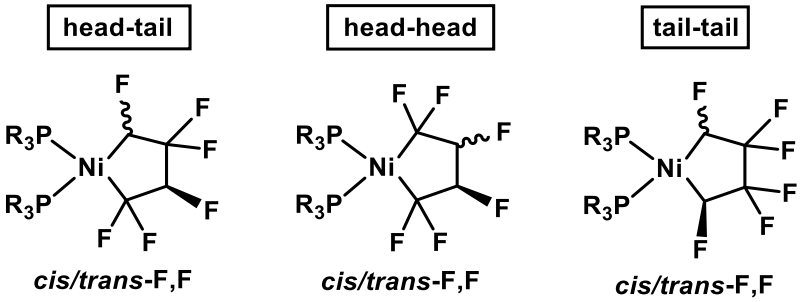

4.3 Results and Discussion

4.3.1 Synthesis and Characterization of Hydrofluoronickelacycle Complexes.

Treatment of Ni(0) complexes **Ni-15a,c,d** and **e** (generated from $Ni(cod)_2$ + 2 equiv of L = PPh_3, **Ni-15a**, PPh_2Me, **Ni-15c**, $PPhMe_2$, **Ni-15d**, or PMe_3, **Ni-15e**), with ~ 7 psi of TrFE at room temperature in toluene gave quantitative conversion (by $^{31}P\{^1H\}$ NMR) to Ni(II) 5-membered metallacycles **Ni-16a,c,d** and **e** (cod = 1,5-cyclooctadiene; Table 4.1). Under an excess of TrFE (~ 12 psi), tetrakis(phosphite)nickel complex **Ni-15b** afforded 80% conversion to product **Ni-16b** as indicated by quantitative NMR yield. On the basis of ^{19}F NMR spectroscopic analysis, it is concluded that oxidative cyclization at Ni(0) is largely selective towards the formation of three nickelacyclopentane isomers: the *cis* and *trans* head-tail isomers and the *trans* head-head isomer, where the CHF group is defined as the TrFE "head". The less-favored tail-tail isomers are observed only for the bulkiest phosphorus ligands. We note first that the effect of the increased π-acidity associated with phosphite ligand in **Ni-15b** (vs. PPh_3 **Ni-15a**) was to increase the *trans* head-head isomer at the expense of the *trans* head-tail isomer. Note that the steric properties of these ligands are similar (cone angle for $P[(O\text{-}o\text{-}tol)_3]$ = 141° and PPh_3 = 145°).[14] On progressing to less bulky phosphines (**Ni-15c,d,e**) by successive replacement of Ph by Me, however, minor amounts of the tail-tail isomers are no longer detected and the ratio of the *trans* head-head isomer to the head-tail isomers

increases from 0.2 (PPh_3) to 0.3, 0.4 and to 1.0 for PMe_3. Preliminary studies with (oxydi-2,1-phenylene)bis(diphenylphosphine) (DPEPhos) show quantitative conversion to the same three major isomers, indicating that bidentate ligands follow the same trend as the monodentate ligands studied herein.[15] DFT (B3LYP-D3/LACV3P**) calculations for the systems $L_2Ni(C_2F_3H) + C_2F_3H$, with L = PMe_3 and PPh_3 (Table 4.2), indicate that metallacycle formation is strongly downhill energetically and unlikely to be reversible under the experimental conditions. While the experimentally observed regiochemistry does reflect the relative thermodynamic stabilities of the metallacyclic isomers for L = PMe_3, the same is not the case for L = PPh_3, suggesting that the product ratios are likely those of kinetic control in the cyclization mechanism. Leaving a C_6D_6 solution of **Ni-16c** in a J Young tube under ~ 7 psi of TrFE at room temperature for 18 h results in no change in the isomer ratios. Moreover,

Table 4.1 Phosphorus ligand effects on selectivity of hydrofluoronickelacyclopentane formation.[a]

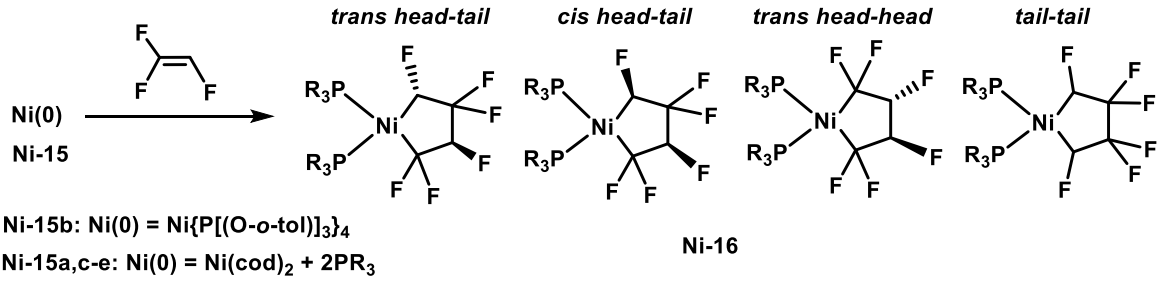

Product	PR_3	Cone Angle	Yield (%)[a]	*Cis h-t (%)*	*Trans h-t (%)*	*Trans h-h (%)*	Tail-tail *(%)*[b]
Ni-16a	PPh_3	145	64	53	25	17	4
Ni-16b	$P(O\text{-}o\text{-}tol)_3$	141	80[c]	53	20	21	6
Ni-16c	PPh_2Me	136	87	53	25	20	2
Ni-16d	$PPhMe_2$	122	83	50	21	28	0
Ni-16e	PMe_3	118	87	38	13	49	0

[a] Yield of isolated product; isomer mix was determined by ^{19}F NMR integration. [b] Both isomers of this minor product were characterized by ^{19}F NMR. [c] Yield estimated by relative integration of product peaks with hexafluorobenzene in the ^{19}F NMR spectrum.

heating the $PPhMe_2$ metallacycle **Ni-16d** at 80°C in C_6D_6 under N_2 for 24 h provided no evidence of isomerization and only a minor amount of decomposition.

The nickelacyclopentane isomers of all **Ni-16** complexes were characterized by multinuclear NMR spectroscopy. Both the *cis* and *trans* head-tail isomers contain no mirror plane (C_s symmetric) and therefore six unique fluorine peaks are observed for each isomer in the ^{19}F NMR spectrum. The *cis* arrangement of the major head-tail stereoisomer is supported by a 2D ^{19}F-^{19}F NOESY experiment (Figure A14). The *trans* head-head and tail-tail isomers each display three unique fluorine resonances, owing to the presence of a C2 axis, with the geminal coupling between the $C_\alpha F_2$ fluorines of the head-head isomer arising from the presence of a chiral centre in the adjacent position ($C_\beta FH$). Surprisingly, there is a large enough chemical shift difference between each fluorine in the three observed major isomers, resulting in fifteen unique fluorine environments in the ^{19}F and $^{19}F\{^1H\}$ NMR spectra of all **Ni-16** complexes (excluding the minor tail-tail resonances). Correlations between fluorines for each isomer were confirmed using 2D ^{19}F-^{19}F COSY experiments (Figures A15-A17). Consistent with

Table 4.2 DFT calculated (B3LYP-D3/LACV3P) relative free energies (kcal/mol) of hexafluoro-nickelacyclopentane isomers.**

	Relative G	Relative G of metallacycle isomers	Relative G	Relative G of metallacycle isomers
	L = PMe_3		L = PPh_3	
$L_2Ni(CF_2CFH)$ + CF_2CFH	0.0		0.0	
Trans head-head (F equatorial)	-28.1	0.0	-24.6	0.0
Cis head-head	-27.2	0.8	-20.5	4.2
Trans head-head (F axial)	-26.3	1.8	-24.6	0.0
Trans head-tail	-24.8	3.3	-19.4	5.2
Cis head-tail	-24.6	3.5	-23.0	1.6
Trans tail-tail	-24.3	3.8	-19.8	4.9
Cis tail-tail	-22.8	5.3	-24.3	0.3

previously reported NMR assignments of perfluoronickelacycles,[16] the $C_\alpha F_2$ signals of hydrofluoronickelacycle isomers appear downfield in the ^{19}F NMR with chemical shifts and geminal coupling constants ranging from δ_F = -83 to -106 and $^2J_{FF}$ = 251-278 Hz. The $C_\beta F_2$ resonances, including $C_\beta F_2$ signals associated with the tail-tail isomers, appear further upfield, displaying shifts ranging from δ_F = -107 to -131 with smaller geminal coupling constants $^2J_{FF}$ = 218-242 Hz. The $C_\alpha FH$ and $C_\beta FH$ fluorines are shifted drastically further upfield at δ_F = -201 to -228. Geminal coupling constants between the fluorine and proton of the *cis* and *trans* head-tail metallacycles are not very dependent on the position of the fluorine (C_α vs. C_β), exhibiting a narrow range of values ($^2J_{FH}$ = 47-50 Hz), whereas $C_\beta FH$ fluorines of the *trans* head-head isomers have larger coupling constants ($^2J_{FH}$ = 57-59 Hz). The $C_\alpha FH$ fluorines of the tail-tail isomers in **Ni-16a,b** and **c** appear as complex multiplets owing to their coupling with phosphorus, proton and $C_\beta F_2$ fluorines. For **Ni-16a,b,c** and **d**, the $^{31}P\{^1H\}$ NMR resonances of all three metallacycles appear as overlapping multiplets, however **Ni-16e** exhibits an apparent broad singlet (Δ□1/2 = 73 Hz) in the $^{31}P\{^1H\}$ NMR spectrum due presumably to nearly identical chemical shifts for the inequivalent phosphine ligand.

Likewise, the ^1H NMR spectra reveal overlapping peaks (integrating to 2H relative to other proton peaks) in the chemical shift range from ca. δ 4.5 to 6 for the metallacyclic protons of all three isomers (the ^1H NMR spectrum for **Ni-16e** is shown in Figure 4.1c). Further NMR experiments for complexes **Ni-16c,d** and **e** were performed to decipher each unique metallacycle proton signal. The 1D ^1H detected ^1H-^{19}F HOESY NMR spectra were obtained to provide NOE correlations by sequentially using a selective pulse on each type of fluorine in the $C_\alpha FH$ and $C_\beta FH$ region (δ_F = -201 to -228).[17] The upfield region of the 1D ^{19}F spectrum for complex **Ni-16e** is depicted in Figure 4.1a. Only strong NOEs were observed for the proton geminal to the fluorine that was being selectively irradiated (Figure 4.1b). The correlation between each proton and its associated geminal fluorine was also corroborated with 2D ^1H-^{19}F HMQC NMR ($^2J_{FH}$ = 50 Hz) data (see Figures A18-A20). Weak NOEs

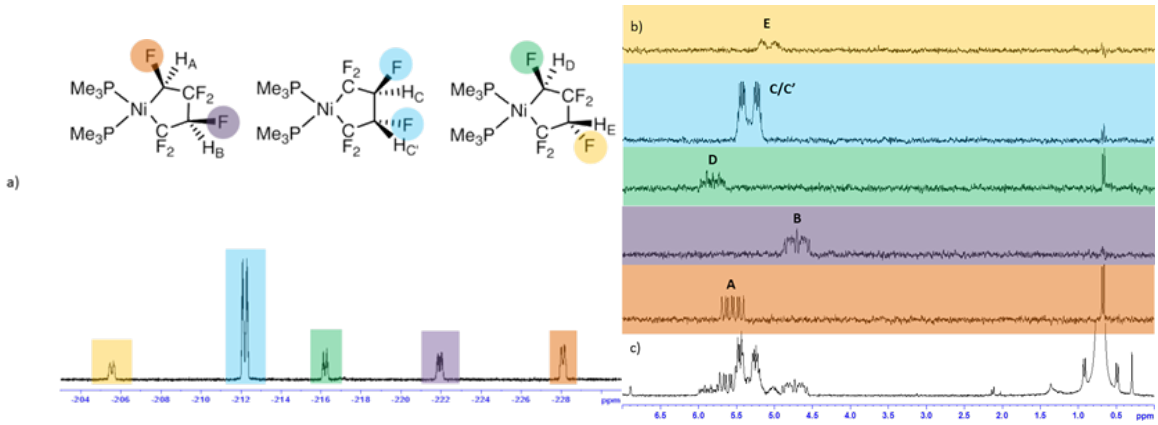

Figure 4.1 a) The 1D ^{19}F NMR spectrum of **Ni-16e** depicting the fluorine peaks that are geminal to a metallacyclic proton (282 MHz, C_6D_6). b) The 1D ^{1}H detected ^{1}H-^{19}F HOESY NMR spectra that are colour coded to indicate the selected fluorine. c) The 1D ^{1}H NMR spectrum for **Ni-16e** (300 MHz, C_6D_6).

are also observed with at least one proton of a P−CH_3 group when the fluorines in the C_α position of the head-tail isomers are selectively irradiated (orange and green spectra in Figure 4.1), indicating that they are also close in space. The ^{1}H detected ^{1}H-^{19}F HOESY NMR spectra of **Ni-16c,d** and **e** (Figure 4.1 and Figures A21-A22) reveal that the protons in the C_β position of the hydrofluorometallacycles appear more upfield (e.g., δ_H = 5.08, 5.32 and 4.71 for H_E, $H_{C/C'}$ and H_B respectively) than the C_α metallacyclic protons (δ_H = 5.81 and 5.55 for H_D and H_A respectively).

The molecular structure of the *trans* head-head isomer of **Ni-16e** was confirmed by a single crystal X-ray diffraction study (Figure 4.2, left). Bond angles about the Ni(II) centre are indicative of a distorted-square-planar geometry (360.5°). Interestingly, there are no significant differences in metallacycle Ni−C and C−C bond lengths when comparing to previously characterized perfluoro-nickelacyclopentanes.[16b,c,d] Furthermore, the distance between the C3 methyl group on the phosphine ligand and F2 is 2.926 Å, supporting the positive NOE observed in the ^{1}H detected ^{1}H-^{19}F HOESY spectrum (*vide supra*).

As noted above, in Stone's original studies of the (tdame)Ni(C_2F_3H) complex (Scheme 4.2) they speculated that reaction with another equivalent of TrFE overnight afforded 5-membered

nickelacycles that were not characterized due to solubility issues.[12] Indeed, we demonstrate here that halting the reaction between *in situ* generated $(PPh_3)_2Ni(cod)$ and TrFE by evacuating the head space of the reaction flask after 1 h at room temperature results in clean isolation of metallacyclopropane **Ni-17** as a bright yellow powder in 74% yield (Scheme 4.3). In the ^{19}F NMR spectrum, a geminally coupled pair is observed at δ_F = -114.3 and -115.6 ($^2J_{FF}$ = 181 Hz) corresponding to the $C_\alpha F_2$ fluorines along with a peak far upfield at δ_F = -221.0 associated with the $C_\alpha FH$ fluorine resonance, revealing couplings of $^2J_{FH}$ = 64 Hz and *trans* $^3J_{FF}$ = 96 Hz. The metallacyclic proton appears at δ_H = 5.45 as a distinctive doublet of doublets in the ^1H NMR spectrum. The coupling constant values for **Ni-17** fall

Scheme 4.3 Synthesis of Ni-17 from Ni-15a and TrFE.

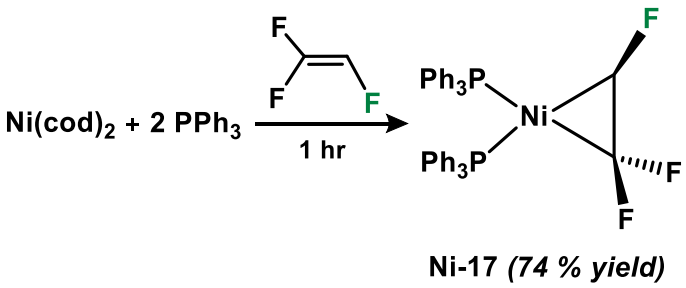

Ni-17 ***(74 % yield)***

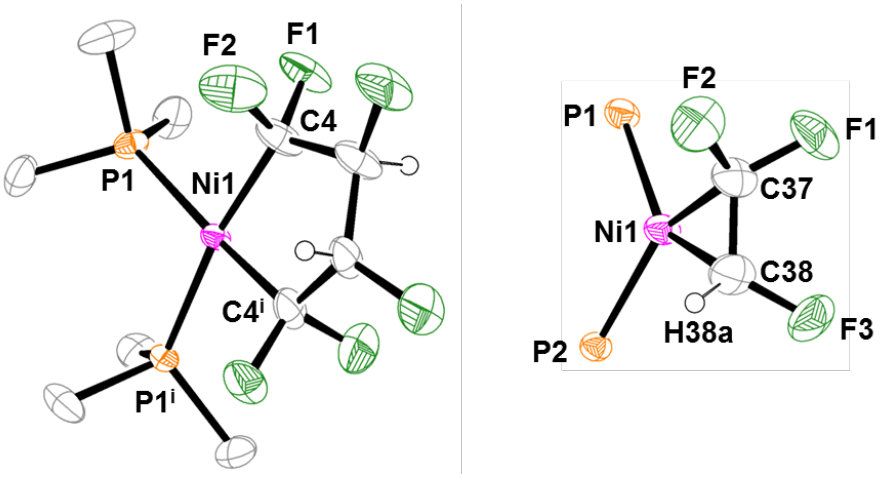

Figure 4.2 ORTEP representation of the molecular structure of the *trans* head-head isomer of complex **Ni-16e** (left) and complex **Ni-17** (right). Thermal ellipsoids are set at the 40% probability level. Hydrogen atoms and phenyl rings from PPh_3 are omitted for clarity. For **Ni-16e**, one of the two orientations for the disordered $C_\beta FH$ groups are shown. For **Ni-17**, one of four orientations of the disordered structure is depicted.

somewhere between typical values expected for fluorines on sp^2 hybridized carbons and sp^3 hybridized ones[16b,d] (e.g., gem-F,F of 181 Hz vs. 251-278 Hz for above nickelacyclopentanes). In the solid state, the Ni-C_α bond lengths are surprisingly shorter than those observed in **Ni-16e** (e.g., 1.903(3) vs. 1.937(4) Å respectively, Figure 2).

The C_α-C_α bond length of 1.385 Å is elongated in relation to that of free TrFE [1.309(6) Å], and the F1-C37- F2 angle of 101.8(9) deviates significantly from sp^2 hybridization.[16c,29] Moreover, the non-planarity of the TrFE moiety, evidenced in the bending away of the substituents from the metal centre, suggests significant back-donation from the nickel to the π^* antibonding orbital of TrFE.[18,19] Overall, the spectroscopic and solid state structural data indicate that **Ni-17** has both metallacyclopropane and η^2-coordinated TrFE olefin-type character. Complex **Ni-17** adds another equivalent of TrFE to form nickelacyclopentanes **Ni-16a**, providing evidence for the intermediacy of TrFE nickelacyclopropanes in the formation of nickelacyclopentanes. In contrast, **Ni-17** behaves more like an η^2-coordinated TrFE olefin complex in the presence of other fluorinated alkenes (e.g., tetrafluoroethylene, hexafluoropropene), liberating free TrFE.

4.3.2 Reactivity of Hydrofluoronickelacycle Complexes.

With the objective of generating functionalized hydrofluorocarbons, we initiated studies on the C−F and Ni−C_α reactivity of hydrofluoronickelacycles **Ni-16c** and **Ni-16d**. The Lewis acid reactivity of bis(phosphine) perfluoronickelacyclopentanes is well documented in the literature; C_α−F fluoride abstraction is accompanied by migration of the phosphorus ligand to C_α, affording phosphonium zwitterions (Scheme 4.4a).[16b,c] We then showed that addition of isonitrile ligands to a P-S ligated analogue effected Ni−C bond cleavage and elimination of a β-F, affording the unusual ring-opened Ni phosphonium dication, **A** (Scheme 4.4b).[16d] However, the reactivity of Lewis acids with partially fluorinated nickelacycles has not been previously investigated.

Scheme 4.4 C_α-F fluoride abstraction/phosphine migration to C_α.

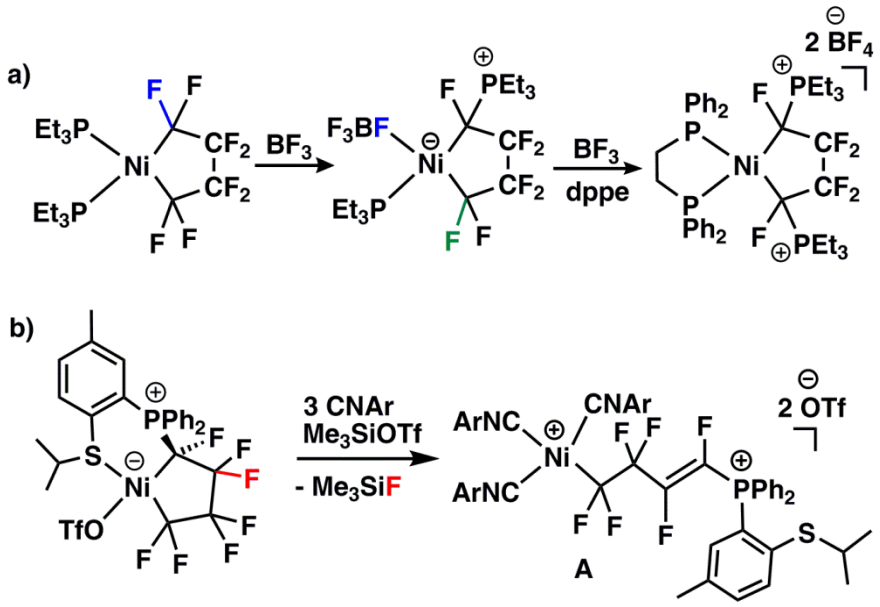

Treatment of the Ni PPh_2Me metallacycle mixture **Ni-16c** with a stoichiometric amount of boron trifluoride etherate, (BF_3•OEt_2) resulted in multiple C−F bond activations in all regioisomers, affording four different organic products. While the *trans* head-head isomer yielded two isomers of the bis(phosphonium) 1,4-difluorobutadienes (**O4a**,**O5a**) from the expected phosphine migration to C_α followed by β-F elimination, the head-tail isomers gave 1,1,2,3-tetrafluorocyclobutene (**O2**) as the major fluorinated product along with a minor amount of (*Z,E*)-1,1,3,4-tetrafluorobutadiene (**O3**; Table 4.3, entry 1). Cyclobutene **O2** is also obtained as the major product when the reaction was performed with the $PPhMe_2$ analogue **Ni-16d** (entry 2). Surprisingly, treatment of **Ni-16c** with either two equivalents of trimethylsilyl trifluoromethanesulfonate (Me_3SiOTf) or a stoichiometric amount of Brønsted acid, *N,N*-dimethylanilinium bromide [$C_6H_5N(CH_3)_2$•HBr] reversed the selectivity, yielding butadiene **O3** as the major organic product and only a minor amount of cyclobutene **O2** (entries 3 and 5). In contrast to the head-tail isomers, the minor head-head regioisomer did not show any acid-dependent selectivity differences. Organic products **O2-O5** were characterized by multinuclear NMR spectroscopy and, for isolated examples, by high resolution MS and X-ray diffraction.

Table 4.3 Reactivity of complexes Ni-16c and Ni-16d with Lewis and Brønsted acids.[a]

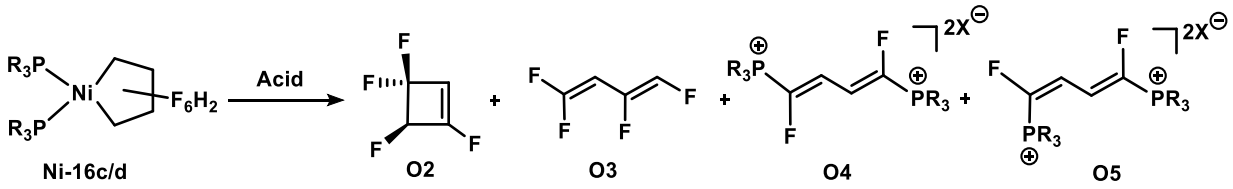

Entry	PR_3	Acid	equiv. Acid	Solvent	Yield **O2** [%]	Yield **O3** [%]	Yield **O4** [%]	Yield **O5** [%]
1	PPh_2Me	$BF_3•(OEt)_2$	1.1	$CDCl_3$	66	3	5	10
2	$PPhMe_2$	$BF_3•(OEt)_2$	1.1	$CDCl_3$	50	3	9	13
3	PPh_2Me	Me_3SiOTf	2.1	DCM	3	45	6	13
4	$PPhMe_2$	Me_3SiOTf	2.1	DCM	< 1	23	8	14
5	PPh_2Me	$[C_6H_5N(CH_3)_2•HBr]$	1.2	DCM	3	61	5	ND
6	$PPhMe_2$	$[C_6H_5N(CH_3)_2•HBr]$	1.2	DCM	4	64	6	6

[a] Yields estimated by relative integration of product peaks with hexafluorobenzene in $^{19}F\{^1H\}$ spectra

Constitutional isomers **O2** and **O3** both have characteristic chemical shifts/coupling constants in their ^1H, ^{19}F and $^{13}C\{^1H\}$ spectra when compared to other geometric isomers of tetrafluorocyclobutene and constitutional isomers of tetrafluorobutadiene respectively.[20-22] The signal for the sp^2 hybridized fluorine in the ^{19}F NMR spectrum of **O2** is located downfield at -95.8 with a *cis* coupling to the alkenyl proton of $^3J_{FH}$ = 8 Hz. The two fluorine signals associated with the CF_2 group at -104.5 and -115.7 ppm depict $^2J_{FF}$ = 199 Hz, a value that is congruous with other reported cyclobutenes containing geminally coupled fluorines (cf. 199 Hz in 1,2,3,3,4-pentafluorocyclobutene)[20b]. The CFH fluorine predictably appears the furthest upfield at -184.2 ppm and exhibits a large coupling constant with the geminal proton (60 Hz).[20] Unsymmetrical butadiene **O3** displays four unique fluorine resonances in the ^{19}F NMR spectrum. The terminal CF_2 difluorovinyl group appears as two signals at -79.2 and -81.3 ppm with *gem*-F,F coupling of 20 Hz.

Terminal fluorine F_A (Figure 4.3) displays a large ($^5J_{FF}$ = 28 Hz) long-range coupling with F_D, consistent with previous assignments made by Servis and Roberts for 1,1,4,4-tetra-fluorobutadiene.[22b] The $F_{C,D}$ signals associated with the 3,4-*cis* fluorines appear further upfield at -143.2 and-159.1 ppm, respectively and are coupled to each other by $^3J_{FF}$ = 13 Hz, in agreement with their *cis* geometry. In the ^{1}H NMR spectrum, the internal proton appears further upfield at δ 3.74 compared to the terminal proton at 5.56. The large *gem*-F,H coupling constant of 72 Hz is characteristic of terminal vinylic CFH groups. The observed and simulated ^{19}F NMR spectra of **O2** are depicted in Figure A29.

Compound **O4c** was fully characterized using multinuclear NMR, X-ray diffraction, and high-resolution ESI-MS. Analogues **O4a,b,d-f** were all identified based on their highly characteristic ^{19}F and ^{31}P{^{1}H} chemical shifts and splitting patterns identical to **O4c**. Structural characterization of **O4b** (Figure 4.4) and **O4c** (Figure A56) was obtained from X-ray quality crystals grown from cooled acetonitrile solutions of each compound. Another minor product of these reactions displays two unique fluorines in the ^{19}F spectrum with large J_{FP} values, and two unique phosphorus peaks with corresponding J_{FP} values. Given the characteristic coupling constants and the decrease in symmetry

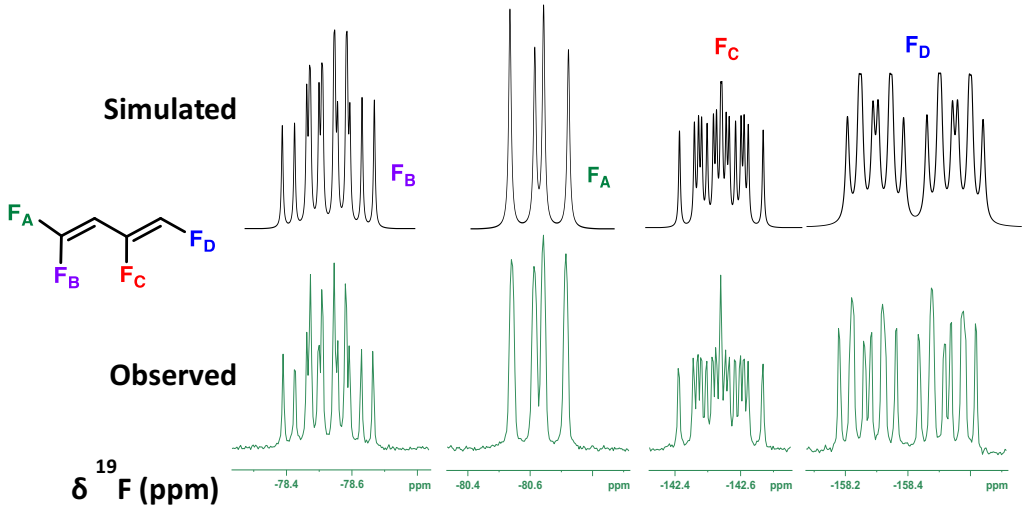

Figure 4.3 Simulated (g-NMR) and observed (282 MHz, C_6D_6) ^{19}F NMR spectra for **O3**.

relative to **O4**, we propose these peaks correspond to the *2Z,4E* isomers **O5a-f**. The lower yield of **O3** in entry 4 of Table 4.3 is accounted for by the presence of another phosphine-functionalized butadiene presumably derived from the head-tail nickelacycle. This competing phosphine migration does not occur when $C_6H_5N(CH_3)_2$•HBr is employed, in which a high yield of **O3** is obtained (entry 6).

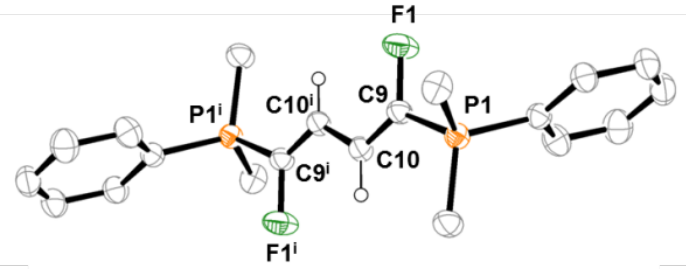

Figure 4.4 ORTEP representation of the molecular structure of **O4b**. Thermal ellipsoids are set at the 40% probability level. Hydrogen atoms and outer-sphere tetrafluoroborate ions are omitted for clarity.

4.3.3 Reaction intermediates and proposed pathways.

Given both the well-established precedent for activation of C−F bonds alpha to a transition metal[16,23] and the asymmetry of the head-tail nickelacycles, we can propose two possible fluoride activation routes to obtain tetrafluorocyclobutene **O2** from metallacycles **Ni-16c**/**Ni-16d**: a) Initial C_α−F activation from $C_\alpha FH$ affords a Ni−cyclobutyl intermediate (***Int 1***) that then undergoes β-fluoride elimination at $C_\beta F_2$ and Ni−C_α bond cleavage to give **O2**; b) initial C_α−F abstraction occurs at the $C_\alpha F_2$ position followed by Ni−C_α cleavage, generating Ni−cyclobutyl intermediate (***Int 2***), that undergoes C_β−F elimination from $C_\beta FH$ and Ni−C_α bond cleavage to afford **O2** (Scheme 4.5). A T-shaped three-coordinate perfluoronickelacyclopentane–NHC complex reported by our group undergoes a similar C_α−F/C_β−F activation to give perfluorocyclobutene, where the slower C_β−F elimination allowed for full characterization of the Ni−cyclobutyl product.[24] Key intermediates also consistent with path (b) were observed by closely monitoring the reaction between BF_3•OEt_2 and **Ni-**

Scheme 4.5 Two proposed routes for the double C−F bond activation of Ni-16c and Ni-16d with BF_3•OEt_2.

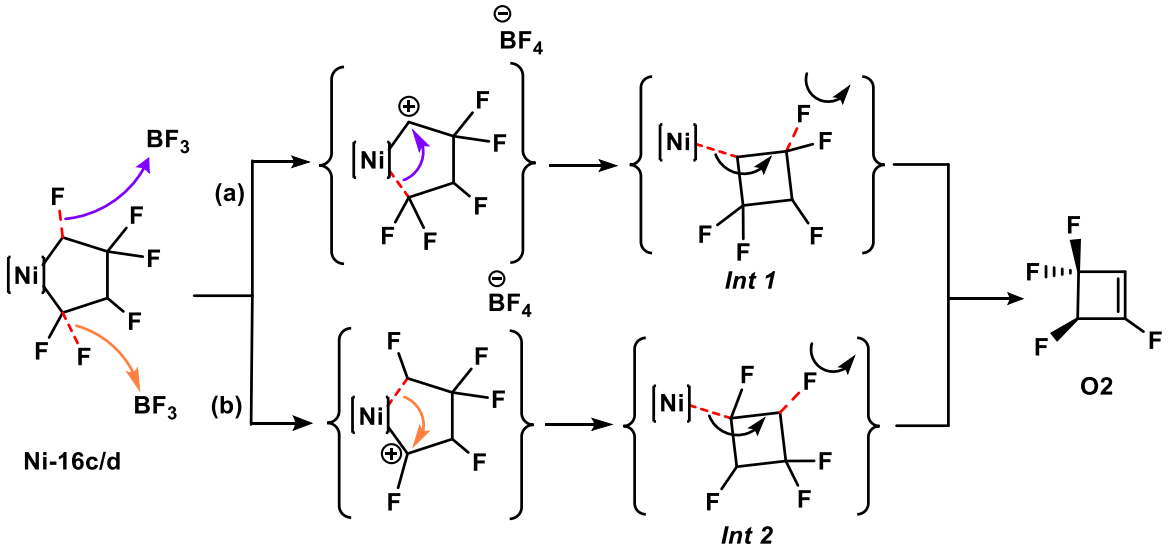

16c by NMR in $CDCl_3$. A colour change to dark purple upon addition of BF_3•OEt_2 was accompanied by complete consumption of starting metallacycle as observed by $^{19}F\{^1H\}$ NMR. The appearance of new peaks in the ^{19}F and $^{19}F\{^1H\}$ spectra is in agreement with the formation of two fluorocyclobutyl intermediates (Chart 4.2) **Ni-18'** and **Ni-19'**, that support an initial selective C_α−F activation from the $C_\alpha F_2$ carbon followed by a nucleophilic attack by the $C_\alpha FH$ group. The characteristic NMR features of **Ni-18'** include an upfield C_α−F peak at δ_F = -192.1 which exhibits an apparent triplet coupling to phosphorus ($^3J_{FP}$ = 36 Hz) with a corresponding doublet in the $^{31}P\{^1H\}$ spectrum at δ_P = 2.0 ppm. Intermediate **Ni-19'** displays a distinguishing resonance with complex coupling well upfield at δ_F = -383.5 ppm representing the bridging Ni fluorides. The $^{19}F\{^1H\}$ spectrum after 15 minutes shows resonances due to **O2** : **Ni-18'** : **Ni-19'** in a ratio of 1.0:0.6:0.5 and those associated with **Ni-18'** decrease at a faster rate than **Ni-19'** (see Figures A30-A33 for detailed NMR spectra). We propose that the minor *trans* cyclobutyl intermediate is not observed by NMR due to a significantly faster rate of β-fluoride activation compared to the *cis* cyclobutyl isomer. We suggest that this faster reactivity

Chart 4.2 Proposed observed intermediates in the reaction between Ni-16c and BF_3•OEt_2 in $CDCl_3$.

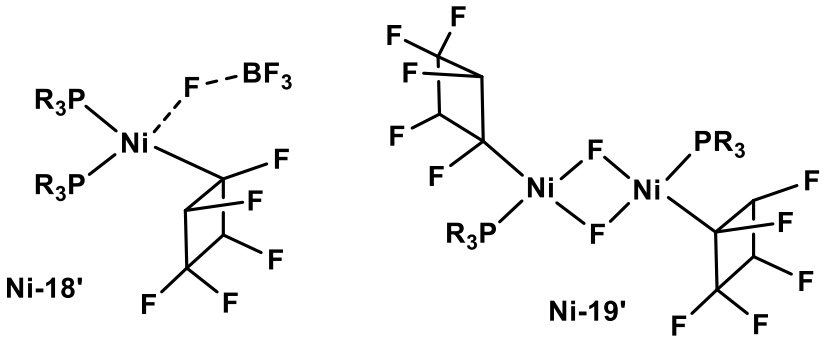

is attributed to an intramolecular β-F elimination to give cyclobutene **O2**. This type of intramolecular $C_\beta F$ activation is not possible with the *cis* arrangement of the cyclobutyl intermediate, where both $C_\beta FH$ fluorines are pointing away from the Ni centre. The selective formation of fluorocyclobutene rather than phosphine-functionalized nickelacycles suggests that the difference in reactivity between the head-head isomer and head-tail isomers stems from the competing nucleophilicity of PR_3 and $C_\alpha FH$.

Performing the reaction between BF_3•OEt_2 and **Ni-16c** in toluene solvent produces the same two cyclobutyl intermediates. Over the course of the reaction, the resonances associated with proposed intermediate **Ni-18'** decrease with time as those assigned to **O2** and **Ni-19'** increase, indicating that competing pathways for the conversion of **Ni-18'** to **Ni-19'** or **O2** exist in toluene. The reaction deposited a deep red-purple crystalline solid that was shown by X-ray diffraction to be a dicationic, difluoro-bridged Ni dimer containing two outer-sphere tetrafluoroborate anions (**Ni-20**, Figure 4.5, right) as the major Ni-containing byproduct resulting from β-fluoride elimination from **Ni-18'**. In contrast to **Ni-18'**, the difluoro-bridged binuclear **Ni-19'** is stable in toluene and does not undergo the second β-fluoride elimination, enabling characterization by multinuclear NMR and an X-ray study that confirms the dimeric structure, where both Ni(II) centres exhibit square-planar geometry (Figure 4.5, left).

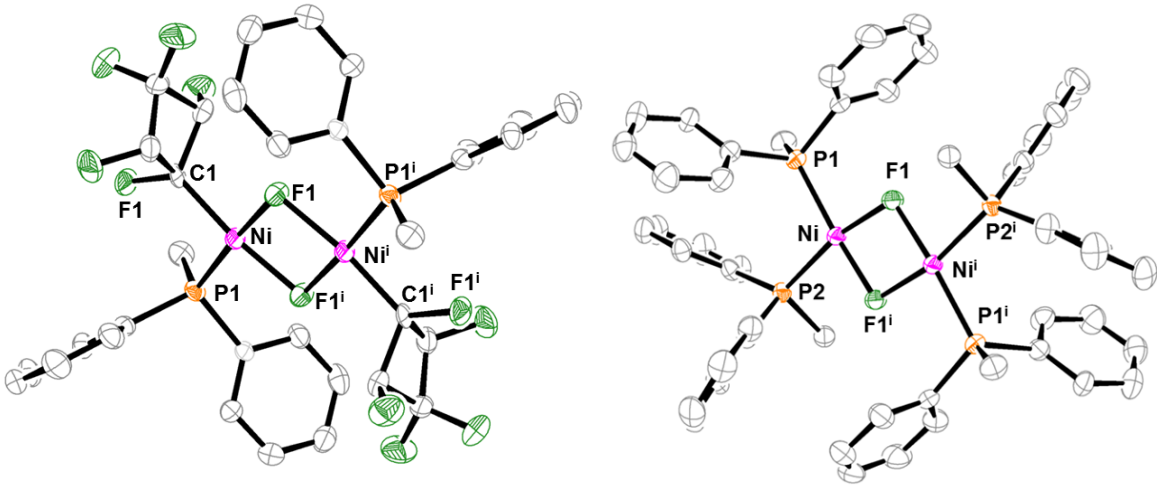

Figure 4.5 ORTEP representation of the molecular structures of **Ni-19'** (left) and **Ni-20** (right). Thermal ellipsoids are set at the 40% probability level. Hydrogen atoms are omitted for clarity.

Compound **O2** can be isolated in 58% yield (89% purity) and **O3** in 56% isolated yield (82% purity) by cryogenic distillation under vacuum. Trace amounts of other small fluorinated organics are detected by ^{19}F NMR: in the spectrum of **O2**; 1,1,2,2-tetrafluorocyclobutene (arising from the head-head metallacycle), **O3** and another isomer of tetrafluorocyclobutene (potentially arising from β-hydride elimination from **Ni-18'** or **Ni-19'**) are detected, and in **O3**; (*Z,Z*)-1,1,3,4-tetrafluorobutadiene, **O2**, and 1,1,4,4-tetrafluorobutadiene[23b] (arising from the head-head metallacycle) are detected.

In contrast to the BF_3•OEt_2 reaction, close monitoring of the reaction between metallacycle **Ni-16c** and Me_3SiOTf or *N,N*-dimethylanilinium bromide at room temperature did not result in the observation of any key intermediates. In the Me_3SiOTf reaction, complete conversion of starting material occurs with only a 45% yield of **O3**. Initially, one species with a cyclobutyl group was observed by ^{19}F NMR, but it slowly transformed to unknown product(s) and did not appear to correspond to an intermediate in butadiene formation. Notably, 3,3,4,4-tetrafluorocyclobutene is known to isomerize to 1,1,4,4- tetrafluorobutadiene at elevated temperatures (550-750°C).[25] A control

Scheme 4.6 Proposed route for the double C-F bond activation of Ni-16c and Ni-16d with Me_3SiOTf and $C_6H_5N(CH_3)_2$•HBr. LA = Lewis acid; HA = Brønsted acid

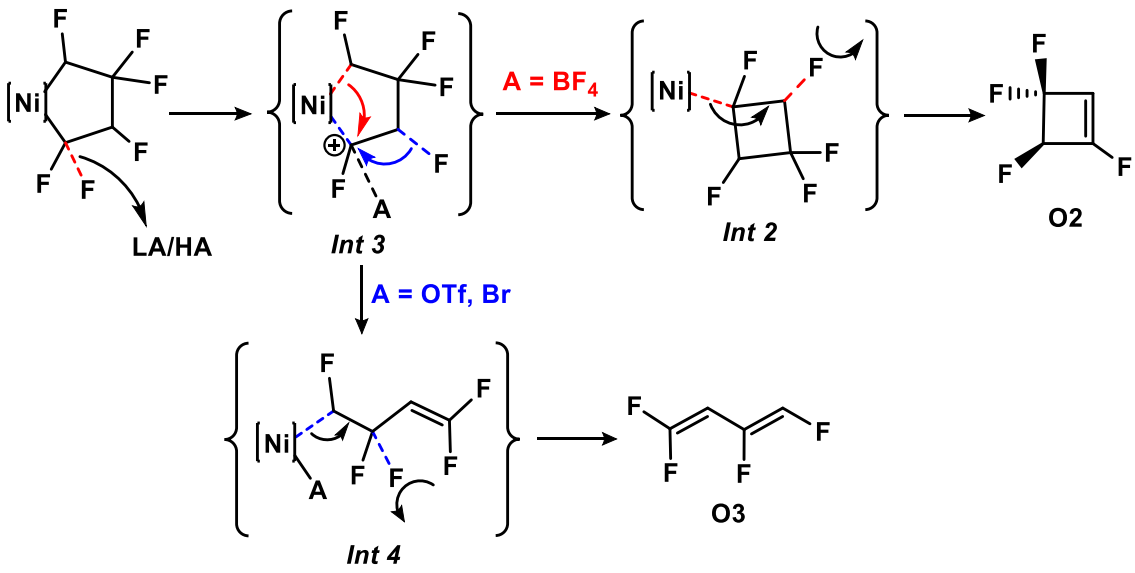

experiment with **O2** in the presence of Lewis acidic $Ni(OTf)_2$ salt showed no conversion to **O3** at room temperature. Furthermore, there is no evidence for the intermediacy of **O2** in the formation of **O3** by reaction monitoring. It is also important to note that there is no observation of a fluoride-bridged intermediate or Ni byproduct over the course of the Me_3SiOTf and $C_6H_5N(CH_3)_2$•HBr reactions. At this point, we surmise that the disparate product selectivities arise from the higher nucleophilicity of the triflate/bromide anions versus the tetrafluoroborate anion. We propose that initial C−F activation still occurs at the $C_\alpha F_2$ position and the generated carbocationic intermediate is partially stabilized by the OTf/Br counterion and the adjacent CHF group (***Int 3***; Scheme 4.6). A [1,2]-fluoride shift/Ni−C_α cleavage generates butenyl intermediate (***Int 4***) that then undergoes β-fluoride elimination to afford **O3**. Such [1,2]-fluoride shifts are well documented in fluoroorganic chemistry.[26] Currently, a detailed DFT study examining the mechanism of C−F activation in hydrofluoronickelacyclopentanes is underway.

4.4 Conclusions

The oxidative cyclization of TrFE at Ni(0) complexes **Ni-15** is selective towards the formation of the *cis* and *trans* head-tail and thermodynamically favored *trans* head-head hydrofluoronickelacyclopentanes **Ni-16**. An analysis of the ^{19}F NMR spectra of **Ni-16** shows that the respective ratio of the three major isomers is dictated by the nature of the PR_3 ancillary ligands. Additionally, a minor amount of tail-tail metallacycle is observed with the larger phosphine/phosphite ligands (PR_3 = PPh_3, $P(O\text{-}o\text{-tol})_3$, PPh_2Me). The effect of ancillary ligands on metallacycle selectivity is both informative on a fundamental level and in terms of potential application for the selective formation of valuable fluoroorganics. At this point, we cannot conclude whether the steric or electronic properties of the ancillary ligands play a bigger role in selectivity. Ongoing studies in our group using different ligands as well as other fluorinated feedstocks (e.g., vinylidene fluoride) aim to shed more light on this. Lewis and Brønsted acids induce a surprising double C−F bond activation of the head-tail regioisomers in **Ni-16c** and **Ni-16d**, affording small functionalized hydrofluoroalkenes. Surprisingly, varying the acid employed dictates the organic product obtained: BF_3•OEt_2 is selective for 1,1,2,3-tetrafluorocyclobutene **O2** as the major organic product, whereas Me_3SiOTf and *N,N*-dimethylanilinium bromide yield (*Z,E*)-1,1,3,4-tetrafluorobutadiene **O3** as the major fluorinated product. Notably, when **Ni-15a** (L = PPh_3) is left to react at room temperature for 24 h under ca. 7 psi of TrFE, minor amounts of butadiene and peaks presumably associated with ring-opened products are observed. This does not occur with any of the other ligands studied and is therefore attributed to the lability of one PPh_3. Furthermore, it indicates that a low-coordinate Ni centre can be sufficiently acidic for presumably intermolecular C−F bond activation. Given the ratio of BF_3•OEt_2 or *N,N*-dimethylanilinium bromide to metallacycle employed, we also presume that this type of nickel-mediated C−F bond activation could be playing a role in the formation of **O2**, **O3**, **O4**, and **O5**. Based on our current understanding, initial C−F activation with BF_3•OEt_2 occurs rapidly followed by a slower second C−F elimination. In contrast, employing Me_3SiOTf and

N,N-dimethylanilinium bromide results in a slower initial C−F bond activation followed by a faster second C−F elimination. The chemistry of phosphine-ligated partially fluorinated nickelacyclopentanes derived from TrFE thus deviates significantly from that of the previously studied perfluorinated analogues. Previously observed phosphine ligand migration to C_α following C_α−F activation is only observed with the *minor* head-head regioisomer and results in an unstable product (in contrast to the TFE-derived analogue)[16a] that undergoes further β-F eliminations. In contrast, the head-tail regioisomers undergo successive C−F activations with no evidence for phosphine migration to C_α of the metallacycle. This chemistry highlights that substitution of CF_2 with CFH in metallacyclopentanes has a significant effect on the reactivity of Ni−C and C−F bonds. Very recently, Ogoshi et. al. communicated some similar differences observed with mixed metallacyclopentanes derived from tetrafluoroethylene and ethylene.[27] Further analysis of the reaction pathways through observation and characterization of key intermediates by NMR/X-ray will be invaluable in the development of catalytic systems for production of **O2** and **O3** which are desirable products in relation to their potential application as refrigerants and blowing agents. Ongoing studies in our lab are exploring the mechanism of C−F bond activation in hydrofluoronickelacycles in addition to further investigations of ligand variation with the goal of designing catalytic methods for the production of C^F_4 products from C^F_2 gases.

4.5 Experimental Section

4.5.1 General

Experiments were conducted under nitrogen, using Schlenk techniques or an MBraun glove box. All solvents were deoxygenated by purging with nitrogen. Toluene, hexanes, diethyl ether and tetrahydrofuran (THF) were dried on columns of activated alumina using a J. C. Meyer solvent purification system. Benzene-d_6 (C_6D_6) was dried by stirring over activated alumina (ca. 10 wt.%)

overnight, followed by filtration. Acetonitrile (CH_3CN), acetonitrile-d_3 (CD_3CN) and dichloromethane (DCM) were dried by refluxing over calcium hydride under nitrogen. After distillation, they were further dried by stirring over activated alumina (ca. 5 wt.%) overnight, followed by filtration. All solvents were stored over activated (heated at ca. 250 °C for >10 h under vacuum) 4 Å molecular sieves. The following chemicals were used as purchased, without further purification: $Ni(cod)_2$ (Strem, 98+%), PPh_3 (Strem, 99%), PPh_2Me (Strem, 99%) $PPhMe_2$ (Strem, 99%), PMe_3 (Strem, 98+%), Me_3SiOTf (Aldrich, 98%), BF_3•OEt_2 (Alfa Aesar, 98+%). $Ni\{P[O(o\text{-}tol)_3]\}_4$ was prepared using reported methods.[8] *N,N*-dimethylanilinium bromide was synthesized using a slightly modified literature procedure.[28] Glassware was oven-dried at 150°C for >2 h. ^1H, ^{19}F, $^{31}P\{^1H\}$, $^{13}C\{^1H\}$ NMR spectra were recorded on a 300 MHz Bruker Avance instrument at room-temperature (21-23°C). ^1H NMR spectra were referenced to the residual proton peaks associated with the deuterated solvents (C_6D_6: 7.16 ppm; CD_3CN: 1.94 ppm). ^{19}F NMR used 1, 3-bis(trifluoromethyl)benzene (BTB) set to –63.5 ppm or hexafluorobenzene (HFB) set to –164.9 ppm. $^{31}P\{^1H\}$NMR data were referenced to external H_3PO_4 (85% aqueous solution) set to 0.0 ppm. For acquisition of quantitative ^{19}F and $^{19}F\{^1H\}$ NMR data, delay times (D1) were set to 5 s. For labelling of **O5a-f**, F_A is used for the *cis* fluorine signal and F_B for the *trans* signal. UV-vis spectra were recorded on a Cary 100 instrument, using sealable quartz cuvettes (1.0 cm pathlength). A Micromass Q-ToF 1 (positive mode) was used for electrospray ionization (ESI), and a Kratos Concept S1 (Hres 7000-10000) was used for electron impact (EI). Elemental analyses were performed by CENTC Elemental Analysis Facility at the University of Rochester. NMR simulations were done using the program g-NMR.

4.5.2 X-ray Crystallography

The crystals of **Ni-16e**, **Ni-17**, **O4b, O4c**, **Ni-19'**, and **Ni-20** were mounted on thin glass fibers using paraffin oil. Prior to data collection, crystals were cooled to 200±2 K. Data were collected on a Bruker AXS single crystal diffractometer equipped with a sealed Mo tube source (wavelength 0.71073 Å) and APEX II CCD detector. Raw data collection and processing were performed with

Bruker APEX II software package.[1] Semi-empirical absorption corrections based on equivalent reflections were applied.[2] Systematic absences in the diffraction dataset and unit cell parameters were consistent with triclinic *P*-1 (#2) for **Ni-17**, **O4c**, **Ni-19'**, monoclinic *C*2/*c*(#15) for **Ni-16e**, monoclinic $P2_1/n$ (#14) for **Ni-20**, **O4b**. The structures were solved by direct methods and refined with full-matrix least-squares procedures based on F^2, using SHELXL[3] and WinGX[4]. All non-hydrogen atoms were refined anisotropically. The positions of hydrogen atoms were calculated based on the geometry of related non-hydrogen atoms.

In the crystal structure of **2e** the molecule lies on a 2-fold rotation axis. The F3 and H5A atoms are disordered over two positions with 0.50:0.50 occupancies. Some restraints were applied to the ADPs and bond distances of the disordered group. The crystal structure of **Ni-17** was refined using HKLF5 file as a two-component twin with 0.55:0.45 ratio of components. The F1, F2, F3, and F4 fluorine atoms were modeled at 75% occupancy and H37A, H37B, H38A, H38B - as 25% occupied. The molecule of **O4b** as well lies on an inversion centre. It crystallizes with two BF_4^- anions per main molecule. The tetrafluoroborate anion is disordered over two positions with 0.76(1):0.24(1) occupancies. The molecule of **O4c** lies on an inversion centre. Half of the molecule and one -OTf anion constitute the asymmetric unit. No restraints or constraints were applied. The molecule of **Ni-19'** lies on an inversion centre. No restraints or constraints were applied. The molecule of **Ni-20** also lies on an inversion centre. There are two BF_4^- anions per molecule. The C8…C13 phenyl ring is disordered over two positions with 0.74(2):0.26(2) occupancies. Some restraints and constraints were applied to the disordered group.

4.5.3 $(PPh_3)_2Ni(C_4F_6H_2)$ (Ni-16a)

$Ni(cod)_2$ (250 mg, 0.909 mmol) was dissolved/suspended in ca. 15 mL of toluene in a 100 mL round-bottom Schlenk flask. Two equivalents of triphenylphosphine (500 mg, 1.909 mmol) were added. The colour changed from yellow to deep red. The flask was degassed, charged with ca. 7 psi

of TrFE, and stirred at room temperature for 16 h. The colour changed to a cloudy brown-yellow over the course of the reaction. The solvent volume was reduced to ca. 5 mL. Hexanes was added (10 mL), and the flask was cooled at -35°C. The product was filtered cold, washed with cold hexanes, and dried *in vacuo*, affording a dark yellow powder. Yield: 435 mg, 0.582 mmol, 64% based on $Ni(cod)_2$. UV-vis (0.7 mM in DCM): $\lambda_{max}(\varepsilon)$ = 265 nm (47 405). ^{1}H NMR (300 MHz, $CDCl_3$) δ 4.19-5.01 (ov m), 5.8 (d d d d, 1H, $^2J_{HF}$ = 64 Hz, $^3J_{HP}$ = 7 Hz), 6.93 (br s, 18H, Ar-H), 7.16 (solvent), 7.47 (br s, 12H, Ar-H). $^{31}P\{^1H\}$ (121 MHz, $CDCl_3$) δ 6.2-11.0 (ov m, 2P, Ni-P). ^{19}F NMR *cis* head-tail: (282 MHz, $CDCl_3$) δ -84.7 (d m, 1F, $^2J_{FF}$ = 256 Hz, $C_\alpha F_2$), -101.2 (d m, 1F, $^2J_{FF}$ = 256 Hz, $C_\alpha F_2$), -110.7 (d m, 1F, $^2J_{FF}$ = 227 Hz, $C_\beta F_2$), -128.1 (d m, 1F, $^2J_{FF}$ = 227 Hz, $C_\beta F_2$), -215.4 (m, 1F, C_αFH), -222.9 (d m, 1F, $^2J_{FH}$ = 50 Hz, C_βFH). ^{19}F NMR *trans* head-tail: (282 MHz, $CDCl_3$) δ -88.1 (d m, 1F, $^2J_{FF}$ = 251 Hz, $C_\alpha F_2$), -97.4 (m, 1F, $^2J_{FF}$ = 251 Hz, $C_\alpha F_2$), -114.7 (d m, 1F, $^2J_{FF}$ = 242 Hz, $C_\beta F_2$), -123.9 (d m, 1F, $^2J_{FF}$ = 242 Hz, $C_\beta F_2$), - 202.0 (d m, 1F, C_αFH), -212.6 (d m, 1F, $^2J_{FH}$ = 49 Hz, C_βFH). ^{19}F NMR *trans* head-head: (282 MHz, $CDCl_3$) δ -90.6 (d, 2F, $^2J_{FF}$ = 231 Hz, $C_\alpha F_2$), -91.9 (d t m, 2F, $^2J_{FF}$ = 231 Hz, $^3J_{FP}$ = 40 Hz, $C_\alpha F_2$), -214.3 (d m, $^2J_{FH}$ = 58 Hz, C_βFH). ^{19}F NMR *cis/trans* tail-tail: (282 MHz, $CDCl_3$) δ -118.0 (d, 2F, $^2J_{FF}$ = 246 Hz, $C_\beta F_2$), -121.1 (d m, 2F, $^2J_{FF}$ = 234 Hz, $C_\beta F_2$), -122.4 (d m, 2F, $^2J_{FF}$ = 234 Hz, $C_\beta F_2$), -128.0 (ov d m, 2F, $^2J_{FF} \approx$ 246 Hz, $C_\beta F_2$), -213.9 (m, 2F, C_αFH), -216.6 (m, 1F, C_αFH).

4.5.4 $[P(O\text{-}o\text{-}tol)_3]_2Ni(C_4F_6H_2)$ (Ni-16b)

$Ni[P(O\text{-}o\text{-}tol)_3]_4$ (301 mg, 0.205 mmol) was dissolved in ca. 3 mL of toluene and transferred to a 50 mL ampoule. The flask was degassed, charged with ca. 8 psi of TrFE, and stirred at 40°C for 40 h. The colour changed to a dark yellow with minor amount of Ni black observed. An aliquot was filtered through a pipet with a Celite plug into an NMR tube containing HFB (0.026 mmol). Yield of **Ni-16a** was determined by integration of C_βFH peaks with HFB in the ^{19}F spectra. Yield: 0.164 mmol, 80% based on $Ni[P(O\text{-}o\text{-}tol)_3]_4$. ^{1}H NMR (300 MHz, C_6D_6) δ 4.19-5.01 (ov m), 5.8 (d d d d, 1H, $^2J_{HF}$

= 64 Hz, $^{3}J_{HP}$ = 7 Hz), 6.93 (br ov m, 18H, Ar-H), 7.16 (solvent), 7.47 (br s, 12H, Ar-H). $^{31}P\{^{1}H\}$ (121 MHz, C_6D_6) δ 116.0-121.9 (ov m, 2P, Ni-P). ^{19}F NMR *cis* head-tail: (282 MHz, C_6D_6) δ -83.6 (app d t m, 1F, $^{2}J_{FF}$ = 257 Hz, $^{3}J_{FP}$ = 53 Hz $C_\alpha F_2$), -98.4 (d m, 1F, $^{2}J_{FF}$ = 257 Hz, $C_\alpha F_2$), -110.8 (d m, 1F, $^{2}J_{FF}$ = 224 Hz, $C_\beta F_2$), -130.0 (d m, 1F, $^{2}J_{FF}$ = 224 Hz, $C_\beta F_2$), -216.0 (d d m, 1F, $^{3}J_{FP}$ = 106 Hz, $^{2}J_{FH}$ = 55 Hz, $C_\alpha FH$), -224.5 (d m, 1F, $^{2}J_{FH}$ = 45 Hz, $C_\beta FH$). ^{19}F NMR *trans* head-tail: (282 MHz, C_6D_6) δ -86.2 (d m, 1F, $^{2}J_{FF}$ = 246 Hz, $C_\alpha F_2$), -91.8 (d m, 1F, $^{2}J_{FF}$ = 246 Hz, $C_\alpha F_2$), -108.6 (d m, 1F, $^{2}J_{FF}$ = 241 Hz, $C_\beta F_2$), -112.6 (d m, 1F, $^{2}J_{FF}$ = 241 Hz, $C_\beta F_2$), -202.7 (d d m, 1F, $^{3}J_{FP}$ = 96 Hz, $^{2}J_{FH}$ = 49 Hz, $C_\alpha FH$), -203.4 (d m, 1F, $^{2}J_{FH}$ = 49 Hz, $C_\beta FH$). ^{19}F NMR *trans* head-head: (282 MHz, $CDCl_3$) δ -86.9 (d m, 2F, $^{2}J_{FF}$ = 243 Hz, $C_\alpha F_2$), -88.8 (app d t m, 2F, $^{2}J_{FF}$ = 43 Hz, $^{3}J_{FP}$ = 58 Hz $C_\alpha F_2$), -213.2 (d m, $^{2}J_{FH}$ = 58 Hz, $C_\beta FH$). ^{19}F NMR *cis/trans* tail-tail: (282 MHz, C_6D_6) δ -118.0 (d, 2F, $^{2}J_{FF}$ = 246 Hz, $C_\beta F_2$), -121.1 (d m, 2F, $^{2}J_{FF}$ = 234 Hz, $C_\beta F_2$), -122.4 (d m, 2F, $^{2}J_{FF}$ = 234 Hz, $C_\beta F_2$), -128. (ov d m, 2F, $^{2}J_{FF} \approx$ 246 Hz, $C_\beta F_2$), -213.9 (m, 2F, $C_\alpha FH$), -216.6 (m, 1F, $C_\alpha FH$).

4.5.5 $(PPh_2Me)_2Ni(C_4F_6H_2)$ (Ni-16c)

$Ni(cod)_2$ (320 mg, 1.16 mmol) was dissolved/suspended in ca. 15 mL of toluene in a 100 mL round-bottom Schlenk flask. Two equivalents of diphenylmethylphosphine (455 µL, 2.44 mmol) were added to the $Ni(cod)_2$/toluene solution. The colour changed from yellow to orange-yellow. The flask was degassed, charged with ca. 7 psi of TrFE, and stirred at room temperature for 16 h. The solvent volume was reduced of the resulting cloudy yellow reaction mixture to ca. 3 mL. Hexanes was added (10 mL), and the flask was cooled at -35°C. The product was filtered cold, washed with cold hexanes, and dried *in vacuo*, affording a light yellow powder. Yield: 631 mg, 1.01 mmol, 87% based on $Ni(cod)_2$. UV-vis (0.7 mM in DCM): $\lambda_{max}(\varepsilon)$ = 386 nm (400). ^{1}H NMR (300 MHz, C_6D_6) δ

1.09 (d, 1.4H, $^2J_{HP}$ = 7 Hz, P-CH_3), 1.16 (d, 0.67H, $^2J_{HP}$ = 7 Hz, P-CH_3), 1.46 (d, 1.3H, $^2J_{HP}$ = 7 Hz, P-CH_3), 1.61 (ov d d, 2.3H, P-CH_3), 4.68 (d d d, 0.5H, $^2J_{HF}$ = 49 Hz), 5.13-5.85 (ov m, 1.5H, CFH), 6.71-7.06 (ov m, 12H, Ar-H), 7.16 (solvent), 7.09-7.61 (ov m, 8H, Ar-H). $^{31}P\{^1H\}$ (121 MHz, C_6D_6) δ 6.5-11.0 (ov m, 2P, Ni-P). ^{19}F NMR *cis* head-tail: (282 MHz, C_6D_6) δ -84.8 (ov d m, 1F, $^2J_{FF}$ = 262 Hz, $C_\alpha F_2$), -102.7 (d m, 1F, $^2J_{FF}$ = 262 Hz, $C_\alpha F_2$), -108.9 (d m, 1F, $^2J_{FF}$ = 221 Hz, $C_\beta F_2$), -129.7 (d m, 1F, $^2J_{FF}$ = 221 Hz, $C_\beta F_2$), -219.9 (m, 1F, $C_\alpha FH$), -221.4 (d m, 1F, $^2J_{FH}$ = 49 Hz, $C_\beta FH$). ^{19}F NMR *trans* head-tail: (282 MHz, C_6D_6) δ -84.8 (ov d m, 1F, $^2J_{FF}$ = 264 Hz, $C_\alpha F_2$), -97.4 (br d, 1F, $^2J_{FF}$ = 264 Hz, $C_\alpha F_2$), -112.8 (d m, 1F, $^2J_{FF}$ = 239 Hz, $C_\beta F_2$), -121.6 (d m, 1F, $^2J_{FF}$ = 239 Hz, $C_\beta F_2$), -207.9 (m, 1F, $^2J_{FH}$ = 47 Hz, $C_\alpha FH$), -209.3 (d m, 1F, $^2J_{FH}$ = 50 Hz, $C_\beta FH$). ^{19}F NMR *trans* head-head: (282 MHz, C_6D_6) δ -89.6 (d t m, 2F, $^2J_{FF}$ = 253 Hz, $^3J_{FP}$ = 43 Hz, $C_\alpha F_2$), -94.8 (d m, 2F, $^2J_{FF}$ = 253 Hz, $C_\alpha F_2$), -212.4 (d m, $^2J_{FH}$ = 59 Hz, $C_\beta FH$). See Figures A12-A13 for ^{19}F and $^{31}P\{^1H\}$ NMR spectra.

4.5.6 $(PPhMe_2)_2Ni(C_4F_6H_2)$ (Ni-16d)

$Ni(cod)_2$ (500 mg, 1.82 mmol) was dissolved/suspended in ca. 10 mL of toluene in a 100 mL round-bottom Schlenk flask. Two equivalents of dimethylphenylphosphine (517 μL, 3.64 mmol) were added, resulting in a colour change from yellow to orange-yellow. The flask was degassed, charged with ca. 7 psi of TrFE, and stirred at room temperature for 14 h. A light yellow precipitate was formed throughout the course of the reaction. The flask was degassed, and the solvent volume was reduced to ca. 5 mL. Hexanes was added (10 mL), and the flask was cooled at -35°C. The product was filtered cold, washed with cold hexanes, and dried *in vacuo*, affording a bright yellow powder. Yield: 692 mg, 1.38 mmol, 83% based on $Ni(cod)_2$. UV-vis (0.7 mM in DCM): $\lambda_{max}(\varepsilon)$ = 373 nm (950), 299 nm (4153). Anal. Calc. for $C_{20}H_{24}F_6NiP_2$: C, 48.14, H, 4.85. Found: C, 48.11, H, 4.78. ^1H

NMR (300 MHz, C_6D_6) δ 0.07-1.19 (ov m, 12H), 4.85 (ov m, 0.5H, CFH), 5.12-6.04 (ov m, 1.5H, CFH), 6.80-7.06 (ov m, 10H, Ar-H). $^{31}P\{^1H\}$ (121 MHz, C_6D_6) δ -5.7 (ov m, 2P, Ni-P). ^{19}F NMR *cis* head-tail: (282 MHz, C_6D_6) δ -86.8 (br d, 1F, $^2J_{FF}$ = 269 Hz, $C_\alpha F_2$), -104.4 (br d, 1F, $^2J_{FF}$ = 268 Hz, $C_\alpha F_2$), -108.6 (d m, 1F, $^2J_{FF}$ = 219 Hz, $C_\beta F_2$), -130.1 (d m, 1F, $^2J_{FF}$ = 219 Hz, $C_\beta F_2$), -222.2 (d m, 1F, $^2J_{FH}$ = 49 Hz, $C_\beta FH$), -225.6 (m, 1F, $C_\alpha FH$). ^{19}F NMR *trans* head-tail: (282 MHz, C_6D_6) δ -84.7 (br d, 1F, $^2J_{FF}$ = 277 Hz, $C_\alpha F_2$), -97.6 (br d, 1F, $^2J_{FF}$ = 277 Hz, $C_\alpha F_2$), -113.8 (d m, 1F, $^2J_{FF}$ = 238 Hz, $C_\beta F_2$), -120.7 (d m, 1F, $^2J_{FF}$ = 238 Hz, $C_\beta F_2$), -207.2 (d m, 1F, $^2J_{FH}$ = 50 Hz, $C_\beta FH$), -213.2 (br d, 1F, $^2J_{FH} \approx$ 49 Hz, $C_\alpha FH$). ^{19}F NMR *trans* head-head: (282 MHz, C_6D_6) δ -89.3 (br d t, 2F, $^2J_{FF}$ = 270 Hz, $^3J_{FP}$ = 35 Hz, $C_\alpha F_2$), -99.3 (br d, 2F, $^2J_{FF}$ = 270 Hz, $C_\alpha F_2$), -212.1 (d m, $^2J_{FH}$ = 58 Hz, $C_\beta FH$).

4.5.7 $(PMe_3)_2Ni(C_4F_6H_2)$ (Ni-16e)

$Ni(cod)_2$ (320 mg, 1.16 mmol) was dissolved/suspended in ca. 15 mL of toluene in a 100 mL round-bottom Schlenk flask. Two equivalents of trimethylphosphine (239 µL, 2.33 mmol) were added to the $Ni(cod)_2$/toluene solution. No major colour change occurred. The flask was degassed, charged with ca. 7 psi of TrFE, and stirred at room temperature for 16 h. An immediate colour change to cloudy orange occurred. The flask was degassed, and the solvent volume was reduced to ca. 2 mL. Hexanes was added (10 mL), and the flask was cooled at -35°C. The product was filtered cold, washed with cold hexanes, and dried *in vacuo*, affording a light yellow powder. Yield: 380 mg, 1.01 mmol, 87% based on $Ni(cod)_2$. UV-vis (0.7 mM in DCM): $\lambda_{max}(\varepsilon)$ = 381 nm (877), 299 nm (3277). Anal. Calc. for $C_{10}H_{20}F_6NiP_2$: C, 32.04, H, 5.38. Found: C, 32.11, H, 5.28. ^1H NMR (300 MHz, C_6D_6) δ 0.71 (d, 18H), 4.55-6.00 (ov m, 2H, CFH). $^{31}P\{^1H\}$ (121 MHz, C_6D_6) δ -17.1 (br s, 2P, Ni-P). ^{19}F

NMR *cis* head-tail: (282 MHz, C_6D_6) δ -89.4 (d m, 1F, $^2J_{FF}$ = 269 Hz, $C_\alpha F_2$), -105.6 (d d d, 1F, $^2J_{FF}$ = 269 Hz, $C_\alpha F_2$), -108.2 (d m, 1F, $^2J_{FF}$ = 218 Hz, $C_\beta F_2$), -130.7 (d m, 1F, $^2J_{FF}$ = 218 Hz, $C_\beta F_2$), -205.6 (d m, 1F, $^2J_{FH}$ = 50 Hz, CFH), -216.2 (d m, 1F, $^2J_{FH}$ = 48 Hz, CFH). ^{19}F NMR *trans* head-tail: (282 MHz, C_6D_6) δ -86.8 (d d d, 1F, $^2J_{FF}$ = 278 Hz, $C_\alpha F_2$), -98.6 (ov d m, 1F, $^2J_{FF}$ = 278 Hz, $C_\alpha F_2$), -113.4 (d m, 1F, $^2J_{FF}$ = 238 Hz, $C_\beta F_2$), -118.6 (d m, 1F, $^2J_{FF}$ = 238 Hz, $C_\beta F_2$), -221.9 (d m, 1F, $^2J_{FH}$ = 49 Hz, CFH), -228.1 (d m, 1F, $^2J_{FH}$ = 47 Hz, CFH). ^{19}F NMR *trans* head-head: (282 MHz, C_6D_6) δ -91.8 (br d t, 2F, $^2J_{FF}$ = 271 Hz, $C_\alpha F_2$), -98.6 (br d, 2F, $^2J_{FF}$ = 271 Hz, $C_\alpha F_2$), -212.2 (d m, $^2J_{FH}$ = 58 Hz, $C_\beta FH$).

4.5.8 $(PPh_3)_2Ni(C_2F_3H)$ (Ni-17)

$Ni(cod)_2$ (100 mg, 0.36 mmol) was dissolved/suspended in ca. 6 mL of diethyl ether in a large vial fitted with a septum cap. Two equivalents of triphenylphosphine (191 mg, 0.73 mmol) were added to the $Ni(cod)_2$/diethyl ether solution. The colour changed from yellow to deep red. TrFE (ca. 15 mL, 1.7 equiv) was added via syringe through the septum cap of the vial. The colour changed to cloudy orange. The vial was stirred at room temperature for 1 h. A bright yellow precipitate formed over the course of the reaction. The reaction mixture was filtered through a 15 mL medium pore fritted funnel. The collected powder was washed with cold hexanes and dried *in vacuo*, affording a fluorescent yellow powder. Yield: 178 mg, 0.27 mmol, 74% based on $Ni(cod)_2$. X-ray quality crystals were grown from a cooled (-35°C) saturated solution in chlorobenzene. UV-vis (0.7 mM in DCM): $\lambda_{max}(\varepsilon)$ = 323 nm (10 118). Anal. Calc. for $C_{38}H_{31}F_3NiP_2$: C, 68.60, H, 4.70. Found: C, 67.76, H, 4.62. ^{1}H NMR (300 MHz, C_6D_6) δ 5.45 (d d, 1H, $^2J_{HF}$ = 64 Hz, $^3J_{HP}$ = 7 Hz), 6.87-7.00 (ov m, 18H, Ar-H), 7.16 (solvent), 7.49 (app t, 12H, Ar-H). ^{19}F NMR (282 MHz, C_6D_6) δ -114.3 (d d, 1F, $^2J_{FF}$ = 181 Hz, $^3J_{FF}$ = 18 Hz), -115.6 (d d, 1F, $^2J_{FF}$ = 181 Hz, $^3J_{FF}$ = 96 Hz), -221.0 (d d d, $^3J_{FF}$ = 96 Hz, $^2J_{FH}$ = 64 Hz, $^3J_{FF}$ = 18 Hz). $^{31}P\{^1H\}$ (121 MHz, C_6D_6) δ 26.0 (br s, 2P, Ni-P). See Figures A23-A24 for ^{19}F and ^{1}H NMR spectra.

4.5.9 Reaction of $(PPh_2Me)_2Ni(C_4F_6H_2)$ (Ni-16c) with BF_3•OEt_2

$(PPh_2Me)_2Ni(C_4F_6H_2)$ (48 mg, 0.080 mmol) was dissolved in ca. 1 mL of $CDCl_3$ and transferred to a 25 mL round-bottom Schlenk ampoule containing a quantitative amount of HFB (3 μL, 0.026 mmol). A 1.1 equiv portion of BF_3•OEt_2 (10.5 μL, 0.085 mmol) was added to the **Ni-16c**/$CDCl_3$ solution. The colour changed immediately from yellow to dark red-purple. The flask was stirred at room temperature for 2 h. The reaction mixture was decanted from the white solid that had formed over the course of the reaction into a J Young tube for quantitative NMR analysis. The solid bis(phosphonium) salt was dissolved in ca. 0.7 mL of CH_3CN and transferred to an NMR tube containing HFB (0.026 mmol). Yields were determined by integration of signals with respect to HFB in the $^{19}F\{^1H\}$ spectra.

1,1,2,3-tetrafluorocyclobutene (**O2**): Yield: 0.051 mmol, 66% based on sp^2 CF. ^1H NMR (300 MHz, $CDCl_3$) δ 5.58 (ov d m, 2H, $^2J_{HF}$ = 60 Hz, H_A + H_B), 7.26 (solvent). ^{19}F NMR (282 MHz, $CDCl_3$) δ -95.8 (app t m, 1F, $^3J_{FF}$ = 25 Hz, $^3J_{FF}$ = 23 Hz, F_C), -104.5 (d d d d, 1F, $^2J_{FF}$ = 199 Hz, $^3J_{FF}$ = 25 Hz, $^3J_{FF}$ = 18 Hz, $^3J_{FH}$ = 2 Hz, F_D/$F_{D'}$), -115.7 (d d d d, 1F, $^2J_{FF}$ = 199 Hz, $^3J_{FF}$ = 23 Hz, $^3J_{FF}$ = 15 Hz, $^3J_{FH}$ = 2 Hz, F_D/$F_{D'}$), -184.2 (d t d d, 1F, $^2J_{FH}$ = 60 Hz, $^3J_{FF}$ = 18 Hz, $^3J_{FF}$ = 15 Hz, F_E). $^{13}C\{^1H\}$ NMR (75 MHz, $CDCl_3$) δ 92.3 (d m, 1C, $^1J_{CF}$ = 228 Hz), 112.8 (t d, 1C, $^2J_{CF}$ = 27 Hz, $^2J_{CF}$ = 13 Hz), 113.7 (t d d d, 1C, $^1J_{CF}$ = 275 Hz, $^2J_{CF}$ = 52 Hz, $^2J_{CF}$ = 19 Hz, $^3J_{CF}$ = 3 Hz), 160.5 (d d d d, 1C, $^1J_{CF}$ = 344 Hz, $^2J_{CF}$ = 36 Hz, $^2J_{CF}$ = 21 Hz, $^3J_{CF}$ = 20 Hz). High-resolution EIMS by head space analysis: mass calculated for $C_4F_4H_2$ 126.0093, found 126.0089. See Fugures A25-A26 for ^1H and ^{19}F NMR spectra.

Z,E)-1,1,3,4-tetrafluorobutadiene (**O3**): Yield was 3% based on CFH. ^1H NMR (300 MHz, C_6D_6) δ 3.74 (app t d d d, 1H, $^3J_{HF}$ = 19 Hz, $^3J_{HF}$ = 19 Hz, $^3J_{HF}$ = 2 Hz, $^4J_{HF}$ = 1 Hz, $^4J_{HH}$ = 0.6 Hz, H_A), 5.56 (d d app quin, 1H, $^2J_{HF}$ = 72 Hz, $^3J_{HF}$ = 16 Hz, $^5J_{HF}$ = 2 Hz, $^5J_{HF}$ = 1 Hz, $^4J_{HH}$ = 0.6 Hz, H_B), 7.16 (solvent). ^{19}F NMR (282 MHz, C_6D_6) δ -79.2 (m, 1F, $^2J_{FF}$ = 20 Hz, $^4J_{FF}$ = 24 Hz, $^5J_{FF}$ = 10 Hz, $^3J_{FH}$ = 20 Hz, F_B), -81.3 (d d d, 1F, $^2J_{FF}$ = 20 Hz, $^5J_{FF}$ = 28 Hz, $^3J_{FH}$ ≈ 2 Hz, F_A), -143.2 (m, 1F, $^3J_{FF}$ = 13 Hz,

($^4J_{FF}$ = 24 Hz, $^3J_{FH}$ = 16 Hz, F_C), -159.1 (d d m, 1F, $^2J_{FH}$ = 72 Hz, $^3J_{FF}$ = 13 Hz, $^5J_{FF}$ = 28 Hz, $^5J_{FF}$ = 10 Hz, F_D). $^{13}C\{^1H\}$ NMR (75 MHz, C_6D_6) δ 72.3 (d d d, 1C, $^2J_{CF}$ = 39 Hz, $^2J_{CF}$ = 25 Hz, $^2J_{CF}$ = 14 Hz), 135.5 (d d, 1C, $^1J_{CF}$ = 258 Hz, $^2J_{CF}$ = 16 Hz, $^4J_{CF}$ = 10 Hz, $^4J_{CF}$ = 6 Hz), 141.3 (d m, 1C, $^1J_{CF}$ = 248 Hz), 156.1 (t m, 1C, $^1J_{CF}$ = 289 Hz). See Figures A27-A28 for ^1H and ^{19}F NMR spectra.

2Z,4Z-[(PPh_2Me)(F)C=C(H)−C(H)=C(F)(PPh_2Me)][BF_4]$_2$ (**O4a**): Yield: 5% based on F. ^{19}F NMR (282 MHz, CD_3CN) δ -116.6 (d d, $^2J_{FP}$ = 74 Hz, $^3J_{FH}$ = 33 Hz, 2F), -152.6 (br s, 8F, BF_4). $^{31}P\{^1H\}$ (121 MHz, CD_3CN) δ 20.0 (d, $^2J_{PF}$ = 74 Hz, 2P). *2Z,4E*-[(PPh_2Me)(F)C=C(H)−C(H)=C(F)(PPh_2Me)][BF_4]$_2$ (**O5a**): Yield: 10% based on F_A. ^{19}F NMR (282 MHz, CD_3CN) δ -105.6 (app d t, 1F, $^2J_{FP}$ = 86 Hz, $^5J_{FF}$ ≈ 22 Hz, $^3J_{FH}$ ≈ 22 Hz, F_A), -119.6 (d d d, 1F, $^2J_{FP}$ = 76 Hz, $^5J_{FF}$ ≈ 22 Hz, $^3J_{FH}$ = 32 Hz, F_B), -152.6 (br s, 8F, BF_4. $^{31}P\{^1H\}$ (121 MHz, CD_3CN) δ 19.1 (ov d d, $^2J_{PF}$ = 86 Hz, $^2J_{PF}$ = 76 Hz, 2P).

Isolation of O2:

(PPh_2Me)$_2$Ni($C_4F_6H_2$) (46 mg, 0.074 mmol) was dissolved in ca. 1 mL of $CDCl_3$ and transferred to a 25 mL round-bottom Schlenk ampoule. A 1.1 equiv portion of BF_3•OEt_2 (10.0 µL, 0.081 mmol) was added to the **Ni-16c**/$CDCl_3$ solution. The colour changed immediately from yellow to dark red-purple. The flask was stirred at room temperature for 3.5 h. A J Young tube was loaded with a quantitative amount of HFB (0.026 mmol). On the Schlenk line, one freeze-pump-thaw cycle was performed on both the J Young tube and the reaction flask, respectively. The solvent/volatiles from the Schlenk ampoule were vacuum condensed into the J Young tube kept at -196°C. Yield of **O2** based on sp^2 CF: 0.043 mmol, 58% (ca. 89% purity).

4.5.10 Reaction of ($PPhMe_2$)$_2$Ni($C_4F_6H_2$) (Ni-16d) with BF_3•OEt_2

($PPhMe_2$)$_2$Ni($C_4F_6H_2$) (40 mg, 0.080 mmol) was dissolved in ca. 1 mL of $CDCl_3$ and transferred to a 25 mL round-bottom Schlenk ampoule containing a quantitative amount of HFB (0.026 mmol). A 1.1 equiv portion of BF_3•OEt_2 (10.9 µL, 0.088 mmol) was added, resulting in an immediate colour

change from yellow to dark red-purple. The flask was stirred at room temperature for 2 h. The reaction mixture was decanted from the white solid that had formed over the course of the reaction into a J Young tube. The white solid was dissolved in ca. 0.7 mL of CD_3CN and transferred to an NMR tube containing HFB (0.026 mmol). Yields were determined by integration of signals with respect to HFB in the $^{19}F\{^1H\}$ spectra. Yield of **O2** based on sp^2 CF: 0.040 mmol, 50% and of **O3** based on CFH: 3%.

2Z,4Z-[$(PPhMe_2)(F)C{=}C(H){-}C(H){=}C(F)(PPhMe_2)$][$BF_4$]$_2$ (**O4b**): Yield: 9% based on F. ^{19}F NMR (282 MHz, CD_3CN) δ -114.6 (d d, $^2J_{FP}$ = 74 Hz, $^3J_{FH}$ = 35 Hz, 2F), -151.2 (8F, BF_4). $^{31}P\{^1H\}$ (121 MHz, CD_3CN) δ 18.7 (d, $^2J_{PF}$ = 74 Hz, 2P).

2Z,4E-[$(PPhMe_2)(F)C{=}C(H)$-$C(H){=}C(F)(PPhMe_2)$][BF_4]$_2$ (**O5b**): Yield: 13% based on F_A. ^{19}F NMR (282 MHz, CD_3CN) δ -104.6 (app d t m, 1F, $^2J_{FP}$ = 86 Hz, $^5J_{FF} \approx$ 21 Hz, $^3J_{FH} \approx$ 21 Hz, F_A), -115.9 (d d d, 1F, $^2J_{FP}$ = 77 Hz, $^5J_{FF}$ = 21 Hz, $^3J_{FH}$ = 32 Hz, F_B), -151.2 (8F, BF_4). $^{31}P\{^1H\}$ (121 MHz, CD_3CN) δ 18.3 (ov d d, $^2J_{PF}$ = 77 Hz, $^2J_{PF}$ = 86 Hz, 2P).

4.5.11 Observation of intermediates Ni-18' and Ni-19' by reaction monitoring in $CDCl_3$

$(PPh_2Me)_2Ni(C_4F_6H_2)$ (24 mg, 0.039 mmol) was dissolved in ca. 1 mL of $CDCl_3$ and transferred to a J Young NMR tube. A 1.1 equiv portion of $BF_3{\bullet}OEt_2$ (5.2 µL, 0.042 mmol) was added to the NMR tube. The colour changed immediately from yellow to dark red-purple. The sample was taken immediately to the NMR spectrometer and $^{19}F\{^1H\}$ spectra were acquired every 30 min for 10 h. See Figure A30 for time-elapsed $^{19}F\{^1H\}$ NMR spectra and A31-A33 for initial $^{19}F\{^1H\}$ and $^{31}P\{^1H\}$ spectra.

NMR data for Ni-18': ^{19}F NMR (282 MHz, $CDCl_3$) δ -102.0 (d, 1F, $^2J_{FF}$ = 206 Hz, $C_\gamma F_2$), -139.2 (d m, 1F, $^2J_{FF}$ = 206 Hz, $C_\gamma F_2$), -192.1 (m, 1F, $C_\alpha F$), -218.3 (d m, 2F, $^2J_{FH}$ = 44 Hz, $C_\beta FH$). $^{19}F\{^1H\}$ NMR (282 MHz, $CDCl_3$) δ -102.0 (d, 1F, $^2J_{FF}$ = 206 Hz, $C_\gamma F_2$), -139.2 (d d, 1F, $^2J_{FF}$ = 206 Hz, $^3J_{FF}$ = 8 Hz,

$C_\gamma F_2$), -192.1 (app t m, 1F, $^3J_{FP}$ = 36 Hz, $C_\alpha F$), -218.3 (s, 2F, $C_\beta FH$). $^{31}P\{^1H\}$ (121 MHz, $CDCl_3$ δ 2.0 (d, $^3J_{PF}$ = 36 Hz, 2P). NMR data for **Ni-19'**: ^{19}F NMR (282 MHz, $CDCl_3$) δ -101.0 (d m, 2F, $^2J_{FF}$ = 205 Hz, $C_\gamma F_2$), -139.1 (d m, 2F, $^2J_{FF}$ = 205 Hz, $C_\gamma F_2$), -201.2 (m, 2F, $C_\alpha F$), -221.8 (d m, 4F, $^2J_{FH}$ = 44 Hz, $C_\beta FH$), -383.5 (m, 2F, Ni-F).

Isolation of Ni-19`: $(PPh_2Me)_2Ni(C_4F_6H_2)$ (89 mg, 0.14 mmol) was dissolved in ca. 10 mL of toluene in a large vial. A 1.1 equiv portion of BF_3•OEt_2 (19.4 µL, 0.16 mmol) was added to the **Ni-16c**/toluene solution. The colour changed immediately from yellow to dark red-purple. The reaction was stirred at room temperature for 5 h. Over the course of the reaction, a deep red-purple solid crashed out of solution. The orange supernatant was decanted into a new vial and concentrated *in vacuo* to ca. 1 mL. Hexanes was added (3 mL), precipitating a dark yellow solid. The product was filtered, and washed with hexanes. Yield: 20 mg, 0.05 mmol, 33% based on **Ni-16c**. X-ray quality crystals were grown from a cooled saturated toluene solution. Anal. Calc. for $C_{34}H_{30}F_{12}Ni_2P_2$•$2H_2O$: C, 46.30, H, 3.89. Found: C, 46.282, H, 3.504. ^1H NMR (300 MHz, C_6D_6) δ 1.40 (d, 6H, $^3J_{HP}$ = 10 Hz, P-CH_3), 4.19 (br d, 4H, $^2J_{HF}$ = 45 Hz, $C_\beta FH$), 6.88-7.09 (ov m, 12H, Ar-H), 7.16 (solvent), 7.42 (d d, 8H, Ar-H). ^{19}F NMR (282 MHz, C_6D_6) δ -97.9 (d, 2F, $^2J_{FF}$ = 202 Hz, $C_\gamma F_2$), -136.0 (d m, 2F, $^2J_{FF}$ = 202 Hz, $C_\gamma F_2$), -197.4 (br s, 2F, $C_\alpha F$), -219.1 (d, 4F, $^2J_{FH}$ = 45 Hz, $C_\beta FH$), -379.5 (br s, 2F, Ni-F). $^{31}P\{^1H\}$ (121 MHz, C_6D_6) δ 19.4 (m, 2P, Ni-P).

4.5.12 Reaction of $(PPh_2Me)_2Ni(C_4F_6H_2)$ (Ni-16c) with Me_3SiOTf

$(PPh_2Me)_2Ni(C_4F_6H_2)$ (43 mg, 0.069 mmol) was dissolved in ca. 1.5 mL of DCM and transferred to a 25 mL round-bottom Schlenk ampoule containing a quantitative amount of HFB (0.026 mmol). A 2.1 equiv portion of Me_3SiOTf (25.3 µL, 0.14 mmol) was added, resulting in an immediate colour change from yellow to dark red. The flask was stirred at room temperature for 16 h. The colour

changed to cloudy orange over the course of the reaction. The reaction mixture was decanted from the white solid that had formed over the course of the reaction into a J Young tube. The white solid was dissolved in ca. 0.7 mL of CD_3CN and transferred to an NMR tube containing HFB (0.026 mmol). Yields were determined by integration of signals with respect to HFB in the $^{19}F\{^1H\}$ spectra. Yield of **O2** based on sp^2 CF: 3% and of **O3** based on CFH: 0.031 mmol, 45%.

2Z,4Z-[$(PPh_2Me)(F)C{=}C(H){-}C(H){=}C(F)(PPh_2Me)$][OTf]$_2$ (**O4c**): Yield: 6% based on F. ^1H NMR (300 MHz, CD_3CN) δ 1.94 (solvent), 2.78 (d, 6H, $^3J_{HP}$ = 15 Hz, P-CH_3), 6.86 (d m, 2H, $^3J_{HF}$ = 35 Hz, $^3J_{HP}$ = 4 Hz), 7.68-8.00 (ov m, 10H, Ar-H). ^{19}F NMR (282 MHz, CD_3CN) δ -79.3 (s, 6F, SO_3CF_3), -112.3 (d d m, 2F, $^2J_{FP}$ = 72 Hz, $^3J_{FH}$ = 35 Hz, 2F). $^{31}P\{^1H\}$ (121 MHz, CD_3CN) δ 17.4 (d, $^2J_{PF}$ = 72 Hz, 2P). High-resolution Electrospray Ionisation, solvent: CH_3CN; mass calculated for $C_{30}H_{28}P_2F_2^{++}$ 244.08117, found 244.08172.

2Z,4E-[$(PPh_2Me)(F)C{=}C(H){-}C(H){=}C(F)(PPh_2Me)$][OTf]$_2$ (**O5c**): Yield: 13% based on F_A. ^{19}F NMR (282 MHz, CD_3CN) δ -79.7 (s, 6F, SO_3CF_3), -103.1 (app d t, 1F, $^2J_{FP}$ = 86 Hz, $^5J_{FF}$ = 22 Hz, $^3J_{FH}$ = 22 Hz, F_A), -113.0 (d d d, 1F, $^2J_{FP}$ = 75 Hz, $^5J_{FF}$ = 22 Hz, $^3J_{FH}$ = 32 Hz, F_B). $^{31}P\{^1H\}$ (121 MHz, CD_3CN) δ 16.7 (d, $^2J_{PF}$ = 86 Hz, 1P), 21.1 (d, $^2J_{PF}$ = 75 Hz, 1P).

4.5.13 Reaction of $(PPhMe_2)_2Ni(C_4F_6H_2)$ (Ni-16d) with Me_3SiOTf

$(PPhMe_2)_2Ni(C_4F_6H_2)$ (40 mg, 0.080 mmol) was dissolved in ca. 1.5 mL of DCM and transferred to a 25 mL round-bottom Schlenk ampoule containing a quantitative amount of HFB (0.026 mmol). A 2.1 equiv portion of Me_3SiOTf (30.8 µL, 0.17 mmol) was added, resulting in an immediate colour change from yellow to dark red. The flask was stirred at room temperature for 16 h. The colour changed to cloudy orange over the course of the reaction. The reaction mixture was decanted from the white solid that had formed over the course of the reaction into a J Young tube. The white solid was dissolved in ca. 0.7 mL of CD_3CN and transferred to an NMR tube containing HFB (0.026 mmol). Yields were determined by integration of signals with respect to HFB in the $^{19}F\{^1H\}$ spectra. Yield of **O2** based on sp^2 CF: < 1% and of **O3** based on CFH: 0.02 mmol, 23%.

2Z,4Z-[($PPhMe_2$)(F)C=C(H)−C(H)=C(F)($PPhMe_2$)][OTf]$_2$ (**O4d**): Yield: 8% based on F. ^{19}F NMR (282 MHz, CD_3CN) δ -79.8 (s, 6F, SO_3CF_3), -115.1 (d d, 2F, $^2J_{FP}$ = 74 Hz, $^3J_{FH}$ = 36 Hz, 2F). ^{31}P{^{1}H} (121 MHz, CD_3CN) δ 25.5 (d, $^2J_{PF}$ = 74 Hz, 2P).

2Z,4E-[($PPhMe_2$)(F)C=C(H)−C(H)=C(F)($PPhMe_2$)][OTf]$_2$ (**O5d**): Yield: 14% based on **Ni-16d**. ^{19}F NMR (282 MHz, CD_3CN) δ -79.8 (s, 6F, SO_3CF_3), -105.3 (app d t, 1F, $^2J_{FP}$ = 86 Hz, $^5J_{FF}$ ≈ 21 Hz, $^3J_{FH}$ ≈ 21 Hz, F_A), -116.6 (d d d, 1F, $^2J_{FP}$ = 77 Hz, $^5J_{FF}$ ≈ 21 Hz, $^3J_{FH}$ ≈ 33 Hz, F_B). ^{31}P{^{1}H} (121 MHz, CD_3CN) δ 25.1 (ov d d, $^2J_{PF}$ = 77 Hz, $^2J_{PF}$ ≈ 86 Hz, 2P).

4.5.14 General Procedure for the reaction between $(PR_3)_2Ni(C_4F_6H_2)$ and *N,N*-dimethylaniline Hydrobromide

$(PR_3)_2Ni(C_4F_6H_2)$ (0.069 mmol) was dissolved in ca. 1.5 mL of DCM and transferred to a vial containing a 1.2 equiv portion of *N,N*-dimethylaniline hydrobromide (0.083 mmol). The reaction mixture was transferred to a 25 mL round-bottom Schlenk ampoule containing a quantitative amount of HFB (0.026 mmol) and stirred at room temperature for 16 h. The colour changed to dark red with white precipitate over the course of the reaction. The reaction mixture was decanted from the white solid into a J Young tube. The white solid was dried in vacuo and dissolved in ca. 0.7 mL of CH_3CN for NMR quantification. Yields were determined by integration of signals with respect to HFB in the ^{19}F{^{1}H} spectra.

Reaction of Ni-16c with *N,N*-dimethylaniline hydrobromide: Yield of **O2** based on sp^2 CF: 3% and of **O3** based on CFH: 0.04 mmol, 61%. High-resolution EIMS by head space analysis: mass calculated for $C_4F_4H_2$ 126.0093, found 126.0071.

2Z,4Z-[(PPh_2Me)(F)C=C(H)−C(H)=C(F)(PPh_2Me)][Br]$_2$ (**O4e**): Yield: 5% based on F. ^{19}F NMR (282 MHz, D_2O) δ -111.4 (d d, 2F, $^2J_{FP}$ = 73 Hz, $^3J_{FH}$ = 35 Hz, 2F). ^{31}P{^{1}H} (121 MHz, D_2O) δ 17.9 (d, $^2J_{PF}$ = 73 Hz, 2P).

Reaction of Ni-16d with *N,N*-dimethylaniline hydrobromide: Yield of **O2** based on sp^2 CF: 4% and of **O3** based on CFH: 0.04 mmol, 64%.

2Z,4Z-[($PPhMe_2$)(F)C=C(H)−C(H)=C(F)($PPhMe_2$)][Br]$_2$ (**O4f**): Yield: 6% based on F. ^{19}F NMR (282 MHz, D_2O) δ -114.1 (d d, 2F, $^2J_{FP}$ = 75 Hz, $^3J_{FH}$ = 35 Hz, 2F). ^{31}P{^{1}H} (121 MHz, D_2O) δ 20.9 (d, $^2J_{PF}$ = 75 Hz, 2P).

2Z,4E-[($PPhMe_2$)(F)C=C(H)−C(H)=C(F)($PPhMe_2$)][Br]$_2$ (**O5f**): Yield: 6% based on F_A. ^{19}F NMR (282 MHz, D_2O) δ -104.5 (app d t, 1F, $^2J_{FP}$ = 85 Hz, $^5J_{FF}$ ≈ 21 Hz, $^3J_{FH}$ ≈ 22 Hz, F_A), -114.7 (d d d, 1F, $^2J_{FP}$ = 76 Hz, $^5J_{FF}$ ≈ 21 Hz, $^3J_{FH}$ ≈ 33 Hz, F_B). ^{31}P{^{1}H} (121 MHz, D_2O) δ 20.3 (ov d d, $^2J_{PF}$ ≈ 76 Hz, $^2J_{PF}$ = 85 Hz, 2P).

Isolation of O3: (PPh_2Me)$_2$Ni($C_4F_6H_2$) (43 mg, 0.069 mmol) was dissolved in ca. 1 mL of DCM and transferred to a 25 mL round-bottom Schlenk ampoule. One equiv of *N,N*-dimethylaniline hydrobromide (14 mg, 0.069 mmol) was added to the **Ni-16c**/DCM solution. The flask was stirred at room temperature for 16 h. A J Young tube was loaded with a quantitative amount of HFB (0.026 mmol). On the Schlenk line, one freeze-pump-thaw cycle was performed on both the J Young tube and the reaction flask, respectively. The solvent/volatiles from the Schlenk ampoule were vacuum condensed into the J Young tube kept at -196°C. Yield of **O3** based on CFH: 0.039 mmol, 5% (ca. 82% purity).

4.6 References

[1] For selected examples see: a) Kiplinger, J. L.; Richmond, T. G.; Osterberg, C. E. *Chem. Rev.* **1994**, *94*, 373. b) Lundgren, R. J.; Stradiotto, M. *Angew. Chem. Int. Ed.* **2010**, *49*, 9322. c) Furuya, T.; Kamlet, A. S.; Ritter, T. *Nature* **2011**, *473*, 470. d) Liu, H.; Gu, Z.; Jiang, X. *Adv. Synth. Catal.* **2013**, *355*, 617. e) Zhu, W.; Wang, J.; Wang, S.; Gu, Z.; Aceña, J. L.; Izawa, K.; Liu, H.; Soloshonok, V. A. *J. Fluor. Chem.* **2014**, *167*, 37. f) Campbell, M. G.; Hoover, A. J.; Ritter, T. *Top. Organomet. Chem.* **2015**, *52*, 1. g) Chen, B.; Vicic, D. A. *Top. Organomet. Chem.* **2015**, *52*, 113. h) Ohashi, M.; Ogoshi, S. *Top. Organomet. Chem.* **2015**, *52*, 197. i) Ahrens, T.; Kohlmann, J.; Ahrens, M.; Braun, T. *Chem. Rev.* **2015**, *115*, 931.

[2] a) Chambers, R.D. *Fluorine in Organic Chemistry*, 2nd Ed., Blackwell: Oxford, **2004**. b) Kirsch, P. *Modern Fluoroorganic Chemistry: Synthesis, Reactivity, Applications, 1st ed.* Wiley-VCH: Weinheim, Germany, **2004**.

[3] Ritter, S. K. *Chem. Eng. News* **2010**, *88(5)*, 12.

[4] Yang, L.; da Rocha, S. R. P. *J. Phys. Chem. B* **2014**, *118*, 10675.

[5] Ritter, S. K. *Chem. Eng. News* **2015**, *93(28)*, 27.

[6] a) Tam, W.; Klute, W.; Lautnes, M. *Chem. Rev.* **1996**, *96*, 49. b) Cámpora, J.; Palma, P.; Carmona, E. *Coord. Chem. Rev.* **1999**, *193-195*, 207. c) Hager, E.; Sivaramakrishna, A.; Clayton, H. S.; Mogorosi, M. M.; Moss, J. R. *Coord. Chem. Rev.* **2008**, *252*, 1668. d) Hoyt, J. M.; Sylvester, K. T.; Semproni, S. P.; Chirik, P. J. *J. Am. Chem. Soc.* **2013**, *135*, 4862.

[7] OHashi, M.; Ogoshi, S. *Topics Organomet. Chem.* **2015**, *52*, 197.

[8] Baker, R. T.; Beatty, R. P.; Farnham, W. B.; Wallace, R. L. Jr. EP 0783472 A1, **1997**, E. I. Du Pont de Nemours & Co., USA.

[9] Ogoshi, S.; Kikushima, K.; Taniguchi, T.; Kawashima, T.; Ohashi, M. *Organometallics* **2015**, *34*, 1604.

[10] Ogoshi, S.; Kikushima, K.; Shirataki, H.; Ohashi, M. *J. Am. Chem. Soc.* **2015**, *137*, 6496.

[11] a) Browning, J.; Cundy, C. S.; Green, M.; Stone, F. G. A. *J. Chem. Soc. (A)* **1969**, 20. b) Cundy, C. S.; Green, M.; Stone, F. G. A. *J. Chem. Soc. (A)* **1970**, 1647.

[12] Maples, P. K.; Green, M.; Stone, F. G. A. *J. C. S. Dalton* **1973**, 388.

[13] a) Ristic-Petrovic, D.; Anderson, D. J.; Torkelson, J. R.; McDonald, R.; Cowie, M. *Organometallics* **2003**, *22*, 4647. b) Anderson, D. J.; McDonald, R.; Cowie, M. *Angew. Chem. Int. Ed.* **2007**, *46*, 3741. c) Slaney, M. E.; Anderson, D. J.; Ferguson, M. J.; McDonald, R.; Cowie, M. *J. Am. Chem. Soc.* **2010**, *132*, 16544. d) Slaney, M. E.; Ferguson, M. J.; McDonald, R.; Cowie, M. *Organometallics* **2012**, *31*, 1384.

[14] a) Tolman, C. A. *Chem. Rev.* **1977**, *77*, 313. b) Muller, T. E.; Mingos, D. M. P. *Transition Met. Chem.* **1995**, *20*, 533.

[15] Estimated ratios for (DPEPhos)Ni($C_2F_3H)_2$: *cis* head-tail 46%; *trans* head-tail 41%; *trans* head-head 10%; and tail-tail 3%.

[16] a) Burch, R. R.; Calabrese, J. C.; Ittel, S. D. *Organometallics* **1988**, *7*, 1642. b) Giffin, K. A.; Korobkov, I.; Baker, R. T. *Dalton Trans.* **2015**, *44*, 19587. c) Ohashi, M.; Shibata, M.; Saijo, H.; Kambara, T.; Ogoshi, S. *Organometallics* **2013**, *32*, 3631. d) Giffin, K. A.; Harrison, D. J.; Korobkov, I.; Baker, R. T. *Organometallics* **2013**, *32*, 7424.

[17] Combettes, L. E.; Clausen-Thue, P.; King, M. A.; Odell, B.; Thompson, A. L.; Gouverneur, V.; Claridge, T. D. W. *Chem. Eur. J.* **2012**, *18*, 13133.

[18] Ihrig, A. M.; Smith, S. L. *J. Am. Chem. Soc.* **1972**, *94*, 34.

[19] Stalick, J. K.; Ibers, J. A. *J. Am. Chem. Soc.* **1970**, *92*, 5333.

[20] a) Craig, N. C.; Kim, H.; Lorencak, P.; Sibley, S. P.; Kuczkowski, R. L. *J. Mol. Struct.* **1990**, *223*, 45. b) Kuehnel, M. F.; Holstein, P.; Kliche, M.; Krüger, J.; Matthies, S.; Nitsch, D.; Schutt, J.; Sparenberg, M.; Lentz, D. *Chem. Eur. J.* **2012**, *18*, 10701.

[21] a) Weigert, F. J.; Karel, K. J. *J. Fluor. Chem.* **1987**, *37*, 125. b) Weigert, F. J. *J. Fluor. Chem.* **1990**, *46*, 375.

[22] a) Anderson, J. L.; Putnam, R. E.; Sharkey, W. H. *J. Am. Chem. Soc.* **1961**, *83*, 382. b) Servis, K. L.; Roberts, J. D. *J. Am. Chem. Soc.* **1965**, *87*, 1339. c) Akkerman, F. A.; Kickbusch, R.; Lentz, D. *Chem. Asian. J.* **2008**, *3*, 719.

[23] a) Brothers, P. J.; Burrell, A. K.;Clark, G. R.; Rickard, C. E. F.; Roper, W. R. *J. Organomet. Chem.* **1990**, *394*, 615. b) Burrell, A. K.; Clark, G. R.; Jeffrey, J. G.; Rickard, C. E. F.; Roper, W. R. *J. Organomet. Chem.* **1990**, *388*, 391. c) Burrell, A. K.; Clark, G. R.; Rickard, C. E. F.; Roper, W. R. *J. Organomet. Chem.* **1994**, *482*, 261. d) Huang, D. J.; Koren, P. R.; Folting, K.; Davidson, E. R.; Caulton, K. G. *J. Am. Chem. Soc.* **2000**, *122*, 8916. e) Ferrando-Miguel, G.; Gerard, H.; Eisenstein, O.; Caulton, K. G. *Inorg. Chem.* **2002**, *41*, 6440. f) Hughes, R. P. *Eur. J. Inorg. Chem.* **2009**, 4591. g) Leclerc, M. C.; Bayne, J. M.; Lee, G. M.; Gorelsky, S. I.; Vasiliu, M.; Korobkov, I.; Harrison, D. J.; Dixon, D. A.; Baker, R. T. *J. Am. Chem. Soc.* **2015**, *137*, 16064.

[24] Andrella, N. O.; Sicard, A. J.; Gorelsky, S. I.; Korobkov, I.; Baker, R. T. *Chem. Sci.* **2015**, *6*, 6392.

[25] Anderson, J. L.; Putnam, R. E.; Sharkey, W. H. *J. Am. Chem. Soc.* **1961**, *83*, 382.

[26] Krespan, C.G.; Dixon, D. A. *J. Fluorine Chem.* **1996**, *77*, 117.

[27] Ohashi, M.; Ueda, Y.; Ogoshi, S. *Angew. Chem. Int. Ed.* **2017**, *56*, 2435.

[28] Harrison, D. J.; Gorelsky, S. I.; Lee, G. M.; Korobkov, I.; Baker, R.T. *Organometallics* **2013**, *32*, 12.

[29] Lentz, D.; Bach, A.; Jürgen, B.; Luger, P.; Messerschmidt, M. *Chem. – Eur. J.* **2004**, *10*, 5059.

Chapter 5. Formation and C−F bond functionalization of [P,N]-coordinated perfluoronickelacyclopentanes

K. A. Giffin, L. A. Pua, I. Korobkov and R. T. Baker *manuscript in preparation*.

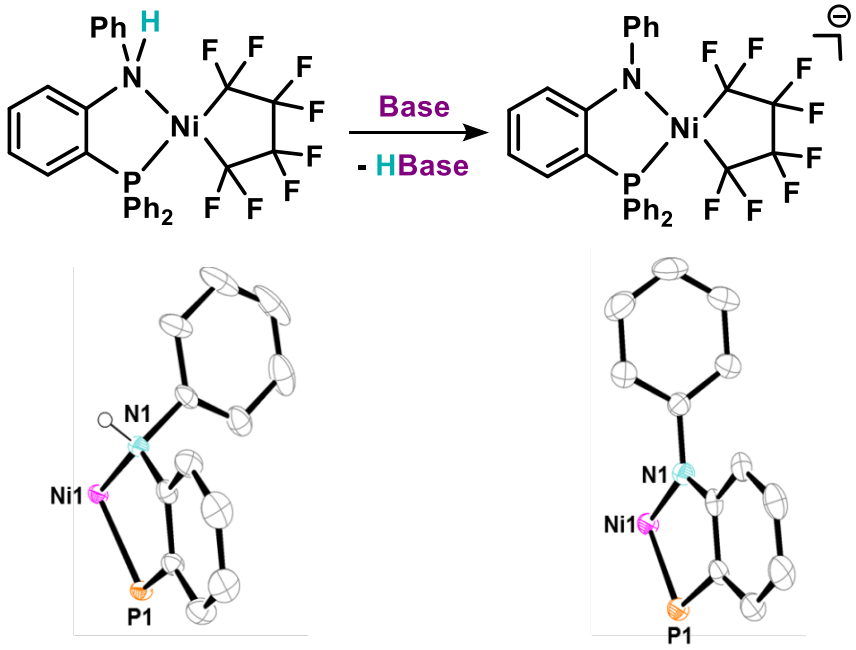

5.1 Author Contributions

Giffin wrote the Chapter. Giffin performed all experiments presented. Pua performed preliminary experimental studies under the supervision of Giffin. Korobkov was responsible for X-ray diffraction studies.

5.2 Abstract

Detailed herein is the synthesis and characterization of **[P,N]**-ligated perfluoronickelacyclopentanes based on the bidentate ligand 2-(diphenylphosphino)phenyl-*N*-phenylaniline **[P,NH]**. A clean, high-yielding substitution reaction between $[P(O\text{-}o\text{-}tol)_3]_2Ni(C_4F_8)$ and **[P,NH]** gives the phosphinoamine-coordinated metallacycle **Ni-21**. Alternatively, **Ni-21** is formed upon treatment of Ni(0) with **[P,NH]** followed by tetrafluoroethylene (TFE). This product reacts quantitatively with base to give an anionic phosphinoamide-coordinated metallacycle.

Additionally, treatment of the deprotonated ligand **[P,N$^-$]** with Ni(0) and TFE, or exclusively with TFE leads to the formation of a nickelacyclopentane complex or a perfluorovinyl compound respectively. Reactivity studies of the new **[P,NH]**- and **[P,N$^-$]**-ligated perfluoronickelacycles are presented and compared/contrasted to previously reported systems.

5.3 Introduction

Complexes incorporating cooperative ligands have become well known as the most active and efficient catalysts for a variety of challenging chemical transformations, most notably the activation of small molecules.[1] The most established metal ligand cooperative systems to date incorporate metal−amido/amino bonds.[1d] For example, ruthenium complex **A** has been reported as a very effective catalyst for ketone/ester hydrogenation to alcohols, and for the dehydrogenation of ammonia-borane (Scheme 5.1).[2] Although the exact nature of cooperativity between the metal and nitrogen has recently been debated[3], a decrease in activity in the absence of the N*H* functionality confirms that some type of cooperativity is responsible for the higher activities observed with such catalysts.[4] In particular, bi- and tridentate ligands based on **[P,N]** scaffolds have been especially successful as catalysts for challenging bond activation reactions.[5] This can perhaps be attributed to an increase in robustness in comparison to chelating ligands based on **[N,N]** scaffolds. Such **[P,N]** platforms have yet to be investigated as ligands for transformations of fluoroalkyl groups at transition metal centres.

Scheme 5.1 [P,N]-type ruthenium catalysts used for various chemical transformations.

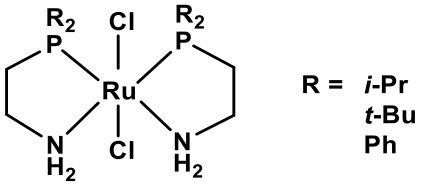

A

As discussed in the Chapters above, there is great interest in discovering more sustainable and atom economical routes to functionalized FCs. We have also noted that transition metal fluoroalkyl complexes are known to be very robust based on the stability of M−R^F and C−F bonds, requiring

high temperatures or pressures to achieve any reactivity.[6] A good example of this is the catalytic hydrodimerization of TFE (proceeding through perfluoronickelacyclopentane intermediates) developed by Baker, where pressures and temperatures of 700 psi and 100°C are needed for productive catalysis (Scheme 5.2a).[7] In this case, the bulky monodentate phosphite ligands act as spectator ligands and also stabilize the Ni(0) intermediate. More recently, Mr. Nick Andrella from the Baker group has explored the effects of employing one equivalent of very bulky ligand to obtain low-coordinate metallacycle complexes (Scheme 5.2b).[8] Unpublished results from Andrella demonstrate that hydrogenolysis of (NHC)Ni(C_4F_8) occurs under mild conditions, with full conversions obtained at room temperature and only ca. 7 psi of H_2! Some selectivity is lost under these conditions and the formation of octafluorobutane is accompanied by formation of another uncharacterized organofluorine product. Furthermore, a competing reaction between SIPr and free TFE renders this system less amenable to catalytic conditions (Scheme 5.3).[9]

Scheme 5.2 Hydrogenolysis reactions of perfluoronickelacyclopentanes.

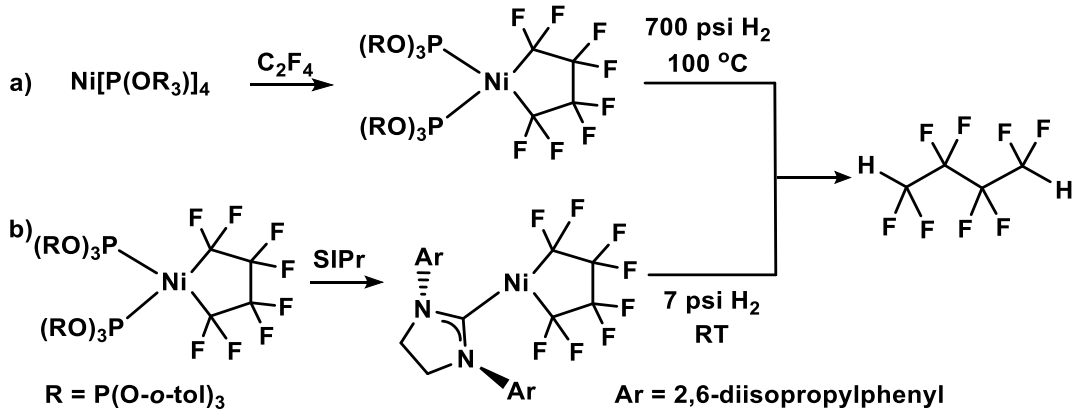

Scheme 5.3 Reactivity of free SIPr NHC with tetrafluoroethylene.

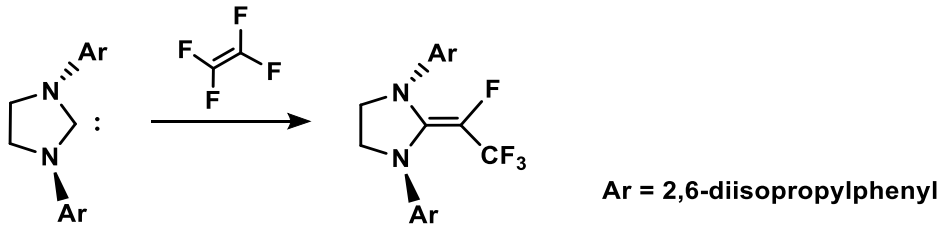

The reactions outlined above highlight some of the progress that has been made in terms of perfluorometallacycle reactivity based on ligand variation. Keeping in line with this, we set out to examine the use of potentially cooperative ligands in perfluoronickelacycle formation and reactivity. We recently reported substitution reactions with bidentate 1,2,4-(HS),(Ph_2P),Me(C_6H_3) **[P,SH]** and (PR_3)$_2$Ni(C_4F_8). When PR_3 equals the phosphite ligand, P(O-*i*-Pr)$_3$, the thiolate group in ***Int 2*** nucleophilically attacks an O−*i*-Pr bond of the phosphonium cation to give thioether-bound product **Ni-2** (Scheme 5.4, left).[10] Alternatively, when PR_3 equals phosphine ligand, regioselective C_α−F activation of ***Int 2*** occurs followed by phosphine installment in the C_α position, affording phosphinothiolate-coordinated functionalized metallacycles **Ni-11a** and **Ni-11b** (Scheme 5.4, right).[11]

In this study, we report the synthesis and preliminary reactivity studies of new amino- and amido-coordinated perfluoronickelacyclopentanes based on both the neutral form **[P,NH]** and anionic form **[P,N$^-$]** of the bidentate ligand, 2-(diphenylphosphino)phenyl-*N*-phenylaniline.[12] We also introduce an interesting reaction between free deprotonated ligand **[P,N$^-$]** and TFE that is proposed to generate the organic product resulting from alkenyl fluoride substitution with the amido nucleophile of the **[P,N$^-$]** compound.

Scheme 5.4 Summary of reactivity between [P,SH] and $(PR_3)_2Ni(C_4F_8)$.

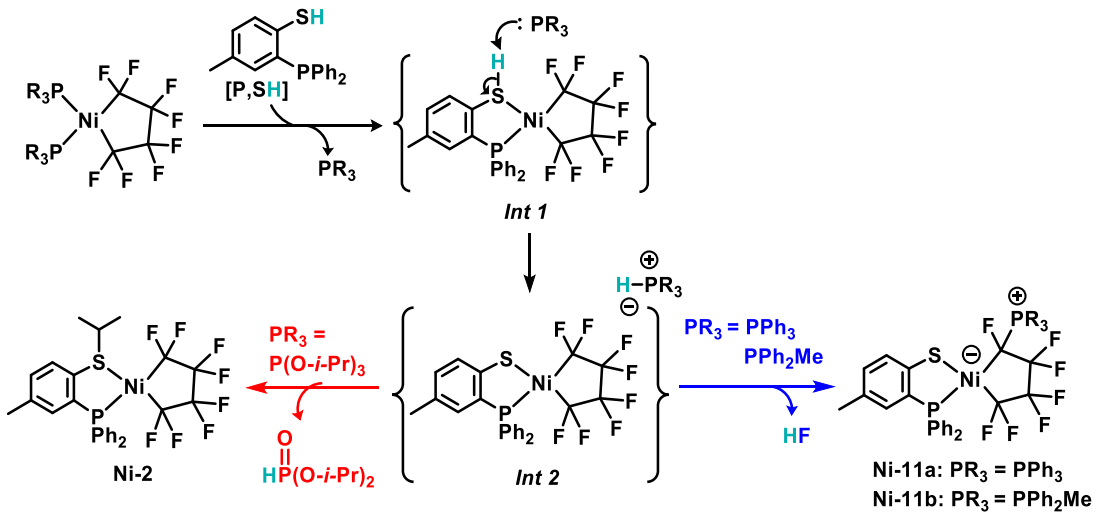

5.4 Results and Discussion

Unlike the **[P,SH]** ligand studied previously, addition of **[P,NH]** to bis(phosphite) perfluoronickelacycle **Ni-8** leads to a clean ligand substitution reaction, exclusively forming the phosphinoamine-coordinated **Ni-21** complex (Scheme 5.5, top). Interestingly, **Ni-21** can also be accessed by addition of **[P,NH]** to low valent $Ni[P(O\text{-}o\text{-}tol)_3]_4$, followed by treatment with sub-atmospheric pressures of TFE (Scheme 5.5, bottom). This is promising in the context of potential future applications in catalytic processes where metallacyclopentanes are desired as intermediates. Previous reports involving TFE addition to Ni(0) complexes containing chelating **[P,P]** [$Cy_2P(CH_2)_2PCy_2$ and $Cy_2P(CH_2)_4PCy_2$][13] or **[N,N]** [tetramethyl(ethylene)diamine][14] ligands afforded 3-membered metallacycles, with the exception of the DPPE-ligated perfluoronickelacycle reported by Stone.[15] The phoshinoamide-coordinated anionic metallacycle **Ni-22•Na** can be formed quantitatively upon treatment of **Ni-21** with a stoichiometric amount of base and 18-Crown-6 (Scheme 5.5).

Scheme 5.5 Synthesis of amino- and amido-coordinated perfluoronickelacycles.

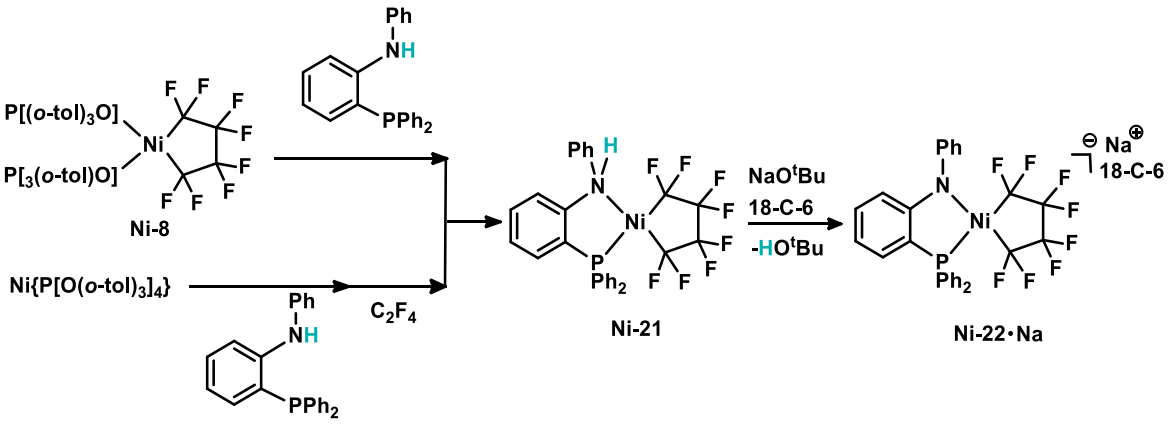

Structural characterization of both **Ni-21** and **Ni-22•Na** reveals significant changes in bond lengths upon moving from an amino-coordinated complex to the amido anionic complex (Figure 4.1). Specifically, a notable shortening of the Ni−N bond and the N−C_{Ar} bond in the ring linking the nitrogen and phosphine groups occurs. In contrast, there is little effect on the N−C_{Ar} bond length of the *N*-phenyl group upon deprotonation. The X-ray structure of **Ni-22•Na** also clearly depicts the roughly planar geometry of the nitrogen atom[16], consistent with the observed change in symmetry from C_l (**Ni-21**) to C_s (**Ni-22•Na**) by multinuclear NMR characterization.

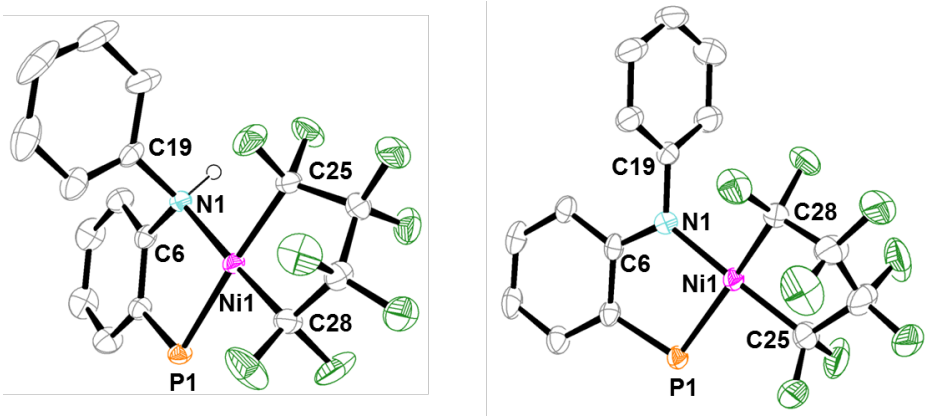

Figure 5.1 ORTEP representation of the molecular structures of complexes **Ni-21** (left) and **Ni-22•Na** (right). Thermal ellipsoids are set at the 40% probability level. Hydrogen atoms and phenyl rings of **P1** are omitted for clarity.

The ^{19}F NMR spectra are most informative when considering this symmetry change. The eight unique fluorine signals for **Ni-21** containing no mirror plane collapse to four signals upon deprotonation to **Ni-22•Na**, indicative of the increase in symmetry (Figure 5.2). An ESI-MS experiment of **Ni-22•Na** in acetonitrile reveals an intense parent ion in the negative mode corresponding to the nickel anion $\{[1,2\text{-}(PhN),(Ph_2P)(C_6H_4)]Ni(C_4F_8)\}^-$ at *m/z* 610.0 (calc'd value: m/z 610.0) with a distinct nickel isotope pattern.

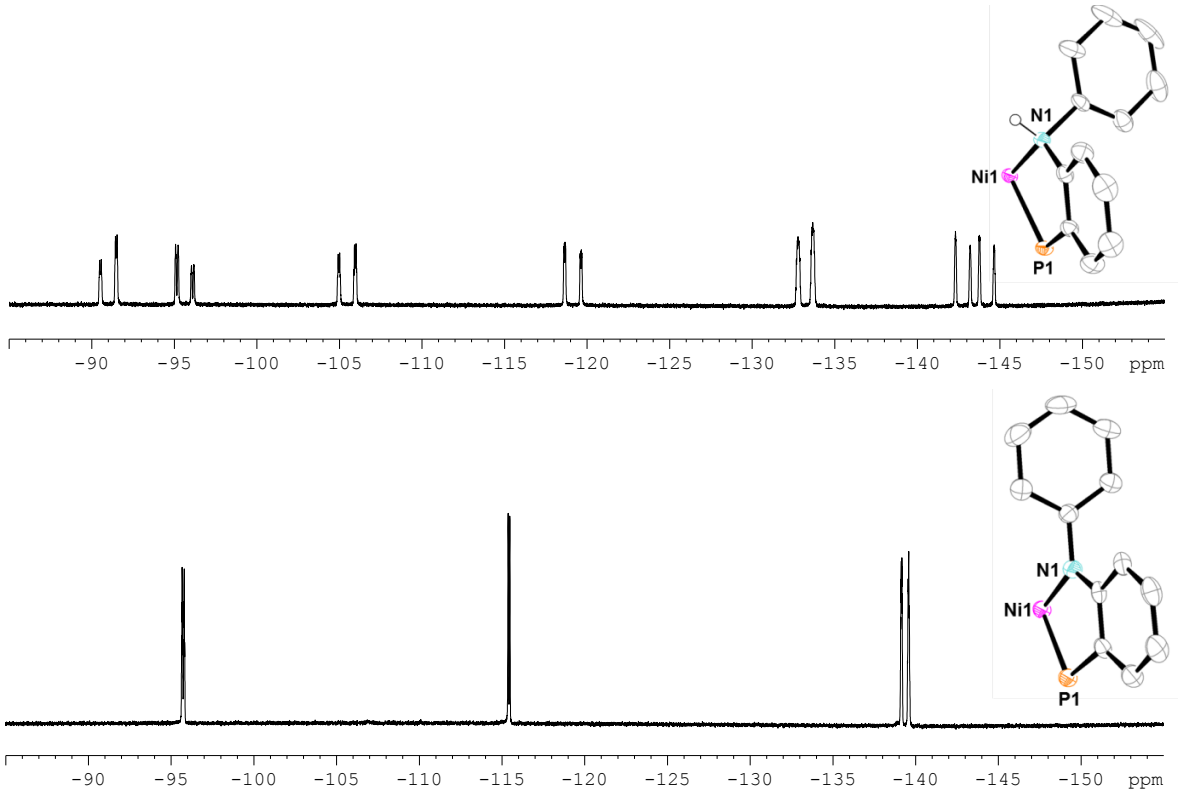

Figure 5.2 Top: The 1D ^{19}F NMR spectrum of **Ni-21** depicting the eight unique fluorine peaks (282 MHz, C_6D_6). Bottom: The 1D ^{19}F NMR spectrum of **Ni-22•Na** (282 MHz, CD_3CN). Additionally, selected portions of the ORTEP representations of **Ni-21** and **Ni-22•Na** are depicted.

Complex **Ni-22•Na** was further characterized electrochemically and the cyclic voltammetry data is presented in Figure 5.3. At a sweep rate of 0.1 V s^{-1} (red voltammogram), an irreversible peak at -0.25 V is consistent with a Ni^{II} to Ni^{III} redox couple. Increasing the sweep rate to 1.0 V s^{-1} (blue voltammogram) results in an improvement in the reversibility, with a more distinct cathodic peak observed at -0.36 V.

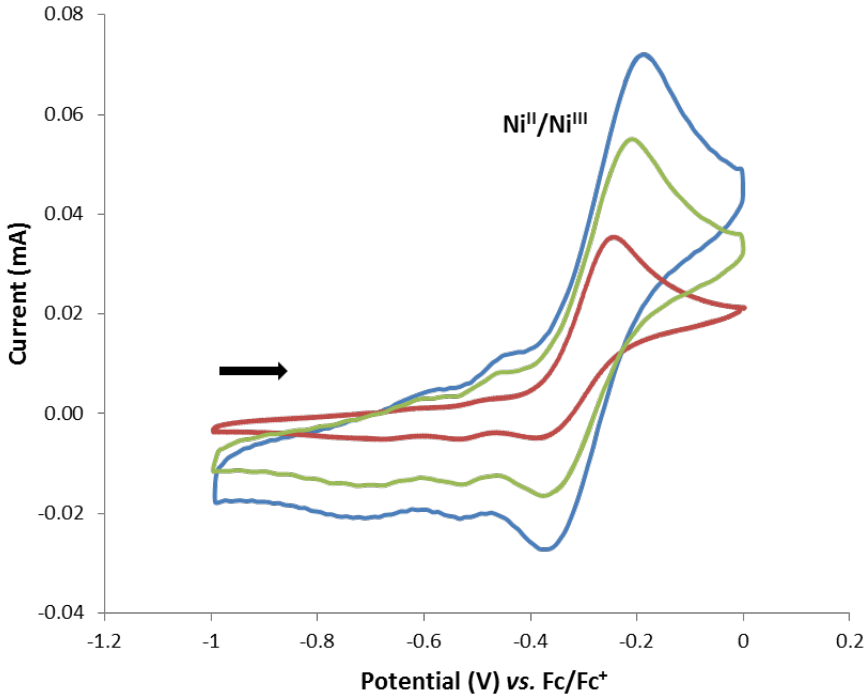

Figure 5.3 Cyclic voltammograms of **Ni-22•Na** in 0.1 M [(nBu)$_4$N][PF$_6$]/THF [v = 0.1 V s^{-1} (red), 0.5 V s^{-1} (green) and 1.0 V s^{-1} (blue)].

The deprotonated form **[P,N$^-$]** of the bidentate ligand can be formed quantitatively *in situ* by addition of NaH to **[P,NH]** in THF, resulting in a shift of the phosphorus signal in the ^{31}P{^{1}H} spectrum from δ_P –19.1 ppm to –9.5 ppm. Anionic metallacycle **Ni-22•K** can alternatively be synthesized by sequential addition of NiP[O-*o*-tol)$_3$]$_4$ and TFE to the phosphinoamide ligand **[P,N$^-$]** (Scheme 5.6, top).

Free **[P,N$^-$]** ligand reacts quantitatively with TFE to give three new products as revealed by ^{31}P{^{1}H} NMR. Based on some signature NMR handles, the major product is proposed to be unsymmetrical fluoroalkenyl compound **O6**, resulting from the formation of a new C–N bond with concomitant NaF elimination (Scheme 5.6, middle). Table 5.2 highlights some of the key features of the ^{19}F and ^{31}P{^{1}H} NMR that are consistent with the proposed structure **O6**. The large $^6J_{PF}$ coupling constant of 26 Hz between P and F$_C$ can perhaps be attributed to a through-space effect. Further

studies including a ^{19}F-$^{31}P\{^{1}H\}$ NOESY experiment would be helpful in confirming the proximity of these two atoms.

Scheme 5.6 Reactivity of [P,N$^-$] ligand.

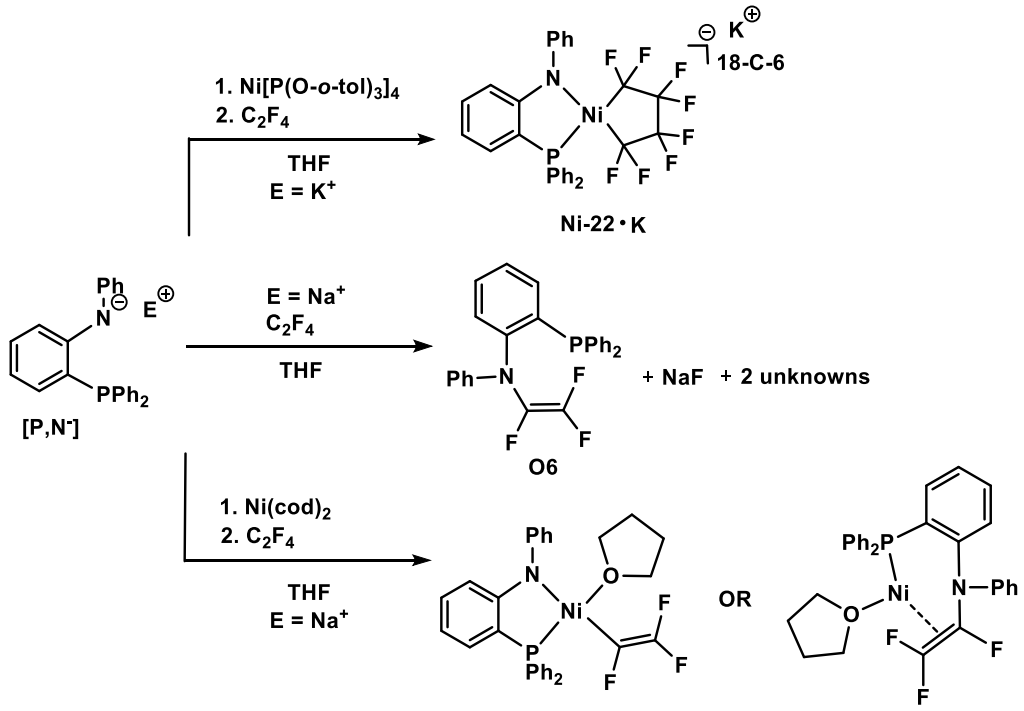

Table 5.1. Selected NMR data for proposed compound O6.

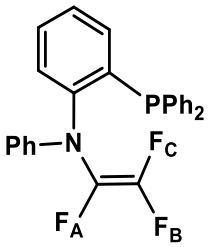

Nuclei	Coupling (Hz)
F_A-F_B	40
F_A-F_C	110
F_B-F_C	68
P-F_C	26
P-F_A	19

This organic reaction is reminiscent of the reactivity reported by Mr. Matthew Leclerc of our group between *N*-heterocyclic polyfluoroalkenyl imidazolium salts and nitrogen-based nucleophiles.[17] Addition of an equimolar amount of $Ni(cod)_2$ to **[P,N⁻]** as the Ni(0) source in place of $Ni\{P[O(o\text{-}tol)_3]\}_4$ does not yield **Ni-22•Na**, but rather gives a major product containing a trifluorovinyl group as evidenced by the distinctive F-F couplings observed by ^{19}F NMR (Scheme 5.6, bottom). At this point, we cannot conclude whether the trifluorovinyl group is coordinated to Ni, or whether it is a complex resulting from a C−N bond forming reaction with the amido group of the ligand. Previously reported perfluorovinyl Ni complexes are typically accessed by heating or addition of a Lewis acid to η^2-TFE complexes[13], and have recently been implicated as important intermediates in Hiyama and Suzuki-Miyaura coupling reactions.[9a,18]

In keeping with the unique reactivity between the **[P,S^{iPr}]**-ligated perfluoronickelacycle and Lewis acids, **[P,NH]**-ligated **Ni-21** gives metallabicyclic **Ni-23** upon treatment with Me_3SiOTf (Scheme 5.7). Again, exclusive formation of the C_α−P functionalized metallacycle is observed with no evidence of any competing migration of the nitrogen donor. The deprotonation reactivity detailed above for **Ni-21** extends to metallabicyclic **Ni-23**; upon treatment with sodium *tert*-butoxide in acetonitrile, **Ni-24** is cleanly formed, with concomitant formation of HO^{t}Bu and NaOTf, retaining a Ni(II) oxidation state in the product.

Scheme 5.7 Synthesis of Ni-23 and Ni-24 metallabicycles.

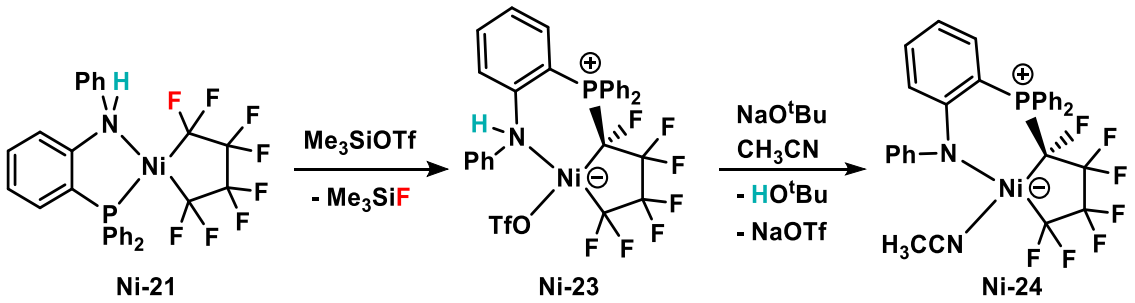

Ni-21 Ni-23 Ni-24

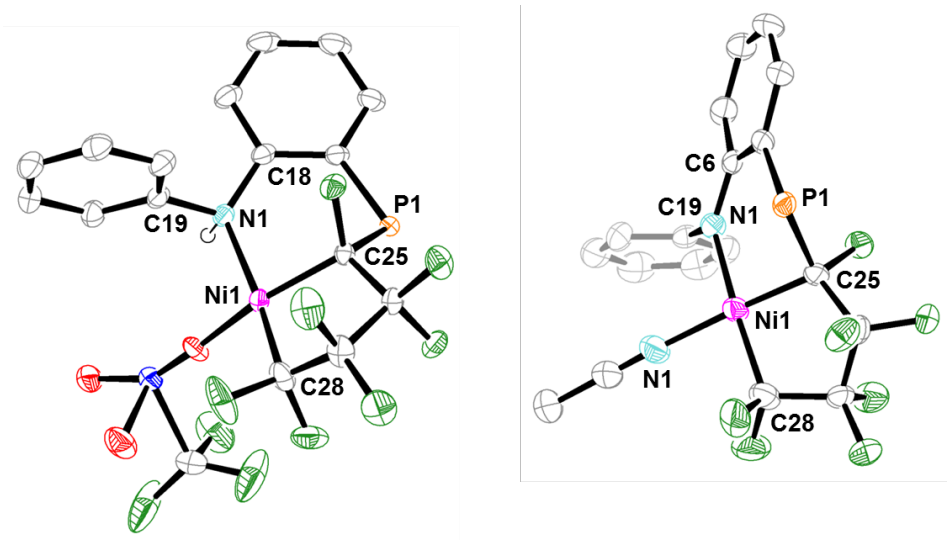

Figure 5.4 ORTEP representation of the molecular structures of complexes **Ni-23** (left) and **Ni-24** (right). Thermal ellipsoids are set at the 40% probability level. Hydrogen atoms and phenyl rings of **P1** are omitted for clarity. Outersphere solvent molecules are removed for clarity. For **Ni-23**, one of two orientations of the disordered OTf group is shown.

Crystallographic studies of **Ni-23** and **Ni-24** show similar trends to the structures depicted above. Both the Ni−N and Ni−C_{Ar} (aryl group linking nitrogen and phosphine donor) contract upon substituting the amino group for an amido (see Table 4.1). The structure of **Ni-24** reveals that the Ni−N bond to the coordinated acetonitrile molecule is notably shorter in comparison to the Ni−N bond of the coordinated amido group.

We next turned our attention to the reactivity of anionic nickelacycle **Ni-22•Na** with Brønsted acids. In contrast to the previously reported phosphinothiolate anionic complex **Ni-12**, which affords phosphine-functionalized products (**Ni-11a** and **Ni-11b**) when treated with tertiary phosphonium salts (see Scheme 3.5), **Ni-22•Na** re-forms **Ni-21** in the presence of the same phosphonium salts, arising from protonation of the amido group and overall loss of free phosphine and NaBr salt as by-products (Scheme 5.8).

Scheme 5.8 Reaction of Ni-22•Na with phosphonium salts.

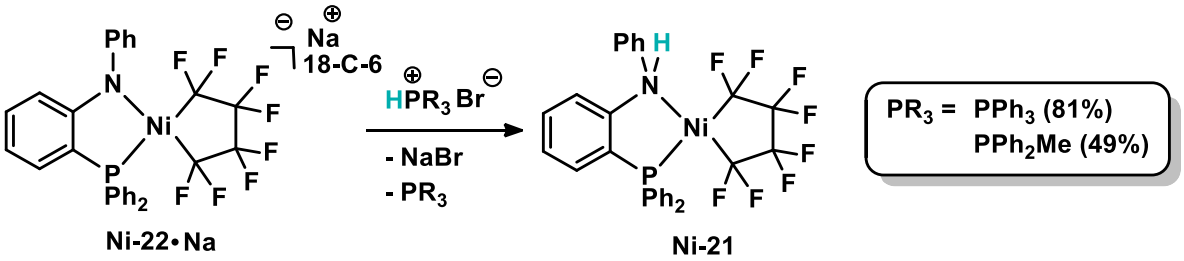

As mentioned above, all examples of perfluoronickelacyclopentane hydrogenolysis afford octafluorobutane as the major fluoroorganic product. We envisaged that **[P,N$^-$]**-ligated metallacycles could potentially proceed through alternative reaction mechanisms in the presence of H_2, involving

Table 5.2 Selected bond lengths (Å) and angles (deg) for Ni-21, Ni-22•Na, Ni-23 and Ni-24.

	Ni-21	Ni-22•Na	Ni-23	Ni-24
Ni-N1	2.0070(17)	1.930(2)	2.049(2)	1.939(2)
Ni-P1	2.2032(6)	2.2007(7)	-	-
Ni-C_α (trans to N)	1.902(2)	1.905(3)	1.905(3)	1.904(3)
Ni-C_α'	1.921(2)	1.946(3)	1.886(3)	1.911(3)
C_α-C_β (avg)	1.515(3)	1.531(4)	1.530(5)	1.518(4)
C_β-C_β'	1.511(3)	1.446(5)	1.526(4)	1.510(4)
C_α-F (avg)	1.386(3)	1.379(4)	1.375(4)	1.384(4)
C_β-F (avg)	1.360(3)	1.395(4)	1.356(4)	1.358(3)
C_α-F (gem to P)	-	-	1.415(3)	1.424(3)
C_α-P	-	-	1.833(3)	1.828(3)
Ni-N2	-	-	-	1.897(3)
Ni-O (avg)	-	-	1.971(4)	-
C_α-Ni-C_α'	85.40(10)	86.26(12)	87.36(13)	86.69(12)
C_α'-Ni-P	95.56(7)	92.95(9)	-	-
N-Ni-P	87.01(5)	85.37(7)	-	-
N1-Ni-C_α	92.07(8)	97.05(11)	94.06(11)	93.28(10)
N-Ni-O	-	-	93.34(15)	-
O-Ni-C_α	-	-	85.44(17)	-
N1-Ni-N2	-	-	-	92.80(10)
N2-Ni-C_α	-	-	-	88.11(12)

cooperative participation of the amido group (Scheme 5.9). The proposed cycle begins with addition of an H_2 molecule across the nickel−amido unit, followed by a ring-opening reaction to give a nickel−fluoroalkyl intermediate. Ideally, the presence of an N−H bond rather than a Ni−H at this stage would instigate a β-fluoride elimination, favouring the generation of targeted hydrofluoroalkenes over hydrofluoroalkanes.

Scheme 5.9 Potential cycle for hydrogenolysis of [P,N]-ligated perfluonickelacycles.

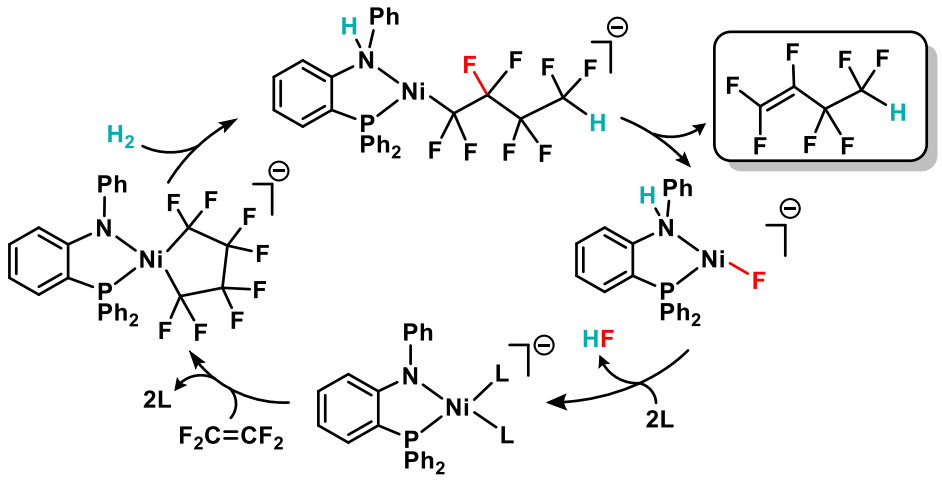

Surprisingly, **Ni-22•Na** remains unreactive towards 740 psi of H_2 at 80 °C and for 24 h! We speculate that the stability of **Ni-22•Na** could be attributed to the resonance stabilization of the nitrogen lone pair, as evidenced by the near planar geometry about nitrogen as well as the short N−C_{Ar} bond. Consequently, we have begun investigations with other **[P,N]**-type ligands, and with more reactive reducing agents, such as silanes.

5.5 Conclusions

In summary, we have outlined the synthesis and full characterization of a neutral phosphinoamine- (**Ni-21**) and an anionic phosphinoamide-coordinated (**Ni-22•Na**) perfluoronickelacyclopentane. We have demonstrated that **Ni-21** can be formed either by a ligand substitution reaction involving **[P,NH]** and $[P(O\text{-}o\text{-tol})_3]_2Ni(C_4F_8)$, or by treating low valent Ni(0) with **[P,NH]** followed by an excess of TFE to afford the oxidative cyclization product. Furthermore, we explored the reactivity of the

deprotonated bidentate **[P,N⁻]** ligand, leading to formation of a new substituted fluoroalkenyl compound through a C−F bond substitution reaction with the amido group of **[P,N⁻]** acting as the nucleophile. Reactivity studies of the **[P,NH]**-ligated metallacycle with Lewis acids expands on previously reported reactions, where phosphine-functionalization of the fluorinated metallacycle is achieved via selective C_α−F activation. Finally, addition of weak phosphonium acids to $\{[P,N]Ni(C_4F_8)\}^-$ results in protonation at the nitrogen position, affording $[P,NH]Ni(C_4F_8)$. In contrast, the anion does not readily promote the heterolytic cleavage of dihydrogen even at 80°C under 700 psi of H_2. Ongoing studies in our group aim to exploit the bifunctional nature of **[P,N]**-ligated metallacycles in order to develop alternative catalytic routes to novel small-molecule functionalized FCs.

5.6 Experimental Section

5.6.1 General

Experiments were conducted under nitrogen, using Schlenk techniques or an MBraun glove box. All solvents were deoxygenated by purging with nitrogen. Toluene, hexanes, diethyl ether and tetrahydrofuran (THF) were dried on columns of activated alumina using a J. C. Meyer solvent purification system. Benzene-d_6 (C_6D_6) was dried by stirring over activated alumina (ca. 10 wt.%) overnight, followed by filtration. Acetonitrile (CH_3CN), acetonitrile-d_3 (CD_3CN), and dichloromethane (DCM) were dried by refluxing over calcium hydride under nitrogen. After distillation, CH_3CN, CD_3CN and DCM were further dried by stirring over activated alumina (ca. 5 wt.%) overnight, followed by filtration. All solvents were stored over activated (heated at ca. 250^{o}C for >10 h under vacuum) 4 Å molecular sieves. Glassware was oven-dried at 150^{o}C for >2 h. The following chemicals were obtained commercially, as indicated: trimethylsilyl trifluoromethanesulfonate (Me_3SiOTf, Aldrich, 99%), bis(1,5-cyclooctadiene)nickel (0) ($Ni(cod)_2$, Strem, 98+%), $P(O\text{-}o\text{-tol})_3$, Strem. Tetrafluoroethylene was made by pyrolysis of polytetrafluoroethylene (Scientific Polymer Products, powdered) under vacuum, using a slightly

modified literature procedure (10−20 mTorr, 650°C, 30 g scale, product stabilized with (R)-(+)-limonene (Aldrich, 97%), giving TFE of ca. 97% purity).[19] Compound $[P(O\text{-}o\text{-}tol)_3]_2]Ni(C_4F_8)$ was made by oxidative addition of tetrafluoroethylene to $Ni[P(O\text{-}o\text{-}tol)_3]_4$ using a slightly modified literature procedure.[7] The **[P,NH]** ligand, 2-(diphenylphosphino)phenyl-*N*-phenylaniline, was synthesized using a slightly modified literature procedure.[12] ^1H, ^{19}F, $^{31}P\{^1H\}$, and $^{13}C\{^1H\}$ NMR spectra were recorded on a 300 MHz Bruker Avance instrument at room-temperature (21-23^oC). ^1H NMR spectra were referenced to the residual proton peaks associated with the deuterated solvents. ^{19}F NMR spectra were referenced to internal 1,3-bis(trifluoromethyl)benzene (BTB) (Aldrich, 99%, deoxygenated by purging with nitrogen, stored over activated 4 Å molecular sieves), set to –63.5 ppm. $^{31}P\{^1H\}$ NMR data were referenced to external H_3PO_4 (85% aqueous solution), set to 0.0 ppm. UV-vis spectra were recorded on a Cary 100 instrument, using sealable quartz cuvettes (1.0 cm pathlength). Electrospray ionization mass spectral data were collected using an Applied Biosystem API2000 triple-quadrupole mass spectrometer. Elemental analyses were performed by CENTC Elemental Analysis Facility at the University of Rochester.

5.6.2 X-ray Crystallography

For **Ni-21**, **Ni-22•Na**, **Ni-23** and **Ni-24**: samples were mounted on thin glass fibers using paraffin oil and were cooled to 200 K prior to data collection. Data were collected on a Bruker AXS KAPPA single crystal diffractometer equipped with a sealed Mo tube source (wavelength 0.71073 Å) APEX II CCD detector. Raw data collection and processing were performed with APEX II software package from BRUKER AXS.[20] Diffraction data were collected with a sequence of 0.5° ω scans at 0, 90, 180, and 270° in ϕ. Initial unit cell parameters were determined from 60 data frames collected at the different sections of the Ewald sphere. Semi-empirical absorption corrections based on equivalent reflections were applied. Systematic absences in the diffraction data set and unit-cell parameters were consistent with a triclinic system for **Ni-22•Na** and monoclinic systems for **Ni-21**, **Ni-23** and **Ni-24**. Solutions in centrosymmetric space group yielded chemically reasonable and computationally stable results of refinement. The structures were solved by direct methods, completed with difference

Fourier synthesis, and refined with full-matrix least-squares procedures based on *F*.[27] In the structure, compound molecules are situated in the general position. All non-hydrogen atoms were refined anisotropically with satisfactory thermal parameters values. Additional crystallographic data and selected data collection parameters are reported in Table A1.

5.6.3 Cyclic Voltammetry

Cyclic voltammetry was performed using a Princeton Applied Research Versastat3 potentiostat controlled by Versastudio software. A conventional single compartment 3-electrode configuration with Pt working and counter electrodes and a silver pseudoreference electrode was employes. The measurements were carried out on acetonitrile solutions containing 0.1 M tetrabutylammonium hexafluorophosphate (Aldrich) as a supporting electrolyte. The experiments were subsequently refererenced to the Fc/Fc^+ redox couple of ferrocene.

5.6.4 Synthesis of [1,2-(H*Ph*N),(Ph_2P)(C_6H_4)]Ni(C_4F_8) (Ni-21)

Method A: **[**P(O-*o*-tol)$_3$]$_2$Ni(C_4F_8)] **(Ni-8)** (700 mg, 0.727 mmol) was placed in a 100 mL round-bottom flask and dissolved in ca. 10 mL of toluene. [1,2-(H*Ph*N),(Ph_2P),(C_6H_4)] (257 mg, 0.727 mmol) was added to the stirred **[**P(O-*o*-tol)$_3$]$_2$Ni(C_4F_8)]/toluene mixture, and stirring was continued at room temperature for ca. 12 h. The cloudy yellow reaction mixture was concentrated in vacuo until ca. 2 mL of yellow paste remained. Around 20 mL of hexanes was added, precipitating a light yellow powder. The flask was cooled to -35°C. The product was filtered cold, washed with pre-cooled hexanes (2 x 3 mL), and dried in vacuo, affording a light yellow powder. Yield: 378 mg, 0.618 mmol, 85% based on **Ni-8**. X-ray quality crystals were grown by slow evaporation from a diethyl ether solution. ^{1}H NMR (300 MHz, C_6D_6) δ 5.81 (br s, 1H, N*H*), 6.26 (m, 1H, Ar-H), 6.64 (d d, 2H, Ar-H), 6.69-6.80 (ov m, 5H, Ar-H), 6.88 (ov m, 7H, Ar-H), 7.16 (solvent), 7.44 (d d, 2H, Ar-H), 7.81 (d d, 2H, Ar-H) . ^{19}F NMR (282 MHz, C_6D_6) δ -91.0 (d d m, 1F$_\alpha$, $^2J_{FF}$ = 271 Hz, $^3J_{FP}$ = 27 Hz), -95.6 (d d d, 1F$_\alpha$, $^2J_{FF}$ = 271 Hz, $^3J_{FP}$ = 42 Hz), -105.4 (d d m, 1F$_\alpha$, $^2J_{FF}$ = 279 Hz, $^3J_{FP}$ = 27 Hz), -119.1 (d d d, 1F$_\alpha$, $^2J_{FF}$ = 279 Hz, $^3J_{FF}$ = 10Hz, $^3J_{FP}$ = 22 Hz), -133.2 (ov d m, 2F$_\beta$, $^2J_{FF}$ = 251 Hz), -142.7 (d m, 1F$_\beta$, $^2J_{FF}$ = 251 Hz), -144.2 (d d t, 1F$_\beta$, $^2J_{FF}$ = 251 Hz). ^{31}P{^{1}H} NMR (121 MHz, C_6D_6) δ 25.9 (m,1P).

Anal. Calc. for $C_{28}H_{20}F_8NNiP$: C, 54.94, H, 3.29. Found: C, 55.07, H, 3.02. See Figures A34-A36 for ^1H, ^{19}F and $^{31}P\{^1H\}$ spectra.

Method B: Ni[P(O-*o*-tol)$_3$]$_4$ (20 mg, 0.014 mmol) was dissolved in ca. 0.7 mL THF and transferred to a vial containing [1,2-(H*Ph*N),(Ph_2P),(C_6H_4)] (5 mg, 0.0.014 mmol). Initial colour of reaction mixture was a clear orange. The reaction mixture was transferred to a screw cap NMR tube containing BTB (2.5 μL, 0.016 mmol) and ca. 3 mL of TFE were injected. The reaction mixture was left to stand at RT for 16 h, over the course of which the colour gradually changed to a clear yellow. Integration of product F peaks relative to BTB in the ^{19}F spectrum indicated 49% yield of **Ni-21**.

5.6.5 Synthesis of [1,2-(*Ph*N$^-$),(Ph_2P)(C_6H_4)]Ni(C_4F_8)(Na)(18-Crown-6) (Ni-22•Na)

Method A: [1,2-(H*Ph*N),(Ph_2P)(C_6H_4)]Ni(C_4F_8) (300 mg, 0.49 mmol) was placed in a 100 mL round-bottom flask and dissolved in THF (ca. 10 mL). NaO^{t}Bu (47 mg, 0.49 mmol) was added to the [1,2-(H*Ph*N),(Ph_2P)(C_6H_4)]Ni(C_4F_8)/THF (ca. 10 mL) solution. An immediate colour change from yellow to orange occurred. Immediately after, one equivalent of 18-Crown-6 was added to the flask (130 mg, 0.49 mmol). The reaction mixture was left to stir at RT for 16 h. The orange reaction mixture was concentrated in vacuo until 10 mL solution remained in the flask (precipitate already beginning to form). Around 10 mL of hexanes was added, precipitating a yellow powder. The flask was cooled at -35°C. The product was filtered cold, washed with pre-cooled hexanes (3 x 3 mL), and dried in vacuo, affording a dark yellow powder. Yield: 405 mg, 0.45 mmol, 92% based on [1,2-(H*Ph*N),(Ph_2P)(C_6H_4)]Ni(C_4F_8). X-ray quality crystals were grown by slow cooling of a supersaturated THF solution. ^1H NMR (300 MHz, CD_3CN) δ 1.94 (solvent), 3.57 (s, 24H, 18-Crown-6), 5.59 (d d, 1H, Ar-H linking P and N), 6.00 (app t, 1H, Ar-H linking P and N), 6.66 (app t, 1H, Ar-H linking P and N), 6.77 (app t, 1H, Ar-H linking P and N), 6.85-7.03 (ov m, 3H, Ar-H), 7.15-7.25 (ov m, 2H, Ar-H), 7.40-7.54 (ov m, 6H, Ar-H), 7.84 (d d, 4H, Ar-H). ^{19}F NMR (282 MHz, CD_3CN) δ -95.7 (d m, $^3J_{FP}$ = 34 Hz, $2F_\alpha$), -115.4 (d m, $^3J_{FP}$ = 28 Hz, $2F_\alpha$), -139.1 (m, $2F_\beta$), -139.6 (m, $2F_\beta$). $^{31}P\{^1H\}$ (121 MHz, CD_3CN) δ 32.1 (app quintet, J_{PF} = 34 Hz, 28 Hz, 1P). Anal. Calc. for $C_{35}H_{40}F_8NaNiO_6PS$: C, 53.48, H, 4.82, N, 1.56. Found: C, 53.116, H, 4.631, N, 1.765. MS [ESI

(negative mode), solvent: MeOH] *m/z* calcd for $C_{28}H_{19}F_8NNiP^-$ (M^-) 610.0, *m/z* found 610.0. See Figures A37-A39 for ^1H, ^{19}F and $^{31}P\{^1H\}$ spectra.

Method B:

1,2-(H*Ph*N),(Ph_2P)(C_6H_4)] (ca. 9 mg, 0.03 mmol) was dissolved in ca. 1 mL THF and transferred to a vial containing KH (ca. 1 mg, 0.0.5 mmol). The reaction mixture was left to stir at RT overnight. The colour had changed to cloudy melon over the course of the reaction. The reaction mixture was filtered through a Celite pipet into a vial containing Ni[P(O-*o*-tol)$_3$]$_4$ (37 mg, 0.014 mmol) and then transferred to a screw cap NMR tube containing BTB (2.5 µL, 0.016 mmol). To the NMR tube, ca. 3 mL of TFE was injected. The reaction mixture was left to stand at RT for 4 h, over the course of which the colour gradually changed to a clear dark yellow. The $^{31}P\{^1H\}$ spectrum indicated ca. 46% conversion to **Ni-22•K**.

5.6.6 Observation of [1,2-(*Ph*N),(Ph_2P)(C_6H_4)](CF=CF_2) (O6)

NMR scale: 1,2-(H*Ph*N),(Ph_2P)(C_6H_4)] (15 mg, 0.04 mmol) was dissolved in ca. 1 mL THF and transferred to a vial containing NaH (ca. 3 mg, 0.11 mmol). Stirred at RT overnight. The colour had changed to cloudy melon over the course of the reaction. The reaction mixture was filtered through a Celite pipet into a screw cap NMR tube and ca. 3 mL of TFE added via syringe. The colour gradually changed to a darker orange colour. The tube was left to stand at RT for 16 h while reaction progress was monitored by NMR. The sample was transferred to a vial in the glovebox and the volatiles were removed in vacuo. The remaining red semi-solid was dissolved in C_6D_6 for NMR analysis. ^{19}F NMR (282 MHz, C_6D_6) δ -106.8 (d d, $^2J_{FF}$(*gem*) = 68 Hz, $^3J_{FF}$(*cis*) = 40 Hz, 1F), -117.2 (d d d, $^3J_{FF}$(*trans*) = 110 Hz, $^2J_{FF}$ (*gem*) = 68 Hz, $^6J_{FP}$ = 26 Hz, 1F), -137.4 (d d d, $^3J_{FF}$(*trans*) = 110 Hz, $^3J_{FF}$(*cis*) = 40 Hz, $^5J_{FP}$ = 19 Hz, 1F). $^{31}P\{^1H\}$ NMR (121 MHz, C_6D_6) δ -20.7 (d d, $^6J_{PF}$ = 26 Hz, $^5J_{PF}$ = 19 Hz, 1P). See Figures A40-A42 for ^1H, ^{19}F and $^{31}P\{^1H\}$ spectra.

5.6.7 Synthesis of [1,2-(H*Ph*N),(Ph_2P)(C_6H_4)]Ni(C_4F_7)(OTf) (Ni-23)

[1,2-(H*Ph*N),(Ph_2P)(C_6H_4)]Ni(C_4F_8) (491 mg, 0.82 mmol) was dissolved in ca. 10 mL of toluene and transferred to a 100 mL Schlenk ampoule. To the **Ni-21**/toluene solution was added Me_3SiOTf

(178 µL, 0.98 mmol). The ampoule was sealed and placed in a 40°C oil bath for 48 h. A dark yellow precipitate was formed over the course of the reaction. The product was filtered through a 15 mL medium pore fritted funnel under nitrogen. The collected dark yellow powder was washed with hexanes (2 x 3 mL), and dried in vacuo. Yield: 542 mg, 0.73 mmol, 89% based on **Ni-21**. X-ray quality crystals were grown by cooling a toluene solution from 40°C to room temperature. UV-vis (0.7 mM in acetonitrile): $\lambda_{max}(\varepsilon)$ = 438(188). ^{1}H NMR (300 MHz, CD_3CN) δ 1.94 (solvent), 6.93 (br s, 1H, N*H*), 7.22 (m, 2H, Ar-H), 7.36-7.61 (ov m, 6H, Ar-H), 7.73-7.83 (ov m, 5H, Ar-H), 7.88-8.19 (ov m, 6H, Ar-H). ^{19}F NMR (282 MHz, CD_3CN) δ -79.3 (s, 3F, OTf), -99.1 (d tr, $^{2}J_{FF}$ = 251 Hz, $^{3}J_{FF}$ = 13 Hz, 1F$_\alpha$), -108.4 (d d, $^{2}J_{FF}$= 242 Hz, $^{3}J_{FF}$ = 17 Hz, 1F$_\alpha$), -114.9 (d m, $^{2}J_{FF}$ = 271 Hz, $^{3}J_{FP}$ = 19 Hz, 1F$_\beta$), -128.6 (d t, $^{2}J_{FF}$ = 271 Hz, 1F$_\beta$), -133.5 (d d d, $^{2}J_{FF}$ = 243 Hz, ^{3} J_{FF} = 29, 14 Hz, 1F$_\beta$), -135.6 (d d d, $^{2}J_{FF}$ = 243 Hz, 1F$_\beta$), -197.7 (d d, $^{2}J_{FP}$ = 70 Hz, $^{3}J_{FF}$ = 28 Hz, 1F$_\alpha$). ^{31}P{^{1}H} NMR (121 MHz, CD_3CN) δ 13.7 (d d d, $^{2}J_{PF}$ = 70, $^{3}J_{PF}$ = 19, 13 Hz). Anal. Calc. for $C_{27}H_{23}F_{10}NiO_3PS_2$: C, 46.93, H, 2.72, N 1.89. Found: C, 47.088, H, 3.001, N, 1.672. See Figures A43-A48 for ^{1}H, ^{19}F and ^{31}P{^{1}H} spectra.

5.6.8 Synthesis of [1,2-(*Ph*N$^-$),(Ph$_2$P)(C$_6$H$_4$)]Ni(C$_4$F$_7$)(NCCH$_3$) (Ni-24)

[1,2-(H*Ph*N),(Ph$_2$P)(C$_6$H$_4$)]Ni(C$_4$F$_7$)(OTf) (100 mg, 0.13 mmol) was dissolved in ca. 5 mL of CH_3CN and transferred to a 50 mL RB Schlenk flask. To the **Ni-23**/CH_3CN solution was added NaO^{t}Bu (13 mg, 0.13 mmol). The colour changed from dark yellow to dark orange. The reaction mixture was left to stir at RT for 16 h. The reaction mixture was concentrated in vacuo until 1 mL solution remained in the flask. The product was extracted into ca. 10 mL of DCM, and filtered through a Celite pipet into a clean 50 mL RB Schlenk flask. The solution was concentrated in vacuo to ca. 1 mL. Around 10 mL of hexanes was added, precipitating a yellow powder. The flask was cooled at -35°C. The product was filtered cold, washed with pre-cooled hexanes (3 x 3 mL), and dried in vacuo, affording a dark yellow powder. Yield: 58 mg, 0.09 mmol, 70% based on **Ni-23**. X-ray quality crystals of the CD_3CN adduct were grown by slow cooling of a supersaturated CD_3CN solution. UV-vis (0.7 mM in acetonitrile): $\lambda_{max}(\varepsilon)$ = 410(923). ^{1}H NMR (300 MHz, CD_3CN) δ 1.94

(solvent), 1.96 (s, 3H, CH_3CN), 2.33 (s, 3H, Me), 5.99 (m, 1H, Ar-H linking P and N), 6.13 (d d, 1H, Ar-H linking P and N), 6.26 (d d d, 1H, Ar-H linking P and N), 6.89 (t m, 1H, Ar-H linking P and N), 7.11 (t m, 1H, Ar-H), 7.21-7.26 (ov m, 2H, Ar-H), 7.34-7.42 (ov m, 2H, Ar-H), 7.62-7.93 (ov m, 8H, Ar-H), 8.34 (ov d d, 2H, Ar-H). ^{19}F NMR (282 MHz, CD_3CN) δ -104.9 (d tr, $^2J_{FF}$ = 269 Hz, $^3J_{FF}$ = 14 Hz, $1F_\alpha$), -113.0 (d m, $^2J_{FF}$= 266 Hz, $^3J_{FP}$ = 23 Hz, $1F_\beta$), -114.5 (d d, $^2J_{FF}$ = 269 Hz, $1F_\alpha$), -127.3 (d t, $^2J_{FF}$ = 266 Hz, $^3J_{FF}$ = 16 Hz, $1F_\beta$), -132.5 (app d quart, $^2J_{FF}$ = 239 Hz, $^3J_{FF}$ = 34, 16 Hz, $1F_\beta$), -137.8 (app d t, $^2J_{FF}$ = 239 Hz, $^3J_{FF}$ = 21, 14 Hz, $1F_\beta$), -204.0 (d d, $^2J_{FP}$ = 69 Hz, $^3J_{FF}$ = 27 Hz, $1F_\alpha$). $^{31}P\{^1H\}$ NMR (121 MHz, CD_3CN) δ 11.0 (d d d, $^2J_{PF}$ = 70, $^3J_{PF}$ = 23, 14 Hz). (**Note:** according to ^{19}F NMR, ca. 2% NaOTf remains in the final isolated product.) See Figures A49-A51 for ^1H, ^{19}F and $^{31}P\{^1H\}$ spectra.

5.6.9 NMR scale reaction of Ni-22•Na with [$HPPh_3$](Br)

[1,2-(*Ph*N^-),(Ph_2P)(C_6H_4)]Ni(C_4F_8)(Na)(18-Crown-6) (10 mg, 0.011 mmol) **(Ni-22•Na)** was dissolved in ca. 1 mL DCM and transferred to a vial containing [$HPPh_3$](Br) (4 mg, 0.011 mmol) dissolved /suspended in ca. 0.5 mL DCM. The initial colour of the reaction mixture was a clear light orange. After stirring at RT for 2 h the colour had changed to a lighter yellow. Integration of product F peaks relative to BTB in the ^{19}F spectrum indicated 81% yield of **Ni-21**.

5.6.10 NMR scale reaction of Ni-22•Na with [$HPPh_2Me$](Br)

[1,2-(*Ph*N^-),(Ph_2P)(C_6H_4)]Ni(C_4F_8)(Na)(18-Crown-6) (10 mg, 0.011 mmol) **(Ni-22•Na)** was dissolved in ca. 1 mL DCM and transferred to a vial containing [$HPPh_3$](Br) (3 mg, 0.011 mmol) dissolved /suspended in ca. 0.5 mL DCM. The initial colour of the reaction mixture was cloudy light orange. After stirring at RT for 2 h the colour had changed to bright cloudy yellow. Integration of product F peaks relative to BTB in the ^{19}F spectrum indicated 49% yield of **Ni-21**. (**Note:** we suspect that protonation at the amido group occurs quantitatively, but is followed by de-coordination of **[P,NH]** ligand and replacement with PPh_2Me, accounting for a decrease in yield. Other peaks consistent with the formation of such metallacycles are observed in the ^{19}F NMR.)

5.7 References

[1] a) Ohkuma, T.; Ooka, H.; Hashiguchi, S.; Ikariya, T.; Noyori, R. *J. Am. Chem. Soc.* **1995**, *117*, 2675. b) Grutzmacher, H. *Angew. Chem. Int. Ed.* **2008**, *47*, 1848. c) Morris, R. H. *Acc. Chem. Res.* **2015**, *48*, 1494. d) Khusnutdinova, J. R.; Milstein, D. *Angew. Chem. Int. Ed.* **2015**, *54*, 12236.

[2] a) Saudan, L. A.; Saudan, C. M.; Debieux, C.; Wyss, P. *Angew. Chem. Int. Ed.* **2007**, *46*, 7473. b) Blaquiere, N.; Diallo-Garcia, S.; Gorelsky, S. I.; Black, D. A.; Fagnou, K. *J. Am. Chem. Soc.* **2008**, *130*, 14034.

[3] a) Dub, P. A.; Henson, N. J.; Martin, R. L.; Gordon, J. C. *J. Am. Chem. Soc.* **2014**, *136*, 3505. b) Dub, P. A.; Gordon, J. C. *Dalton Trans.* **2016**, *45*, 6756.

[4] Fryzuk, M. D.; McNeil, P. A. *Organometallics* **1983**, *2*, 355.

[5] a) Pritchard, J.; Filonenko, G. A.; van Putten, R.; Hensen, E. J. M.; Pidko, E. A. *Chem. Soc. Rev.* **2015**, *44*, 3808. b) Chakraborty, S.; Dai, H.; Bhattacharya, P.; Fairweather, N. T.; Gibson, M. S.; Krause, J. A.; Guan, H. *J. Am. Chem. Soc.* **2014**, *136*, 7869. c) Fairweather, N. T.; Gibson, M. S.; Guan, H. *Organometallics* **2015**, *34*, 335. d) Srimani, D.; Mukherjee, A.; Goldberg, A. F. G.; Leitus, G.; Diskin-Posner, Y.; Shimon, L. J. W.; David, Y. B.; Milstein, D. *Angew. Chem. Int. Ed.* **2015**, *54*, 12357.

[6] a) Taw, F. L.; Clark, A. E.; Mueller, A. H.; Janicke, M. T.; Cantat, T.; Scott, B. L.; Hay, P. J.; Hughes, R. P; Kiplinger, J. L. *Organometallics* **2012**, *31*, 1484. b) Algarra, A. G.; Grushin, V. V.; Macgregor, S. A. *Organometallics* **2012**, *31*, 1467.

[7] Baker, R. T.; Beatty, R. P.; Farnham, W. B.; Wallace, R. L. Jr. EP 0783472 A1, **1997**, E. I. Du Pont de Nemours & Co., USA.

[8] Andrella, N. O.; Sicard, A. J.; Gorelsky, S. I.; Korobkov, I.; Baker, R. T. *Chem. Sci.* **2015**, *6*, 6392.

[9] a) Ohashi, M.; Saijo, H.; Shibata, M.; Ogoshi, S. *Eur. J. Org. Chem.* **2013**, 443. b) Leclerc, M. C.; Gorelsky, S. I.; Gabidullin, B. M.; Korobkov, I.; Baker, R. T. *Chem. –Eur. J.* **2016**, *22*, 8063.

[10] Giffin, K. A.; Harrison, D. J.; Korobkov, I.; Baker, R. T. *Organometallics* **2013**, *32*, 7424.

[11] Giffin, K. A.; Korobkov, I.; Baker, R. T. *Dalton Trans.* **2015**, *44*, 19587.

[12] Eggenstein, M.; Thomas, A.; Theuerkauf, J.; Franciò, G.; Leitner, W. *Adv. Synth. Catal.* **2009**, *351*, 725.

[13] Ohashi, M.; Shibata, M.; Saijo, H.; Kambara, T.; Ogoshi, S. *Organometallics* **2013**, *32*, 3631.

[14] Kaschube, W.; Schröder, W.; Pörschke, K. R.; Anfermund, K.; Krüger, C. *J. Organomet. Chem.* **1990**, *389*, 399.

[15] Cundy, C. S.; Green, M.; Stone, F. G. A. *J. Chem. Soc. (A)*, **1970,** 1647.

[16] Bezpalko, M. W.; Foxman, B. M.; Thomas, C. M. *Inorg. Chem.* **2013**, *52*, 12329.

[17] Leclerc, M. C.; Gabidullin, B. M.; Da Gama, J. G.; Daifuku, S. L.; Iannizzi, T. E.; Neidig, M. L.; Baker, R. T. *Organometallics* **2017**, *36*, 849.

[18] Ohashi, M.; Kambara, T.; Hatanaka, T.; Saijo, H.; Doi, R.; Ogoshi, S. *J. Am. Chem. Soc.* **2011**, *133*, 3256.

[19] (a) Siegle, J. C.; Muus, L. T.; Lin, T. P.; Larsen, H. A. *J. Polym. Sci., Part A : Polym. Chem.* **1964**, *2*, 391. (b) Lonfei, J.; Jingling, W.; Shuman, X. *J. Anal. Appl. Pyrol.* **1986**, *10*, 99. (c) Meissner, E.; Wróblewska, A.; Milchert, E. *Polym. Degrad. Stab.* **2004**, *83*, 163. (d) Bhadury, P. S.; Singh, S.; Sharma, M.; Palit, M. *J. Anal. Appl. Pyrol.* **2007**, *78*, 288.

[20] APEX Software Suite v.2010; Bruker AXS: Madison, WI, **2005**.

Chapter 6. Conclusions and Future Outlook

Organofluorine compounds have proven to be indispensable products that are currently used in a wide range of applications on a global scale. Marketed FC compounds are ever-evolving in order to provide products with the desirable properties imparted by C−F bonds while constantly striving to reduce their potential environmental and health impacts. This is particularly true for those FC products that are essential for refrigerant and surfactant applications. The industrial synthesis of many small-molecule FC derivatives is problematic, utilizing ozone depleting chlorocarbons and catalysts based on toxic heavy metals such as antimony. All of the above points present a great opportunity for the development of novel synthetic routes to valuable FC products. We aimed to design new transition metal-mediated routes to offer alternative, more sustainable synthetic strategies for the production of novel small-molecule functionalized FCs from fluoroalkene feedstocks. Specifically, we focused on metallacyclopentane complexes as C_4^F units are particularly valuable in both refrigerant and surfactant applications. This *Thesis* covered progress towards the final goal of catalysis by exploring the fundamental reactivity of key fluoronickelacyclopentane intermediates as a function of their ancillary ligand(s) and the fluorinated feedstock employed.

In terms of perfluoronickelacyclopentane reactivity, previous studies focused solely on symmetrical complexes bearing two monophosphine/monophosphite ligands. Given the promising effects that bidentate and bifunctional ligands have had in other areas of transition metal chemistry, including challenging bond activation reactions, we set out to study such ligands in the context of fluoroorganometallic chemistry. Chapter 2 examined the addition of 1,2,4-(HS),(Ph_2P),Me(C_6H_3) **[P,SH]** to a bis(tri-*iso*-propylphosphite) nickelacycle, wherein an interesting isopropyl migration to the sulfur atom takes place to afford a phosphinothioether-ligated product. Upon treatment with a Lewis acid, the new metallacycle undergoes C_α−F activation, followed by chemoselective migration of the phosphorus arm of the bidentate ligand to C_α, affording a unique fused metallabicyclic product. Addition of a stoichiometric amount of aryl isonitrile CNAr led to the expected displacement of the weakly bound OTf ligand, giving a cationic Ni centre in which the metallabicycle remained intact.

However, a superstoichiometric amount of CNAr induced an unexpected ring-opening reaction through cleavage of the Ni−S^{iPr} and Ni−C_αFP bonds with presumed loss of C_β−F. Furthermore, hydrolysis of the original metallabicycle product afforded a single isomer of hexafluoro-1-butene, demonstrating that selective production of unsaturated C_4 hydrofluorocarbons from C_2 fluoroalkenes through nickel complex mediated processes can be achieved. Although the mechanism of this reaction is still unclear, it likely involves loss of C_β−F in a similar fashion to what we have proposed for the CNAr ring-opening reaction. Although we suspect that this surprising reactivity may be attributed to the metallabicyclic nature of the complex, further experimental and DFT studies would be needed to confirm this effect.

Despite the noteworthy reactivity obtained with the *in situ* formed phosphinothioether-coordinated perfluoronickelacycle, this study concluded that **[P,S]**-ligated metallacycles, where S represents a thiolate or thiol group, could not be accessed from bis(phosphite) nickelacycle derivatives. Other starting metallacyles thus needed to be investigated, with the goal of designing a system that could favour a comparatively more direct route to functionalized FCs such as hexafluoro-1-butene. Chapter 3 investigated the reactivity of the **[P,SH]** ligand with perfluoronickelacycles bearing two monodentate ligands that do not offer a potential alkyl transfer to the sulfur as was observed with the tri-*iso*-propylphosphite ligands. Prior to studying substitution reactions with **[P,SH]**, we wanted to establish the propensity for the $L_2Ni(C_4F_8)$ (where L = PPh_3, PPh_2Me, Pyr) complexes of interest in this study to undergo C_α−F activation/ligand migration in the presence of a Lewis acid. This reaction had only been shown to work previously with the bis PEt_3 analogue reported by Burch and with the **[P,S^{iPr}]** analogue detailed in Chapter 2. Herein, we concluded that the C_α−F activation/ligand migration reactivity extends to bulky, electron deficient phosphines as well as to N-donor ligands, giving a series of new L-functionalized fluoronickelacycles. Treatment of the $(PR_3)_2Ni(C_4F_8)$ complexes with **[P,SH]** also afforded PR_3 functionalized metallacycles bearing a phosphinothiolate ligand via a ligand-assisted/Brønsted acid-protomoted C_α−F activation without the use of strong Lewis acid co-additives. A variable temperature NMR experiment was performed to analyze the

mechanism of the reaction between **[P,SH]** and $(PR_3)_2Ni(C_4F_8)$. This study confirmed the presence of an intermediate consisting of an anionic nickel centre with an outer sphere phosphonium counter ion in the generation of the final product, which lends support to the originally proposed mechanism for $[P,S^{iPr}]Ni(C_4F_8)$ formation in Chapter 2.

Lastly, employment of the deprotonated chelate **[P,S$^-$]** in a substitution reaction with $(PR_3)_2Ni(C_4F_8)$ cleanly formed the first example of an anionic phophinothiolate-cooordinated perfluoronickelacycle. The basic anionic metallacycle was reactive towards weakly acidic tertiary phosphonium salts, affording phophine-functionalization at the C_α position while the **[P,S$^-$]** ligand retained its κ^2-coordination to the metal centre.

The two different types of L-functionalized metallacycles introduced in this Chapter offer a significant opportunity for future studies in this area. It would be interesting to establish whether productive reactivity with H_2 or silanes is favoured with the functionalized metallacycles containing a weakly coordinating site such as the OTf group, or with those bearing the phosphinothiolate ligand. Given that the ligand migration reaction has been established to work with a series of different nucleophiles, there is also potential to exploit such reactivity for the catalytic formation of functionalized highly fluorinated organics that are attractive as surfactants, or as building blocks for either oligomer synthesis (e.g., Scotchgard, see Introduction) or perhaps pharmaceutical applications (Scheme 6.1).

In Chapter 4 we took a different approach to FC synthesis by investigating one of the comparatively less studied fluoralkene feedstocks, trifluoroethylene. Owing to the reduced symmetry of TrFE, there are six potential nickelacyclopentanes with varying regio-/stereoselectivity that can

Scheme 6.1 Proposed mechanism for catalytic functionalized FC production.

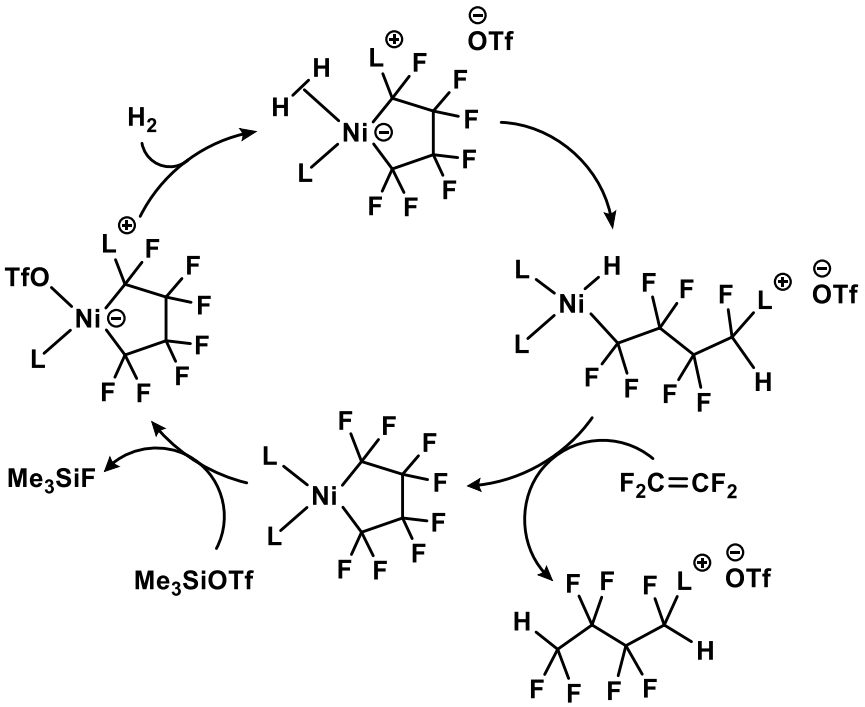

form upon oxidative cyclization. The oxidative cyclization of TrFE at Ni(0) was found to be selective towards the formation of three of the six potential isomers: the *cis* and *trans* head-tail and the thermodynamically favoured *trans* head-head hydrofluoronickelacyclopentanes $L_2Ni(C_4F_6H_2)$ (L = PPh_3, $P(O\text{-}o\text{-}tol)_3$, PPh_2Me, $PPhMe_2$, PMe_3). Moreover, a systematic analysis involving modification of the ancillary ligands employed demonstrated that the ratio of the three major isomers was influenced by the nature of the PR_3 ancillary ligands wherein smaller phosphines favoured the *trans* head-head isomer (cf. 50% with PMe_3) and the largest phosphine and phosphite afforded small amounts of the tail-tail isomers with less bulky CHF groups bound to Ni. The characterization of each isomer was supported through a range of multinuclear 1D and 2D NMR experiments. Double C−F bond activation of the head-tail regioisomers was observed upon addition of Lewis or Brønsted acids to the PPh_2Me and $PPhMe_2$ analogues, releasing small functionalized organics from the metal. Interestingly, varying the acid allowed for control in selecting the fluorinated product obtained: Me_3SiOTf and *N,N*-dimethylanilinium bromide yielded (*Z,E*)-1,1,3,4-tetrafluorobutadiene as the major organic product, while BF_3 cleanly formed 1,1,2,3-tetrafluorocyclobutene as the major organic

product. A minor amount of unique bis(phosphonium) difluorobutadiene products were generated concomitantly from the head-head isomer. The chemistry outlined in Chapter 4 highlights the significant effect that replacing a fluorine with a hydrogen in the fluorinated feedstock can have on the subsequent reactivity of the nickelacyclopentane unit. Previous Chapters showed that L_2-ligated perfluorinated systems consistently form L-functionalized metallacycles upon C_α−F activation with a Lewis acid. Here it is evidenced that when one $C_\alpha F_2$ group is replaced with a $C_\alpha FH$ group, the reactivity deviates significantly, as two successive C−F bond activations occur with no L migration observed. This type of in-depth study on ligand effects in metallacycle selectivity and reactivity aids us in re-designing systems more suitable for catalytic conditions.

As we alluded to in the Conclusions of Chapter 4, ^{19}F NMR reveals minor amounts of butadiene as well as signals presumably arising from ring-opened products with the PPh_3 analogue after 24 h at room temperature. We reason that this results from the lability of PPh_3 from the metal, which suggests furthermore that a low-coordinate Ni centre can be sufficiently acidic for intermolecular C−F bond activation. Indeed, more recent results from Mr. Alexander Sicard of the Baker group using vinylidene fluoride as the fluorinated feedstock support this theory. Our new collaboration with Arkema, Inc. aims to further develop the promising results we have achieved in functionalized FC production from hydrofluorometallacycles. Encouraging results from Sicard, including examples of nickel-catalyzed hydrodefluorodimerization to give 2,4,4-trifluorobutene by employing vinylidene fluoride as the fluorinated feedstock and a stoichiometric amount of silane, will be built on in the future. This reaction will be further optimized and scaled up to determine the physical properties of the novel FCs in order to assess their potential commercial value. Another exciting future project involves the design and construction of a new gas handling apparatus for the Baker lab that will enable: a) the introduction of two different gases at variable pressures, b) real-time reaction analysis by using a sampling loop, and c) facile volatile product isolation via vacuum transfer. This custom system will facilitate reactions meant to explore the syntheses of either mixed metallacycles or the

fluoroorganic products derived from said metallacycles with a series of different C_2 fluorinated feedstocks, including TrFE.

Finally, we explored the synthesis and reactivity of perfluoronickelacyclopentanes based on a bidentate **[P,NH]** [2-(diphenylphosphino)phenyl-*N*-phenylaniline] ligand. In contrast to the previously studied **[P,SH]** ligand, the decreased acidity of the amino group in **[P,NH]** *vs.* the thiol of **[P,SH]** enables a clean substitution reaction to occur between **[P,NH]** and $[P(O\text{-}o\text{-}tol)_3]_2Ni(C_4F_8)$, quantitatively yielding a new phosphinoamine-coordinated nickelacycle. Deprotonation of $[P,NH]Ni(C_4F_8)$ occurred readily upon addition of NaO^tBu and 18-Crown-6 to give an anionic Ni product. Studies were also performed with pre-formed deprotonated ligand **[P,N$^-$]**, including a reaction that takes place between free ligand and TFE to give a fluoroalkenyl compound as the major product along with two other as-yet uncharacterized products. Reactivity studies of the **[P,NH]**-ligated metallacycle include the generation of a metallabicyclic complex via C_α−F activation/phosphine migration in the presence of Lewis acid, adding another example to the growing number of L-functionalized metallacycles. Lastly, we noted the stability of the anionic metallacycle $\{[P,N]Ni(C_4F_8)\}^-$ towards H_2.

Future studies in this area would benefit from a one-pot approach to determine optimal conditions for functionalized FC synthesis [e.g., ligand, base, Ni(0) source, fluoroalkene feedstock and reducing agent]. As mentioned in Chapter 5, the resonance stabilization of the nitrogen lone pair in the anionic complex could contribute to the stability of the metallacycle under high pressures of H_2. This project could benefit from a DFT study of $\{[P,N]Ni(C_4F_8)\}^-$ to examine the extent of π donation from the amido lone pair to the metal. In parallel to the theoretical work, an experimental study examining the effects of varying the nature of the bidentate [P,N] ligand on the reactivity of [P,N]-ligated perfluoronickelacycles would be informative (Chart 6.1).

Chart 6.1. Examples of [P,N] ligands for future studies.

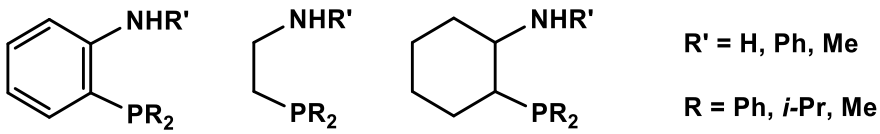

Another point to be studied in the future is the effects of having the cation trap, 18-Crown-6, present in the reactions, as recent studies have implicated cooperative interactions between the Lewis acidic cation and the bifunctional ligand as being crucial for catalyst activity. Notably, upon exposure to air, a THF solution of $\{[P,N]Ni(C_4F_8)\}^-(Na^+)$ in the presence of 18-Crown-6 remains yellow, whereas in the absence of 18-Crown-6, an immediate colour change to dark purple occurs. One other potential avenue to explore in the future for the phosphinoamide-coordinated metallacycle is its reactivity in other oxidation states. Although this point has not been discussed throughout this *Thesis* as it was not the focus of the work presented here, oxidation of Ni^{II} metallacycles to either Ni^{III} or Ni^{IV} states is another promising strategy for activation of Ni−C_α and C_α−F bonds towards functionalized FC production.

Lastly, it would be interesting to expand the reactivity of both the phosphinothiolate- and the phosphinoamide-coordinated metallacycles towards E−H bond activation (E = Si and B). Although some preliminary experiments have proven unsuccesful, the promising results achieved by Oestrich and colleagues, employing Ru−sulfur bonds for generation of silicon cations (from silanes, see Scheme 1.24) and subsequent C−F activation, are good motivation for continued pursuit of this type of reactivity. It is worth noting here that both the **[P,N$^-$]** and **[P,S$^-$]** metallacycles do not give C−F abstraction products upon treatment with Lewis acids (*e.g.*, Me_3SiOTf or BF_3) but rather give products that would be consistent by NMR with N−E or S−E bond formation.

As the work presented in this *Thesis* was being carried out over the past five years, incredible progress was made in many different areas in the field of fluoroorganometallic chemistry. Studies focused on furthering the understanding of coordinated fluoroalkyl groups at transition metal centres

will undoubtedly aid the development of greener catalytic routes to commercially relevant fluorocarbon compounds.

Appendices

NMR Spectra

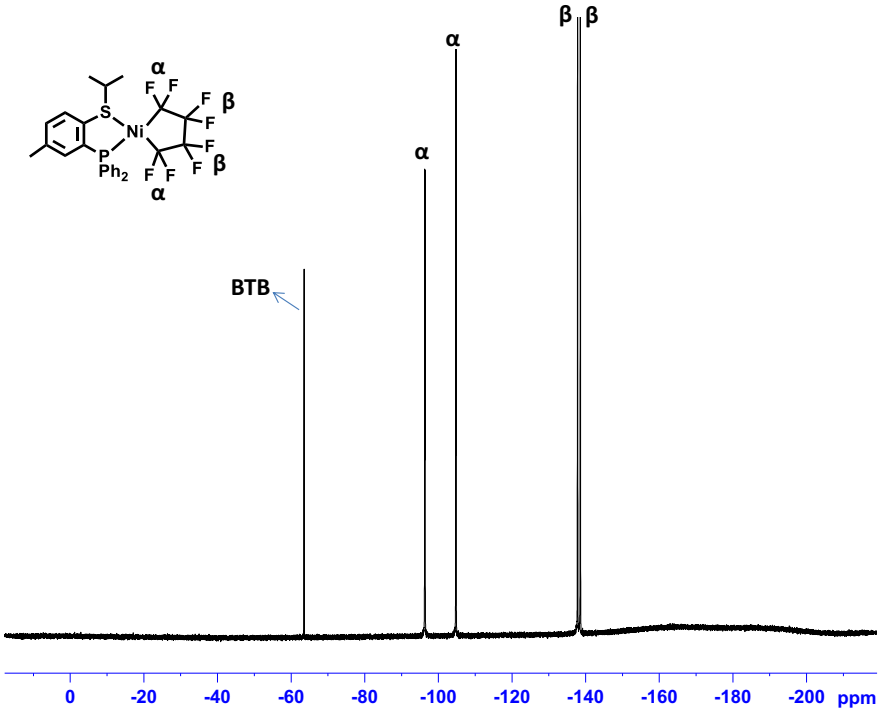

Figure A1. ^{19}F NMR (282 MHz, C_6D_6) spectrum for complex **Ni-2**. 1,3-Bis(trifluoromethyl)benzene (BTB) used as an internal NMR standard.

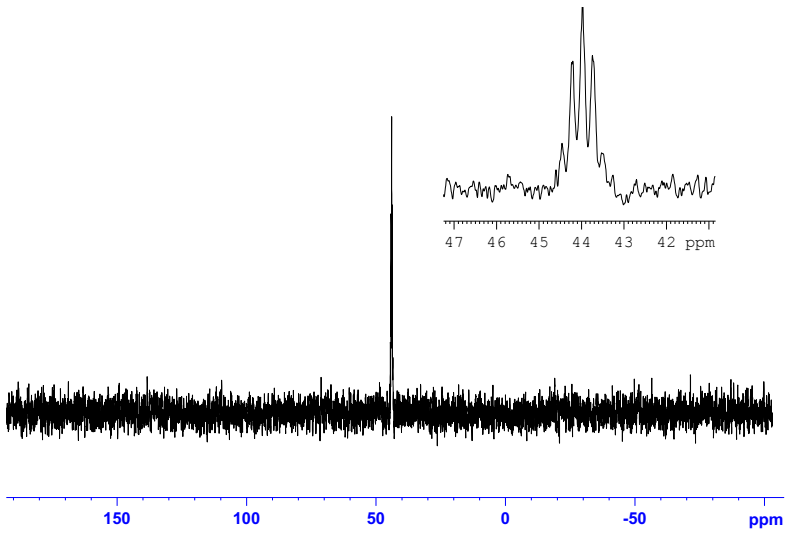

Figure A2. $^{31}P\{^1H\}$ NMR (121 MHz, C_6D_6) spectrum for **Ni-2**. The inset shows the expanded (horizontal scale) signal.

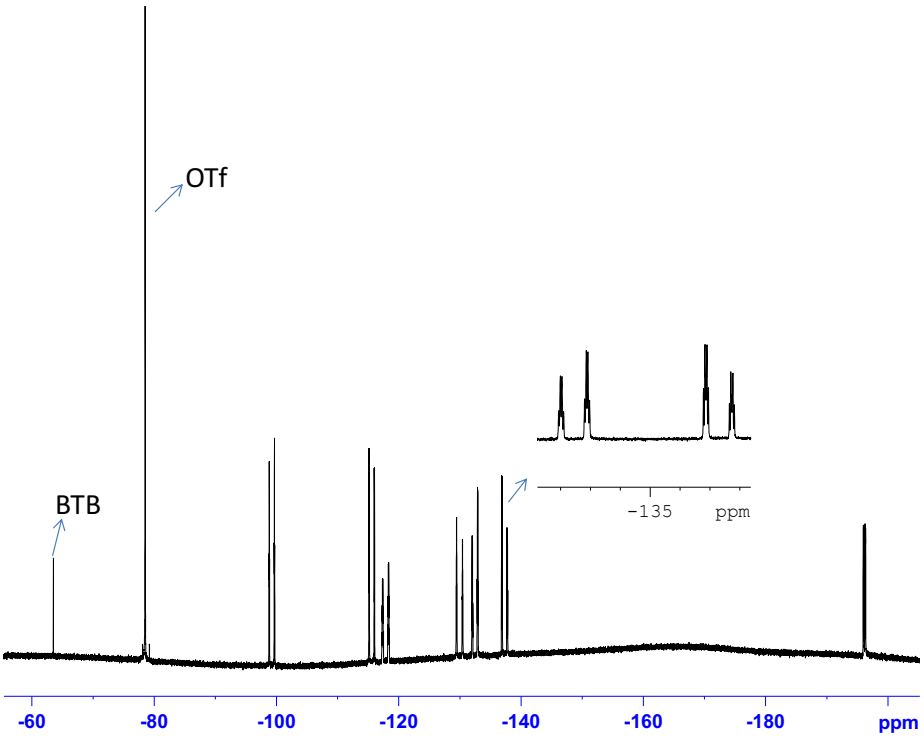

Figure A3. ^{19}F NMR (282 MHz, CD_2Cl_2) spectrum of **Ni-3** with all fluorine peaks labeled. The inset shows the expanded (horizontal scale) peaks associated with the two indicated fluorines.

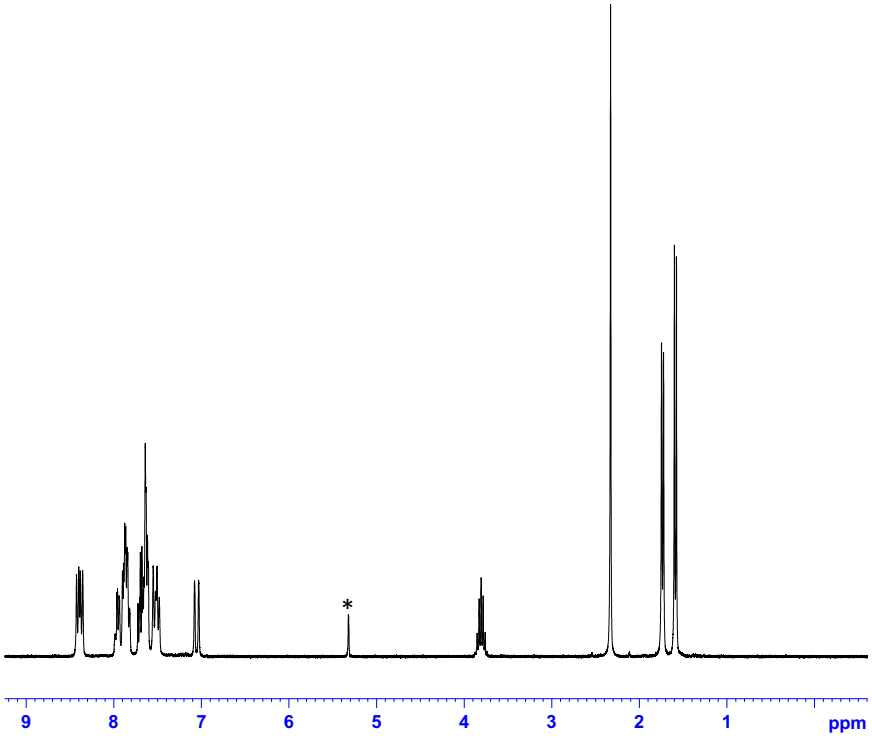

Figure A4. ^{1}H NMR (300 MHz, CD_2Cl_2) spectrum for complex **Ni-3**. Residual solvent peak labeled '*'.

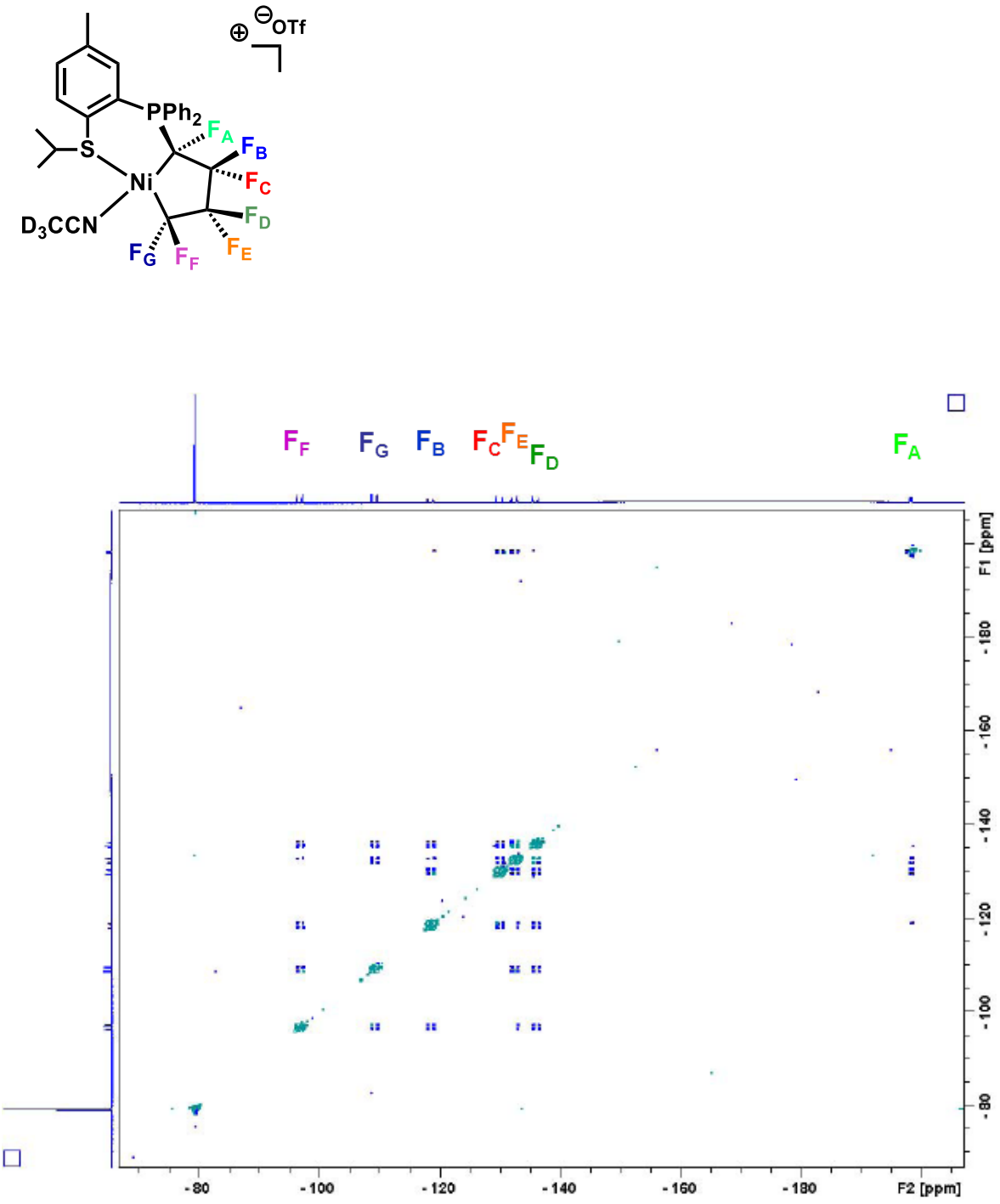

Figure A5. ^{19}F NOESY NMR (282 MHz, CD_3CN) data for complex **3·CD$_3$CN**.

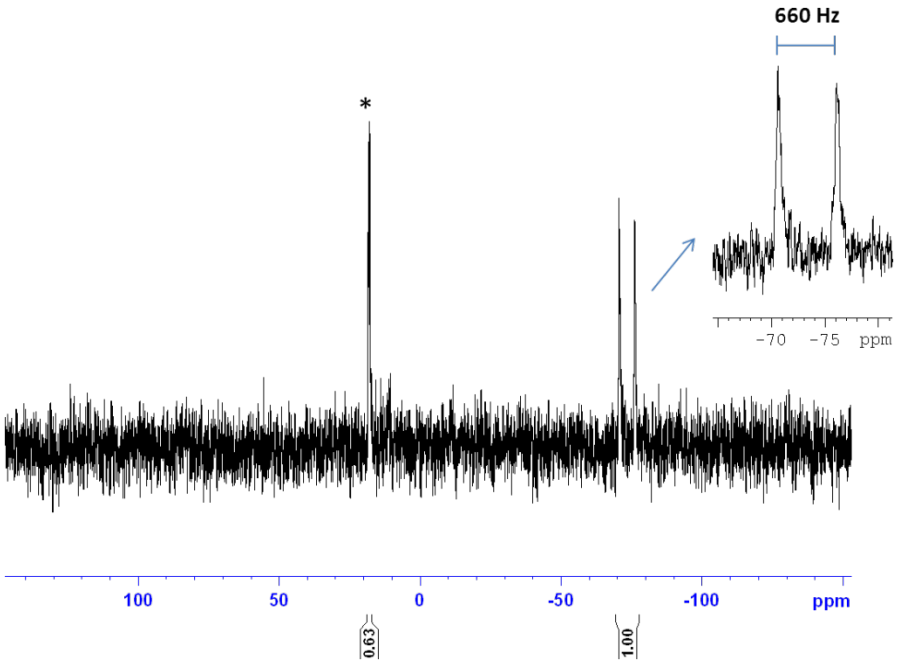

Figure A6. $^{31}P\{^{1}H\}$ NMR (121 MHz, C_6D_6) spectrum of **Ni-6**. The inset shows the expanded (horizontal scale) signal. Intermediate en route to **Ni-7** labeled '*.

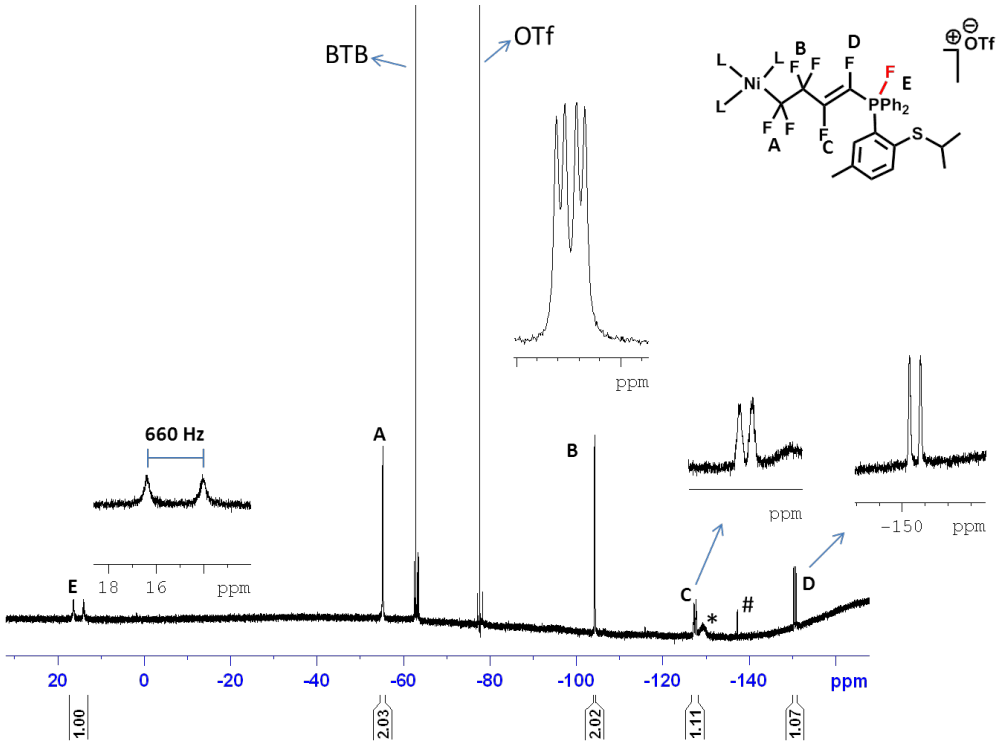

Figure A7. ^{19}F NMR (282 MHz, C_6D_6) spectrum of **Ni-6**. The insets show the expanded (horizontal scale) peaks associated with the indicated fluorines. Broad peak associated with uncharacterized intermediate(s) labeled '*'. Minor impurity (< 5%) labeled with '#'.

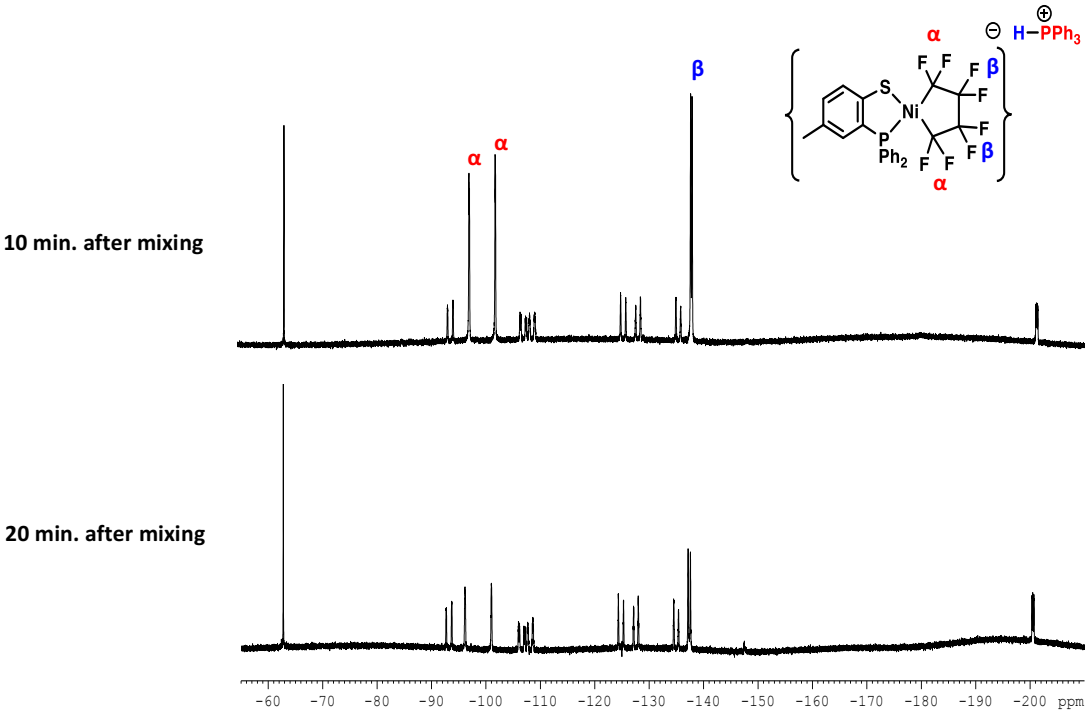

Figure A8. ^{19}F NMR (282 MHz, C_6D_6) spectra at room temperature displaying a mixture of ***Int 4*** and **Ni-11**.

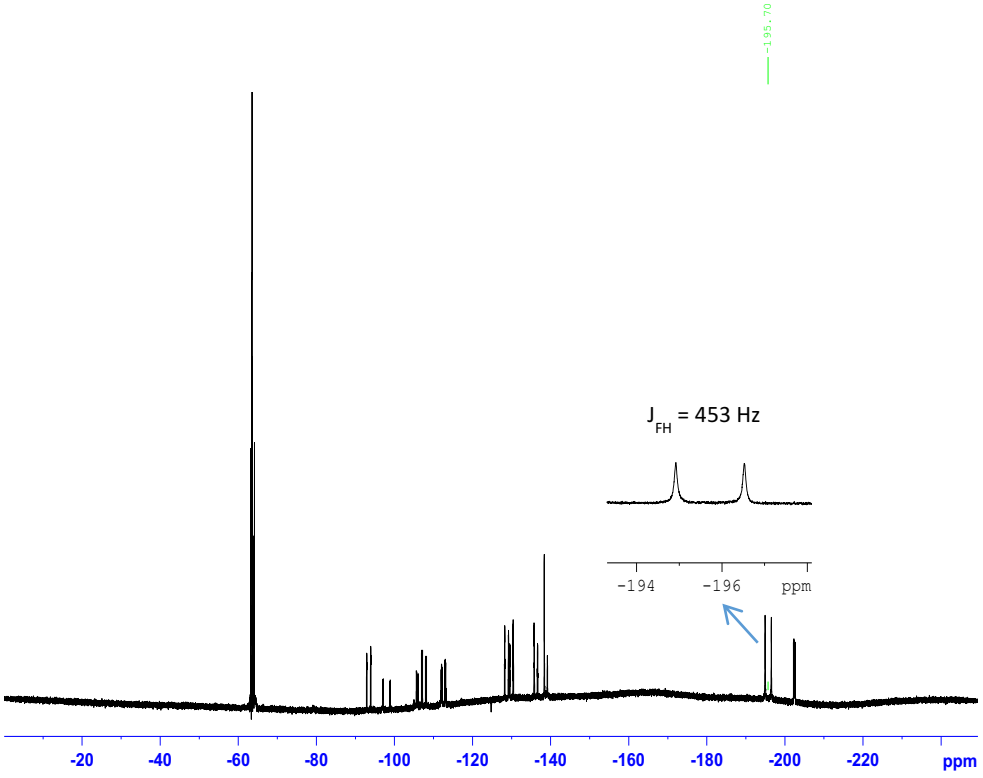

Figure A9. ^{19}F NMR (282 MHz, THF/C_6D_6 lock) spectrum of the reaction between **[P,SH]** and **Ni-9b** at room temperature. The inset shows the expanded (horizontal scale) signal for HF.

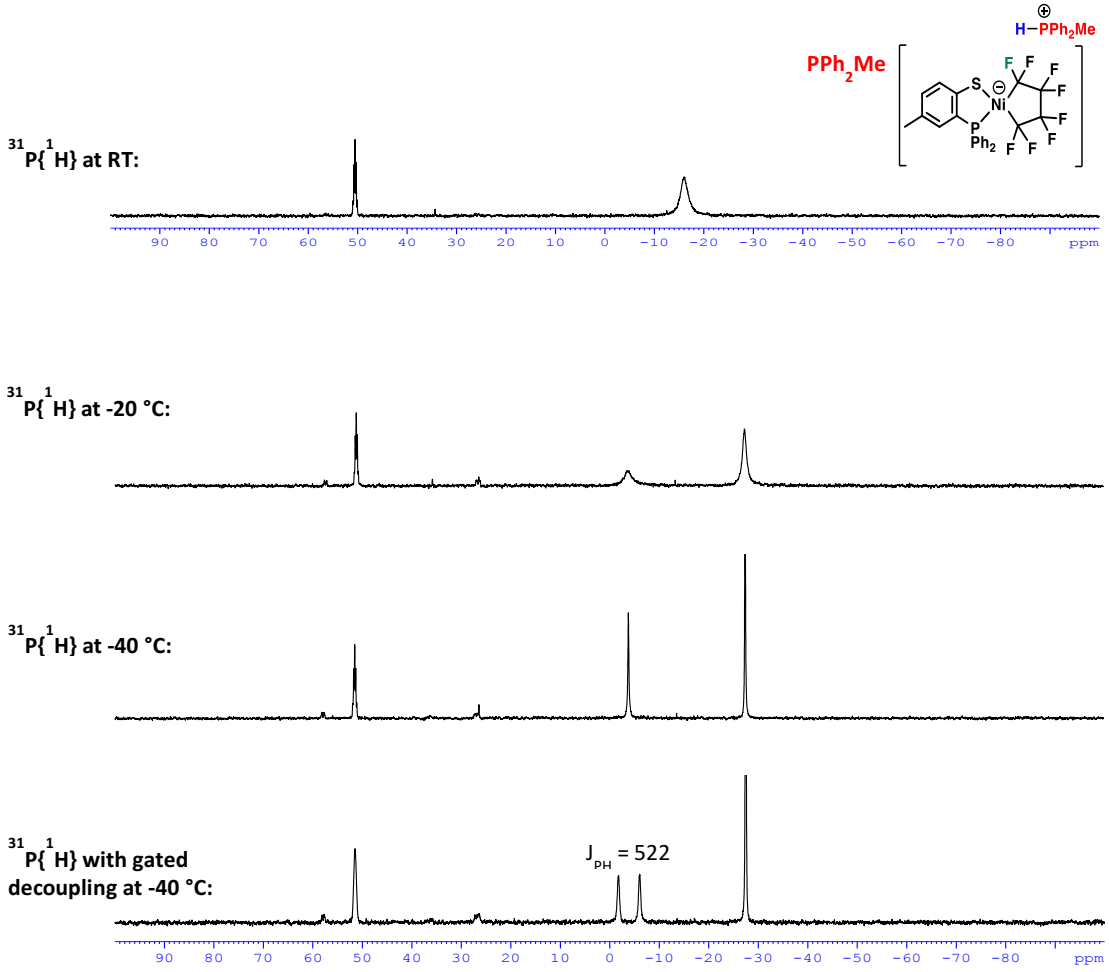

Figure A10. Variable temperature $^{31}P\{^{1}H\}$ and $^{31}P\{^{1}H\}$ with gated decoupling NMR (121 MHz, $CDCl_3$) spectra of the reaction between **[P,SH]** and **Ni-9b**.

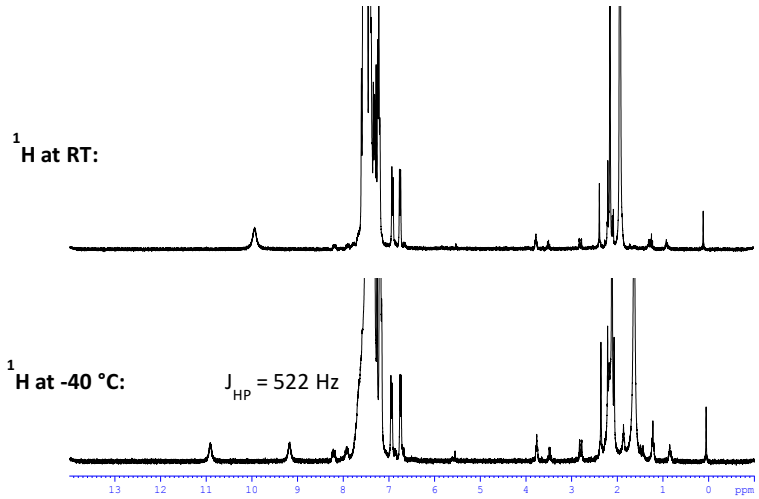

Figure A11. Variable temperature ^{1}H NMR (300 MHz, $CDCl_3$) spectra of the reaction between **[P,SH]** and **Ni-9b.**

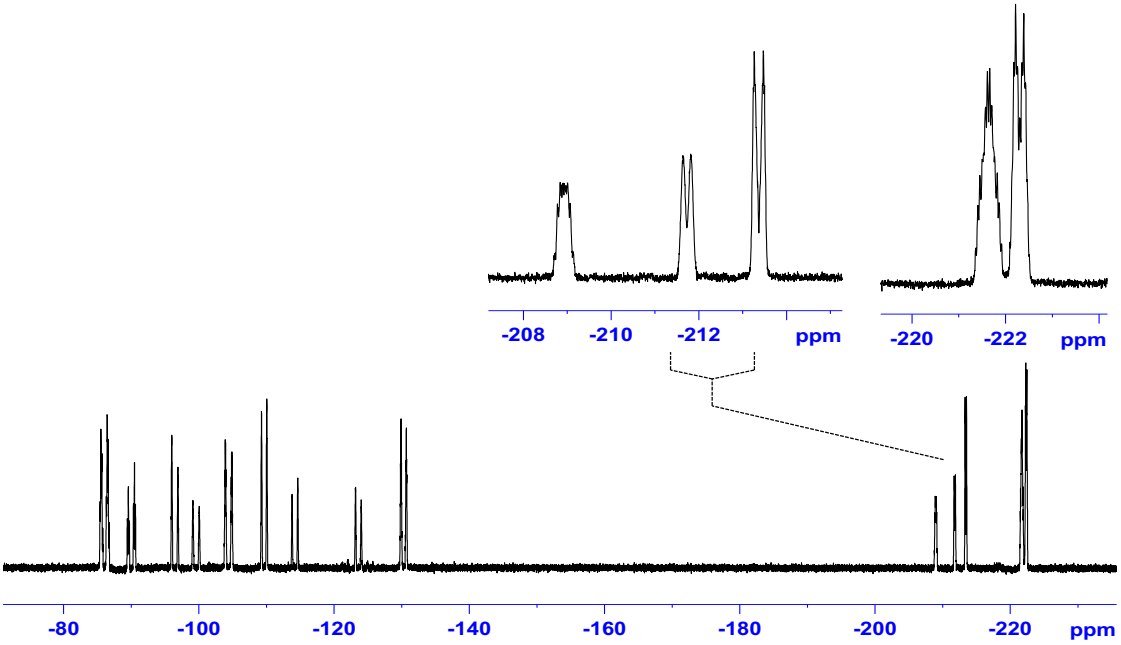

Figure A12. ^{19}F NMR (282 MHz, $CDCl_3$) spectrum for complex **Ni-16c**. The inset shows the expanded (horizontal scale) signal.

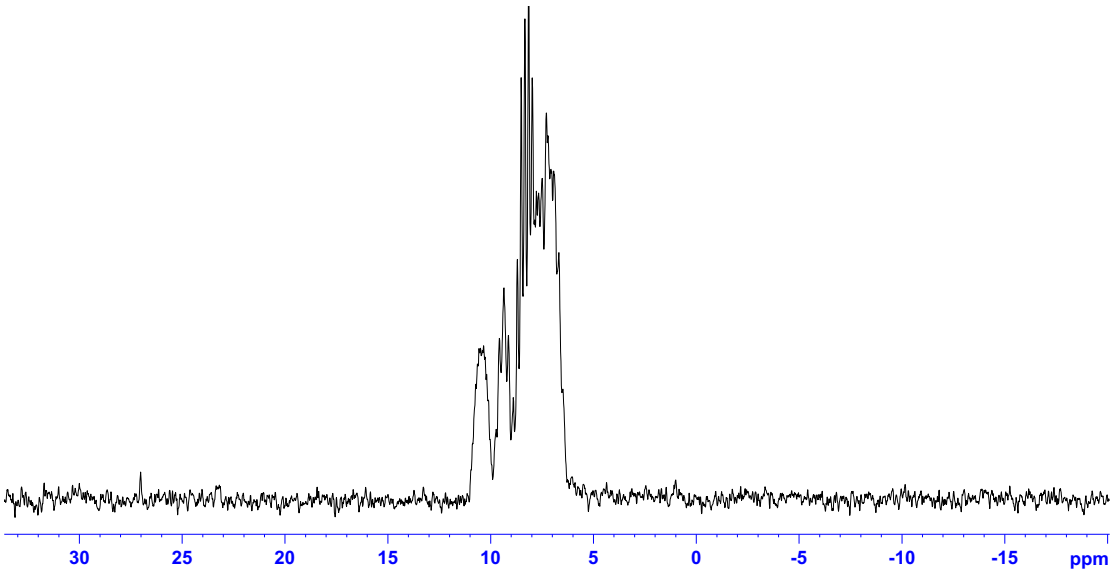

Figure A13. $^{31}P\{^1H\}$ NMR (121 MHz, $CDCl_3$) spectrum for **Ni-16c**.

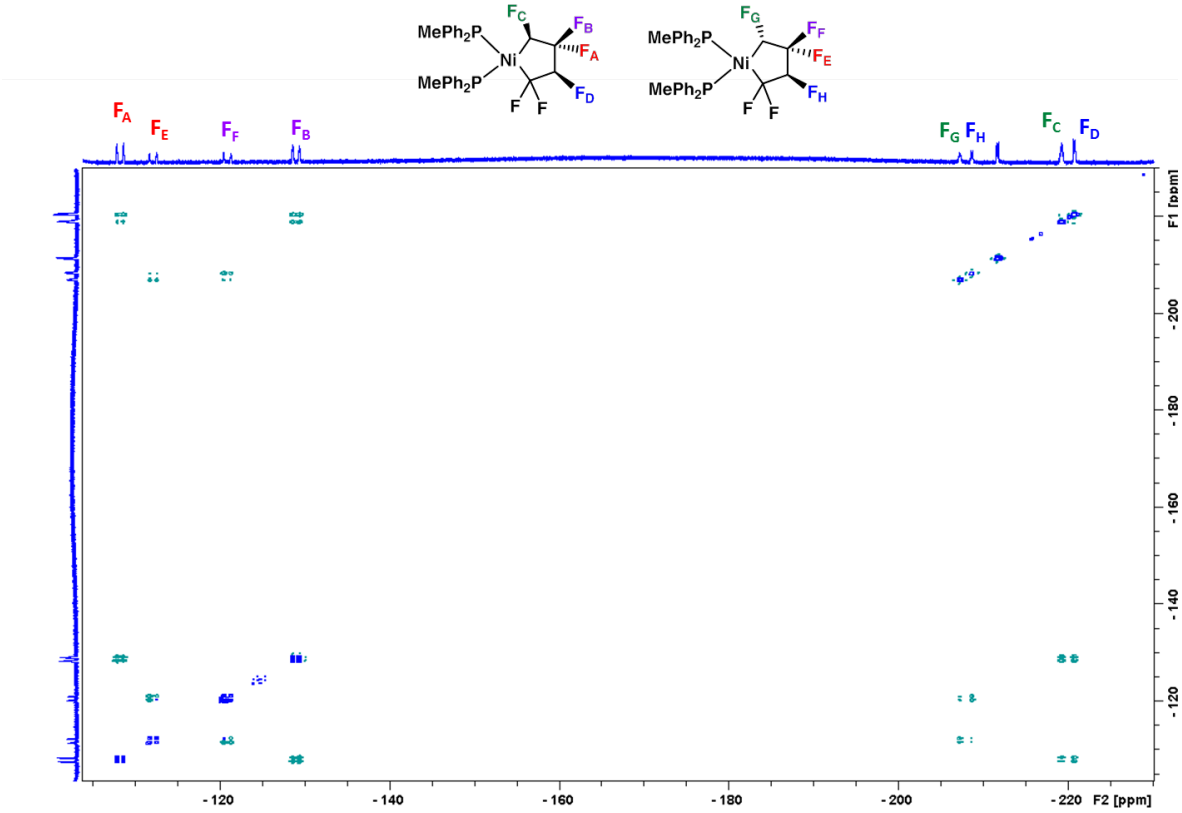

Figure A14. ^{19}F-^{19}F NOESY NMR (282 MHz, C_6D_6) spectrum for complex **Ni-16c**.

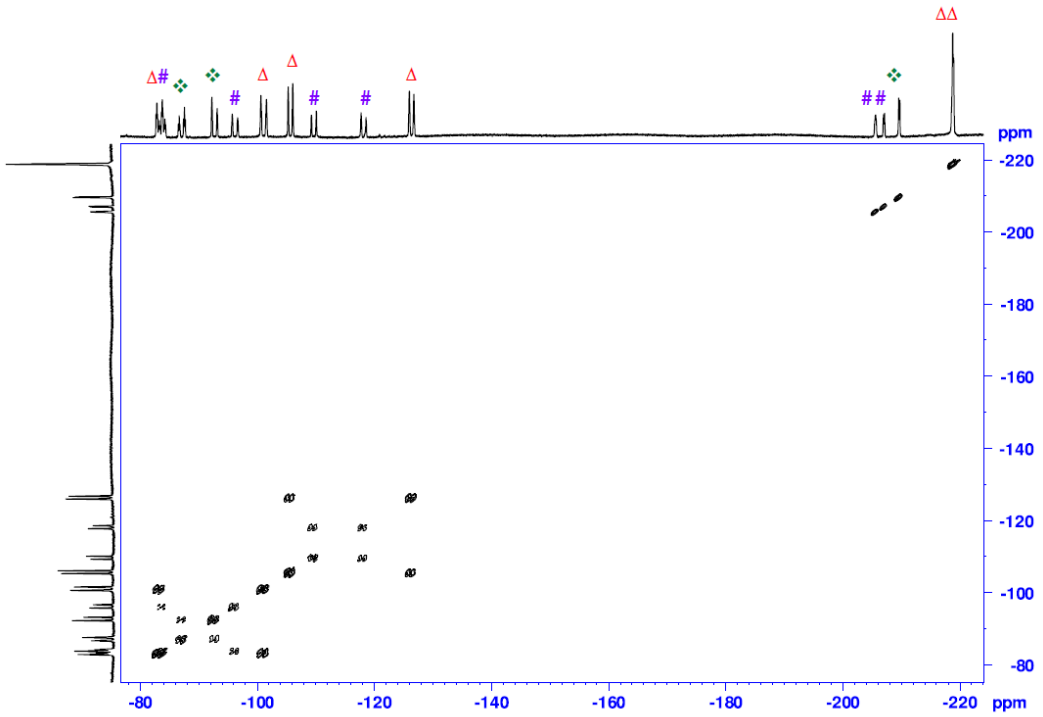

Figure A15. ^{19}F-^{19}F COSY NMR (282 MHz, DCM) spectrum for complex **Ni-16c**.

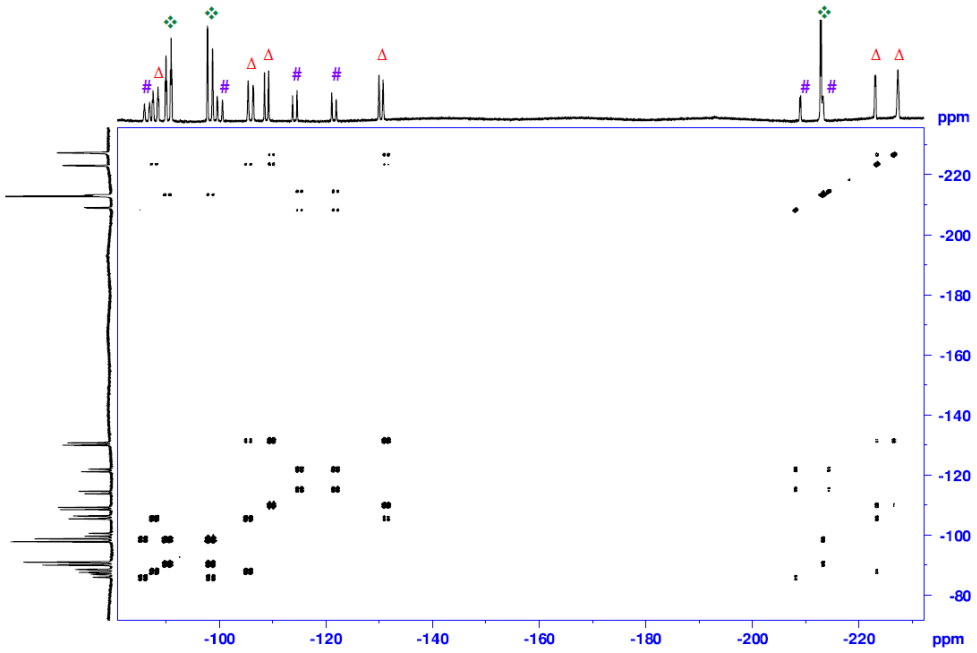

Figure A16. ^{19}F-^{19}F COSY NMR (282 MHz, DCM) spectrum for complex **Ni-16d**.

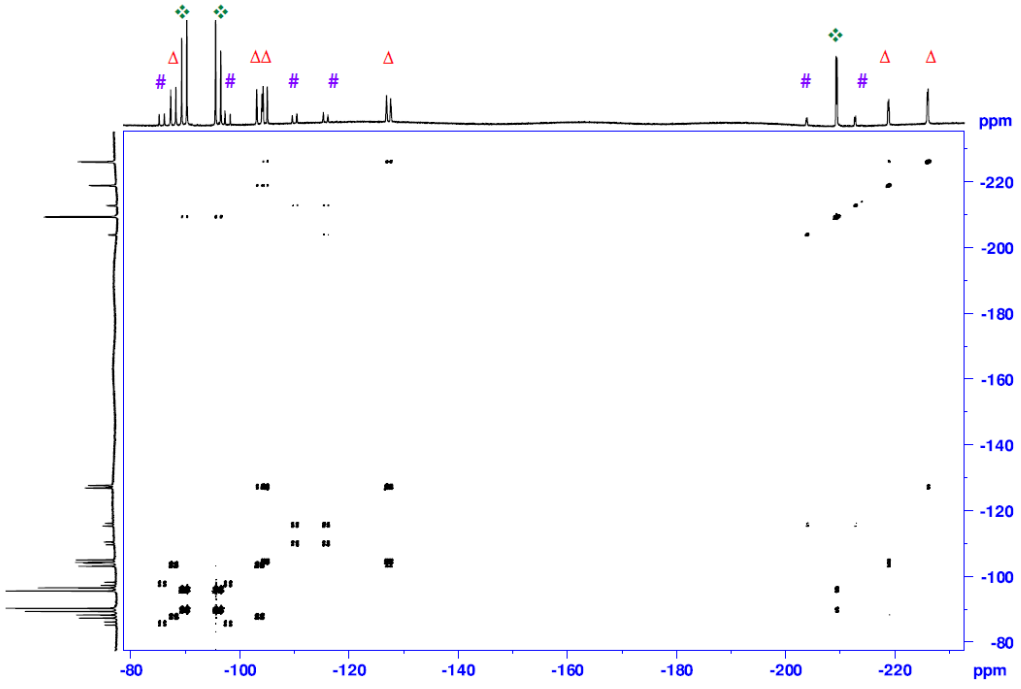

Figure A17. ^{19}F-^{19}F COSY NMR (282 MHz, DCM) spectrum for complex **Ni-16e**.

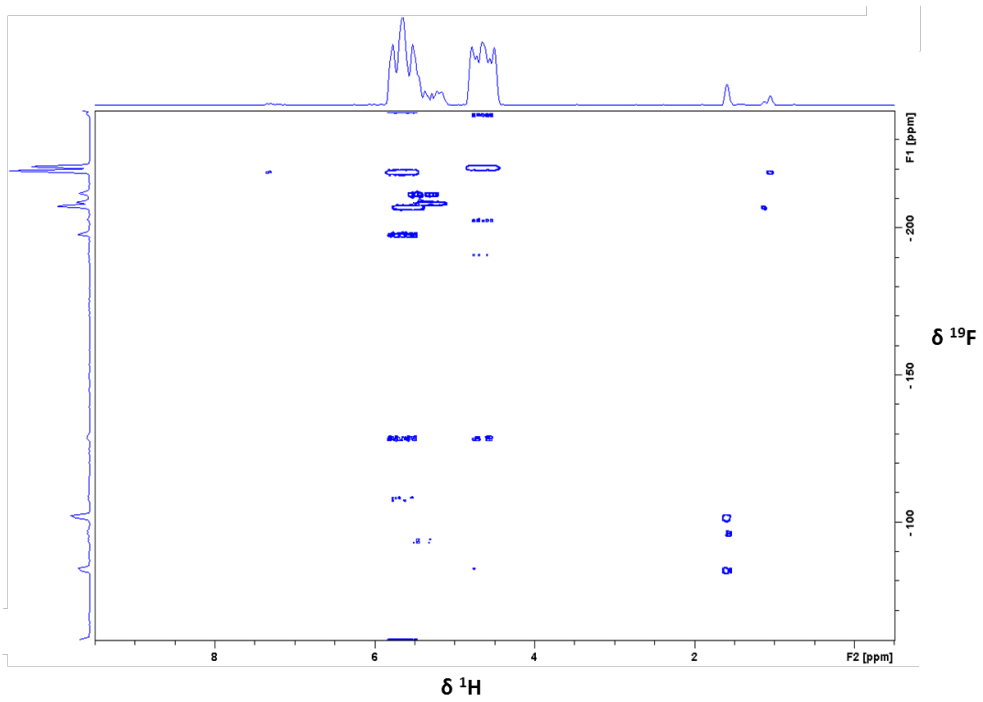

Figure A18. 2D ^{1}H-^{19}F HMQC NMR ($^{2}J_{FH}$ = 50 Hz) spectrum for complex **Ni-16c**.

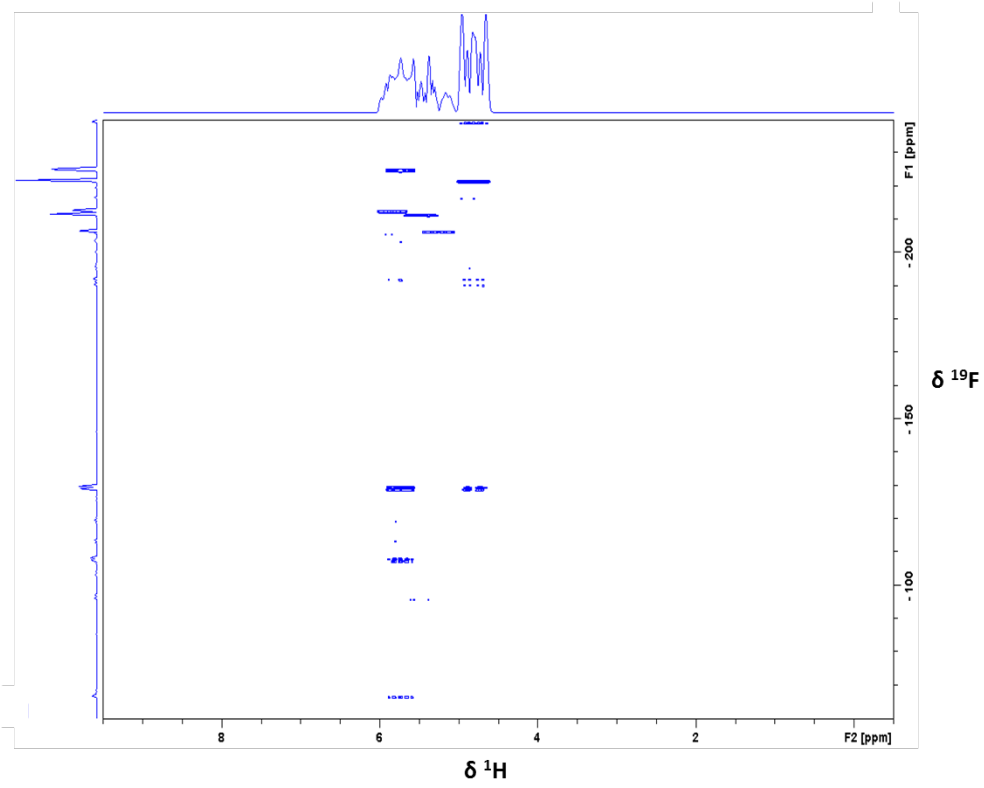

Figure A19. 2D ^{1}H-^{19}F HMQC NMR ($^{2}J_{FH}$ = 50 Hz) spectrum for complex **Ni-16d.**

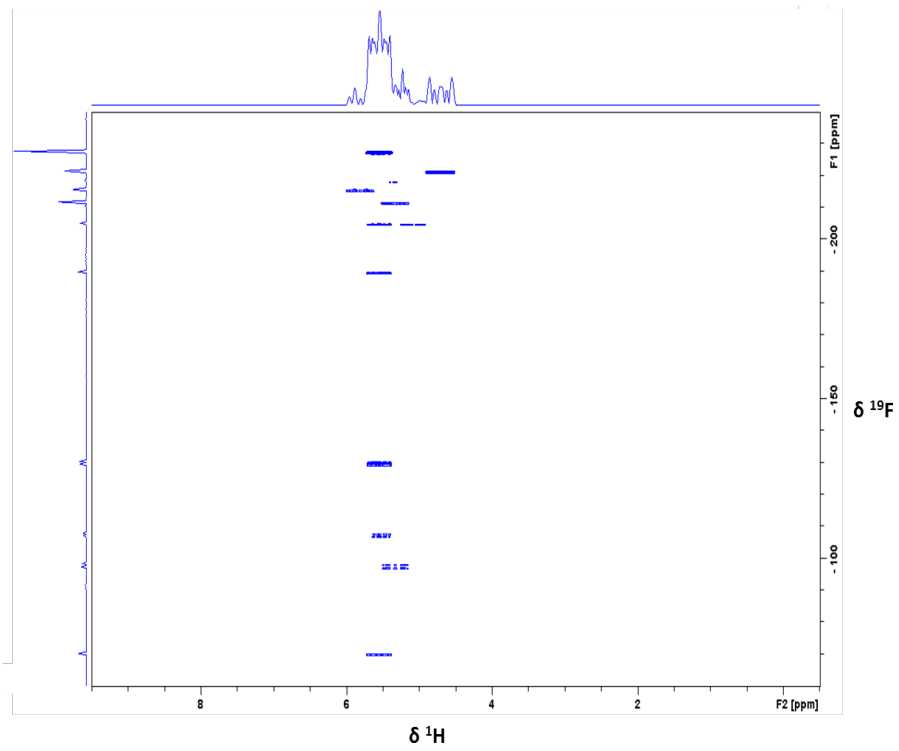

Figure A20. 2D ^{1}H-^{19}F HMQC NMR ($^{2}J_{FH}$ = 50 Hz) spectrum for complex **Ni-16e.**

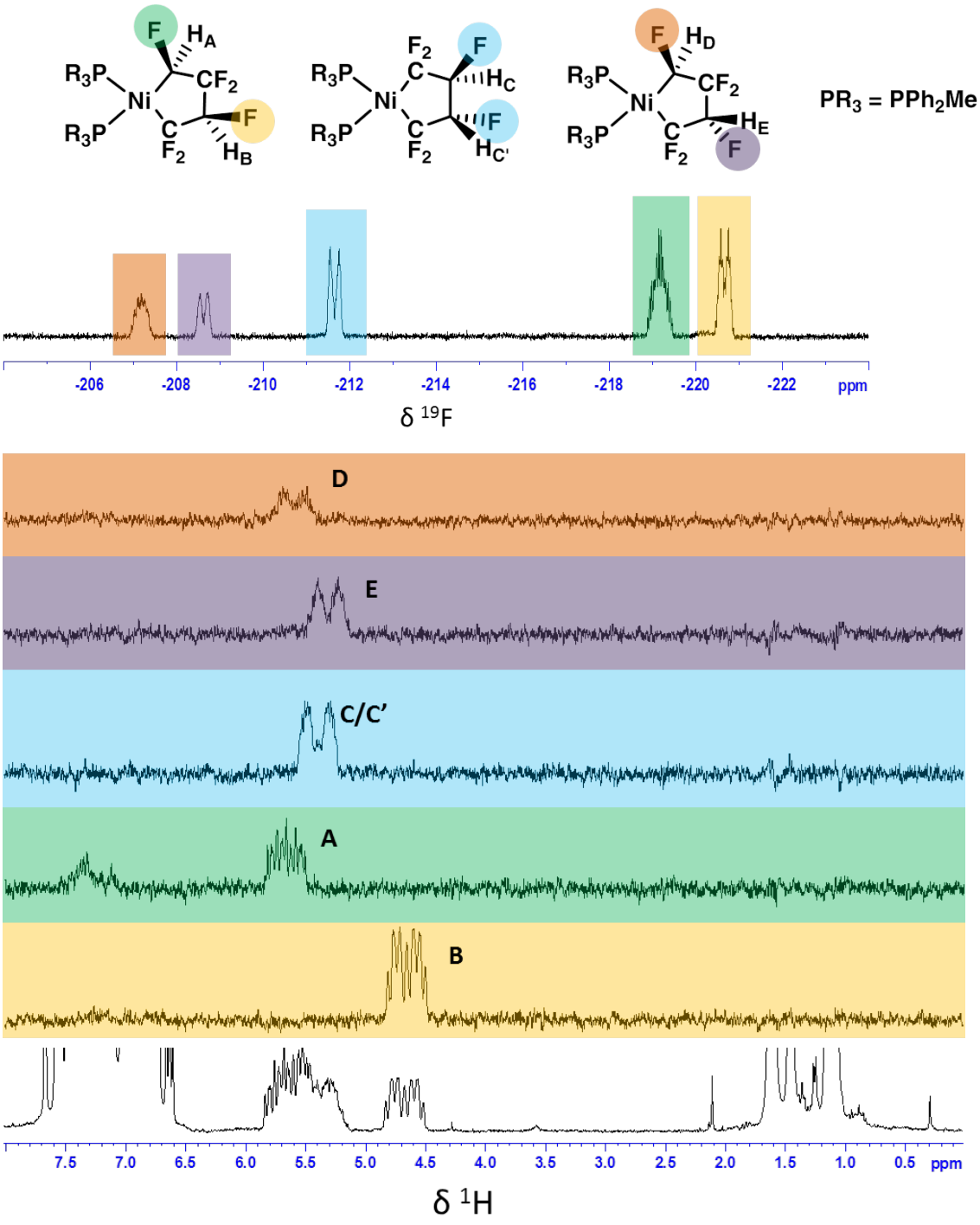

Figure A21. Selective 1D ^{1}H-^{19}F HOESY NMR spectra for complex **Ni-16c**.

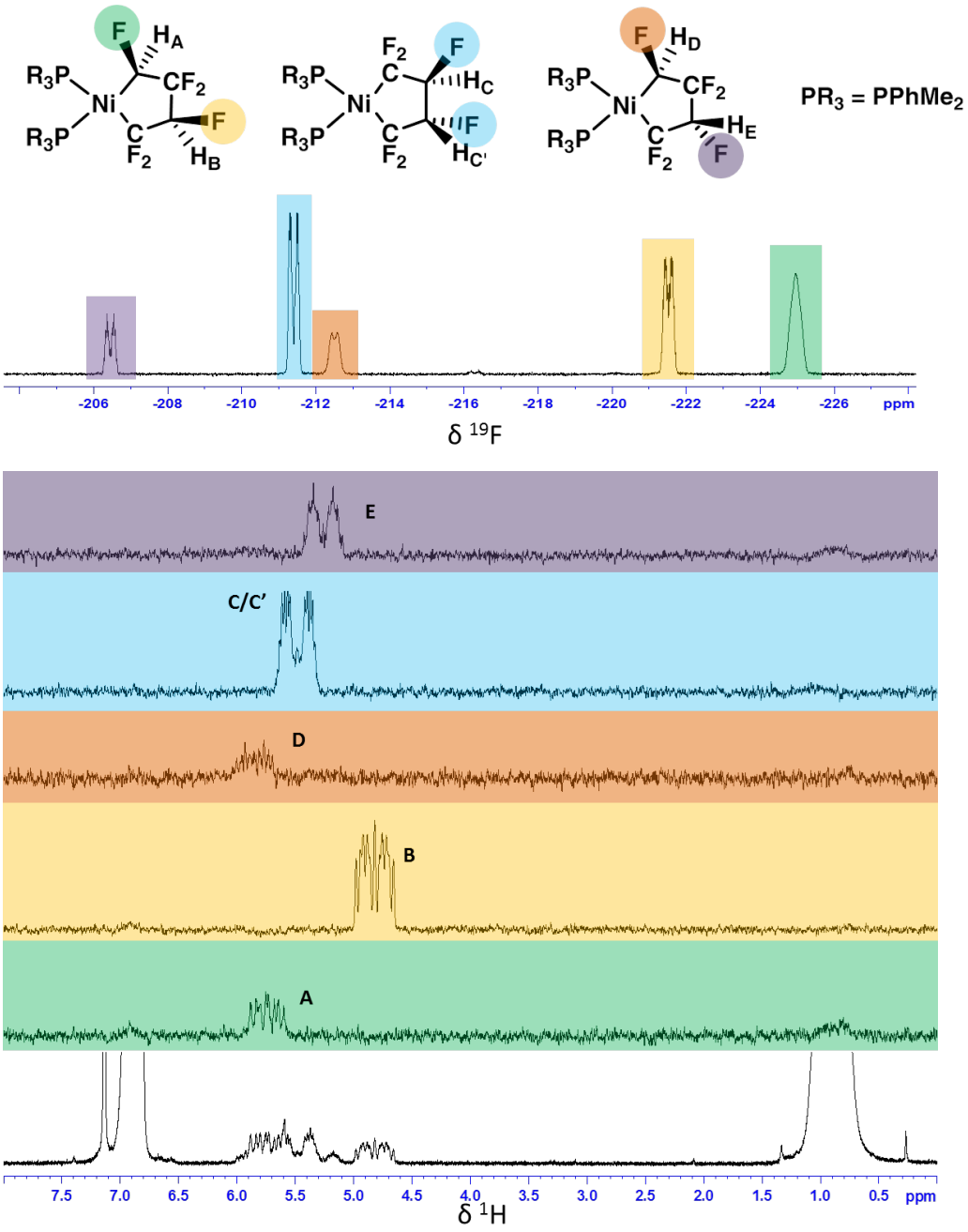

Figure A22. Selective 1D ^{1}H-^{19}F HOESY NMR spectra for complex **Ni-16d**.

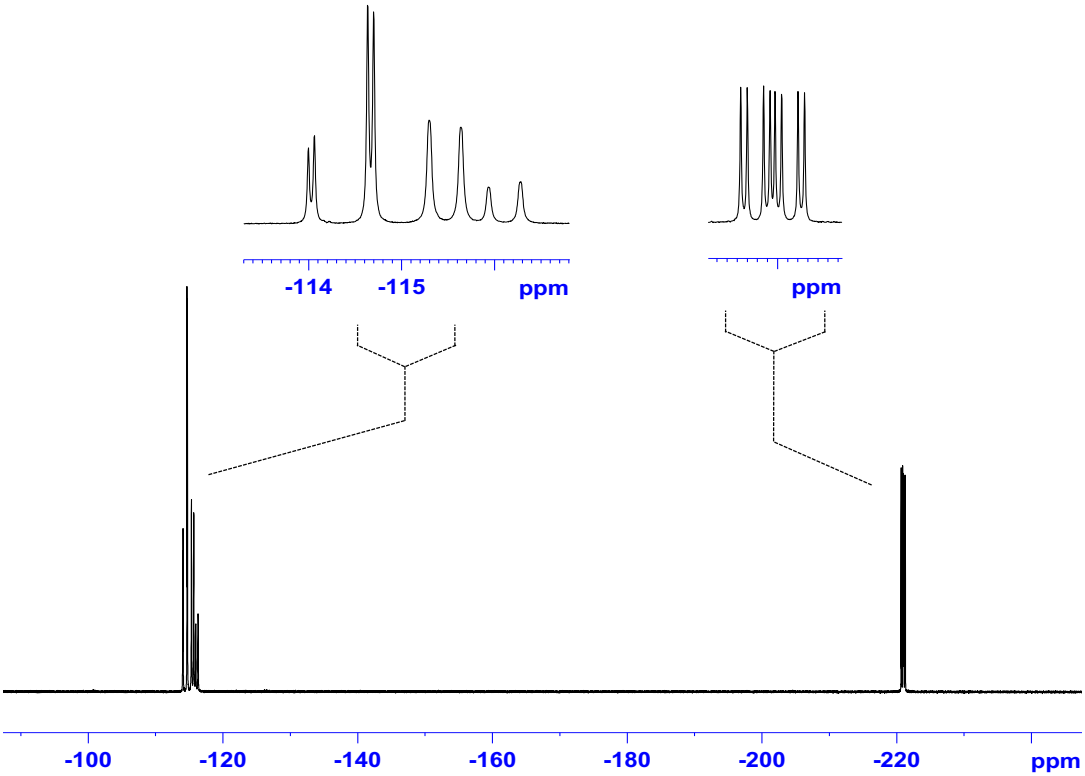

Figure A23. ^{19}F NMR (282 MHz, C_6D_6) spectrum for complex **Ni-17**. The inset shows the expanded (horizontal scale) signal.

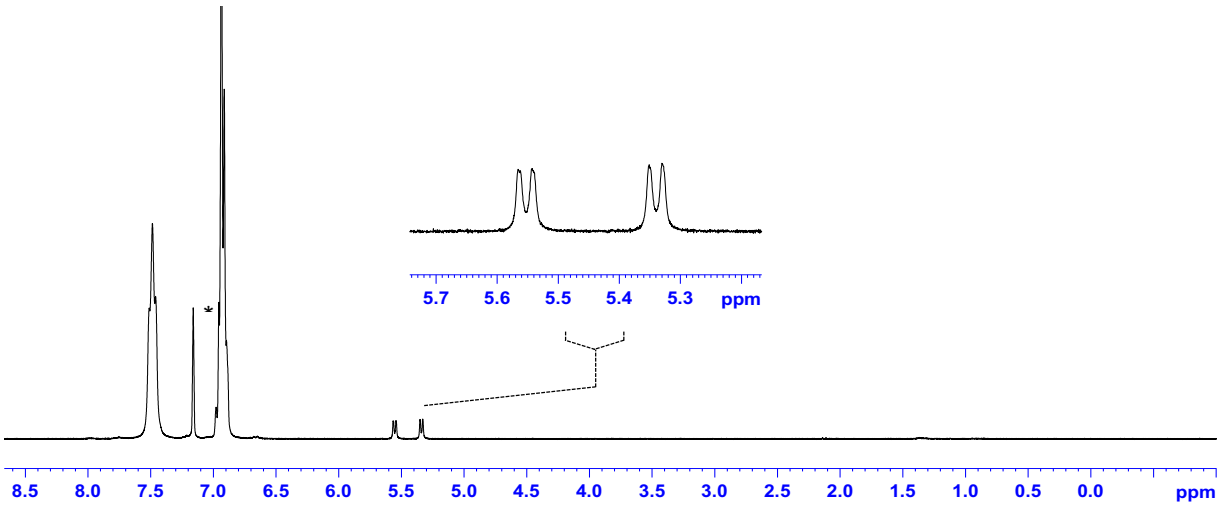

Figure A24. ^{1}H NMR (300 MHz, C_6D_6) spectrum for complex **Ni-17**. The residual solvent peak is labeled '*'. The inset shows the expanded (horizontal scale) signal.

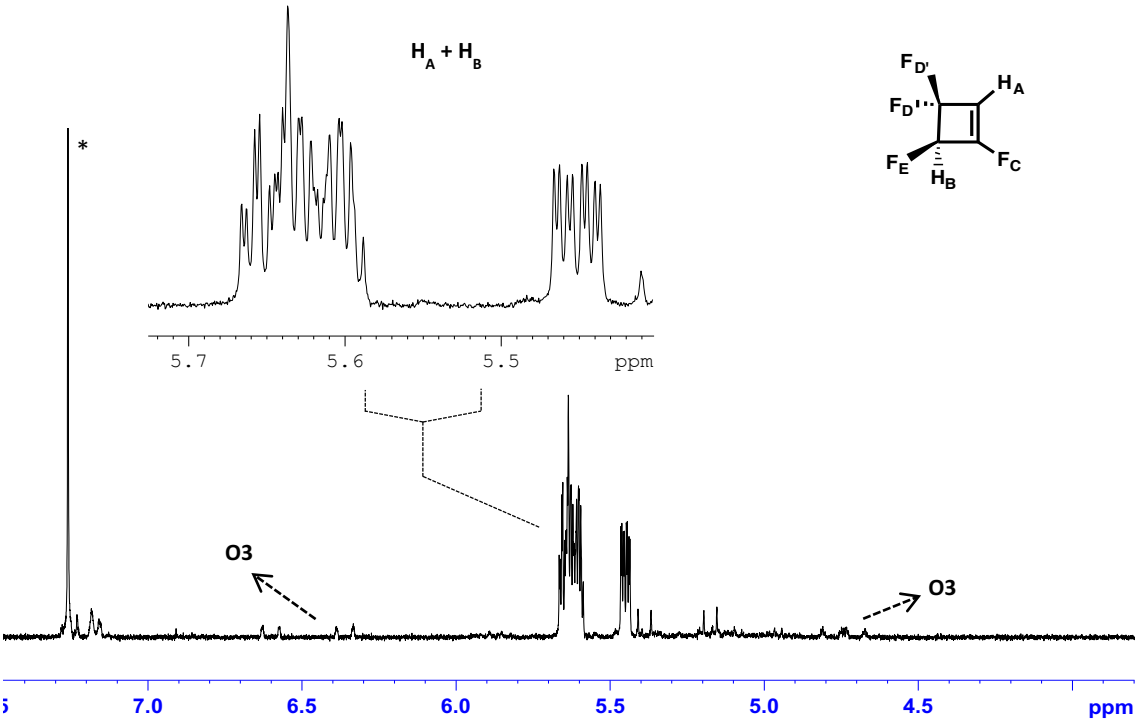

Figure A25. ^{1}H NMR (300 MHz, $CDCl_3$) spectrum of **O2** from the reaction between **Ni-16c** and $BF_3{\cdot}OEt_2$. The residual solvent peak is labeled '*'.

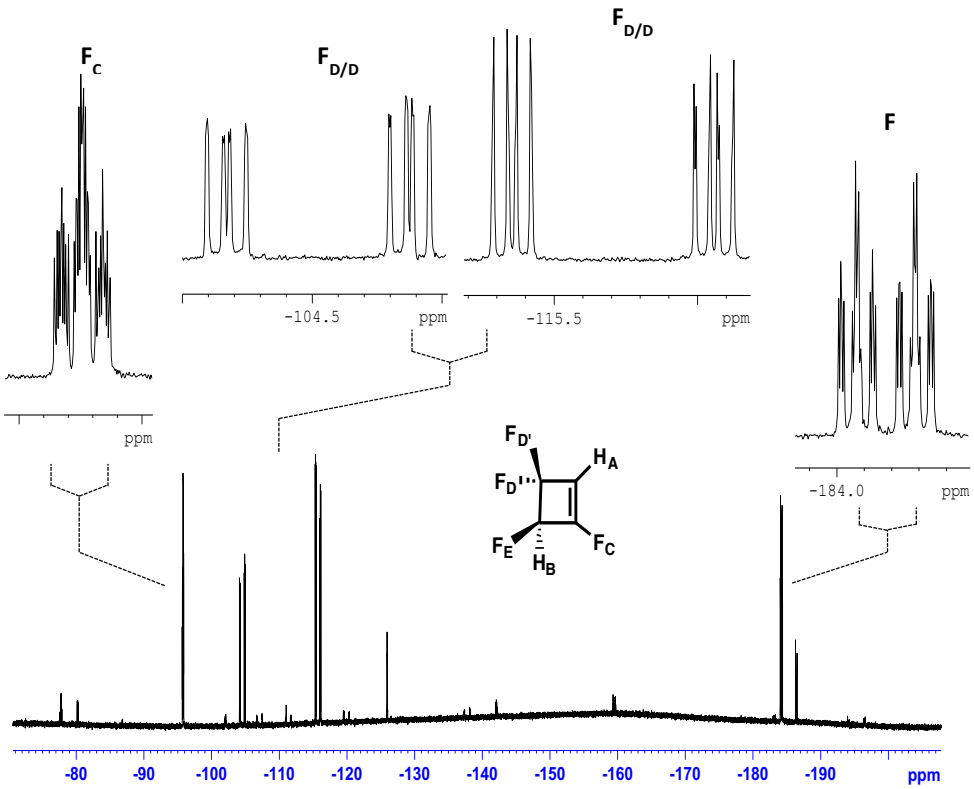

Figure A26. ^{19}F NMR (282 MHz, $CDCl_3$) spectrum of **O2** from the reaction between **Ni-16c** and $BF_3{\cdot}OEt_2$.

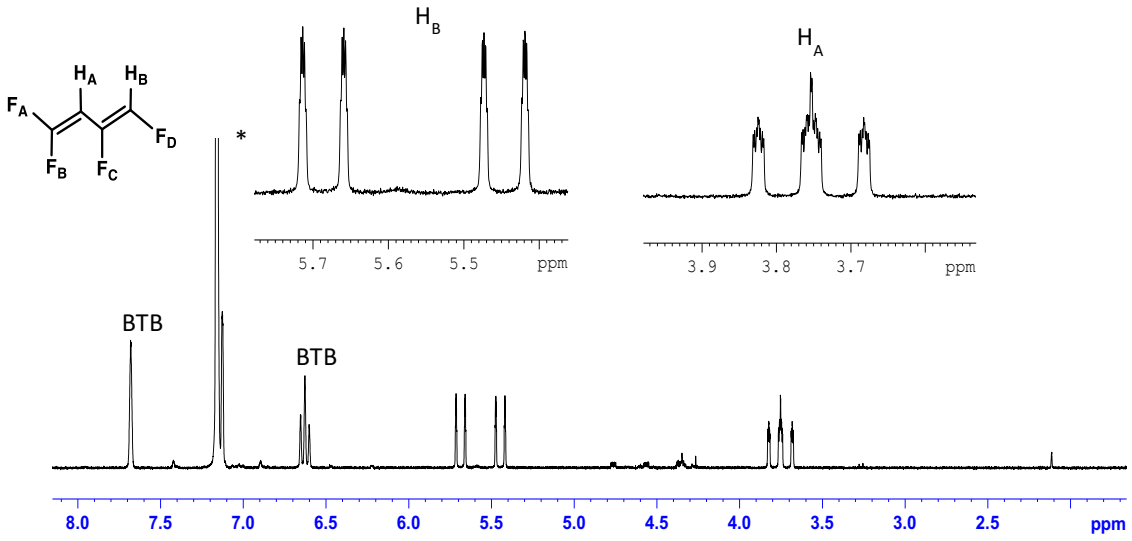

Figure A27. ^{1}H NMR (300 MHz, C_6D_6) spectrum for **O3**. The inset shows the expanded (horizontal scale) signals. The residual solvent peak is labeled '*'.

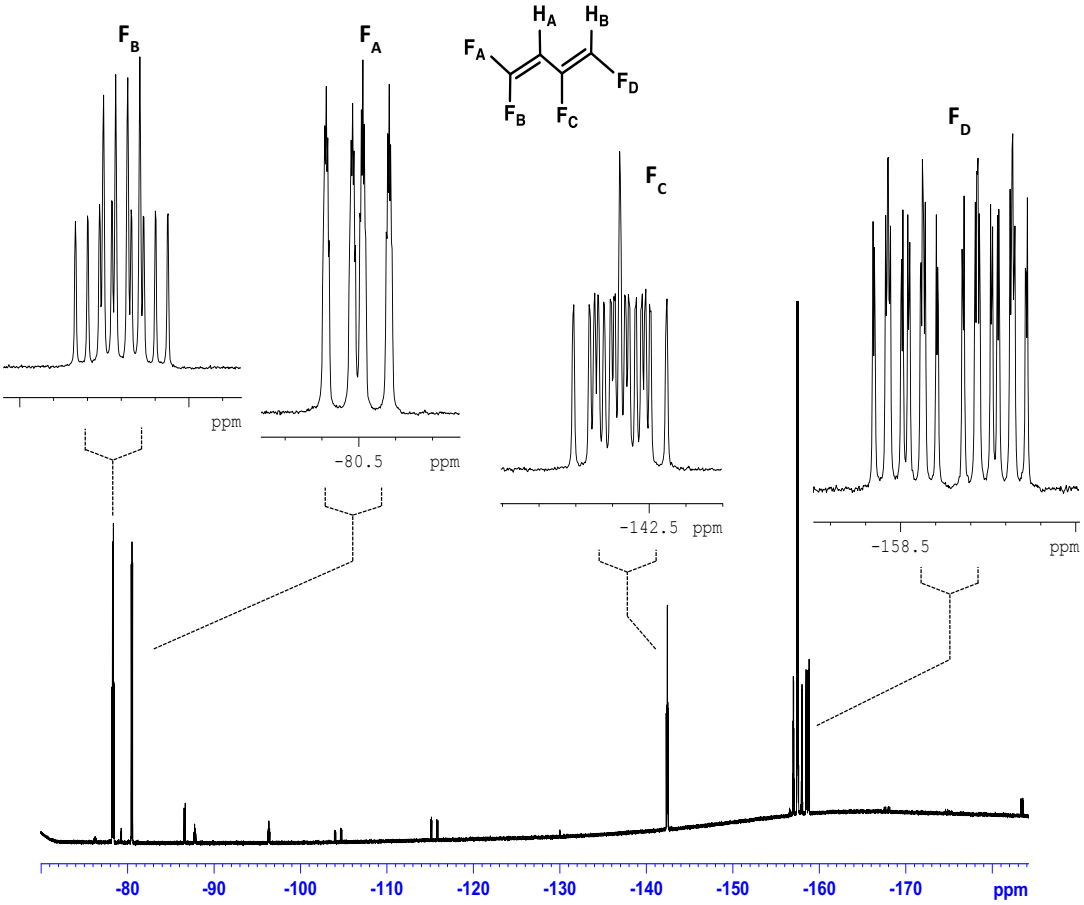

Figure A28. ^{19}F NMR (282 MHz, C_6D_6) spectrum for **O3**. The inset shows the expanded (horizontal scale) signals.

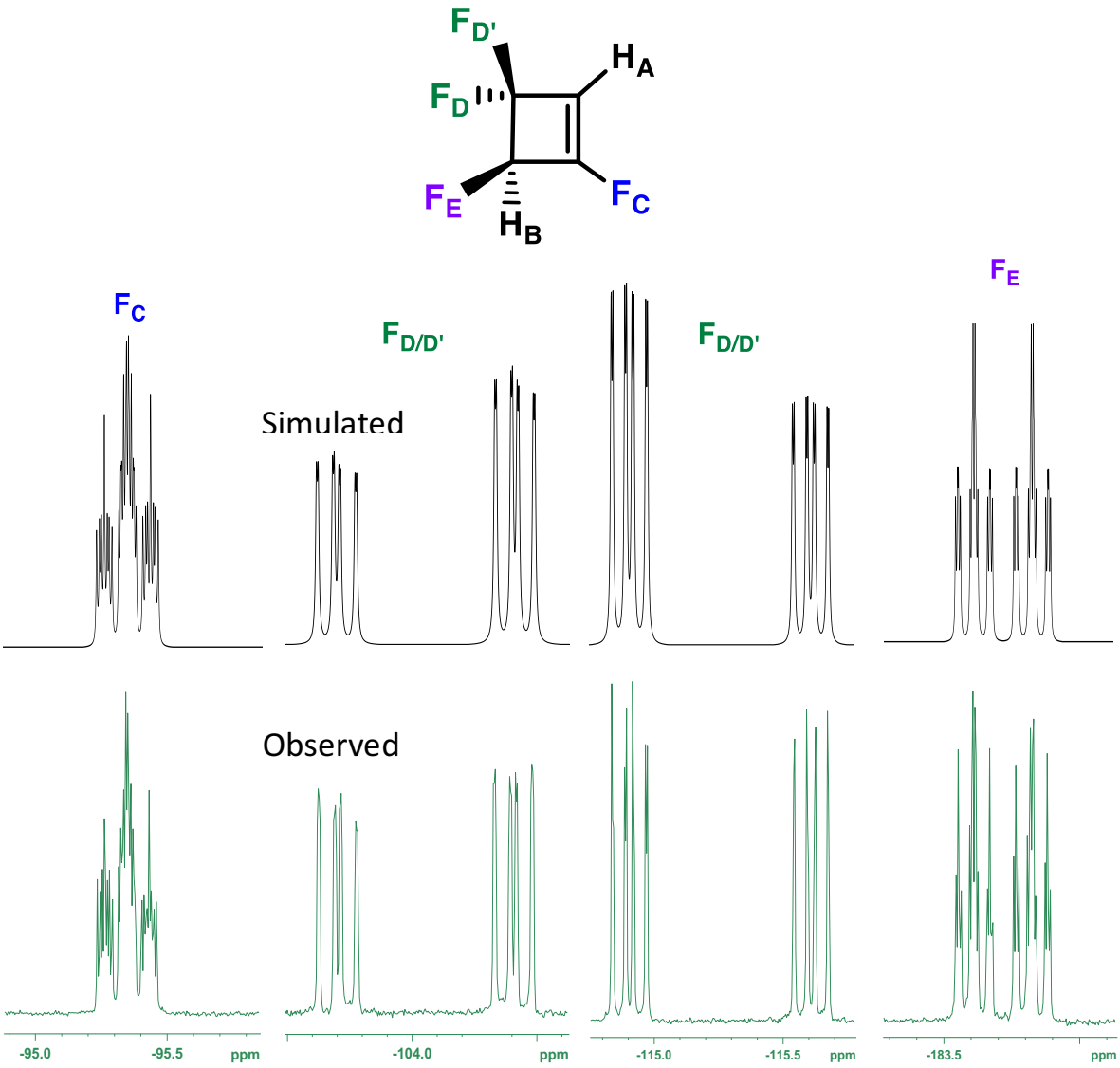

Figure A29. Simulated/observed (282 MHz, $CDCl_3$) ^{19}F NMR spectra for 1,1,3,4-tetrafluorocyclobutene **O2**. Simulations were calculated using the program g-NMR.

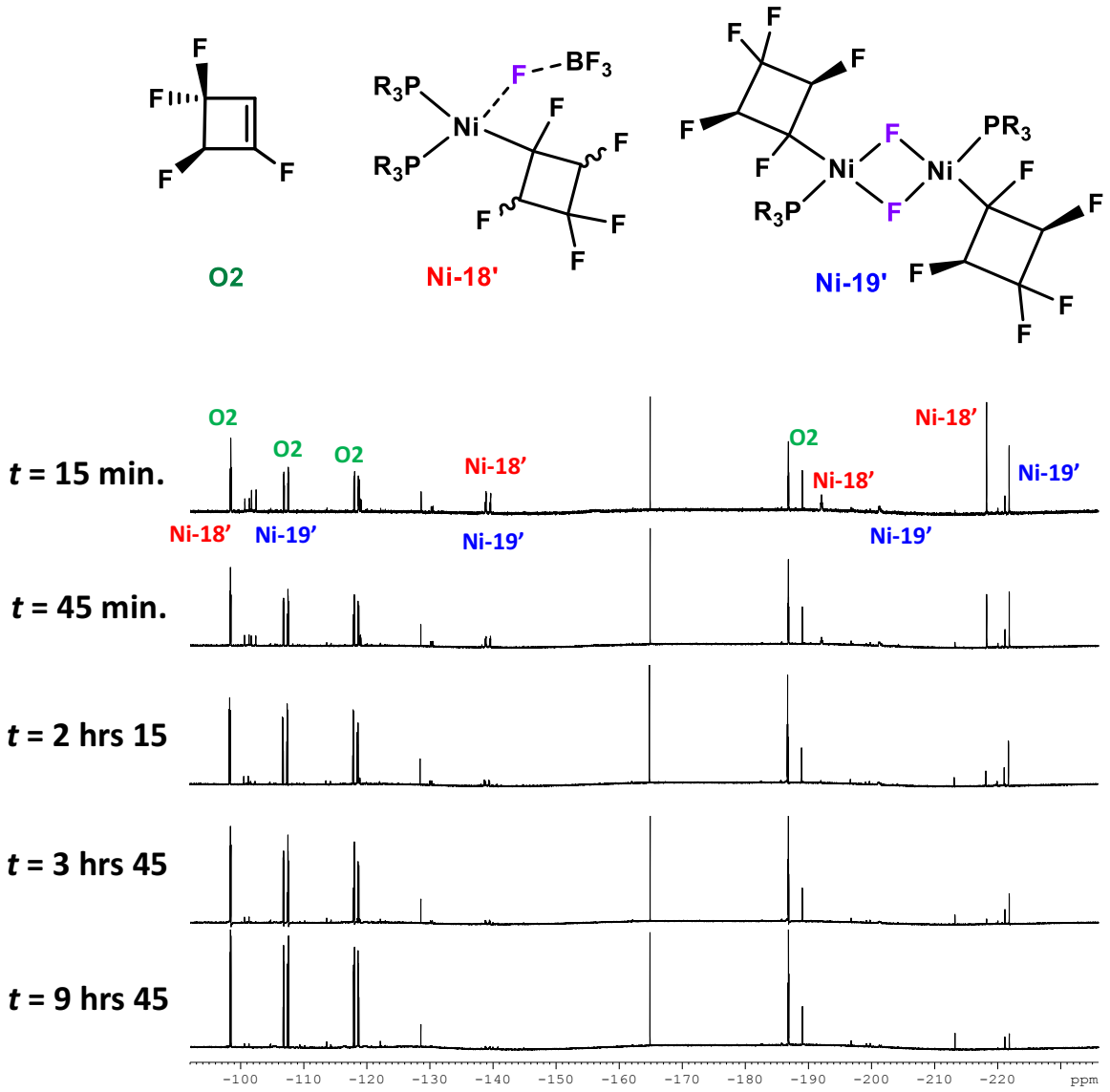

Figure A30. Selected time-elapsed $^{19}F\{^{1}H\}$ NMR (282 MHz, $CDCl_3$) spectra for the reaction between **Ni-16c** and $BF_3{\cdot}OEt_2$. Peaks associated with product **O2** are indicated as well as peaks associated with both proposed intermediates **Ni-18'** and **Ni-19'**.

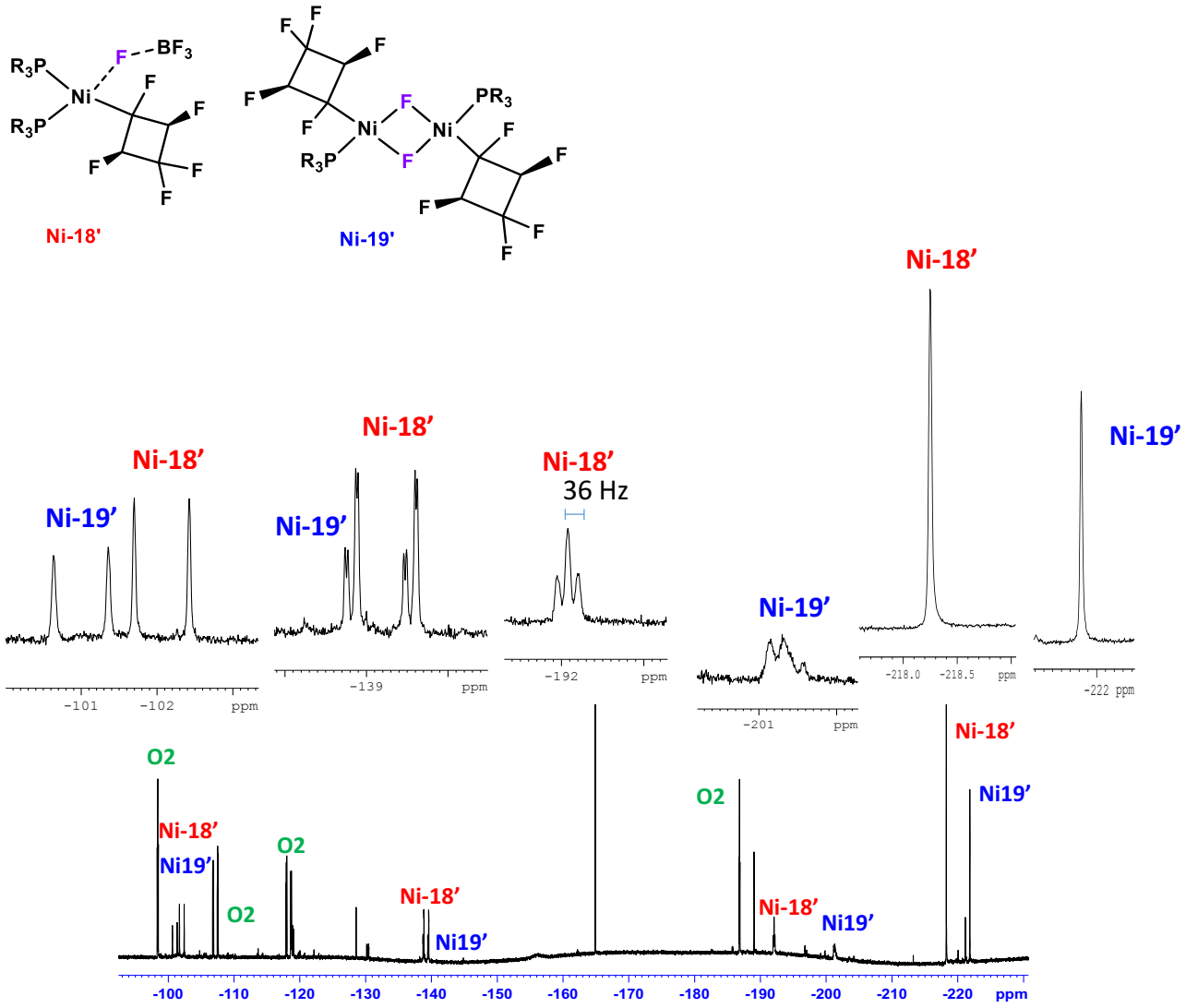

Figure A31. $^{19}F\{^{1}H\}$ NMR (282 MHz, $CDCl_3$) spectrum for ***t* = 15 min.** from **Figure A30**. Peaks associated with product **O2** are indicated as well as peaks associated with both proposed intermediates **Ni-18'** and **Ni-19'**. The inset shows the expanded (horizontal scale) signals.

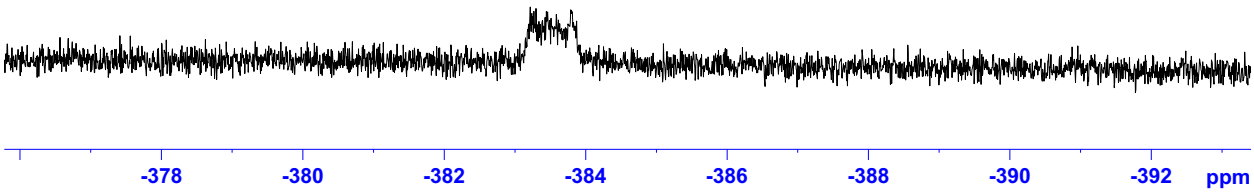

Figure A32. $^{19}F\{^{1}H\}$ NMR (282 MHz, $CDCl_3$) upfield region of the spectrum for ***t* = 15 min.** from **Figure A30** displaying the Ni-F resonance.

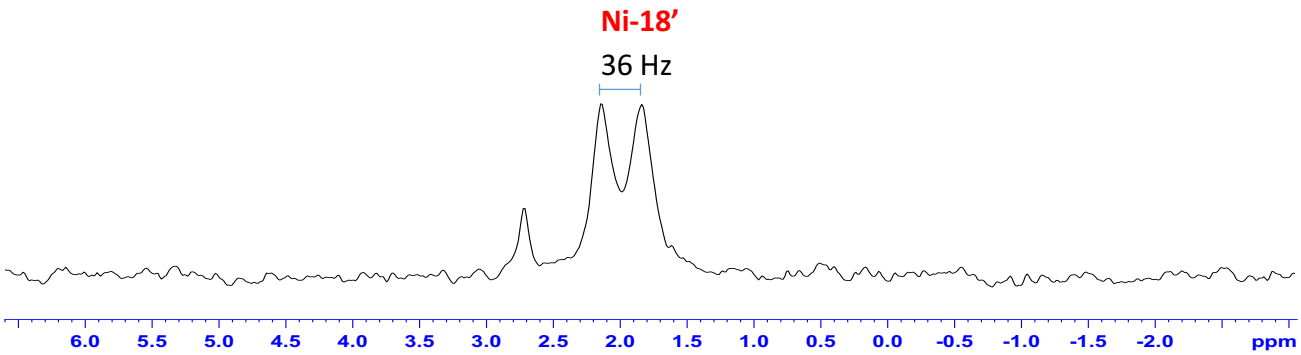

Figure A33. $^{31}P\{^{1}H\}$ NMR (121 MHz, $CDCl_3$) spectrum highlighting phosphorus peak associated with intermediate **Ni-18'**. Spectrum acquired *ca.* 5 min. after initial mixing of **Ni-16c** and $BF_3{\cdot}OEt_2$. Corresponding coupling constant shown in **Figure A31** with C_α-F.

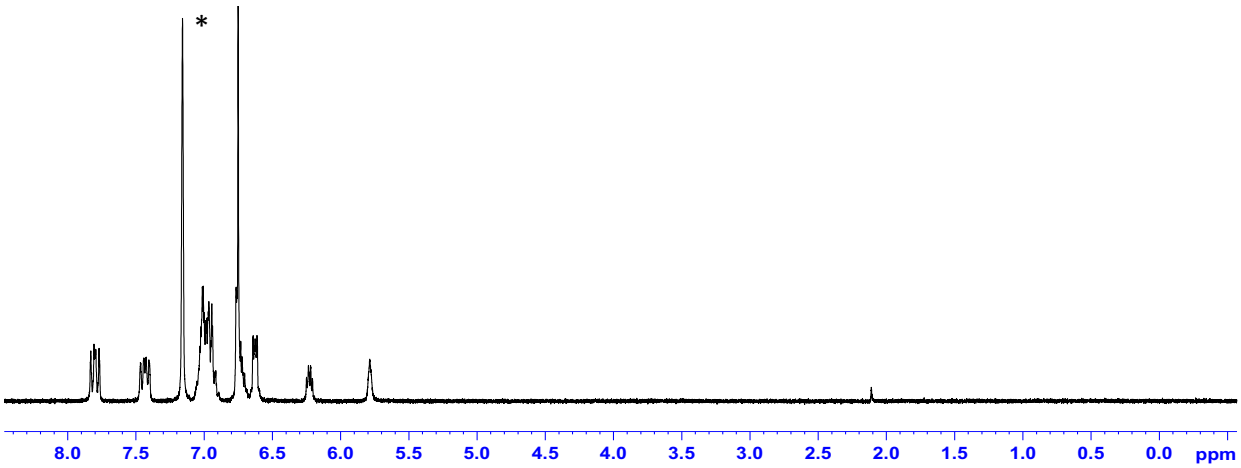

Figure A34. ^{1}H NMR (300 MHz, C_6D_6) spectrum for complex **Ni-21**. The residual solvent peak is labeled '*'.

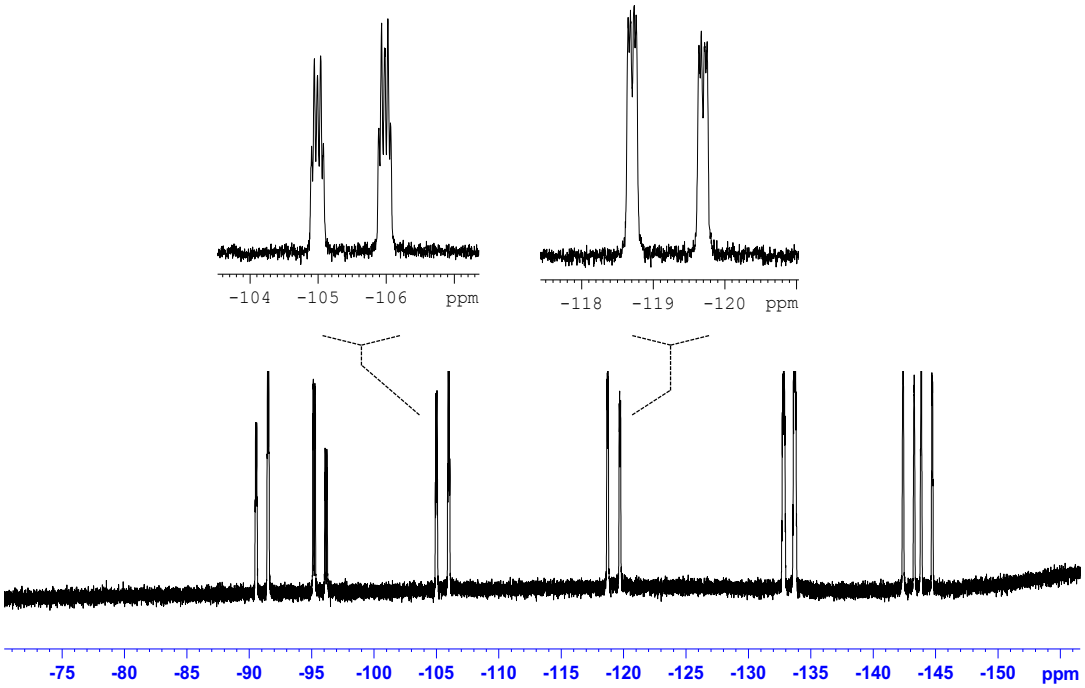

Figure A35. ^{19}F NMR (282 MHz, C_6D_6) spectrum for **Ni-21**. The inset shows the expanded (horizontal scale) signals.

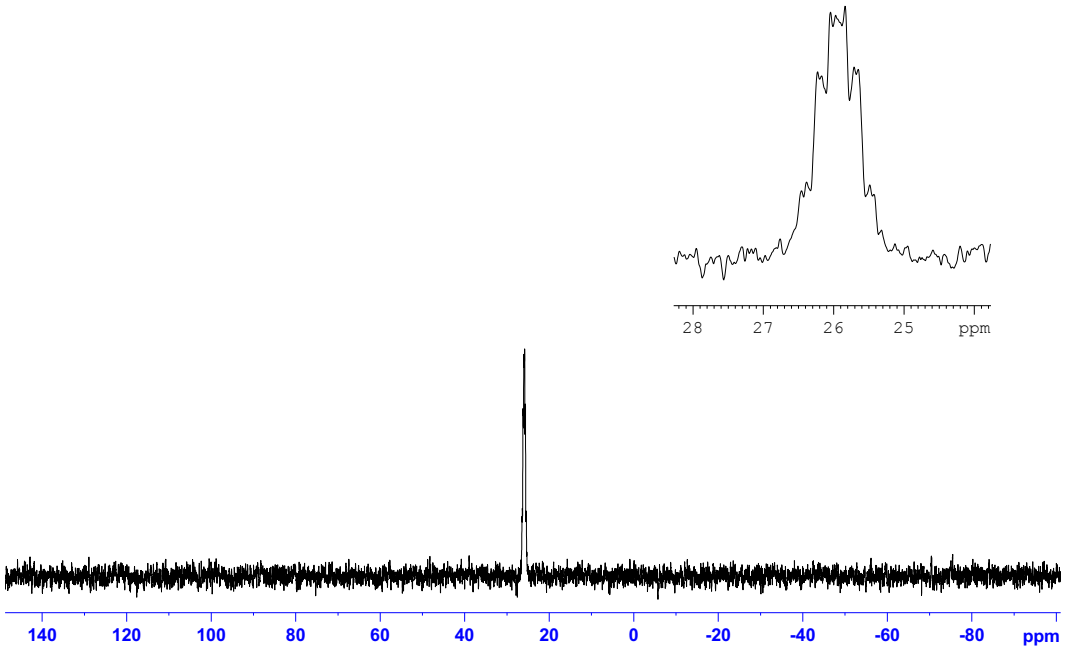

Figure A36. $^{31}P\{^1H\}$ NMR (121 MHz, C_6D_6) spectrum for **Ni-21**. The inset shows the expanded (horizontal scale) signal.

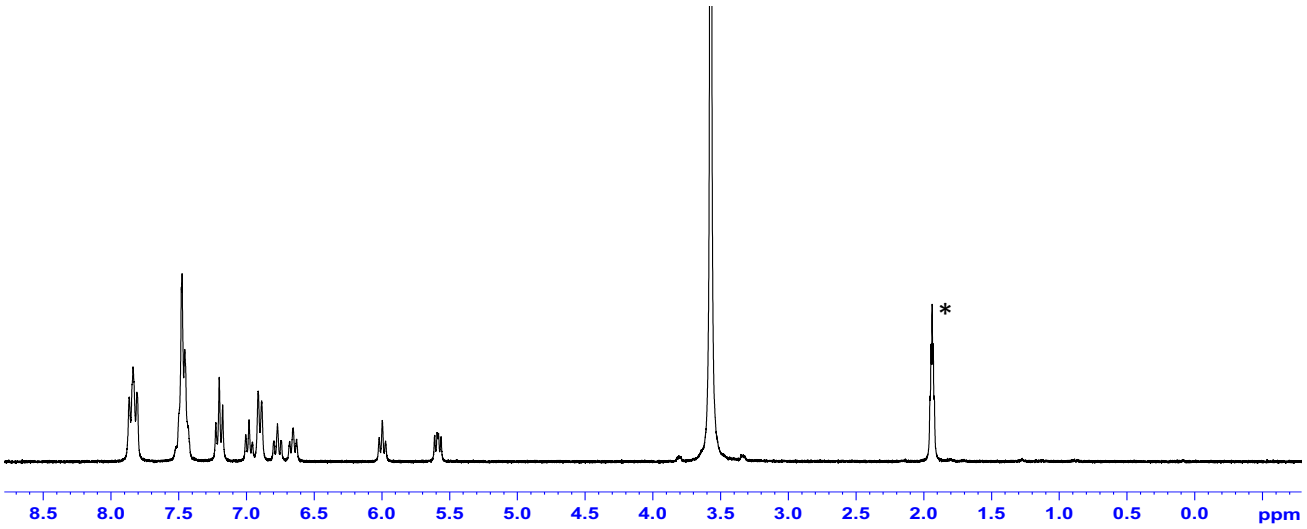

Figure A37. ^{1}H NMR (300 MHz, CD_3CN) spectrum for complex **Ni-22•Na**. The residual solvent peak is labeled '*'.

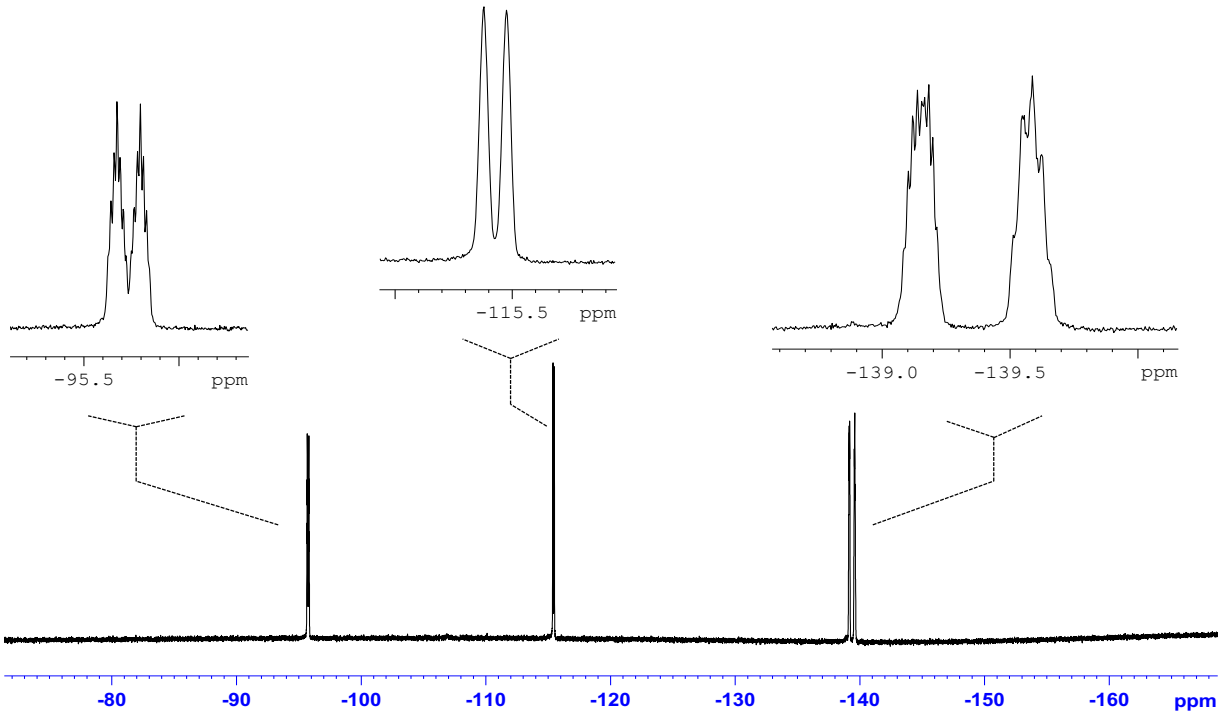

Figure A38. ^{19}F NMR (282 MHz, CD_3CN) spectrum for **Ni-22•Na**. The inset shows the expanded (horizontal scale) signals.

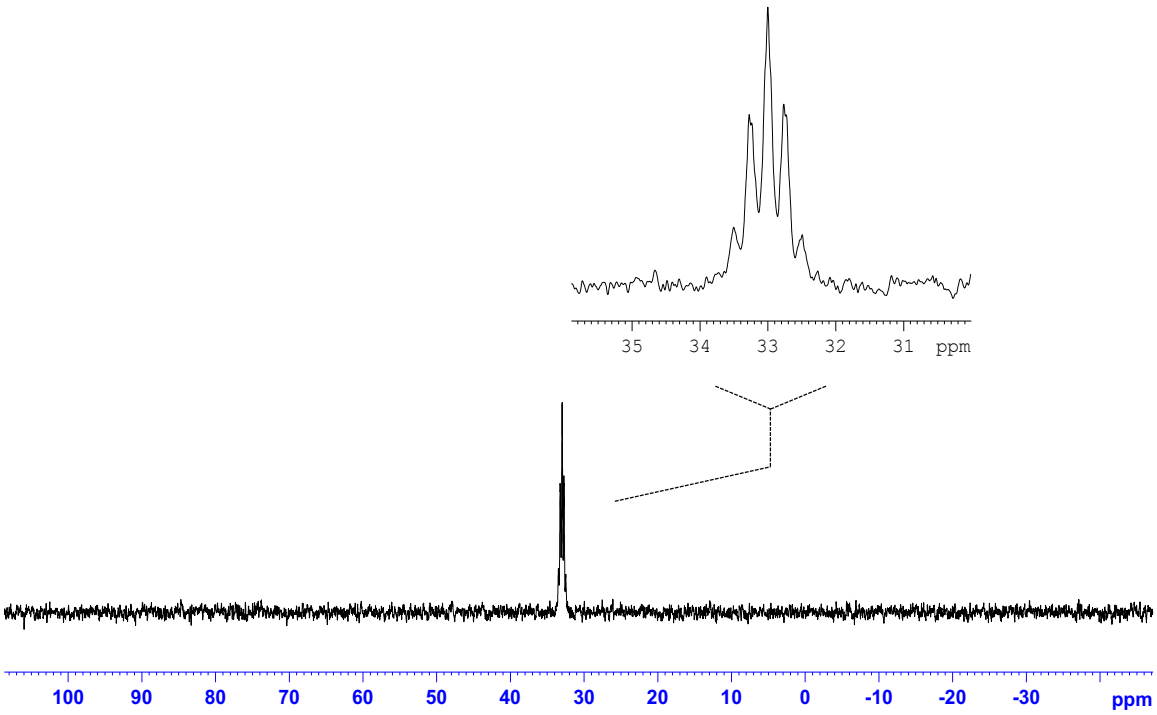

Figure A39. $^{31}P\{^{1}H\}$ NMR (121 MHz, CD_3CN) spectrum for **Ni-22•Na**. The inset shows the expanded (horizontal scale) signal.

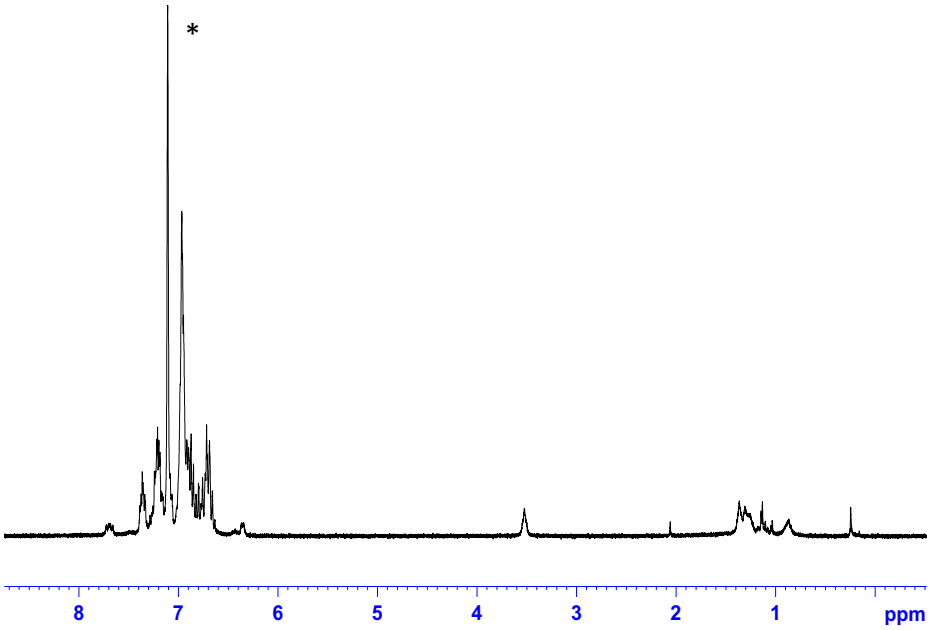

Figure A40. ^{1}H NMR (300 MHz, C_6D_6) spectrum of the reaction between **[P,N$^-$]Na**$^+$ and TFE. The residual solvent peak is labeled '*'.

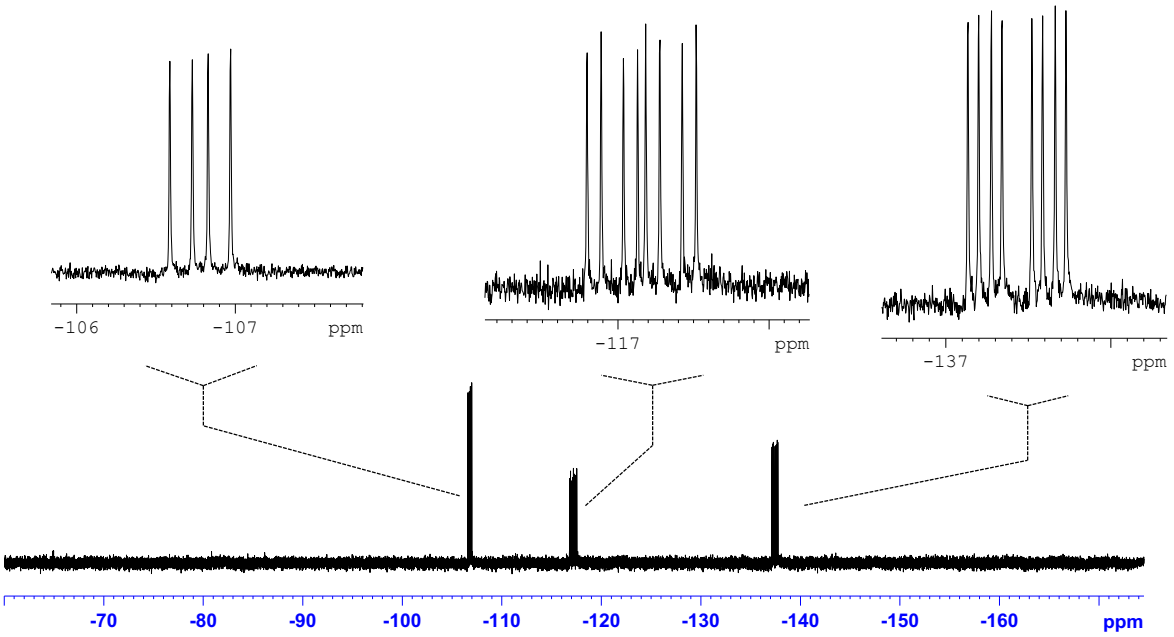

Figure A41. ^{19}F NMR (300 MHz, C_6D_6) spectrum of the reaction between **[P,N$^-$]Na$^+$** and TFE. Expanded peaks correspond to proposed **O6** product.

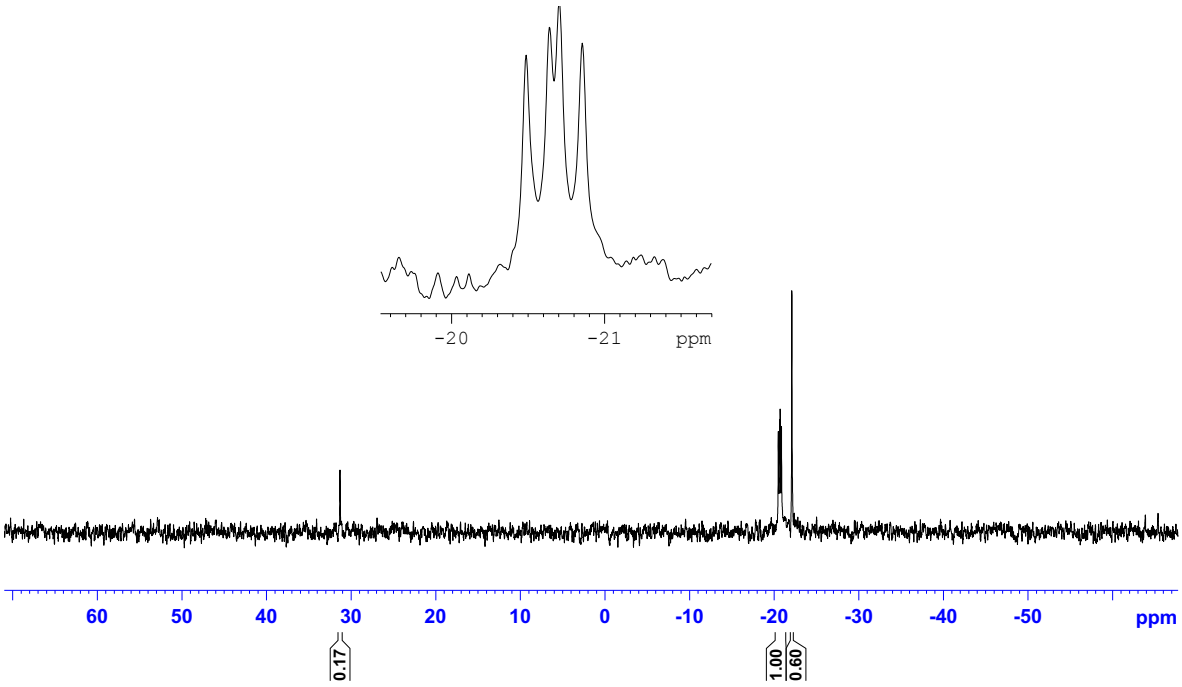

Figure A42. $^{31}P\{^1H\}$ NMR (121 MHz, C_6D_6) spectrum of the reaction between **[P,N$^-$]Na$^+$** and TFE. Expanded peak corresponds to proposed **O6** product.

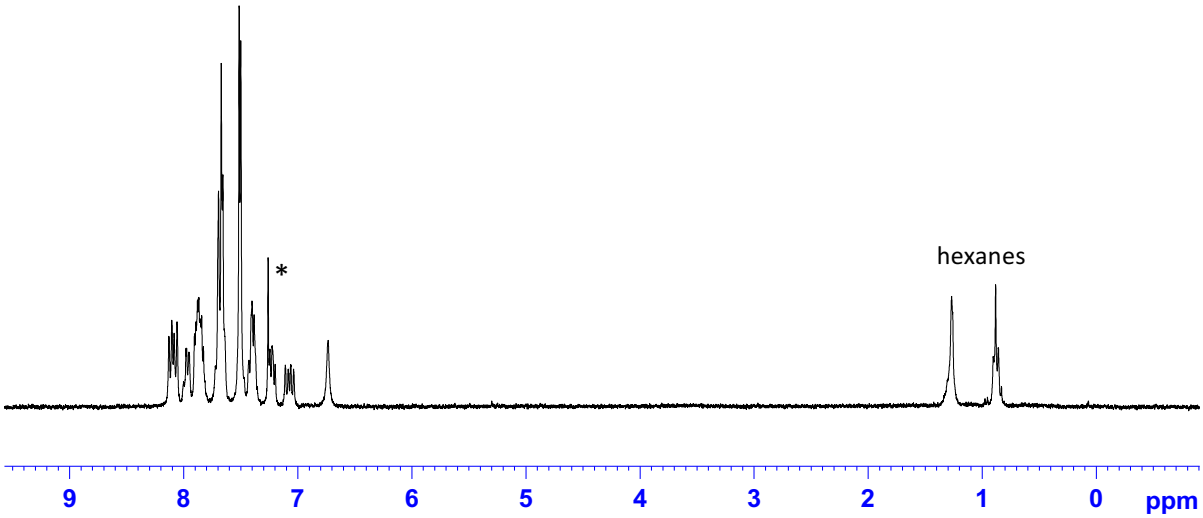

Figure A43. ^{1}H NMR (300 MHz, $CDCl_3$) spectrum for **Ni-23**. The inset shows the expanded (horizontal scale) signals.

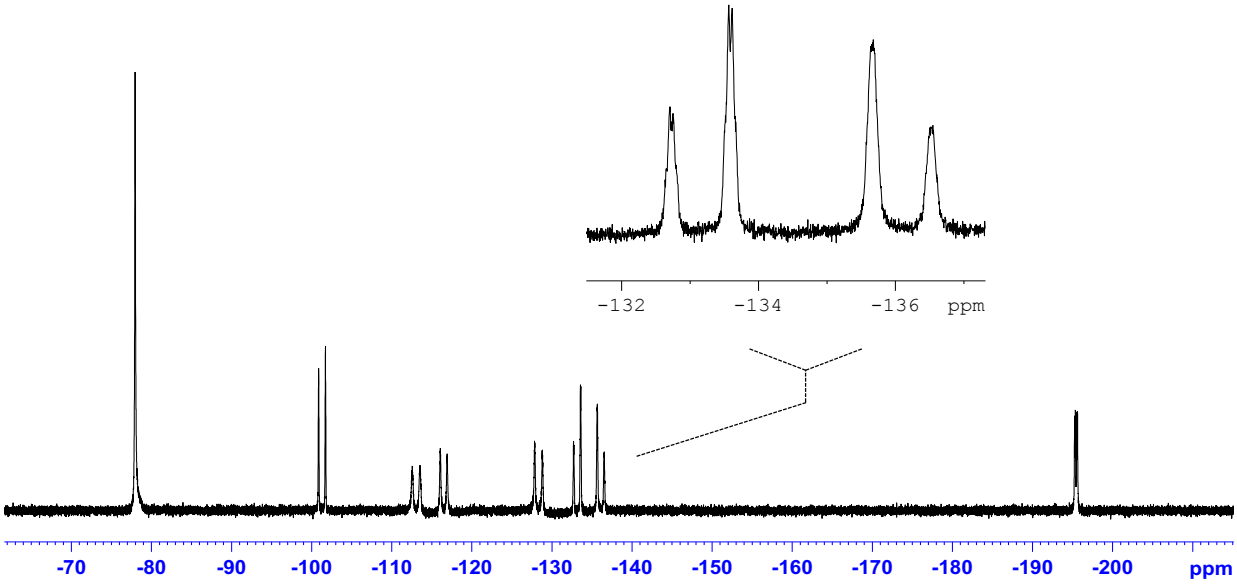

Figure A44. ^{19}F NMR (282 MHz, $CDCl_3$) spectrum for **Ni-23**. The inset shows the expanded (horizontal scale) signals.

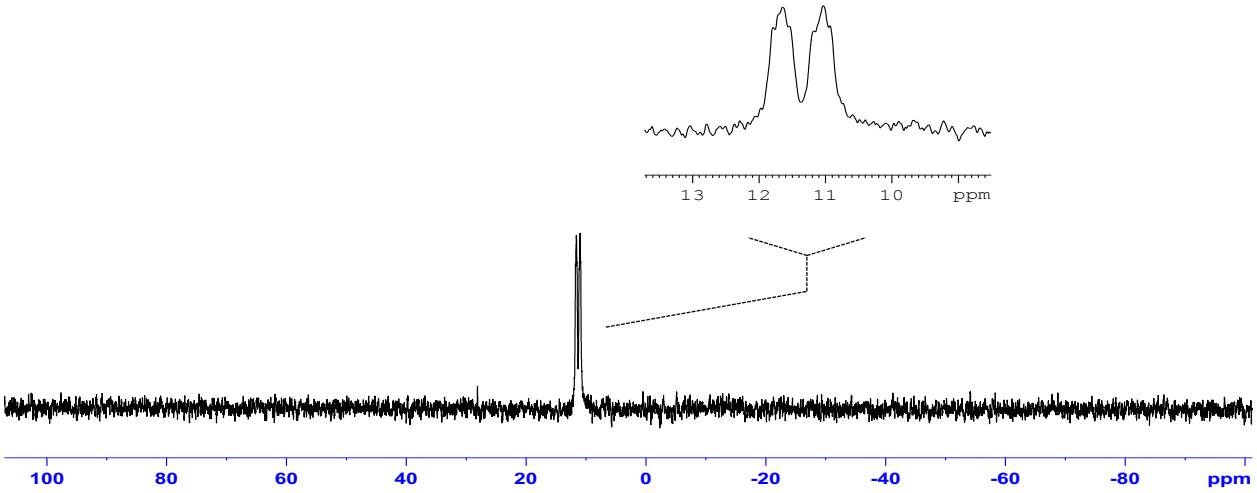

Figure A45. $^{31}P\{^{1}H\}$ NMR (121 MHz, $CDCl_3$) spectrum for **Ni-23**. The inset shows the expanded (horizontal scale) signal.

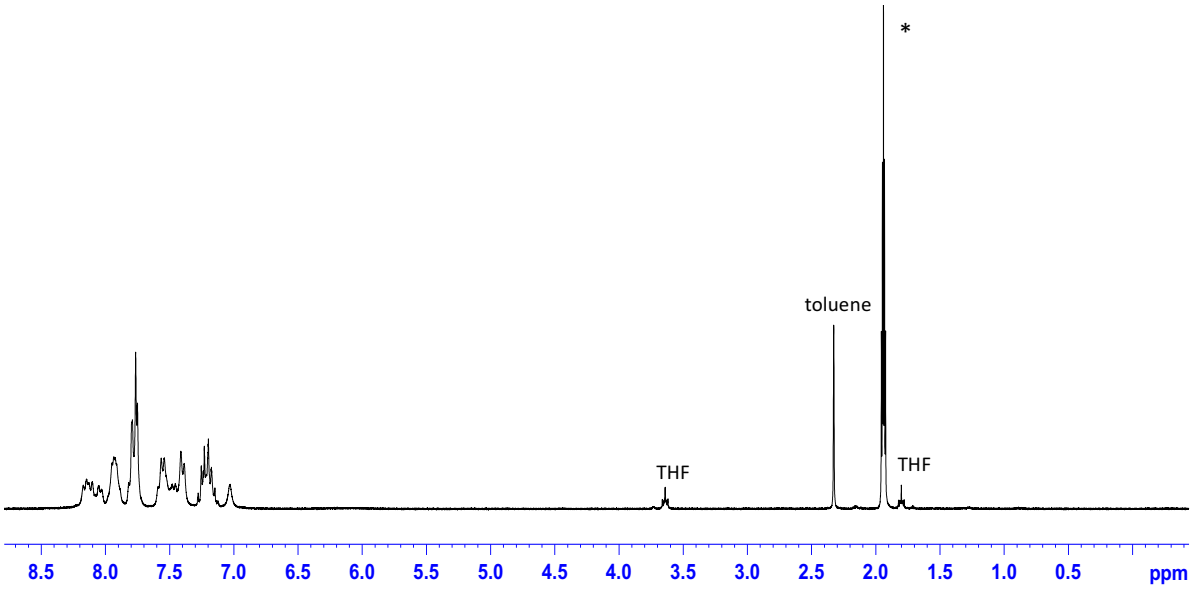

Figure A46. ^{1}H NMR (300 MHz, CD_3CN) spectrum for complex **Ni-23•CD_3CN**. The residual solvent peak is labeled '*'.

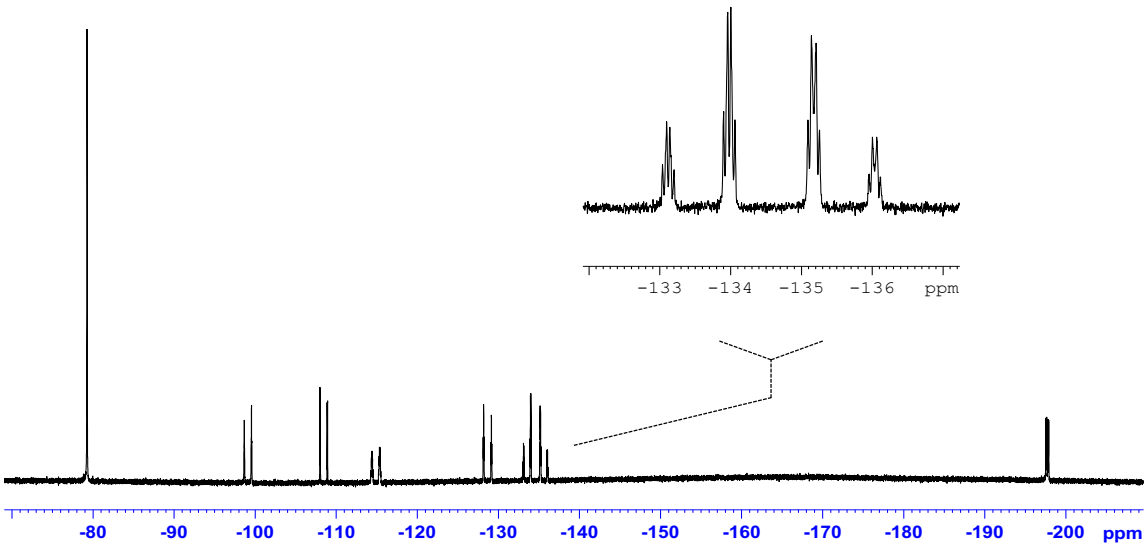

Figure A47. ^{19}F NMR (282 MHz, CD_3CN) spectrum for **Ni-23•CD3CN**. The inset shows the expanded (horizontal scale) signals.

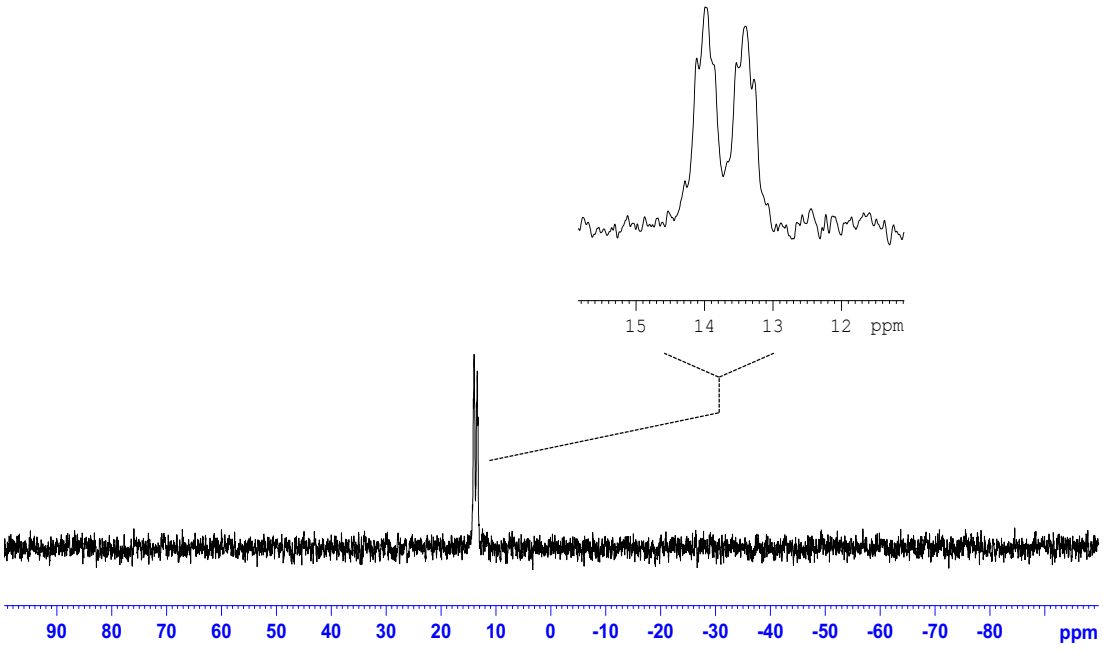

Figure A48. $^{31}P\{^1H\}$ NMR (121 MHz, CD_3CN) spectrum for **Ni-23•CD_3CN**. The inset shows the expanded (horizontal scale) signal.

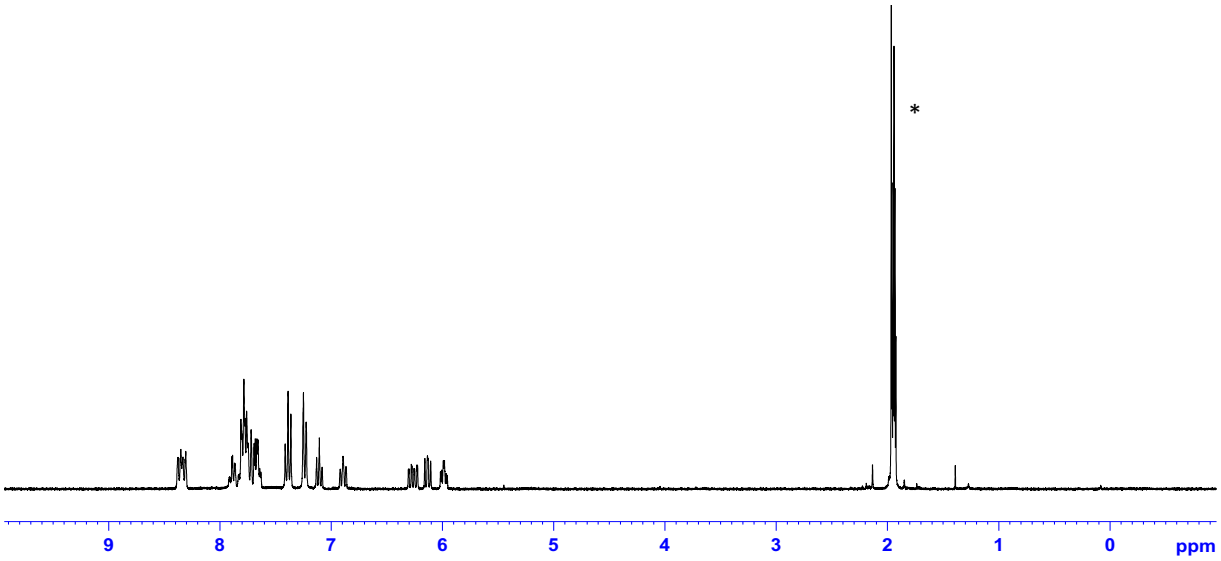

Figure A49. ^{1}H NMR (300 MHz, CD_3CN) spectrum for complex **Ni-24**. The residual solvent peak is labeled '*'.

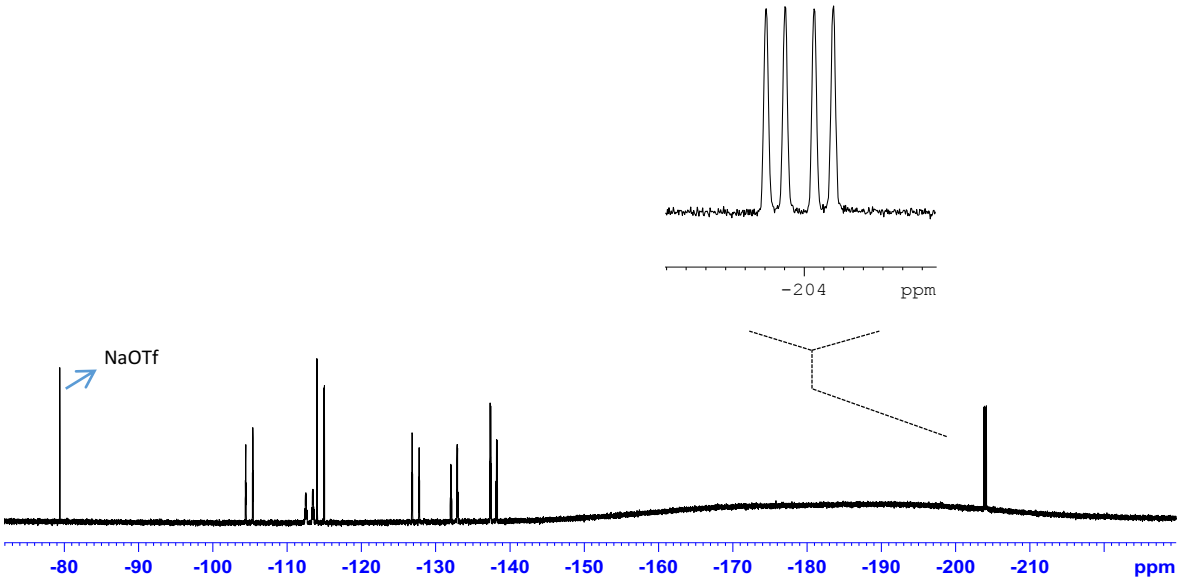

Figure A50. ^{19}F NMR (282 MHz, CD_3CN) spectrum for **Ni-24**. The inset shows the expanded (horizontal scale) signals.

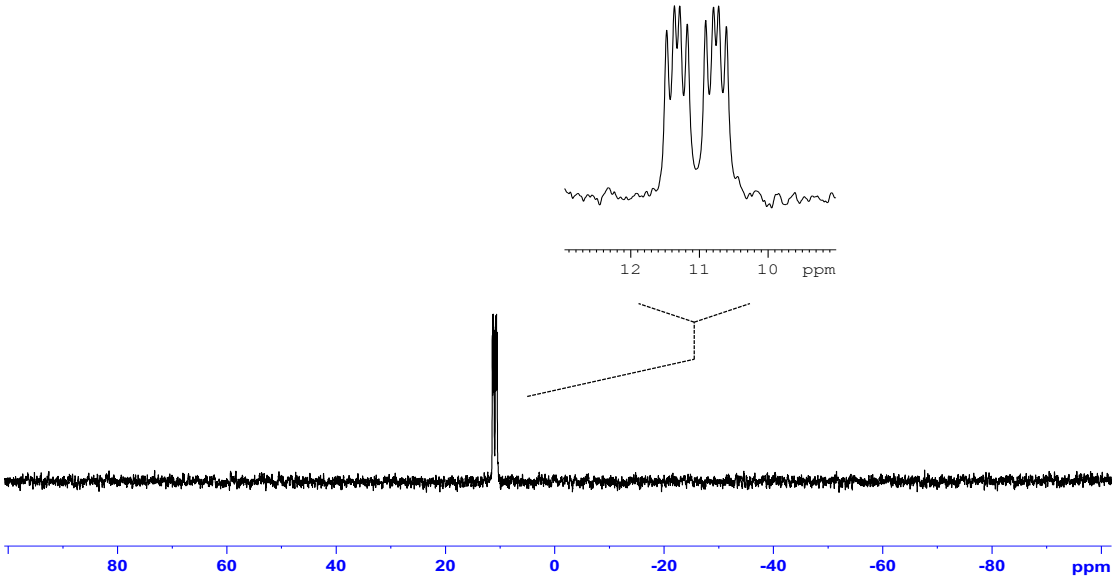

Figure A51. $^{31}P\{^{1}H\}$ NMR (121 MHz, CD_3CN) spectrum for **Ni-24**. The inset shows the expanded (horizontal scale) signal.

Mass Spectrometry Data

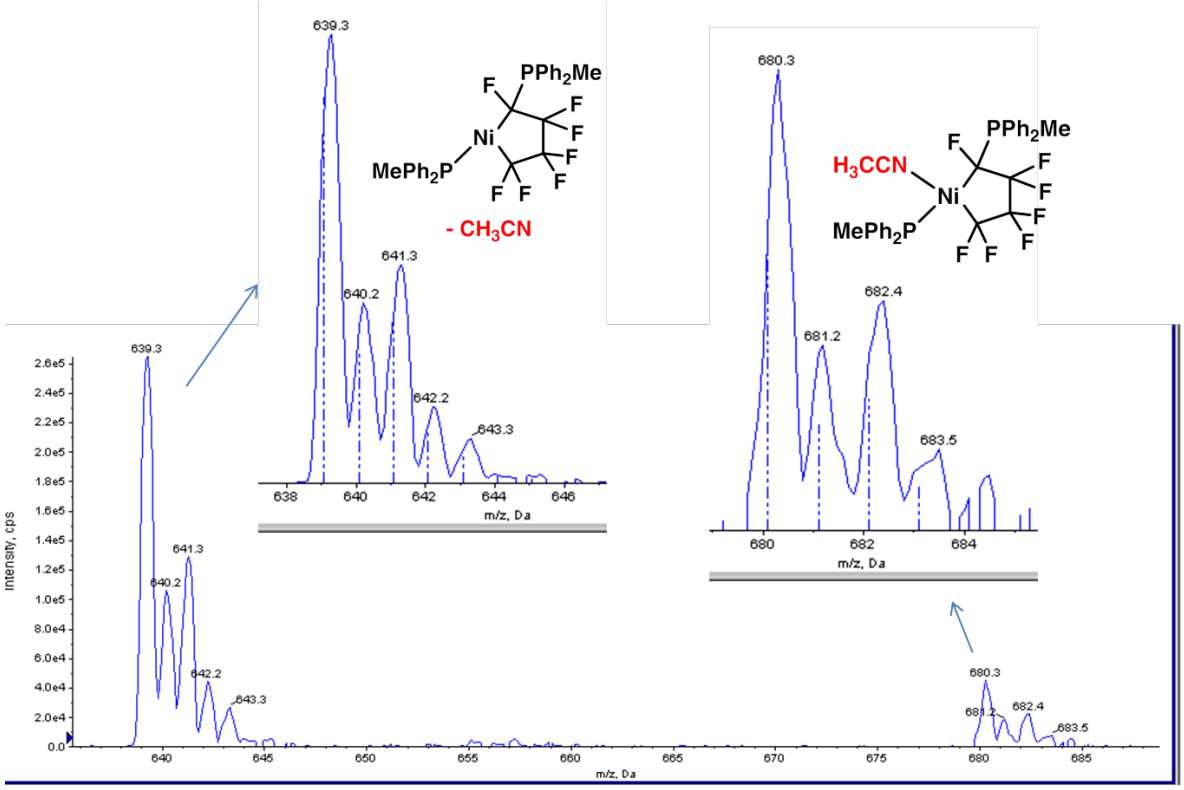

Figure A52. Selected peaks from the ESI mass spectrum (positive mode, CH_3CN) of complex **Ni10-b**.

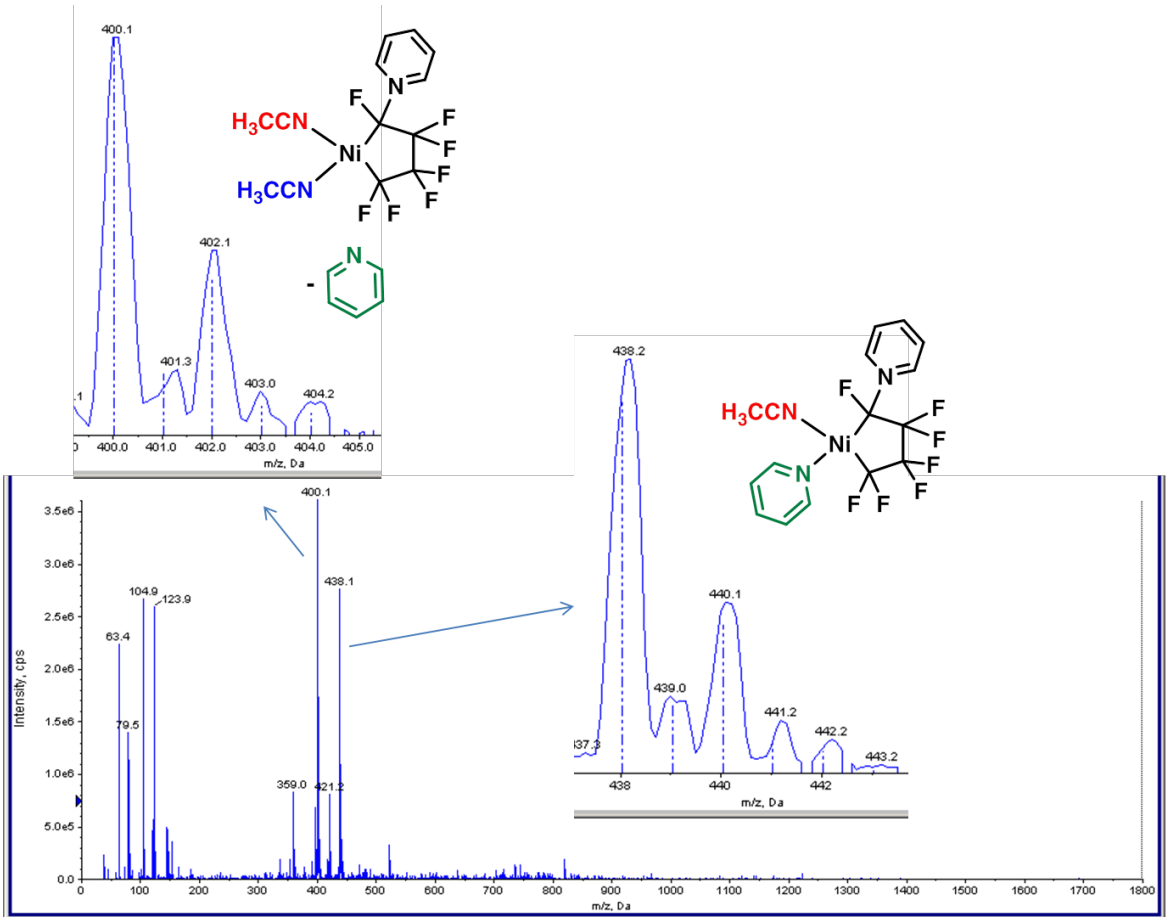

Figure A53. Selected peaks from the ESI mass spectrum (positive mode, CH_3CN) of complex **Ni-10c**.

X-ray Crystallography Data

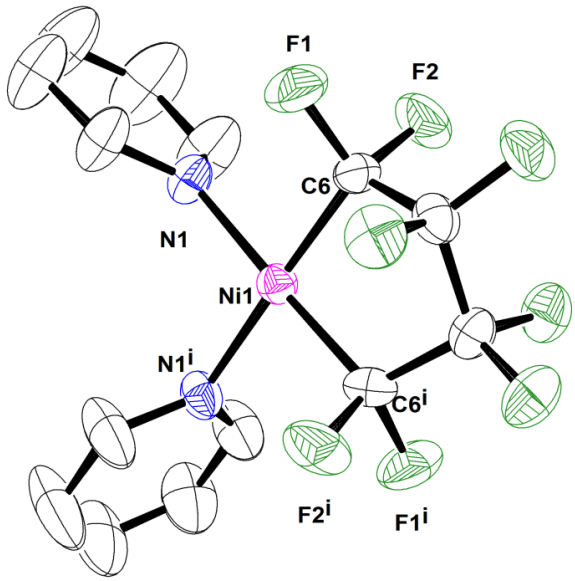

Figure A54. ORTEP representation of the molecular structure of complex **Ni-9c**. Thermal ellipsoids are set at the 40% probability level. Hydrogen atoms of pyridine rings are omitted for clarity.

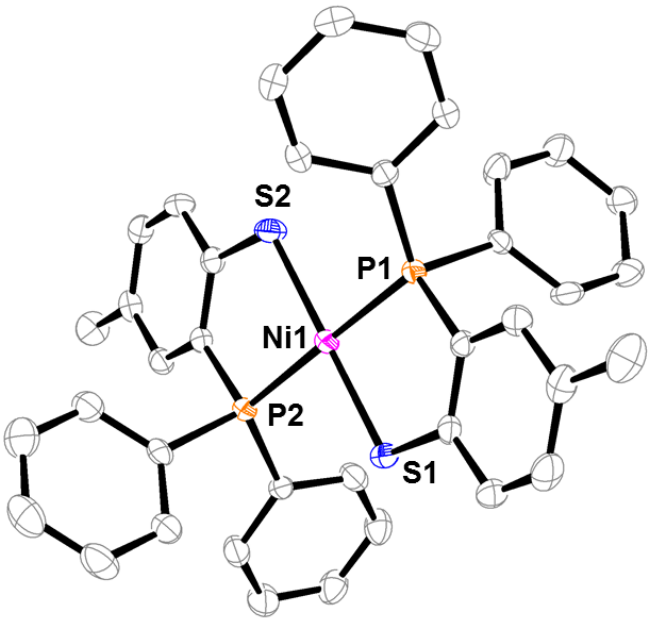

Figure A55. ORTEP representation of the molecular structure of complex **Ni-14**. Thermal ellipsoids are set at the 40% probability level. Hydrogen atoms are omitted for clarity.

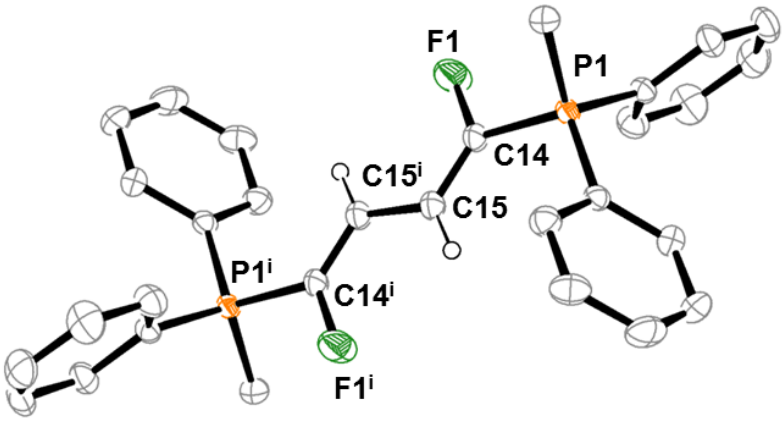

Figure A56. ORTEP representation of the molecular structure of **O4c**. Thermal ellipsoids are set at the 40% probability level. Hydrogen atoms and outer-sphere triflate ions are omitted for clarity.

Table A1 X-ray diffraction data collection and refinement parameters for Ni-21, Ni-22•Na, Ni-23 and Ni-24.

	Ni-21	**Ni-22•Na**	**Ni-23**	**Ni-24**
Formula	$C_{28}H_{20}F_8NNiP$	$C_{48}H_{59}F_8NNaNiO_8P$	$C_{36}H_{28}F_{11}NNiO_3PS$	$C_{32}H_{25}F_7N_3NiP$
Fw	612.13	1042.63	853.33	674.23
Color	Light yellow	Yellow	Yellow	Orange
Temperature/K	200(2)	200(2)	200(2)	200(2)
Crystal system	Monoclinic	Triclinic	Monoclinic	Monoclinic
Space group	P 2(1)/c	P-1	P 2(1)/n	P 2(1)/n
a/Å	17.6812(5)	10.1065(3)	9.8480(4)	11.0743(4)
b/Å	8.8730(2)	13.8945(4)	11.0845(4)	9.4288(4)
c/Å	18.2889(5)	18.2862(6)	30.9463(11)	29.0345(12)
α/deg	90	83.3020(10)	90	90
β/deg	115.8190(10)	87.599(2)	90.7550(10)	97.623
γ/deg	90	75.4930(10)	90	90
V/Å^3	2582.83(12)	2468.78(13)	3377.8(2)	3004.9(2)
Z	4	2	4	4
D_c/Mg m^{-3}	1.574	1.403	1.678	1.490
μ/mm^{-1}	0.890	0.517	0.785	0.770
F(000)	1240	1088	1732	1376
Crystal size/mm	0.12 x 0.09 x 0.03	0.14 x 0.09 x 0.08	0.12 x 0.10 x 0.07	0.14 x 0.06 x 0.04
Reflections collected/unique	10308/1883	40220/10075	53395/8333	27533/5065
θ range/deg	2.24 to 28.32	1.52 to 26.40	2.18 to 28.33	1.90 to 24.73
Index range	-23<=h<=22, -11<=k<=11, -24<=l<=23	-12<=h<=12, -17<=k<=13, -22<=l<=18	-13<=h<=13, -14<=k<=14, -41<=l<=39	-11<=h<=13, -11<=k<=11, -34<=l<=34
R(int)	0.0648	0.0455	0.0221	0.0475
Completeness to θ	28.32°, 99.0 %	26.40°, 99.3 %	28.34°, 98.8 %	24.73, 98.9 %
Max. and min. transmission	0.9738 and 0.9007	0.9598 and 0.9312	0.9471 and 0.9117	0.9699 and 0.8999
Data/restraints/parameters	6369 / 0 / 352	10075 / 134 / 640	8333 / 18 / 496	5065 / 96 / 418
Goodness-of-fit on F^2	1.025	1.014	1.016	1.037
R1, wR2 [I>2σ(I)]	0.0399, 0.0794	0.0523, 0.1090	0.0548, 0.1521	0.0392, 0.0854
R1, wR2 (all data)	0.0750, 0.0890	0.0980, 0.1253	0.0644, 0.1611	0.0755, 0.0969